ACTA UNIVERSITATIS SZEGEDIENSIS

ACTA MINERALOGICA-PETROGRAPHICA

Tomus XXX

SZEGED, HUNGARIA
1989

NOTE TO CONTRIBUTORS

General

The Acta Mineralogica—Petrographica publishes original studies on the field of geochemistry mineralogy and petrology, first of all studies of Hungarian researchers, papers resulted in by cooperation of Hungarian researchers and those of other countries and, in a limited volume, papers from abroad on topics of global interest.

Manuscripts schould be written in English and submitted to the Editor-in-chief, Institute of Mineralogy, Geochemistry and Petrography, Attila József University, H-6701 Szeged, Pf. 651 Hungary.

The authors are responsible for the accuracy of their data, references and quotations from other sources.

Manuscript

Manuscripts should be typewritten with double spacing, 25 lines on a page and space for 50 letter, in a line. Each new paragraph should begin with an indented line. Underline only words that should be typed in italics.

Manuscripts should generally be organized in the following order:

Title
Name(s) of author(s) and their affiliations, in foot-note the address of the author to whom the correspondence should be sent.
Abstract
Introduction
Methods, techniques, material studied, description of the area investigated, etc.
Results
Discussion or conclusions
Acknowledgement
Explanation of plates (if any)
Tables
Captions of figures (drawings, photomicrographs, etc.)

Abstract

The abstract cannot be longer than 500 words.

Tables

The tables should be typewritten on separate sheets and numbered according to their sequence in the text, which refers to all tables.

The title of the table as well as the column headings must be brief, but sufficiently explanatory.

The tables generally should not exceed the type-area of the journal, i.e. 12.5×18.5 cm. Fold-outs can only exceptionally be accepted

ACTA UNIVERSITATIS SZEGEDIENSIS

ACTA MINERALOGICA-PETROGRAPHICA

Tomus XXX

SZEGED, HUNGARIA
1989

HU ISSN 0365—8066
HU ISSN 0324—6523

SERIES NOSTRA AB INSTITUTIS MINERALOGICIS, GEOCHIMICIS PETROGRAPHICIS UNIVERSITATUM HUNGARICUM ADIUVATUR

Editor

Institut Mineralogicum, Geochimicum et Petrographicum
Universitatis Szegediensis de Attila József nominatae

Nota

Acta Miner. Petr., Szeged

Szerkeszti

SZEDERKÉNYI TIBOR

Kiadja

a József Attila Tudományegyetem Ásványtani, Geokémiai és Kőzettani Tanszéke
H-6722 Szeged, Egyetem u. 2—6

Kiadványunk címének rövidítése
Acta Miner. Petr., Szeged

SOROZATUNK A MAGYARORSZÁGI EGYETEMEK ROKON TANSZÉKEINEK TÁMOGATÁSÁVAL JELENIK MEG

CONTENTS

Acta Mineralogica-Petrographica, Szeged, XXX, 5—17, 1989

IN MEMORIAM DR. JÁNOS BÉRCZI

LIESEGANG LAYERED CLINOPYROXENE MEGACRYST INCLUSION FROM SZENTBÉKKÁLLA, HUNGARY

Sz. Bérczi*

Department of General Technics, Eötvös Loránd University

Cs. Szabó**

Department of Petrology and Geochemistry, Eötvös Loránd University

ABSTRACT

Fourteen parallel bands composed from submillimeter sized olivine grains scattered along planes form an almost uniformly spaced (7—9 mm) layered structure in the large, decimeter sized single crystal of clinopyroxene of our Spx—3 inclusion. A medium range of uniformly enriched REE abundances, the spinel-olivine components and a small (1 cm) grain of lherzolite xenolith inclusion in the Al-augite megacryst suggest a complex history of the Spx—3 specimen. Measurements carried out by optical microscopy, X-ray and electron diffraction, INAA and electron microprobe analyses have revealed textural, chemical and REE characteristics of the Spx—3 specimen's mineral components from which its formation can be reconstructed. They indicate its origin in an approximately 15% partial melting of the primary lherzolithic mantle, subsequent lherzolite inclusion transfer to the place of crystallization of this melt in the deep crust or upper mantle region where a cooling process in a concentration gradient field resulted in Liesegang layering of olivine (and partly spinel) in the megacryst producing plutonic massivum, to the final stage of uplift from the upper mantle — lower crust region by volcanic eruption which delivered the specimen to the surface and embedded it in the alkali basalt tuff of Szentbékkálla about 5 million years ago.

INTRODUCTION

REE abundance and corresponding petrological and mineralogical investigations on the Szentbékkálla series of peridotite inclusions have revealed genetic relationships between different upper mantle and lower crust inclusions and host alkali basalts (Sz. Bérczi, J. Bérczi, 1986). During this work a unique specimen was found at Szentbékkálla by one of our students on mathematics and technology, L. Kőszegi in 1984. Initial inspection showed that the specimen was the size of a fist clinopyroxene megacryst nodule broken into four pieces. The interesting and puzzling aspect of its otherwise megacryst appearance was about dozen thin, parallel ribs protruding from its smooth rounded surface. The ribs were visible in low angle incident light. However, a centimeter sized peridotite inclusion was embedded in the speciment together with many smaller and larger spinel crystals. The Spx—3 speci-

* H—1088 Budapest, Rákóczi út 5. Hungary.
** H—1088 Budapest, Múzeum krt. 4/A. Hungary.

men seemed so unique and promising that the four fragments were given to colleagues working in different Departments of the Eötvös Loránd University and the Budapest Technical University who had different measuring facilities. The results of our investigations are summarized on the following pages.

DISCOVERY SITE AND SPECIMEN DESCRIPTION

The Spx—3 specimen was found on the Church hill of Szentbékkálla, North edge of Káli-Basin, Nort-West Balaton Region, Hungary. The specimen was an inclusion protruding from the basalt tuff in a cart-track and hence free of grass vegetation *(Fig. 1.)*, The specimen was extracted in four pieces as shown in *Fig. 2.* Preli-

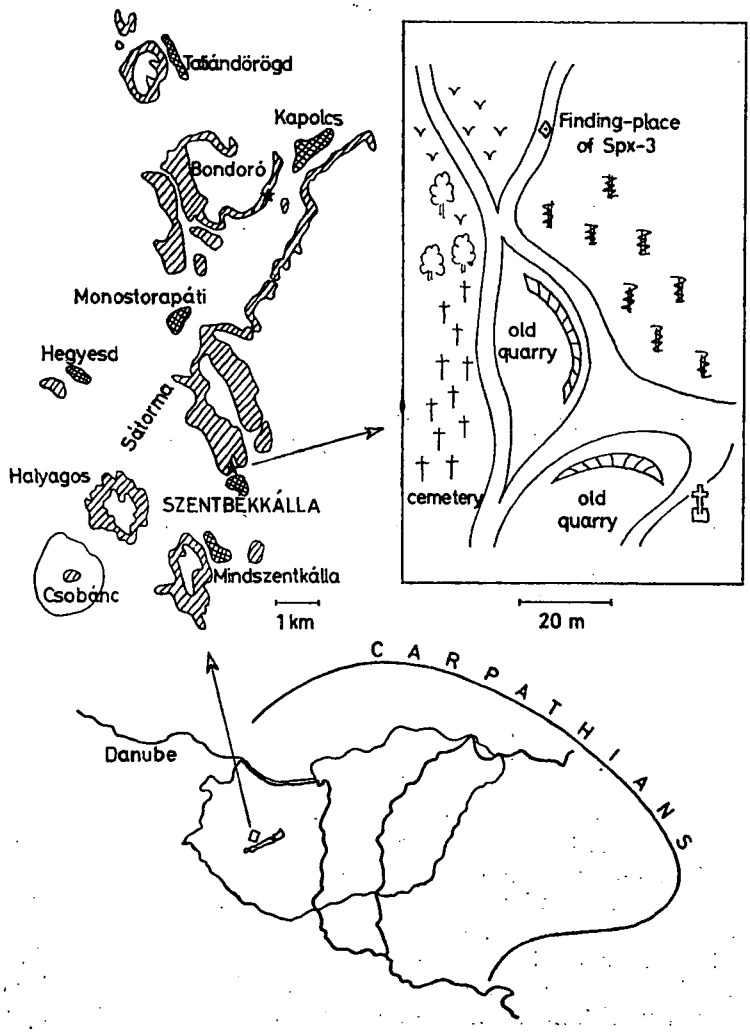

Fig. 1. The site of discovery of Spx—3 sample and that of samples chosen for comparison from Szentbékkálla and Kapolcs, NW Balaton region, Hungary. The upper left part shows piroclastic rock from the geologic map of Lóczy (1920)

minary observations in low angle incident light revealed the almost equidistant rib system of protruding mineral layers running parallel to each other. One of the fractures which divided the sample in to four parts occurred along one of these layers (that separating A+B and C+D pairs in *Fig. 2.*). On the surface of this fracture could be seen olivine crystals 0.1—0.5 mm in size which populated and so formed the layers. As well as these parallel layers, black spinels arranged along the layers also protruded from the nodule although not so densely as the olivines. Moreover a rounded, 1 centimeter sized lherzolite inclusion was embedded in the specimen (fragment C, *Fig. 2.*).

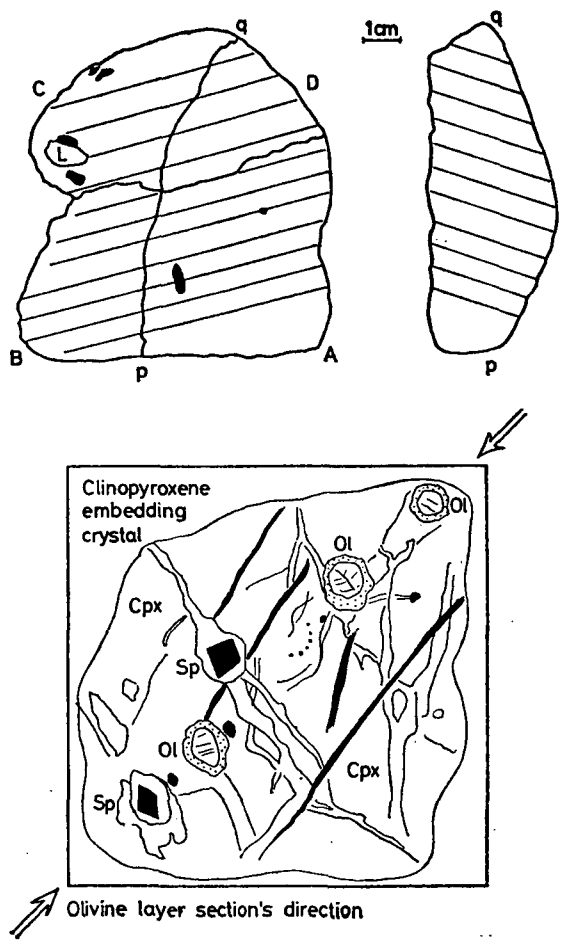

Fig. 2. The fist sized Spx—3 specimen. a The 14 parallel bands of scattered olivine grains arranged along planes protruding from the surface of the sample. The protruding lherzolite (L) grain in C fragment and some of the large spinels in A and C fragments are also drawn in. b The cross section of the Spx—3 sample at the p-q breaking-line shows the position of olivine layers. c Sketch of a cut layer region enlarged from a thin section. Arrows indicate the position of the olivine layer and show that olivine grains rarely populate the planes and that spinels accumulated along these planes.

TEXTURAL CHARACTERISTICS

The mineral phases which constitute the sample have a very strange arrangement. The host clinopyroxene exhibits no optical zoning and twinning, but effects of mechanical strain. The whole large megacryst of Spx—3 seems to be homogeneous, and according to its optical characteristics it is augite.

The olivine and spinel occur as poikilitically embedded minerals arranged near to the direction of cleavage planes of the host clinopyroxene megacryst *(Fig. 2.)* Sometimes these accompanying minerals form aggregates along the planes. The olivine grains are between 0.1—0.5 mm in size and are isometric and euhedral according to their appearance in thin sections. No mechanical twinning or other deformations can be seen in the olivines, except in one larger grain 2 mm-s in diameter. The cleavage planes are clearly visible and there is no sign of their metamorphic transformation.

The spinel grains are generally 0.2—0.9 mm in size but exceptionally crystals of spinel larger than 5 mm-s occur in the Spx—3 sample. On the basis of their triangular or square sections the spinel grains are euhedral and on the basis of their uniform dark-grey color they seem to be homogeneous.

Textural types of Hungarian basic-ultrabasic xenoliths have been reviewed by EMBEY—ISZTIN (1984). The Spx—3 sample belongs to the black pyroxene (Al, Ti-augite) group of xenoliths but does not belong strictly to any of the textural types classified there because of its unique layered texture and its almost decimeter sized single crystal structure. Our sample can, however, be related (interpolated) to two textural types in this classification: clinopyroxene megacryst xenoliths and composite xenoliths.

The general assertions on black clinopyroxene group xenoliths about their almost monomineralic composition, the Al-augite composition of clinopyroxene and the presence of scattered olivine and spinel accessory accompanying minerals are valid for the Spx—3 sample. The poikilitical enclosing of the more frequent smaller, rounded or subhedral olivine and the rare but larger, mostly euhedral spinels by the megacryst clinopyroxene in Spx—3 shows a close relation to the Szg—3005 Embey—Isztin's sample. However in Spx—3 the olivines are evenly distributed along the parallel planes and spinels are also scattered rather uniformly, frequently accumulating along the olivine layers contrary to the unordered texture of Szg—3005 sample.

The embedded lherzolite nodule also relates Spx—3 to the composite xenolith EMBEY—ISZTIN's group, but the extraordinary characteristic of Spx—3 specimen is the ordered texture with the strictly parallel olivine grain populated planes, which might have been formed by a resonance effect (standing weaves) or by special causes during the very quiet, large single crystal growing crystallization process. We have found only one (probable) similar sample from the literature: SKEWES and STERN (1979) reported what we assume to be similarly textured clinopyroxene megacrysts from the Palei-Aike lavas in Chile. These "megacrysts contain opaque inclusions *regularly distributed along curved planes*". We propose forming a distinct subgroup of such black clinopyroxenes with an ordered poikilitical texture and enlarge with this subgroup EMBEY—ISZTIN's classification of Hungarian xenoliths, of which such types with unusual texture may preserve the detailed structure of the process of magmatic events of melts on their way from the mantle to the surface.

THE COMPOSITION OF MINERAL COMPONENTS OF SPX—3

The estimated mineral composition of Spx—3 is as follows: clinopyroxene — 94%, spinel — 3%, olivine — 3%. The compositional data of the microprobe analysis are shown on Table 1. Compositional zoning of the main elements — which could have been reflected by the supposed Liesegang layering in Spx—3. — has not been observed for any of the mineral components of Spx—3, in accordance with the optical characteristics of these minerals.

TABLE 1.

Comparison of maior element composition of spinel and clinopyroxene components of two Spx and one Cpx samples (Microprobe analysis by K. G. SOLYMOS *and* CS. SZABÓ*)*

	Spx—A		Spx—3		Cpx—Kap
	cpx	spinel	cpx	spinel	cpx
SiO_2	49.22	n.a.	48.4	n.a.	48.84
TiO_2	1.17	0.49	0.99	0.40	0.97
Al_2O_3	7.87	61.89	9.25	60.90	7.63
FeO_t	6.24	16.50	5.81	16.80	5.82
MnO	0.18	0.06	n.a.	n.a.	0.10
MgO	15.10	21.41	15.50	20.90	16.12
CaO	18.64	n.a.	18.85	n.a.	18.94
Na_2O	1.24	n.a.	1.48	n.a.	1.17
Cr_2O_3	n.d.	n.a.	n.d.	n.a.	0.12
Sum	99.66	100.44	99.93	99.0	99.71
$\frac{10\ Mg}{Mg+Fe}$	81.2	69.8	82.6	68.9	83.2

n.a. = non analysed, n.d. = non detected.

The clinopyroxene of Spx—3 appears to be very near in composition to the two earlier spinel-pyroxenite and clinopyroxene samples (BÉRCZI, BÉRCZI 1986) in the Ca—Mg—Fe diagram *(Fig. 3)*. These three clinopyroxenes with their average $Ca_{42}Mg_{48}Fe_{10}$ metal composition seem to be richer in Mg and poorer in Ca than the Australian, French and Nógrád—Gömör (Medves) Hungarian black clinopyroxene megacrysts which have been investigated in more detail earlier (WILKINSON 1975, WASS 1979, LIOTARD *et al.* 1988, DIENES 1979) so our NW Balaton regional samples can be found in the endiopside region of the Ca—Mg—Fe pyroxene triangle.

The high Al_2O_3 and Na_2O content of clinopyroxene suggests a considerable amount of jadeite (10.2 percent) and $CaAlAlSiO_6$ (6.4 percent) end members. Clinopyroxenes characterized by a high Mg value (about 80) a greater proportion of jadeite and $CaAlAlSiO_6$ components and a low Cr content are widespread in alkali basalts (WHITE 1966, BINNS *et al.* 1970, IRVING 1974.) and such clinopyroxenes are called Al-augite after WILSHIRE and SHERVAIS (1975).

Most of the authors (for example AOKI and KUSHIRO 1968, AOKI 1971, SKEWES and STERN 1979, WASS 1979, IRVING and FREY 1984,) have considered clinopyroxene inclusions embedded in the host magmatite as cognate precipitates in equilibrium with the host basalt under high pressure and temperature conditions. Using to this model we could estimate the two thermodynamic parameters of the source region of our three samples. In the AOKI—KUSHIRO diagram of Al^{IV}/Al^{VI} ratios *(Fig. 4)* the

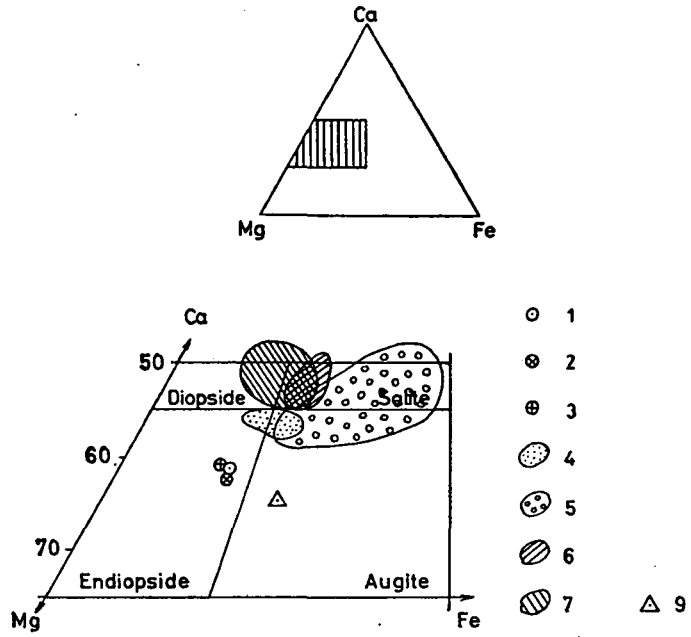

Fig. 3. The position of composition of clinopyroxenes from the Spx—3 sample, from two earlier NW Balaton region samples and the compositional regions of the Australian, French and Chilean clinopyroxenes used for comparison in the Ca—Mg—Fe diagram. (**1.** — cpx from Spx—3. **2.** — cpx from Spx—A. **3.** — cpx of Cpx—Kap. (2.—3. from BÉRCZI, BÉRCZI 1986), **4.** black cpx megacrysts (WILKINSON, 1979.). **5.** French cpx megacrysts (LIOTARD *et al.* 1988), **6.** French cpx megacrysts, **7.** Australian cpx megacrysts (6.—7. from WASS, 1979), 9. — Chilean cpx (SKEWES, STERN 1979.).)

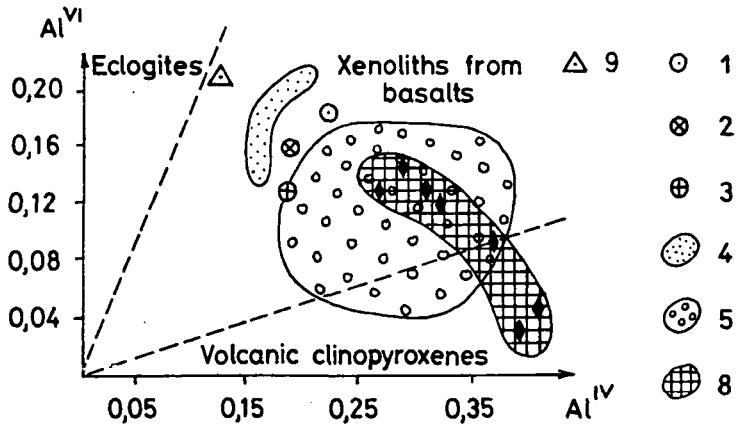

Fig. 4. The Al^{IV}/Al^{VI} positions of clinopyroxenes from our three samples (1., 2. and 3.) and the region of the (4.) Australian (WILKINSON, 1979) and (5.) French (LIOTARD *et al.* 1988) comparison samples in the AOKI—KUSHIRO diagram. (The numbers refer to the indications used on *Fig. 3.*) According to their positions the Nógrád—Gömör samples from Medves (DIENES, 1968) have a partly low pressure origin (8.). The Chilean clinopyroxene megacryst (9.) is the only sample which may have similar ordered texture to that of Spx—3. (The 9. point from SKEWES, STERN 1979.)

clinopyroxenes of Spx—3, Spx—A and Cpx—Kap samples fall within the 10—15 kbar pressure range. On the basis of the experimental data of THOMPSON (1974) the temperature at their source region would probably have been in the 1200—1300 °C range. (THOMPSON's data confirm the pressure estimation of 10—15 kbar from the AOKI—KUSHIRO diagram, too.)

The composition of olivine crystals of Spx—3. (Table 2) can be compared to two different earlier measurements. The olivine of Spx—3. is similar in composition to the megacrysts of alkalic basalts from the Nógrád—Gömör region (ÁRGYELÁN 1987, FORGÁČ *et al.* 1986.) which are always richer in Fe than the olivine phenocrysts of the basalt. This fact agrees with the results of WILKINSON (1975) who also concludes that olivine connected to Al-augite shows similarities in its chemical character to megacrysts.

TABLE 2

Comparison of the composition of olivines from Spx—3, from wehrlite and from basalts as megacrysts
(1. and 2. K. G. SOLYMOS and Cs. SZABÓ, 3. ÁRGYELÁN (1987) average of 7 samples. 4. FORGÁČ et al. (1986) average of 4 samples; 1.—2. Szentbékkálla, 3.—4. Nógrád-Gömör)

	Spx—3	Wehrlite	Av. Megacrysts	Av. Megacrysts
SiO_2	39.4	38.31	39.6	39.5
Al_2O_3	0.10	0.07	0.03	0.04
FeO	16.0	13.90	14.7	17.8
MnO	n.a.	0.27	0.20	0.36
MgO	43.6	47.12	45.3	42.8
CaO	0.15	0.05	0.21	n.a.
Sum	99.25	99.72	100.04	100.5
Mg value	82.9	8.58		

n.a. = non analysed.

The second sample for comparison is from our earlier work (BÉRCZI, BÉRCZI 1986): a wehrlite sample. Not only the Fe enriched composition of its olivine, but also its REE abundance connects this sample more closely to the clinopyroxenite group of inclusions from the Szentbékkálla Series.

Because of its very high Al_2O_3 content, the spinel of Spx—3. is rich in the $MgAl_2O_4$ phase, and so it is the same in composition as spinels of our earlier spinel-pyroxenite samples, Spx—A and Spx—D (BÉRCZI, BÉRCZI 1986). The X-ray diffraction measurements carried out with associated salt crystal also confirm this high $MgAl_2O_4$ content: the grid-unite from the (220) lattice's reflection is 0.812 nm, from the (111) planes it is 0.813 nm and from the (311) planes' reflection it is 0.806. The average of 0.810 nm is very near to the 0.808 nm for true spinels.

REE ABUNDANCES OF CLINOPYROXENE AND SPINEL FROM SPX—3 AND FROM OTHER SPINEL-PYROXENITE NODULES

The chondrite normalized REE abundance pattern of clinopyroxene and spinel of Spx—3, that of Spx—A and Spx—D (BÉRCZI, BÉRCZI 1986) and that of Spx—7 and Spx—Kap (this work for comparison) all have similar shapes in two distinct ranges *(Fig. 5)*. The clinopyroxenes are enriched about 10 times as compared to the

chondritic values, the spinels are on chondritic abundances except in the light REE region, where they are enriched in La to the clinopyroxene level. The run of the REE curves of clinopyroxenes show little HREE depletion and thus a modest decreasing trend from light to heavy REE *(Fig. 5)*. The global range of spinel-pyroxenites is between the range of basalts and that of lherzolites *(Fig. 6)* in the Szentbékkálla series and it is the smoothest of them. Our REE values are in close agreement with the data and range for clinopyroxenes given by IRVING and FREY (1984), (except that our samples exhibit a little negative Eu anomaly proving the differentiated, partly exhausted nature of the source region). From the fact that the clinopyroxene/host basalt distribution coefficients at these authors fall within the range of experimentally investigated clinopyroxene/melt ratios in the case of middle and heavy REE, the conclusion that clinopyroxene megacrysts were in equilibrium with their host basalts is widely accepted (e.g. LIOTARD *e t al.* 1988). But IRVING and FREY in their paper (1984) emphasize that there only *may* be equilibrium between clinopyroxenes and host basalts and they did not exclude other kinds of genetics as well.

Contrary to the rather smooth (compared to chondritic) range of clinopyroxenes from spx-samples the corresponding contribution coefficient range *(Fig. 7)* clearly reflects only the inverse of the LREE enrichment of basalts. The experimental data do not fit those of clinopyroxenes in the LREE region alone. A smoother REE range of host melt could give a better approach to the calculated distribution coefficients:

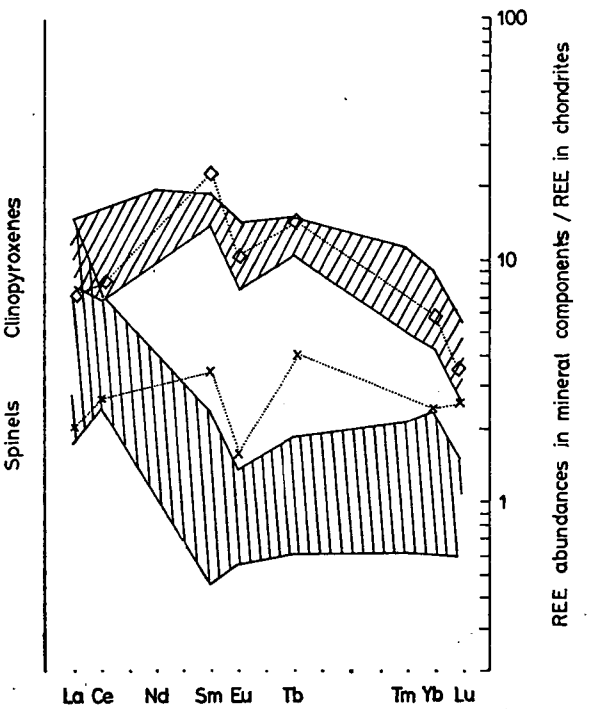

Fig. 5. Chondrite normalized REE abundances of the clinopyroxene and spinel components of Spx—3 and the REE abundance range of these two mineral fractions from the NW Balaton region Hungarian spinel-pyroxenites.) ▽ — cpx of Spx—3, × — sp of Spx—3)

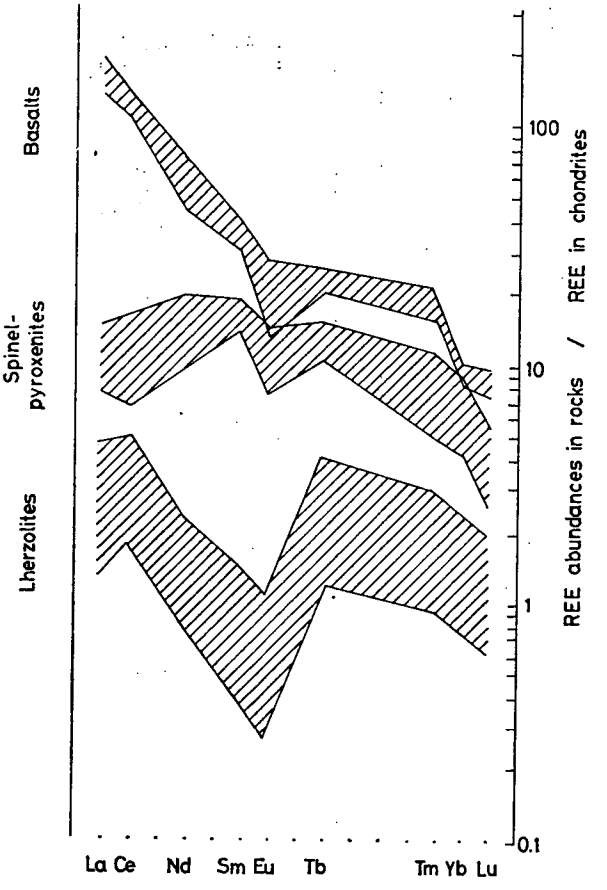

Fig. 6. The REE abundance range of spinel-pyroxenites (this work) between the REE ranges of lherzolites (below) and alkalic basalts (upper) (BÉRCZI, BÉRCZI 1986). The spinel-pyroxenite range is represented with the range of clinopyroxenites, because of their one order of magnitude greater REE content, than that of spinels, except in the LREE region, where they shift of the range to higher values

this may be a 15—20 percent partial melt of the peridotitic mantle which should produce a more even distribution of REE because of the more extended partial melting. This model is in accordance with our earlier suggestion (BÉRCZI, BÉRCZI 1986).

LIESEGANG LAYERING OF OLIVINES IN SPX—3

The periodic precipitation phenomenon is known since the work of R. E. LIESEGANG (1896). The periodic precipitation pattern (PPP) was later commonly called Liesegang phenomenon or Liesegang-rings from its experimental reproduction in Petri dish. The PPP may be formed in the presence of concentartion gradients of two reactants in a background system (liquid or solid state). In their physical-chemical experimental studies S. C. MÜLLER, SHOICHI KAI and J. ROSS (1982) have

TABLE 3

REE content in mineral components of Hungarian s inel-pyroxenite inclusions (data in ppm).
(+ measurements by J. BÉRCZI, *X measurements by* Zs. MOLNÁR*)*

	Szentbékkálla								Kapolcs	
	Spx—A+		Spx—D+		Spx—3+		Spx—7x		Spx—Kapx	
	Sp	Cpx	Sp	Cpx	Sp	Cpx	Sp	Cpx	Sp	Cpx
La	4.3	2.9	0.5	3.2	0.6	2.1	1.8	2.50	3.28	4.85
Ce	5.7	5.8	2.0	8.9	2.1	6.6	n.a.	n.a.	n.a.	n.a.
Nd	<5.0	7.0	<2.0	5.8	n.a.	n.a.	n.a.	n.a.	b.a.	n.a.
Sm	0.40	3.34	0.09	3.88	0.7	4.7	0.45	3.2	0.51	3.1
Eu	0.10	0.98	0.04	0.04	0.12	0.75	n.a.	0.98	n.a.	0.74
Tb	0.09	0.55	0.03	0.7	0.2	0.7	n.a.	n.a.	n.a.	n.a.
Tm	0.07	0.16	0.02	0.36	n.a.	n.a.	n.a.	n.a.	n.a.	n.a.
Yb	<0.5	<0.5	<0.5	<0.5	0.4	1.0	≦0.2	1.07	≦0.4	0.77
Lu	<0.05	0.17	<0.02	0.08	0.08	0.11	≦0.03	0.10	≦0.05	0.11
Cr.	240	29	430	44	91	30	760	38	1040	270

n.a. = non analysed.

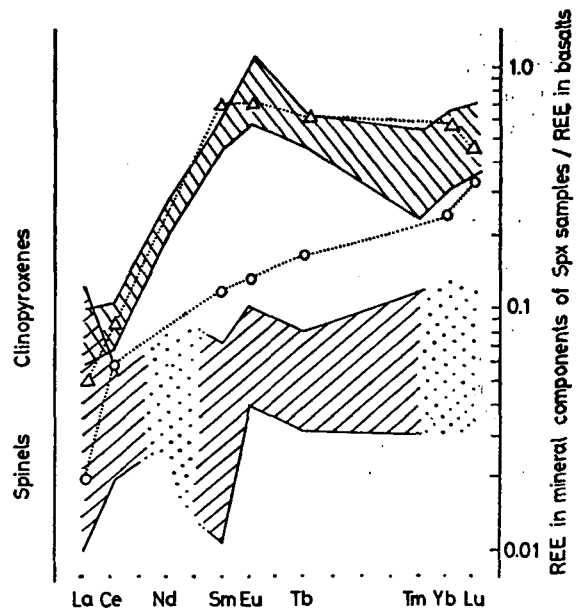

Fig. 7. Clinopyroxene/host basalt and spinel/host basalt distribution coefficients ranges for the mineral components of Hungarian spinel-pyroxenites. (△ — distribution coefficients for the clinopyroxene of Spx—3, ⊙ — distribution coefficients for the spinel of Spx—3.)

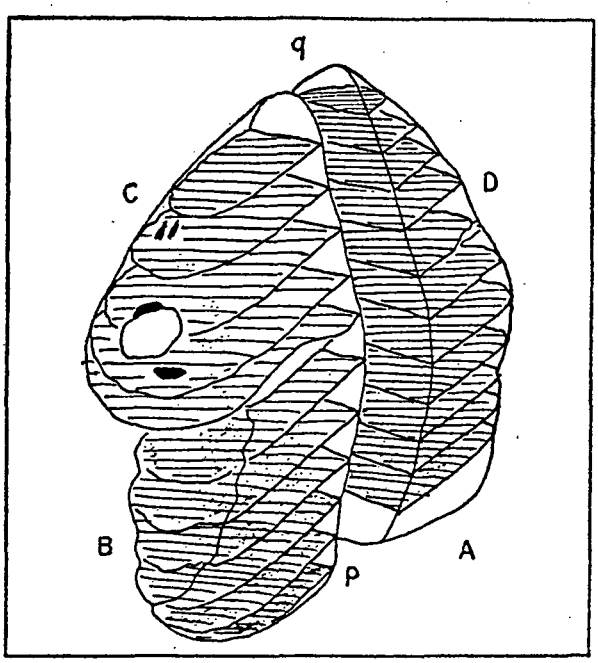

Fig. 8. Perspectivical view the Liesegang layers in the Spx—3. clinopyroxene megacryst inclusion.

concluded the dependence of PPP on the initial concentrations of reactants. According to their work the relevant parameters in the formation of PPP were the initial concentration difference of reactants and the initial ion-concentartion product of reactants. When both of these two parameters were large they have got large number of thin precipitating layers in their experiments. On the basis of the studies of S. C. MÜLLER *et al.* a preliminary inference can be given here to the PPP formation in our Spx—3 specimen *(Fig. 8)*.

In the parent liquid of Spx—3 SiO_4^{2-} and Mg^{2+} ions might have been the main actors of the PPP process. Large initial concentration difference might have been produced by large Mg^{2+} and small SiO_4^{2-} concentration (at the sides of) or gradient (through) the PPP region. The more agile Mg^{2+} ions could have moved — and concentrated by the colloid formation and the subsequent focusing mechanism (MÜLLER *et al.* 1982.) — against the small SiO_4^{2-} gradient in the liquid to form the Mg_2SiO_4 layers in the extended clinopyroxene environment. (In a similar process Mg^{2+} and Al^{3+} ions — which might have been in excess over the average clinopyroxene background — could have formed the $MgAl_2O_4$ spinels against the small oxigene gradient.) These suggestions should be studied in more details if a collection of different Liesegang layered clinopyroxene megacryst specimens makes comparison possible.

SUMMARY

Texture, composition, chemistry and REE abundances of mineral components of Spx—3 megacryst inclusion from alkali basalt of Szentbékkálla prove its origin by crystallization from melt.

1. The primary melt nature of the liquid of Spx—3 is proved by an embedded lherzolite xenolith in the specimen.
2. The melt might have been produced by a 15—20 percent partial melting of the parental mantle peridotite. (according to the REE concentrations)
3. During crystallization olivine and spinel might have been precipitated together with or from clinopyroxene (as shown by their equal Mg-values in Table 2 and 3).
4. Concentration gardients might have resulted in Liesegang layered precipitation arrangement of olivine (and partly the spinel) crystals.
5. According to the compositional data of clinopyroxene of Spx—3 the specimen crystallized in the 10—15 kilobar pressure and the 1200—1300 °C temperature ranges.
6. The crystallization in deep was the first stage of uplifting of the specimen from a mantle region. The second stage was the alkali basaltic eruption which embedded the specimen into the basalt tuff of Szentbékkálla.

CALL FOR COOPERATION IN LIESEGANG LAYERED MEGACRYSTS

We ask investigators of mantle and lower crust xenoliths to kindly inform us if they have measured Liesegang layered structures (PPP) in megacrysts similar to those in our Spx—3 specimen. A comprehensive comparison of these Liesegang layered megacrysts may give us a new method for determination of lower crust — upper mantle conditions where these megacrysts have been formed from partial melts of mantle peridotites.

ACKNOWLEDGEMENTS

The authors are indebted to Zs. Molnár and her colleagues at the Training Reactor of Budapest Technical University for completing the INAA measurements after the death of our colleague, János Bérczi whose memory is consecrated by this paper. We are also indebted to K. G. Solymos for electron-microprobe analysis, to M. Soós for electron microscope measurements of clinopyroxene crystal-structure, to G. Zsolt for X-ray diffraction measurements and to Z. Rácz for the worthy discussions on Liesegang structures. Finally authors express their thanks to I. Kubovics who supported their work by making available the instrumental facilities of the Department of Petrology and Geochemistry, Eötvös Loránd University.

REFERENCES

AOKI, K. (1971): Petrology of mafic inclusions from Itinomegata, Japan. Contrib. Mineral. Petrol. **30,** 314—331.

AOKI, K. KUSHIRO, I. (1968): Some clinopyroxenes from ultramafic inlcusions in Dreiser Weiher, Eifel. Contrib. Mineral. Petrol. **18,** 326—337.

ÁRGYELÁN, G. (1987): A Nógrád-gömöri bazaltok bázisos és ultrabázisos zárványainak kőzettani-geokémiai vizsgálata. (Petrological and geochemical investigations of mafic and ultramafic xenoliths from basalts of Nógrád-Gömör, Hungary.) M. Sc. Thesis (in Hungarian) Eötvös Loránd University, Budapest.

BÉRCZI, SZ., BÉRCZI, J. (1986): Rare earth element content in the Szentbékkálla Series of peridotite inclusions. Acta Mineral. Petrog. Szeged. **28,** 61—73.

BINNS, R. A., DUGGAN, M. B., WILKINSON, J. F. G. (1970): High pressure megacrysts in alkaline lavas from northeastern New South Wales. Amer. J. Sci. **269,** 132—168.

DEER, W. A., HOWIE, R. A., ZUSSMANN, J. (1963): Rock forming minerals. Vol. **III.** Longmass, London.

DIENES, I. (1968): Klinopiroxén megakristályok a medvesi bazaltból. (Clinopyroxene megacrysts from the Medves basalt.) Annual Rep. of Hung. Geol. Survey from 1968. 125—130. (in Hungarian).

EMBEY-ISZTIN, A. (1984): Textural types and their relative frequencies in ultramafic and mafic xenoliths from Hungarian alkali basaltic rocks. Annls. Hist.-nat. Mus. Nat. Hung. **76,** 27—42.

FORGÁČ, J., HATÁR, J., KRISTIN, J., MEDVEGY, J. (1986): Olivines in the Western Carpathians basalts. Geol. Carpathica **37,** 147—165.

IRVING, A. J. (1974): Megacrysts from the Newer basalts and other basaltic rocks of Southwestern Australia. Geol. Soc. Am. Bull. **85,** 1503—1514.

IRVING, A. J., FREY, F. A. (1984): Trace element abundances in megacrysts and their host lavas: constraints on partition coefficients and megacryst genesis. Geochim. Cosmochim. Acta. **48,** 1201—1221.

LIESEGANG, R. E. (1896): Periodische precipitation. Naturwiss. Vochenschr. 11, p. 353.

LIOTARD, J. M., BROIT, D., BOIVIN, P. (1988): Petrological and geochemical relationships between pyroxene megacrysts and associated alkali basalts from Massif Central (France). Contrib. Mineral. Petrol. **98,** 81—90.

LÓCZY, L. (1920): A Balaton tó környékének részletes geológiai térképe. (Detailed geological map of the environment of Lake Balaton.) Hungarian Geographical Society, Budapest.

MÜLLER, S. C., SHOICHI KAI, ROSS, J. (1982): Periodic precipitation patterns in the presence of concentration gradiens: dependence on ion product and concentration difference. J. Phys. Chem. **86,** 4078—4087.

SKEWES, M. A., STERN, C. R. (1979): Petrology and geochemistry of alkali basalts and ultramafic inclusions from the Palei-Aike volcanic field in Southern Chile and the origin of the Patagonian Plateau lavas. Journ. Volcan. Geotherm. Res. **6,** 3—25.

THOMPSON, R. N. (1974): Some high pressure pyroxenes. Miner. Mag. **39,** 768—787.

WASS, S. Y. (1979): Multiple origins of clinopyroxenes in alkali basaltic rocks. Lithos. **12,** 115—132.

WHITE, R. W. (1966): Ultramafic inclusion in basaltic rocks from Hawaii. Contrib. Mineral. Petrol. **12,** 245—314.

WILKINSON, J. F. G. (1975): Ultramafic inclusions and high pressure megacrysts from nephelinite sill, Nandewar Mountains, Northeastern New South Wales, and their bearing on the origin of certain ultramafic inclusions in alkaline volcanic rocks. Contrib. Mineral. Petrol. **51,** 235—262.

WILSHIRE, H. G., SHERVAIS, J. W. (1975): Al-auqite and Cr-diopside ultramafic xenoliths in basaltic rocks from the Western United States. Phys. Chem. Earth. **9,** 257—272.

Manuscript received, 12 December, 1988

Acta Mineralogica-Petrographica, Szeged, XXX, 19—34, 1989

COMPARATIVE PETROLOGICAL INVESTIGATIONS OF METAGABBROS FROM WESTERN ALPS OPHIOLITES

A-A. M. ABDEL-KARIM—Z. PUSKÁS

Department of Petrology and Geochemistry, L. Eötvös University

ABSTRACT

Data on field relation, petrography and trace element geochemistry are presented for metagabbro bodies from a few small tectonic slices in the Piedmont oceanic — type sequence. They are from east Arc valley and Monviso from the eastern internal Piedmont unit and from middle Arc valley, Montgenevre, and Cristillan from western external Piedmont unit.

The metagabbros from Monviso are re-equilibrated under early Alpine eclogitic conditions and were successively involved in a polyphase retrograde tectono-metamorphic evolution. They include eclogitic — and smaragdite — metagabbros which underwent into greenschist facies metamorphism of a later stage. Some gabbros have partially escaped the Alpine metamorphism.

The Arc metagabbros are characterized by glaucophaneschist facies which retrogressed to greenschist facies. The well-preserved gabbroic sequence ranging from talc serpentine metagabbro to late gabbroic differentiated products (albitite) are present in Chenaillet.

In these gabbros, the early — Alpine HP prograde metamorphic events produced blueschist and eclogitic mineral assemblages (glaucophane, phengite, clinozoisite and omphacite ± zoisite ± garnet ± rutile) while the HP retrograde events produced blueschist, greenschist and amphibolite mineral assemblages.

These gabbros appear to be derived from different magma sources in different geotectonic environments and suffered different kinds of metamorphism. Moreover during the early stage of crystallization, Mg—Al gabbros were produced, characterizing a primitive magma while late stage crystallization produced more differentiated Fe—Ti gabbros.

KEYWORDS: petrology, trace element geochemistry, metamorphic evolution, ophiolite metagabbros, Piedmont Zone, Western Alps.

INTRODUCTION

The metaophiolite nappes of the Western Alps display a close connection with some sequences of the Piedmont ophiolite. They are described as remnants of the Tethyan oceanic crust structurally pinched between the Austro-Alpine continental crust (Sesia-Lanzo Zone) and European continental margin (Monte Rose—Grand Paradiso and Grand Saint Bernard nappes) (DAL PIAZ, 1974; COMPAGNONI *et al.* 1977; CARON, 1977, 1984; NISIO and LARDEAUX, 1987). Recently, the ophiolitic associations of the Western Alps were described as rocks formed in the Piedmont-Ligurian oceanic basin during Jurassic time (MESSIGA, 1987). They contain eo-Alpine HP-LT metamorphic assemblages of eclogite and/or blueschist facies, overprinted by a later Alpine re-equilibration in the greenschist facies (DAL PIAZ *et al.* 1972; OBERHAENSLI *et al.* 1982; CARPENA, 1983; NISIO and LARDEAUX, 1987; KUBOVICS and ABDEL-KARIM (1, 2), in press; ABDEL-KARIM and BILIK in press).

The metagabbro bodies of the Western Alps are either strongly metamorphosed, or partly preserved their igneous mineralogy and original relations with ultramafics, basalts and sedimentary sequences.

H—1088 Budapest, Múzeum krt. 4/a, Hungary.

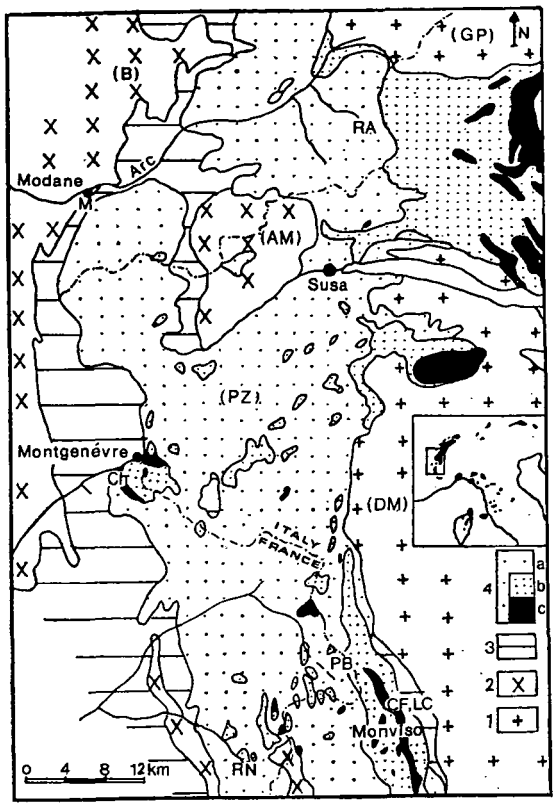

Fig. 1. Tectonic sketch map of the Internal Western Alps showing the location of the main ophiolite complexes. 1. Dora-Maire (DM) and Gran Paradiso (GP) continental units (European Paleomargin); 2. Vanoise, Ambin (AM) and Brianconnais (B) continental units (European Paleomargin); 3. Mesozoic epicontinental covers; 4. Piedmont Zones (PZ) Schistes Lustrés' nappe (Mesozoic, mainly oceanic material): a) undifferentiated metasediments with subordinate ophiolites, b) ophiolite complex with minor metasediments, c) metagabbro bodies.
Location of samples: Arc valley: RA) Refuge d'Averole, M) Modane; Monviso: PB) Petit Belvedere, CF: Colletto Fiorenza, LC: Lago Chiaretto, Montgenévre: CH) Chenaillet; RN) Roche Noire

The distribution of the gabbroic rocks in the Piedmont Zone is, as follows: (1) Large bodies associated with ultramafics and metabasalts in an ophiolite nappe (Eastern Piedmont unit) *(Fig. 1.)*. They derived from the oceanic crust and mantle of the Mesozoic Piedmont-Ligurian basin (BERTOLAMI and DAL PIAZ, 1970; DAL PIAZ and ERNST, 1978; LOMBARDO *et al.* 1978, LOMBARDO and POGNANTE, 1982) and display widespread eclogotic assemblages which are believed to reflect a late Cretaceous subduction (DAL PIAZ, 1974). (2) Smaller tectonic slices or olistoliths associated with metasediments in a westernmost composite unit (Western Piedmont unit) (BEARTH, 1967; DAL PIAZ, 1974; DIETRICH, 1980; LOMBARDO and POGNANTE, 1982) *(Fig. 1.)*. In this unit only blueschist facies assemblages were produced.

Other units, consisting of Ligurian-type sedimentary series and resting on ophiolite bodies are believed to have been formed in the fracture zone of the Piedmont-Ligurian ocean (LEMOINE, 1980).

Geological setting and primary features of metagabbros

Field study and sampling of the ophiolitic metagabbros were carried out from Arc valley in the north, Montgenévre in the central as well as Cristillan and Monviso in the south Piedmont zone *(Fig. 1.)*. Some of the gabbroic bodies partly escaped the Alpine deformation. Although the magmatic features of some bodies are similar, as a result of their different structural setting, different relationship between the gabbros and the other ophiolite members (peridotites, basalts and sediments) can be observed.

The *Arc metagabbros* from Zermatt-Saas zone have been collected in Modane and Refuge d'Averole between Ambin and Gran Paradiso units *(Fig. 1.)*. They represent heterogeneous metamorphic rocks and show strong effects of the Alpine deformation and all the magmatic minerals and structures are more or less oblite rated. (a) Refuge d'Averole metagabbros (greenschistic metagabbros) are situated in the east Arc valley, about 15 km North of Susa *(Fig. 1.)*. They are covered by metabasites (prasinites and ovardites) and overlying metaultramafics (serpentinites and metapyroxenites). They are schistose, flasered and porphyroblastic and usually variable in grain size. (b) Modane metagabbros (glaucophanites) are interposed between Mesozoic epicontinental covers and the western Piedmont zone, forming a small body enclosed in marble and gyps. They are massive, coarse-grained with appearance of gabbroic texture.

The *Chenaillet gabbroic sequence* (on the western side of the Alpine belt) is a part of the Montgenévre-unit which represents one of the best preserved ophiolite complexes in the W. Alps (BERTRAND *et al.* 1987). The primary structure and, in part, the primary mineral assemblage are well preserved. The gabbroic, ultramafic and basaltic rocks occur as separate tectonic units. The Chenaillet gabbroic sequence (130 m thick) has a typically Alpine-character with green cpx and whitish-green plagioclase. Grain size varies widely and sometimes is pegmatitic. They are separated from the pillow lavas by a shear zone which in some places contains serpentinite lenses. They finally differentiated into albitites.

The *Monviso rocks* were collected near Petit Belvedere (Guil valley, French Monviso) and Colletto Fiorenza and Lago Chiaretto (Italian Monviso) on the eastern side of the Alpine belt. The Monviso ophiolite represents a section of the Piedmont-Ligurian oceanic lithosphere and constitutes the most complete metamorphic ophiolite section in the Western Alps (KIENAST and MESSIGA, 1987). It shows four stages of metamorphism namely oceanic event, eclogitic, blueschist and greenschist facies metamorphism.

In the basement of the Monviso gabbroic sequence one can find the Dora-Maire unit and other metasediments. The tectonic contact (few m. thick) consists mainly of strongly sheared serpentinite and talc carbonate schist. Small bodies of ultramafics and layers of eclogitic Fe-gabbros occur within the isotropic metagabbros. The metagabbros exhibit a well developed foliation consisting of bright-green phenoclasts of smaragdite (Cr-omphacite) up to 2 cm length. They sometimes occur within the eclogitic sequence (few cm — few dm thick). The eclogitic metagabbros which are strongly retrogressed mostly consist of greenschist facies mineral assemblage. Some relics of the original pegmatoid gabbroic structure are preserved within the mylonitic foliation of the layered eclogites. Some gabbroic (smaragditic) rocks are crosscut by fine grained greenish coloured metabasalt dykes (several dm thick).

The *Roche Noire metagabbros* (Cristillan) occur in one of the small ophiolitic bodies enclosed in the calcschists found in the southern Piedmont nappe, internal Western Alps *(Fig. 1.)*. They are usually composed of big blocks and crosscut by

TABLE 1

Main petrographic features of representative rocks from Western Alps metagabbros

Rock name	Texture	Main primary minerals (magmatic and late-stage magmatic)	Main secondary minerals (hydrothermal and metamorphic)	Metamorphic facies	Possible primary rock
		1.1. Arc valley; Refuge d'Averole			
(a) Chl-actin metagab.	porph, poikil, nemato, flas		actin-trem, chl, ab, clinoz, ep, leuc, cc	greensch. f.	Mg—Al gab.
(b) Clinoz-chl metagab.	poikil, she		chl, clinoz, actin, trem, ab, gar, tit	greensch. f.	Mg—Al gab.
		1.2. Arc valley; Modane			
Glaucophanite	fibro, nemato		rut. glau, ep, chl, ab, bio, white mi, law, qz, cros	glau. sch. — greensch. f.	Fe—Ti gab.
		2.1. Montgenèvre; Chenaillet			
(a) Talc-serp-gab.	hypid	cpx, pl	trem, serp, talc, preh	greensch. f.	Mg—Al gab.
(b) Chloritized metagab.	hypid	pl	chl, ep, preh, tit	greensch. f.	Mg—Al gab.
(c) Cpx. metagab.	flas, hypid	cpx, pl, Fe-oxide	amp, ep, clinoz, chl	greensch. f.	Mg—Al gab.
(d) Leucogab.	hypid	pl	ep, zo, preh, chl	greensch. f.	Fe-gab.
(e) Albitite	hypid, gran	olig, qz, hb	chl, ep, ab	greensch. f.	plagiogr.
		3.1. Monviso; Petit Belvedere (Guil valley)			
(a) Corund cumm. gab.	pseudoph, sch	pl	Corund, cumm, preh, chl, white mi	glau. sch. —	Mg—Al gab.
(b) She. cpx. metagab.	oph, she, kink	cpx, ap	trem-actin, ep. leuc, cc, preh, glau	greensch. f.	Mg—Al and Fe—Ti gab.
		3.2. Monviso; Colletto Fiorenza			
(a) Smaragdite metagab.	porph	cpx	Cr—omp, trem, jad, talc, ab, qz, chl, gar, tit	eclogite--greensch. f.	Mg—Al gab.
(b) Eclogitic metagab.	porph	cpx	omp, trem, zo, gar, qz, tit, blue amp, phen	eclogite f.	Fe—Ti gab.
		4.1. Cristillan valley; Roche Noire			
Hb-metagab.	hypid, sch	pl, hb	ep, trem, chl	amph?-greensch. f.	Fe—Ti gab.

Abbreviations: cpx=clinopyroxene; jad=jadeite; omp=omphacite; amp=amphibole; cumm=cummingtonite; glau=glaucophane; cros=crossite; trem-actin=tremolite-actinolite; hb=hornblende; ep=epidote; clinoz=clinozoisite; zo=zoisite; chl=chlorite; preh=prehnite; cc=calcite; ap=apatite; leuc=leucoxene; rut=rutile; tit=titanite; bio=biotite; mi=mica; phen=phengite; gar=garnet; law=lawsonite; ab=albite; olig=oligoclase; qz=quartz; pl=plagioclase; porph=porphyroblastic; poikil=poikiloblastic; nemato=nematoblastic; fibro=fibroblastic; flas=flaser; hypid=hypidiomorphic; oph=ophitic; pseudoph=pseudoophitic; interg=intergranular; she=sheared; gran=granoblastic; sch=schistose; gab=gabbro; amph=amphibolite; greensch=greenschist; glau. sch=glaucophane schist; f=facies; plagiogr=plagiogranite

basalt dykes. The small fragments of gabbros and minor basalt in a matrix of the same materials are usually composed of an ophiolitic breccia. These gabbros are coarse-grained, massive, banded and whitish-green in colour. They appear to be overprinted by amphibolite facies.

Mineralogy and petrography

The primary (magmatic and late-stage magmatic) as well as the secondary (hydrothermal and metamorphic) mineral assemblages and textures are summarized in Table 1. The metamorphic evolution and some petrographic features are given in Table 2.

TABLE 2

Metamorphic evolution of the Western Alps ophiolitic metagabbros

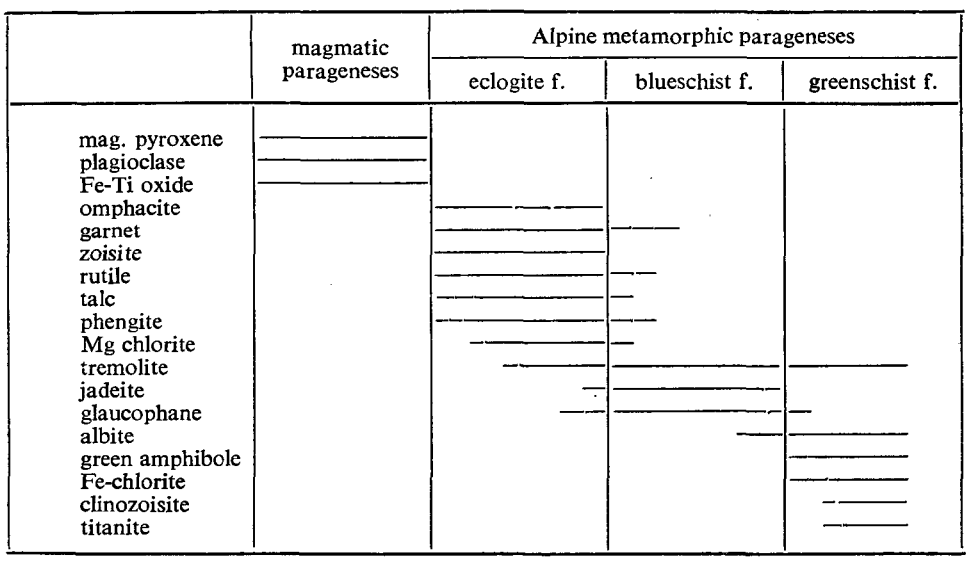

1.1. Two varieties of metagabbros in greenschist facies have been recorded in the Piedmont zone from Refuge d'Averole (Arc), French Western Alps:

(a) *Chlorite actinolite metagabbros* show large crystals (5—7 mm long) of actinolitic amphibole (pseudomorph after magmatic pyroxene) which in turn enucleated aggregates of actinolite. The granoblastic matrix consists of albite, epidote-clinozoisite, chlorite, actinolite-tremolite *(Fig. 2.)* and minor titanite-leucoxene and calcite (Table 1.). The albite (25.1 v%*) forms anhedral crystals, sometimes contains epidote, clinozoisite, tremolite and titanite as inclusions. The chlorite (23.8 v%) is rich in Mg and replaced the former olivine (?). The epidote-clinozoisite (20 v%) is strongly pleochroic and is embedded in a chloritic matrix. The actinolite-tremolite (30.8 v%) replaced the former pyroxene and sometimes altered to chlorite. Leucoxene/titanite is usually associated with epidote. Fine grains of calcite replaced the plagioclase.

* v%: volume per cent.

TABLE 3

Trace element composition of some gabbroic rocks from the Western Alps ophiolites (in ppm)

Locality	Arc valley (Refuge d'Averole)		Monviso (Petit Belvedere)				Montgenevre (Chenaillet)			
Rock name	Greenschist metagabbros		Corund cumm. gab.	Sheared cpx metagabbros			Cpx metagabbro	Ferrogabbro	Albitites	
Sample No. Symbol	1▲	2▲	3▲	4▲	5■	6●	A (9)■	B (4)●	9 ×	C (7) ×
Be	1	<1	<1	<1	<1	<1	—	—	21	—
Sc	27	32	5	26	34	75	33.8	51	2	0.7
Rb	3.2	3.8	14.1	2.9	<4	<4	<4	<4	<2.5	<4
Sr	330	157	110	172	390	420	233	383.7	10	79.6
Y	20	8	<2	21	35	150	22.5	69	224	215.8
Zr	70	29	8	72	290	320	187.5	152.5	465	815.5
Nb	4	2	4	2	8	6	3	3.5	16	22.8
Ba	688	579	739	718	27	80.5	25	70.3	89	30.8
La	10	<10	16	11	20	35	<12	45.8	40	13
M.I.	0.4	0.32	0.24	0.38	0.45	0.71	0.38	0.69	0.71	0.48

▲: Mg—Al metagabbros; ■: altered (intermediate) metagabbros; ●: Fe—Ti metagabbros; × = albitites A, B, and C: average of samples, after Bertrand et al. (1987)

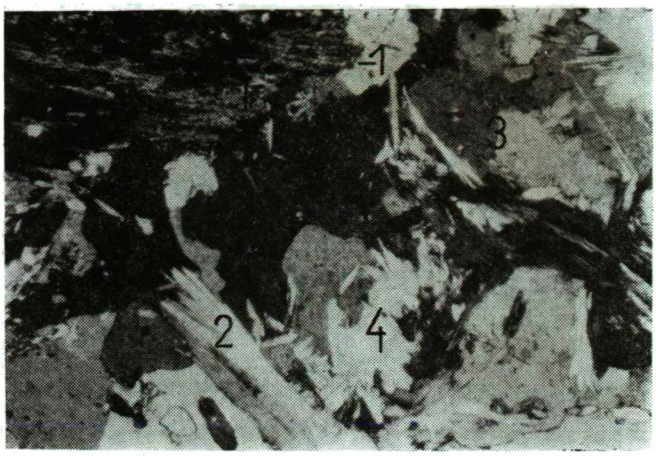

Fig. 2. Photomicrograph of chlorite actinolite greenschist metagabbros from Refuge d'Averole (Arc valley) W. Alps showing the pseudomorphic replacement of pyroxene (1) by actinolite (2) and the growth of albite (3) and tremolite (4) C. N., X = 50

b) The primary textures in the *clinozoisite chlorite metagabbros* have nearly adpTpeared, and from the primary minerals only relics of clinopyroxene are preserved. egy(s are composed of Mg-chlorite, clinozoisite-epidote, albite, actinolite-tremolite, harnet and minor titanite and iron oxide. The Mg-chlorite (30 v%) probably replaced former olivine (?), while the clinozoisite-zoisite (37 v%, up to 2—5 mm long) with characteristic zonation and anomalous blue-grey interference colour, replaced the former plagioclase. They contain fine grains of garnet and titanite. The actinolite - tremolite (10.5 v%) mostly replaced the former pyroxene. Interstitial albite (9.7 v%, 0.4—1.8 mm across) and chloritized garnet (8.5 v%) were determined, too.

1.2. In the *glaucophanites,* collected near Modane (Arc), the primary pyroxene is completely replaced by glaucophane-crossite, chlorite and albite; with large amounts of rutile-leucoxene and minor jadeite, biotite, phengite, lawsonite and quartz *(Fig. 3.)*. The glaucophane (43 v%) preserved the shape of the former pyroxene-crystals and sometimes is associated with crossite. It is often rimmed by actinolite. The Fe-rich chlorite (18.2 v%) occurs as aggregated matrix *(Fig. 3.)*. Fe-rich epidote and scarce lawsonite (5.9 v%) form euhedral prisms usually embedded in the matrix. The albite (12 v%) is sometimes replaced by calcite. Rutile-leucoxene (12.2 v%, 4.2—5.2 mm) is rarely transformed to titanite. Biotite is Ti-rich, usually grew along chlorite edges. The jadeite (2.3 v%) is partially replaced by chlorite and glaucophane, while phengite were only locally observed.

2. The Chenaillet metagabbros (Montgenévre ophiolite) have a complete gabbroic sequence (Table 1.), that are;

(a) *Talc serpentine gabbros* mainly consist of olivine, clinopyroxene and plagioclase with minor tremolite, serpentine, talc and prehnite (Table 1.). The augitic clinopyroxene (40.6 v%) is moderately replaced by tremolite and chlorite. Olivine is replaced by serpentine and talc *(Fig. 4.)*. The bytownitic plagioclase (An_{85-95}, 24.5 v%) is often traversed by veinlets of serpentine and is transformed to prehnite. Serpentine (20 v%) is often replaced by talc (14.6 v%, *Fig. 4.*).

(b) *Chloritized metagabbros* essentially consist of plagioclase and chlorite, with epidote, titanite and prehnite as only accessory minerals. The plagioclase

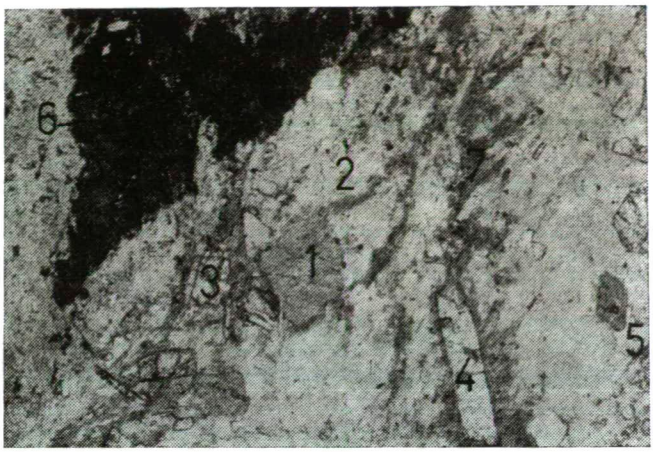

Fig. 3. Photomicrograph of glaucophanite from Modane (Arc valley) W. Alps showing the replacement of the former clinopyroxene by single crystal of glaucophane (1), chlorite (2) and epidote (3) +/− lawsonite (4) +/− quartz (5), and usually associated with leucoxene (6) Ti-biotite (stilpnomelane, 7) grew along the chlorite edges, P. P., X=44

Fig. 4. Photomicrograph of talc serpentine gabbro from Chenaillet (Montgenévre) W. Alps showing the replacement of olivine by serpentine (1) and talc (2); clinopyroxene (3) and plagioclase (4) by chlorite (5). C. N., X=50

(40.7 v%) is of magmatic origin, which survived metamorphism and is commonly deformed and transformed to epidote, kaoline, prehnite and chlorite. Chlorite (52 v%) formed single pseudomorphs after magmatic pyroxene. Epidote (6.3 v%) replaced the plagioclase or is embedded in chlorite. Titanite is enclosed in chlorite, particularly along cracks and grain boundaries. Prehnite is also embedded in the plagioclase.

(c) The *clinopyroxene gabbros* are mainly made up of magmatic clinopyroxene (diallage) and plagioclase. Amphibole, epidote-clinozoisite, chlorite and iron oxide are subordinate constituents. The diallage (48 v%) usually show kink-band defor-

mation, and is partially transformed to hornblendic and actinolitic amphibole and, rarely to chlorite. The plagioclase (38.5 v%) changed into albite and epidote-clinozoisite. Amphiboles (8.5 v%) are represented by actinolite and hornblende. The Mg-Fe rich chlorite (4.2 v%) usually forms pseudomorphs after pyroxene and is associated with iron oxides.

(d) The *leucogabbros* are composed of hypidiomorphic plagioclase with subordinate epidote, zoisite, prehnite and chlorite. The bytownitic (An_{80-85}) plagioclase (more than 90 v%, *Fig. 5.)* is always transformed to epidote, zoisite and prehnite. The last three minerals usually fill the cracks and cavities of the leucogabbros.

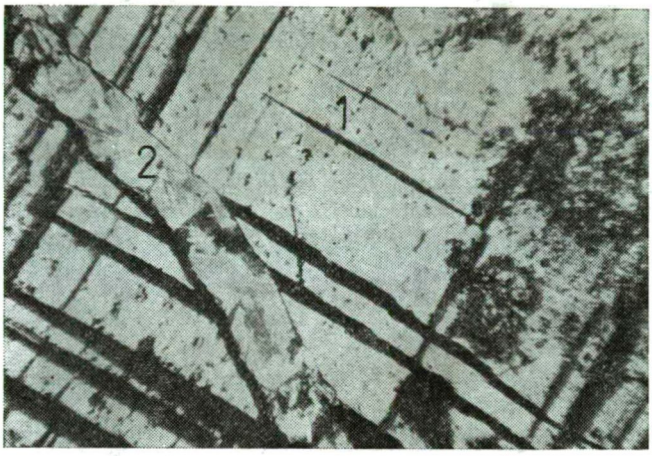

Fig. 5. Photomicrograph of leucogabbro from Chenaillet (Montgenévre), W. Alps showing the dislocated twinned labradorite (1) with several glide planes. The cracks in the rock are occupied by prehnite, epidote and zoisite (2). C. N., X=44

(e) *Albitites* are considered to be final products of the differentiation processes in the gabbroic magma at Chenaillet. They consist mainly of oligoclase-albitic plagioclase (94.8 v%), and minor amphibole, quartz, biotite and chlorite *(Fig. 6.)*. Epidote and titanite are accessories (Table 1.). The plagioclase is cataclastically deformed and included fine grains of other minerals. Hornblende (3 v%), quartz (0.7 v%) were also determined. Biotite (0.6 v%) and pale green chlorite are also present.

3. The Monviso metagabbros have the following petrographic features (Table 1.):

3.1. (a) In the *corund cummingtonite gabbros* which were collected in Petit Belverede (French Monviso) the primary magmatic minerals (plagioclase) are plastically deformed and tectonized *(Fig. 7.)*. Prehnite, chlorite and white mica are the main accessories.

The cummingtonite (64.3 v%, 2.1—3.4 mm long) usually contains fine grains of plagioclase, sometimes is transformed into white mica, chlorite and/or prehnite. The anorthitic plagioclase (An_{85-95}, 14.4 v%) is frequently replaced by prehnite. Corund (2.2 v%) usually appear in thin layers (1 mm thick). The matrix (19.2 v%) consists of fine grained prehnite, white mica and Mg-chlorite.

(b) *Sheared clinopyroxene metagabbros* are either massive or layered and display rapid grain size variations from fine to pegmatoid varieties. From the primary mine-

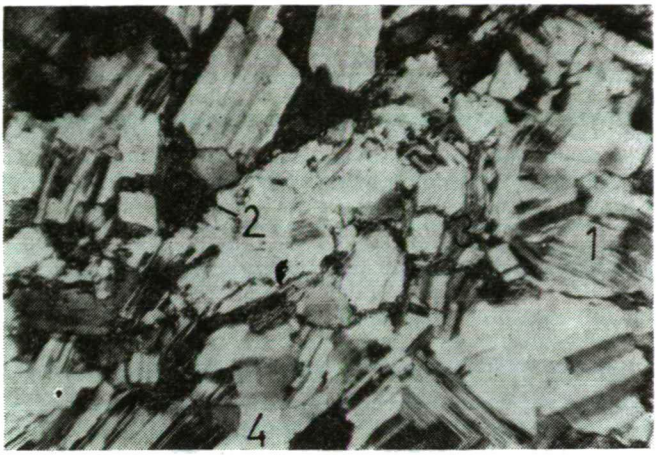

Fig. 6. Photomicrograph of albitite from Chenaillet (Montgenévre) W. Alps showing the cataclastically deformed twinned plagioclase (1) hornblende (2), biotite (3) and quartz (4) giving rise to granitic texture. C. N., X=44

Fig. 7. Photomicrograph of corund-cummingtonite metagabbros (Monviso), W. Alps showing oriented and plastically deformed corund (1), cummingtonite (2) and plagioclase (3). C. N., X=44

rals only cpx could remain. They consist of cpx, plagioclase and tremolite-actinolite as well as scarce hornblende and glaucophane. Some epidote, clinozoisite, leucoxene, calcite, prehnite and apatite are also present. The augite-diallage clinopyroxene (37.5 v%) occur in two generations *(Fig. 8.)*. There are magmatically resorbed augite on the one hand and strongly sheared, deformed and kink-banded diallage on the other hand. They are always rimmed by hornblendic amphibole *(Fig. 8.)*. The plagioclase (54 v%) is replaced by epidote, clinozoisite, albite and calcite or greenish masses of prehnite, chlorite and albite. The amphiboles (8.5 v%) are usually derived from clinopyroxene. They consist of older blue glaucophane which were subsequently replaced by tremolite-actinolite. Later, the tremolite-actinolite was replaced by

Fig. 8. Photomicrograph of sheared clinopyroxene metagabbro from Petit Belvedere (French-Monviso), W. Alps showing two generations of clinopyroxene (1 and 2) replaced by tremolite-actinolite along the rim and cleavage plane (3). The plagioclase is replaced by albite and saussurite (4). C. N., X = 50

actinolite or hornblende. Leucoxene-titanite can be derived from ilmenite, and calcite from plagioclase.

3.2. (a) In the *smaragdite metagabbros* from Colletto Fiorenza a well developed foliation can be observed: in whitish matrix, bright-green phenoclasts of smaragdite occur. They consist of Cr-omphacite phenoclasts (14 v%), which are embedded in a fine matrix of zoisite, jadeite, garnet, Mg-chlorite, talc, rutile or retrograde products such as albite, tremolite-actinolite, Fe-chlorite, clinozoisite-epidote, quartz and titanite. The magmatic clinopyroxene (diopside) is replaced by single crystals of Cr-omphacite and/or tremolite and/or talc ("-smaragdite") or by aggregates of fine-grained omphacite. Tremolite (7 v%) and plagioclase (totally transformed to jadeite, albite, Mg-Fe chlorite and zoisite) are usually enclosed in the matrix. The olivine is also completely altered to talc and/or tremolite.

(b) *Eclogitic metagabbros* from the same locality originally make up of porphyroclastic omphacite (pseudomorphs after cpx) enclosed in a matrix of tremolite, zoisite, fine-grained omphacite, garnet, rutile and accessory apatite, quartz and titanite. Phenoblasts of blue amphibole and phengite locally were also found. The rock is strongly retrogressed and mostly consists of greenschist facies mineral assemblages. During retrograde processes omphacite was usually replaced by tremolite and Mg-Fe chlorite along their margins and cleavages. The plagioclase is completely altered to albite and/or epidote-clinozoisite and/or chlorite. Porphyroblasts of glaucophane-crossite (up to 11 mm long) and sometimes phengite (0.5 mm long) are embedded in the matrix. Fine grains of garnet (up to 0.3 mm across) are partly resorbed and altered to chlorite. Very fine grains of fresh quartz are usually enclosed in the matrix.

4. The gabbroic rock from Roche Noire (Cristillan) are mainly hornblende gabbros. They generally consist of hornblende and plagioclase (Fig. 9.) with minor epidote/clinozoisite, tremolite, chlorite and titanite (Table 1.). The hornblende (63 v%) is usually replaced by tremolite or chlorite. The andesinic (An_{35-45}) plagioclase (31.0 v%) is partly replaced by epidote/clinozoisite and kaoline *(Fig. 9.)*. It is cracked, the cracks are filled by titanite, epidote/clinozoisite and chlorite.

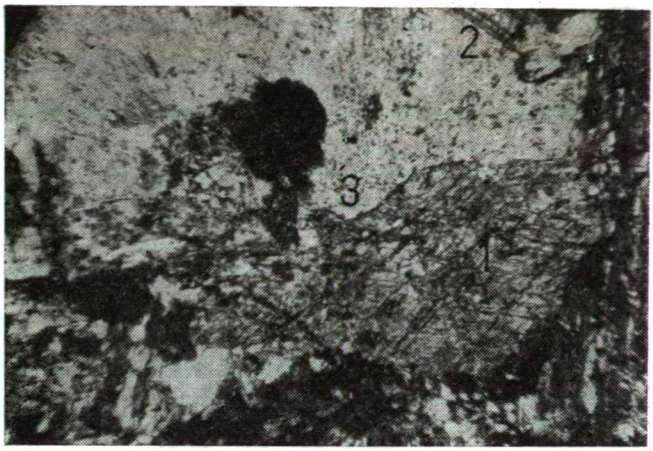

Fig. 9. Photomicrograph of hornblende gabbro from Roche Noire (Cristillan), W. Alps showing the abundance of hornblende (1) with variable size. Plagioclase (2) is partly transformed into kaolin and epidote (3). C. N., X=44

PETROGENESIS

Trace element composition (Table 3.) and their variations against MI $[FeO^+/(FeO^+ + MgO)]$, *(Fig. 10.)*, as well as Zr and Y *(Fig. 11.)* are consistent with mineral and textural evidences for most gabbroic rocks.

Trace element analyses for Be, Sc, Y, Zr, Nb and La have been quantitively carried out by optical atomic spectrographical method (Model PGS, Zeiss Jena) and for Rb, Sr and Ba by atomic absorption spectrophotometric method (Model AA. 475 Varian).

According to the chemical as well as mineralogical composition, these gabbroic rocks can be separated into Mg-Al metagabbros, altered (intermediate) metagabbros and Fe-Ti metagabbros (ABDEL-KARIM and BILIK, in press).

Since the gabbros result mostly from cumulate liquidus phases plus variable amounts of trapped liquid, their composition will not define a liquid line-of-descent, but would only provide a rough idea on fractionation processes of the parental magma (POGNANTE *et al.*, 1982). The evolutionary trends shown in diagrams *(Fig. 10.* and *11.)* indicate their enrichment in Sc, Zr, Y, La and Y/Sc during differentiation.

The early stages of crystallization are characterized by segregation of pl, cpx, Mg-olivin which produced large amount of Mg-Al rich gabbros, indicating little fractionation. The results are consistent with a more primitive nature of the magma. They appear to have occurred under low fO_2 conditions. The rather erratic variation of Sr and Ba should be an effect of post-magmatic transformations.

The later stages of crystallization producing Fe-Ti-rich gabbros probably occurred in relatively rather oxidative condition. Processes producing a peculiar partition of Zr into the more SiO_2-rich liquid may have accompanied this differentiation (POGNANTE *et al.*, 1982). Geochemical data show high Zr, Sc and Y contents

FeO^+ = total iron as FeO.

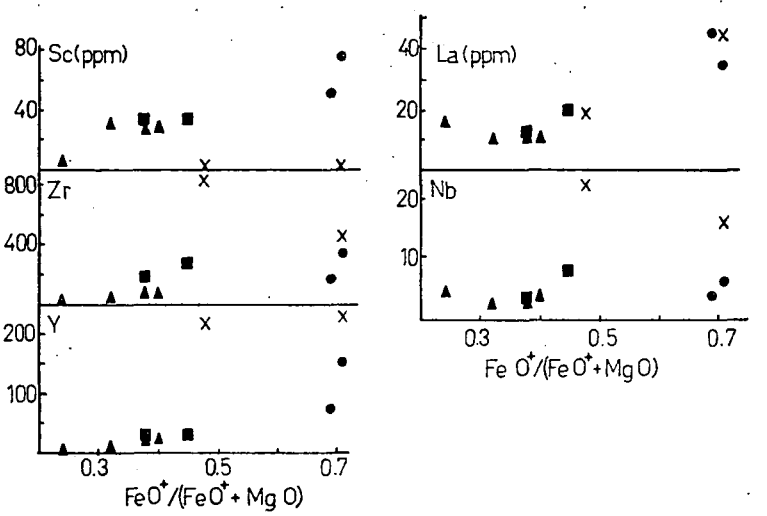

Fig. 10. Some trace elements variation diagrams vs. MI[$FeO^+/(FeO^+ + MgO)$ ratio] in the gabbroic rocks from W. Alps ophiolites. (Symbols as in table 3)

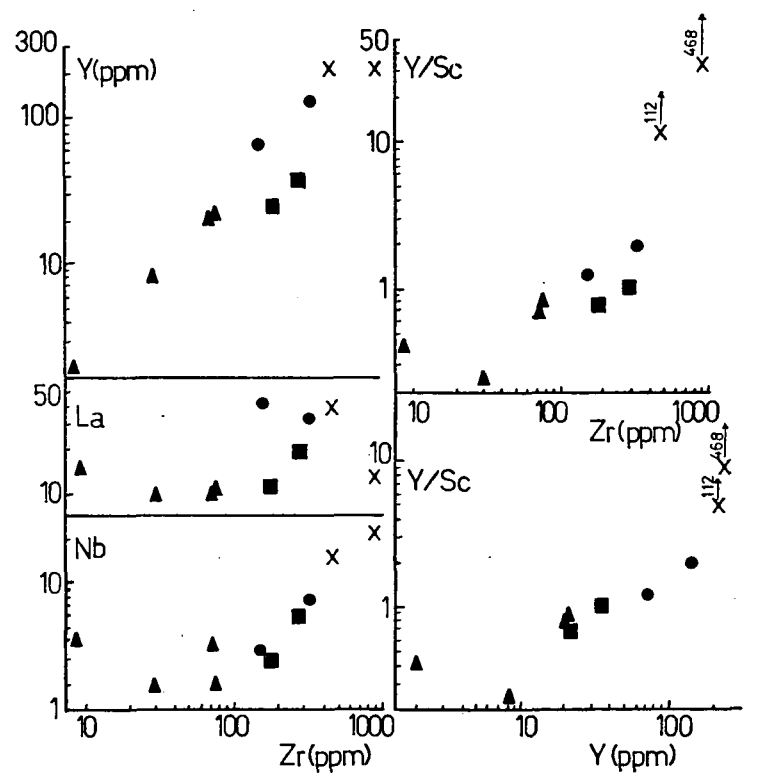

Fig. 11. Y, La and Nb vs. Zr and Y/Sc ratio vs. Zr and Y diagrams showing the evolution trend of the gabbroic rocks from W. Alps ophiolites. (Symbols as in table 3)

indicating that they are highly differentiated with abundant amphibole and Fe-Ti oxides. Higher contents of Ba and La might be attributed to their enrichment in the evolved melt or to later hydrothermal activity.

The albitites from Chenaillet show very high concentration of Be, Nb, Y and Zr supporting the idea of their crystallization from late differentiated melts. Low Sc, Ti, Mn and Ba values are also consistent with this interpretation.

Similar processes and evolution trends have been discussed for gabbroic and basaltic rocks from Lanzo and Montgenevre (POGNANTE *et al.*, 1982; BERTRAND *et al.*, 1987).

CONCLUDING REMARKS

The Piedmont Zone of the Western Alps consists of metamorphic dismembered ophiolite bodies and their Mesozoic metasedimentary cover.

I. In the eastern Piedmont Zone, two of the most significant ophiolitic metagabbros with eclogitic overprint were studied. They are from south to north:

1. The *Monviso metagabbros* can be characterized by prograde glaucophane and eclogite and retrograde glaucophane and greenschist facies metamorphism. The eclogitic stage produced dominantly Na-cpx, garnet, Mg-epidote, Mg-chlorite, rutile$\pm$talc$\pm$white mica$\pm$tremolite paragenesis. During the retromorphism in smaragdite metagabbros (Mg-Al rich metagabbros) and eclogitic metagabbros (Fe-Ti metagabbros), Cr-omphacite pseudomorphosed after magmatic cpx; jadeite, albite and zoisite after plagioclase; Mg-chlorite$\pm$tremolite$\pm$talc after cpx and olivine.

The sheared cpx metagabbros (Mg-Al and Fe-Ti metagabbros) are characterized by the presence of magmatic cpx in two generations. The cpx is altered to hornblende indicating ocean floor metamorphism.

Some gabbroic rocks have partially escaped the Alpine metamorphism. They show magmatic clinopyroxene, amphibole and plagioclase which are plastically deformed with preferred orientation.

2. The *Arc metagabbros* consist of two greenschist-facies metagabbroic body. They are considered as Mg-Al metagabbros.

II. In the western Piedmont Zone, three metagabbroic bodies were studied (from north to south):

1. *Arc glaucophanites* (Fe-Ti metagabbros) that partly retrogressed into greenschist facies (green amphibole grew around blue amphibole; titanite/leucoxene after ilmenite; chlorite after jadeite, biotite after white mica).

2. *Chenaillet metagabbros* are well preserved gabbroic bodies ranging from talc serpentine metagabbros (Mg-Al rich) to leucocratic gabbros (Fe-Ti metagabbro) and albitite. In these gabbros olivine is replaced by tremolite-actinolite and chlorite; plagioclase is transformed to albite and saussurite. Fe-Ti oxide appear as leucoxene/titanite assemblage. Cpx is rimmed by hornblende which has in turn been overgrown by actinolite.

3. *Cristillan metagabbros* (Fe-Ti rich) show an amphibolite facies overprint, in which the plagioclase and hornblende are the dominant minerals.

These gabbros can probably be regarded as separated differentiated rocks derived from different magma sources at different times, in different geotectonic environments that subsequently suffered different types of metamorphism.

During the early stage of crystallization plagioclase, cpx$\pm$Mg-olivine produced Mg-Al rich gabbros which characterized the primitive magma. They have low Zr, Sc and Y contents, and were probably formed under low fO_2 condition.

The later stage of crystallization producing Fe-Ti rich gabbro is characterized by more oxidative conditions, abundance of amphibole and Fe-Ti oxide and higher Zr, Sc and Y content with more signs of differentiation.

In some places, the late differentiated melts of gabbros produced albitites, which are also consistent with this interpretation.

REFERENCES

ABDEL—KARIM, A-A. M., I. BILIK: Geochemistry of Mg-Al rich, Fe-Ti rich metagabbros and albitites from the Western Alps ophiolites. Acta Geol. Hung. (in press)

BEARTH, P. (1967): Ophiolite der zone von Zermatt-Saas fee. Beitr. Geol. Karte Schweiz. **132,** p. 130.

BERTRAND, I., V. DIETRICH, P. NIEVERGELT, M. VUAGNOT (1987): Comparative major and trace element geochemistry of gabbroic and volcanic rock sequences, Montgenévre ophiolite, W. Alps. Schweiz. Mineral. Petrogr. Mitt. **67,** 147—169.

BERTOLAMI G., G. V. DAL PIAZ (1970): Il substrato cristallino del l'anfiteatro meronico di Rivoli-Avigliana (Prov. Torino). Mem. Soc. Ital. Sci. Nat. **18,** 125—169.

CARON, J. M. (1977): Evolution paléogéographique et tectonique de la zone piemontaise dans les Alps Cottiennes. Bull. Soc. Géol. Fr. **7, 19/4,** 893—899.

CARON, J. M. (1984): The diversity of geodynamic regimes leading to HP-LT metamorphism (W. Alps and Corsica). Terra Cognita. **4,** 39—43.

CARPENA, J. (1983): Ophiolite fission track ages in the French Occidental Alps. Terra Cognita. **3, 2—3,** 183.

COMPAGNONI, R., G. V. DAL PIAZ, J. C. HUNZIKER, G. GOSSO, B. LOMBARDO, P. F. WILLIAMS (1977): The Sesia-Lanzo Zone, a slice of continental crust with Alpine HP-LT assemblages in the W. Italian Alps. Rend. Soc. It. Min. Petr. **33,** 281—334.

COMPAGNONI R., J. R. KIENAST, B. LOMBARDO (1988): The Monviso eclogitic meta-ophiolite (Cottian Alps); in the IGCP 235 Excursion to the Alps; HP eclogitic re-equilibration in the W. Alps, Part 1. 81—112.

DAL PIAZ, G. V., J. C. HUNZIKER, G. MARTINOTTI (1972): La zona Sesia-Lanzo e l'evoluzione tectonico-metamorfica della Alpi nordoccidentali internce. Mem. SGI. 11, 433—466.

DAL PIAZ, G. V. (1974): Le métamorphisme eoalpine de haute pression et basse température dans l'evolution structurale du bassin ophiolitique alpino-apenninique. 1. Considérations paléogéographiques. Boll. Soc. Geol. It. **93,** 437—468.

DAL PIAZ, G. V., W. G. ERNST (1978): Areal geology and petrology of eclogites and associated metabasites of the piemonte ophiolite nappe, Brueil, st. Jacques area, Italian W. Alps, Tectonoph. **51,** 99—126.

DIETRICH, V. J. (1980): The distribution of ophiolites in the Alps. Ofioliti, special issue: Tethyan ophiolites. **1,** 7—51.

KIENAST, J. R., B. MESSIGA (1987):: Cr-rich chloritoid, a first record in HP metagabbros from Monviso (Cottian Alps), Italy. Min. Mag. **51,** 681—687.

KUBOVICS, I., A-A. M. ABDEL-KARIM: Petrology of some HP-metavolcanics from Piedmont Zone, Western Alps. Acta Geol. Hung., in press.

KUBOVICS, I., A-A. M. ABDEL-KARIM: Geochemistry of some HP-metavolcanics from the Western Alps ophiolites. Acta Miner-Petr., Szeged, in press.

LEMOINE, M. (1980): Serpentinites, gabbros and ophicalcites in the Piemonte-Ligurian domain of the W. Alps: possible indicators of oceanic fracture zones and of associated serpentinite protrusions in the Jurassic-Cretaceous Tethys. Intern. symp. on tectonic inclusions and associated rocks in serpentinites, Geneve, 1979. Arch. Sci. Genéve. **33,** 103—115.

LOMBARDO, B., R. COMPAGNONI, B. MESSIGA, J. R. KIENAST, C. MEVEL, L. FIORA, G. B. PICCARDO, R. LANZA (1978): Osservazioni preliminari sulle ofioliti metamorfiche del Monviso (Alpi occidentali). Rend. Soc. It. Min. Petrol. **42, 2,** 253—305.

LOMBARDO, B., U. POGNANTE (1982): Tectonic implications in the evolution of the W. Alps ophiolite metagabbros. Ofioliti. **2/3,** 371—394.

MARTIN, R. F. (1984): Patterns of albititization in the Montgenévre ophiolite, W. Alps. Bull. Minéral. **107,** 345—356.

MESSIGA, B. (1987): Alpine metamorphic evolution of Ligurian Alps (N-W. Italy): chemography and petrological constraints inferred from metamorphic climax assemblages. Contrib. Mineral. Petrol. **95,** 269—277.

MONVISO (1980): The Monviso complex. In Panayiotou A. (Ed.), Ophiolite, Proceed. Intern. Ophiol. Symp. Cyprus. **1979**, 332—340.
NISIO, P., J. M. LARDEAUX (1987): Retromorphic Fe-rich talc in Low-T eclogites: example from Monviso (Italian W. Alps). Bull. Mineral. **110**, 427—437.
OBERHAENSLI, R., J. C. HUNZIKER, G. MARTINOTTE, W. STERN (1982): Mucronites an example of eo-Alpine eclogitisation of Permian granitoids. Terra Cognita. **3**, 325.
POGNANTE, U., B. LOMBARDO, G. VENTURELLI (1982): Petrology and geochemistry of Fe-Ti gabbros and plagiogranites from the Western Alps ophiolites. Schweiz. Min. Petr. Mitt. **62**, 457—472.

Manuscript received, 4 November, 1989

Acta Mineralogica-Petrographica, Szeged, XXX, 35—54, 1989

COMPARATIVE PETROLOGY AND GEOCHEMISTRY OF HIGH-PRESSURE METAMORPHIC ROCKS FROM EASTERN CUBA AND WESTERN ALPS

I. KUBOVICS, J. ANDÓ, GY. SZAKMÁNY

Department of Petrology and Geochemistry, Eötvös University

ABSTRACT

The paper deals with HP metamorphic rocks from E-Cuba in the surroundings of Holguin. Thes rocks are mainly eclogitic which occur in blocks of different size in serpentinite along with other oceanic and island arc type rocks. The eclogitic rocks are mainly of oceanic type, related to subduction. The rocks underwent greenschist facies retrogression followed by metasomatism during their tectonic evolution. Chemical and REE analyses were applied in geochemical studies of these rocks. Garnet, pyroxene and amphibole compositions were measured by electron microprobe, and the results were compared with the data of the well-known HP rocks of W-Alps obtained from the literature. On the basis of the analytical results it has been concluded that the eclogitic rocks of E-Cuba were ophilitic, regarding their origin, which underwent high rpessure conditions during subduction. The retrogression can be related to obduction and overthrusting which are due to an uplift caused by a new subduction. The geochemical features of the eclogitic rocks E-Cuba allow us to interpret the petrologic processes the same way as it was done in the case of the W-Alps.

OUTLINE OF GEOLOGY OF CUBA AND GEOLOGICAL SETTING OF THE METAMORPHIC ROCKS FROM WESTERN ALPS

The geological evolution and the present geographic location of Cuba within the Caribbean intercontinental sea are the results of crustal evolution processes which acted between the end of Lower Cretaceous and the Palaeogene. Plate tectonic reconstructions (DIETZ and HOLDEN, 1970) indicate that the oceanic crust of the region have been formed durint Late Jurassic time, as a western extension of the Tethys Sea. After a while the connection between the two regions was ceased due to the opening of the Atlantic Ocean. However, the structural evolution, geology and petrology of the two areas display several similar characters, like rocks of the ophiolite association, and the closely related eclogites and eclogite-derived metamorphites. Their comparative investigation, and the interpretation of the analogous Alpine formations may provide clues for the understanding of the position of the similar Cuban metamorphites.

The geology and structure of Cuba is shown by the latest, 1:500 000 geological and tectonical maps based on the geosyncline principle, but applying certain elements of plate tectonics (1985, 1986). The latest study, based on plate tectonics, was published by ITURRALDE—VINENT (1988).

Definite zonality can be recognized in the geology of Cuba *(Fig. 1)*. Along the northern shores there are outcrops of carbonatic-evaporitic formations of the Bahamian platform. To the south there are terrigenous-carbonatic and siliceous formations (Upper Jurassic — Lower Cretaceous) deposited on the continental slope.

H—1088. Budapest, Múzeum krt. 4/a.

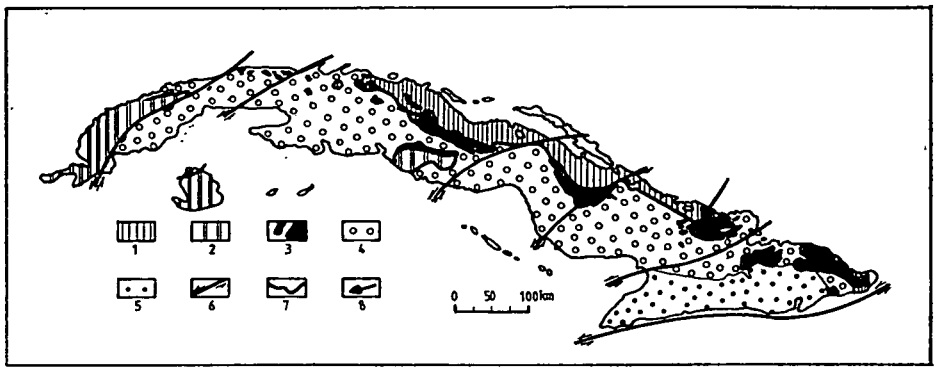

Fig. 1. Geological map of Cuba without Cenozoic cover. Legend: 1. Sedimentary formations of the Bahama Platform and its southern continental slope (J_3—K_1). 2. Terrigenous clastic and carbonate rocks metamorphosed to different grades (J—K_1). 3. Ophiolite association. 4. Cretaceous volcanic arc. 5. Palaeogene volcanic arc. 6. Fault. 7. Thrust zone. 8. Localities of the discussed metamorphic rocks. (After ITURRALDE—VINENT, 1988, simplified)

There are Jurassic, terrigenous clastic and Upper Jurassic — Lower Cretaceous terrigenous-carbonatic-siliceous formations, covering extensive regions in the western part of Cuba, in some isolated outcrops along the southern shores (Isla de Juventud, Escambray Mountains) and in the easternmost zones. The sediments of the continental platform and that of the intracontinental sea have suffered different degrees of metamorphism.

The ridge of the island is formed by a northern Mesozoic ophiolite belt and a southern, Cretaceous island arc, partly mixed with the former one, forming melange.

In the southern part of Eastern Cuba there are volcanic rocks of a younger, Palaeogene island arc sequence. The uplift of the ophiolites to teh surface, and their overthrust on the northern foreland together with the island arc occurred during Late Cretaceous time.

The eclogitic formations are always connected to the ophiolites, i.e. to the serpentinites and the ophiolite melange, in the form of minor blocks or lenses. Besides the investigated occurrence at Holguin, these are known from Central and Western Cuba and from the Escambray Mountains.

The eclogite facies metamorphites of the Western Alps occur along an arc between the Po Plain and the Voltri Massif in several tectonic units *(Fig. 2)*. The so-called Early Alpine high-pressure metamorphism, the rocks, and their plate tectonic implications were initially described by ERNST (1971) and DAL PIAZ et al. (1972). The latest results were published in the field trip guide of IGCP Project 235 (PICCARDO, 1988).

The high-pressure metamorphism in the Western Alps due to the Cretaceous subduction and nappe formation can be recognized on the rocks of both the pre-Alpine continental and oceanic crust (ERNST, 1971, DAL PIAZ *et al.*, 1972). The metamorphic rocks have been formed from igneous, sedimentary and metamorphic rocks of variable mineralogical and chemical composition. The original rocks were some members of the ophiolite association, e.g. the mafites (Cottian Alps, Monviso region, Voltri Massif), ultramafites (Lanzo Massif), pre-Alpine continental rocks (e.g. Sesia Zone), oceanic sedimentary formations (Voltri Massif),

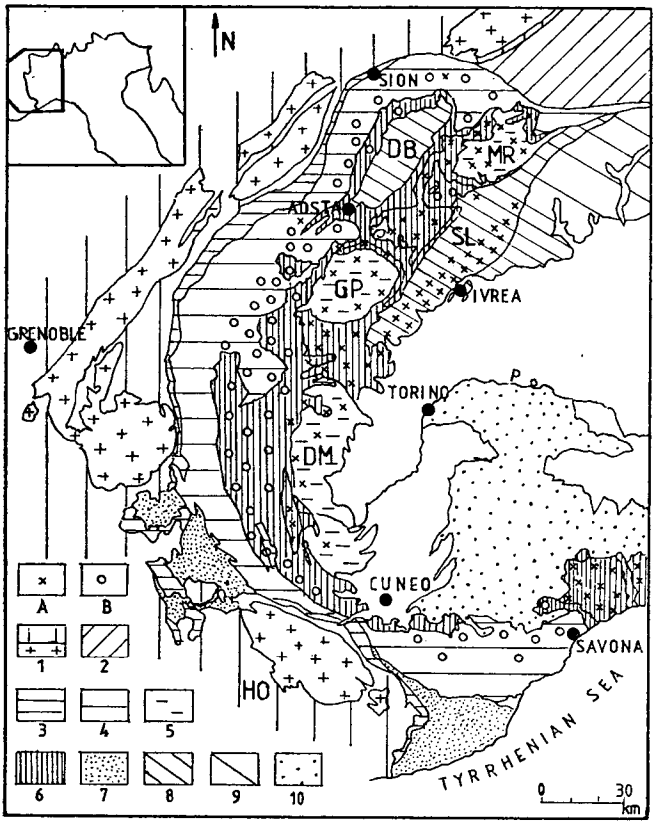

Fig. 2. Tectonic map of the Western Alps, with high-pressure metamorphite localities. Legend: units of the Palaeo-European margin: 1. Helvetic-Dauphinois zone with basement massifs; 2. Lower Penninic nappe; 3. Subbrianconnais unit and Sion-Courmayeur zone; 4. Gran Bernardo nappe; 5. Upper Penninic nappes: Monte Rosa (MR), Gran Paradiso (GP), Dora Maira (DM); 6. Piedmont ophiolite nappe with the Voltri Massif; 7. Helminthoid flysch; units of the Palaeo-African continent: 8. Austro-Alpine Sesia-Lanzo (SL) and Dent Blanche nappes (DB); 9. Southern Alps and the Ivrea Zone; 10. Late orogenic sedimentary sequence. High-pressure associations: A: eclogite, B: blueschist. (After DAL PIAZ—LOMBARDO, 1986)

and pre-Alpine crystalline schists (e.g. Dora Maira Massif, Gran Paradiso, Monte Rosa, Ligurian Alps).

The tectonic and metamorphic evolution of the Western Alps is summarized as follows: The Alpine metamorphism is subdivided into an Early Alpine phase, connected to the subduction-collision process, and into a Late Alpine one, related to uplifting. During the Cretaceous subduction a predominantly blueschist then an eclogite-facies metamorphism were formed in the internal zones of the Western Alps. In the collision realm a blueschist-facies diaphthoresis was predominant during Late Cretaceous and Early Tertiary time. In the outer zones of the Western Alps blueschist-facies rocks were probably formed during the Palaeocene and Early Eocene due to the subduction and collision.

The Late Alpine greenschist-facies diaphthoresis is related to strong uplift. The metamorphic rocks well reflect the above-mentioned alteration processes.

Characteristic minerals of the progressive blueschist facies are glaucophane, clinozoisite, titanite, white mica and Ca- and Mn-rich garnet. The eclogite-facies rocks are characterized by pyroxenes (omphacite or jadeite), almandine- or pyrope-rich garnet, zoisite (rarely epidote) and rutile, according to the description. Quartz was found in the more acidic original rocks. This composition indicate an extended interpretation of eclogite facies by the above cited authors. Some of the listed minerals, e.g. zoisite, epidote, are stable rock-forming minerals in metamorphites of lower P-T range, like in greenschist. The presence of these components and jadeite may indicate that the high pressure — and associated high temperature — characteristic for eclogite facies did not last long enough to reach complete equilibrium. The metamorphic process may have been terminated in a lower, possibly partly greenschist-facies P-T range. Therefore, most of the mineral assemblage of the above-mentioned rocks have been formed due to retrograde metamorphism*. In the retrograde blueschist facies (or glaucophanite facies) there are large amounts of albite, Fe-chlorite, Fe-rich epidote besides Na-amphibole. Also there are stilpnomelane, titanite altered from rutile, and clinozoisite. The Na-amphibole is frequently rimmed by Na-Ca- or Ca-amphibole. The latter phenomena indicate the diaphthoresis.

The eclogite-facies rocks of the Western Alps usually were formed under 450—500 °C temperature and 10—15 kb pressure. The blueschist was formed under

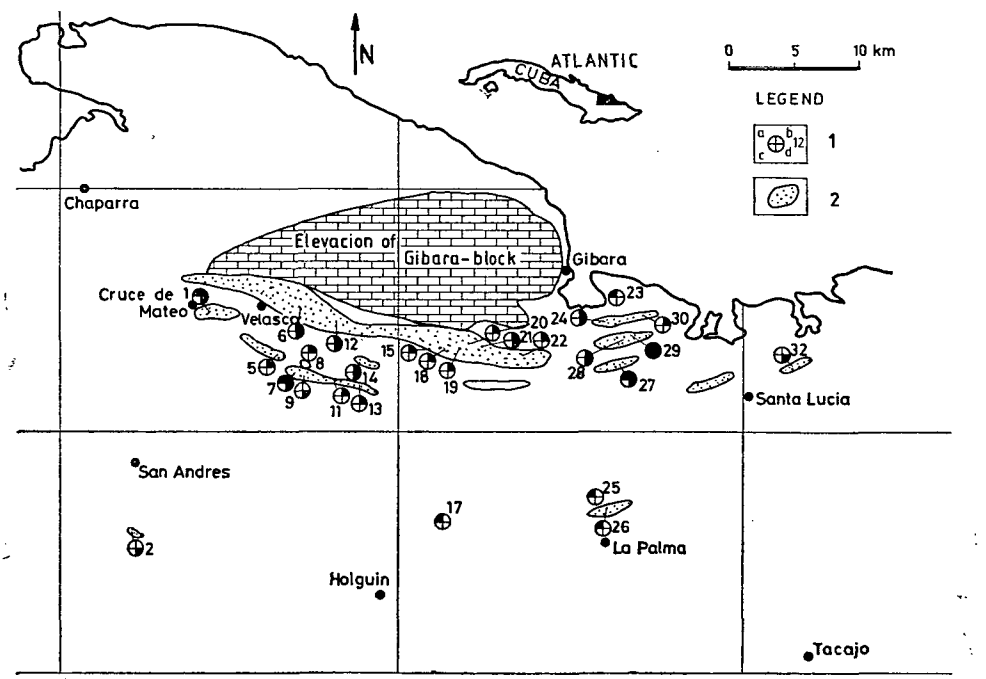

Fig. 3. Locality map of the metamorphic rocks in NW Oriente. Legend: metamorphite localities: La Palma (a) Formation; Mateo Formation (b—d); eclogite, diaphthorized eclogite (c) mafic rocks from the lower crust; (d) metamorphic rocks from the obduction overthrust zone. 2. Probable scattered localities.

* The notion retrograde metamorphism is used after ANGEL (1965).

450 °C and 7—8 kb, while the greenschist-facies metamorphites were formed at about 400 °C and 3—5 kb.

The Cuban-Hungarian Geological Expedition (1984—1988) has found unknown or marginally known (NAGY E. *et al.* 1978) metamorphic rocks (ANDÓ—KOZÁK, 1987).

Various local and regional metamorphites are very widespread; in this paper we discuss only those completely recrystallized rocks of definitely metamorphic texture, which form smaller or larger isolated blocks in melange- or olistostrome-like sedimentary formations *(Fig. 3)*.

DISTRIBUTION, GEOLOGICAL SETTING AND MAIN TYPES OF THE METAMORPHIC ROCKS OF E. CUBA

The pre-Neogene geological structure of NW Oriente is formed by two, completely different structural units. The Cretaceous limestone-dolomite ranging along the northern shores belong to the southernmost outcrops of the North American continental plate (Remedios Zone). The adjoining, southern Zaza Zone is made of mostly tectonic metamorphites (serpentinite), ophiolite and island arc-like formations. It may be considered as an allochthonous melange (KOZÁK—ANDÓ, 1987; ANDÓ—KOZÁK, 1987).

Metamorphic grade allows us to differentiate between low and medium grade (La Palma Formation) and high pressure (Mateo Formation) rocks *(Fig. 3)*.

The La Palma Formation is a 250 m long, elongated metamorphic blocks made of black shales (rich in organic materials) and orthogneisses wedged into the serpentinite scales.

The original material of the organic-rich, graphitic black shale and calcareous phyllite was mostly made of clastics derived from the erosion of mostly pelitic-carbonate, and less granodiorite or low-grade metamorphic orthogneiss terrains. Derivatography indicates partial graphitization of the organic matter, arranged in sheared, fine bands.

The also low-grade metamorphic orthogneiss is of granodioritic origin, too. Its margins display cataclastic-mylonitic structures.

The clastic-carbonatic or granodioritic origin of the metamorphites described here are well shown by their composition (Table 1).

Separated muscovites from the orthogneiss show 196 Ma K/Ar ages*, therefore the original igneous rock was older than Triassic. The 91 Ma age of the feldspars may be related to the Upper Cretaceous tectonic processes. Based on these results the orthogneiss and its original rock, the granodiorite is correlated by the old granodiorites in the northern part of Central Cuba (SOMIN—MILLÁN, 1981) similarly derived from the basement of the continental foreland.

Outcrops of the mafic-ultramafic metamorphites of the Mateo Formation range from metre size up to 20 m *(Fig. 4)*, teherefore siplaying them on the geological maps causes problems. Along the northern part of the region these point-like exposures form an easily recognizable belt about 1 to 10 km south of the present southern edge of the carbonate platform representing the North American continental plate *(Fig. 3)*. The 0,5—1 km wide "metamorphic belt" defined by ca. 25 natural exposures

* The age determinations were made by K. BALOGH and Z. PÉCSKAY at ATOMKI Laboratories, Debrecen.

No.	Sites of sampling	SiO_2	TiO_2	Al_2O_3	Fe_2O_3	FeO	MnO	MgO
1.	30	50.63	1.70	12.70	3.54	7.75	0.534	4.53
2.	13	48.09	1.19	14.02	5.43	8.40	0.278	7.78
3.	1	52.16	0.66	11.81	1.53	8.23	0.153	8.49
4.	27	52.28	0.66	12.18	6.43	2.36	0.159	9.88
5.	27	50.47	1.40	15.53	0.93	8.99	0.137	7.17
6.	20	40.81	1.78	14.51	3.46	7.78	0.249	15.40
7.	21	27.43	3.65	17.61	0.49	20.58	0.534	13.78
8.	29	49.10	1.00	11.84	3.87	5.88	0.201	12.95
9.	PC-444 (1) 2,0 m (1)	48.34	0.75	8.00	3.65	5.69	0.110	21.21
10.	1	55.08	<0.1	4.07	2.00	3.80	0.294	19.63
11.	1	31.13	0.68	15.43	7.28	4.07	0.163	30.07
12.	PC-234 (26) 2.5	70.95	0.17	15.60	1.01	0.77	<0.05	0.80
13.	PC-234 (26)	71.00	0.23	13.70	<0.1	2.13	0.07	0.97
14.	PC-234 (26)	52.08	0.60	12.75	0.59	3.65	0.09	2.28

*=loss of ignition; sites of sampling according to *Fig. 3*

MATEO FORMATION

1—7 = ecologite and metamorphites derived fom eclogites
8. = coarse-grained garnet-amphibolite
9. = tremolite schist with serpentine
10. = tremolite schist
11. = chlorite schist

LA PALMA FORMATION

12—13 = orthogneiss
14 = graphitic phyllite

The analyses were prepared at the Department of Petrology and Geochemistry of Eötvös L. University, Budapest, Hungary (No. s 1—11 and 13) as well as at the Geological Company, Santiago de Cuba, Cuba (no. s 12 and 14)

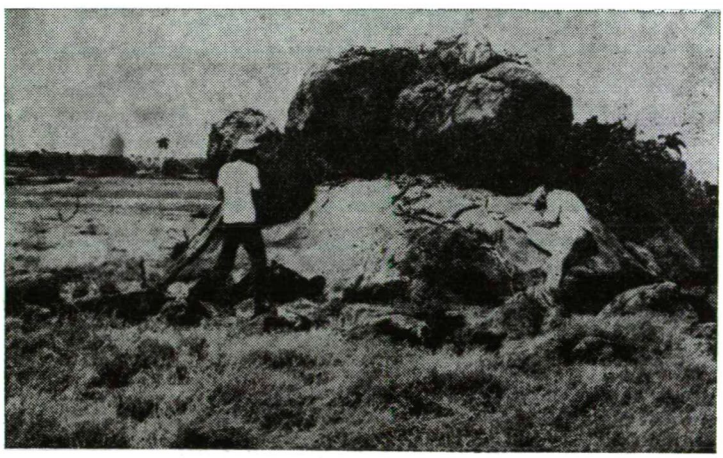

Fig. 4. Eclogite blocks, Cruce de Mateo

TABLE 1

rocks from the environs of Holguin

CaO	Na_2O	K_2O	P_2O_5	$-H_2O$	$+H_2O$	CO_2	SO_2	Total
11.25	5.36	0.55	0.02	0.39	0.49	—	0.76	100.20
11.65	2.10	0.29	0.06	0.07	—	—	—	99.36
10.62	3.47	0.27	0.09	0.13	1.44	—	0.21	99.26
9.82	4.08	0.12	0.01	0.21	1.80	—	—	99.99
6.93	6.15	0.17	0.04	0.07	1.06	—	0.55	99.60
8.14	0.87	<0.1	<0.01	0.75	5.15	—	0.90	99.80
3.06	<0.01	0.02	<0.01	0.61	7.82	3.04	0.74	99.36
8.91	0.91	0.71	0.63	0.33	2.43	—	—	98.76
7.04	0.17	<0.1	0.08	0.20	5.40	—	—	100.64
11.56	0.33	<0.1	<0.01	0.30	2.91	—	—	99.97
0.47	<0.1	0.18	0.01	0.34	10.60	—	—	100.42
0.70	6.30	1.76	0.136		1.69*		<0.1	100.036
0.62	6.56	2.18	0.25	0.40	1.40	—	—	99.51
12.15	3.60	1.32	0.193		10.40*		0.27	99.973

extends from Velasco to Potrerillo to Guardalavaca forming an 50 km long zone. The outcrops at Cruce de Mateo (2 km WSW from Velasco) are regarded as the stratotype of the formation *(see Fig. 3)*.

The mafic-ultramafic metamorphites of the Mateo Formation are subdivided into three groups: (1) eclogite and its diaphtorised and metasomatized varieties; (2) micaceous garnet-amphibolite with slightly oriented structure; (3) schistose amphibolite, amphibole-chlorite-schist, chlorite-talc-schist, actinolite- and tremolite-schist, chlorite-phyllite (antigorite-phyllite) with oriented structure.

The eclogite and its derivatives are distributed all along the zone, while the micaceous garnet-amphibolite occurs in minor amounts only. Members of the third group are widespread, and occur associated with the eclogite varieties, too.

Naturally the main components of the eclogite varieties (derivatives) are eclogite garnet and omphacite *(Fig. 5)*, with a minor amount of glaucophane *(Fig. 6)* provies the formation of these rock-types in a subduction zone. However, the hornblende rim around glaucophane *(Fig. 6)* indicates changes in P-T conditions during metamorphism, the amphibole appearing in the space between albites and pyroxenes, the zoizite and the epidote indicate the termination of the high-pressure process

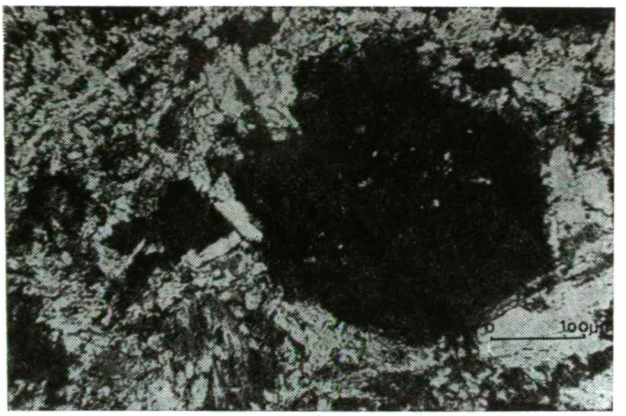

Fig. 5. Euhedral garnet and omphacite from eclogite. Locality No. 8. Crossed nicols, 167x magnification

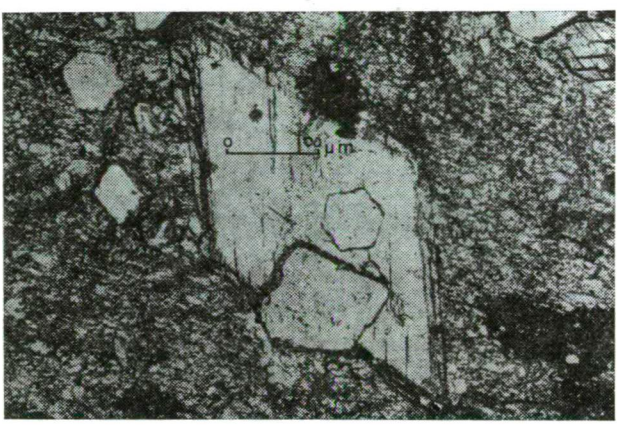

Fig. 6. Hornblende-rimmed glaucophane in diaphthorized eclogite. Locality No. 30. Single nicol 167x magnification

before equilibrium was reached, i.e. retrograde metamorphism. Amphibolization of pyroxene *(Fig. 7)*, leucoxenization of rutile, or its alteration to titanite show a later phase, i.e. diaphthoresis. Therefore the mineral composition of eclogite varieties (derivatives), and the ratio of the above-mentioned components is strongly varied in each locality. Amphibole occurs in larger quantities in these rocks; there are varied amounts of albite together with other minerals (zoisite, epidote, chlorite) stable at lower pressures and temperatures *(Fig. 8)*. It is clearly seen that the cores of titanite grains are made of rutile. This solid phase composition may reflect either retrograde metamorphism or low-grade diaphthoresis. In some localities (e.g. in locality No. 27, see *Fig. 3*) the eclogite almost completely has been transformed to amphibole schist; in this case the pyroxene forms inclusion-like relics only *(Fig. 9)*. The recrystallization brought a coarse crystalline look to the rock.

Diaphthoresis resulted in the formation of metamorphites indicating varied facies from the eclogite. However, the original texture — and partly the mineral com-

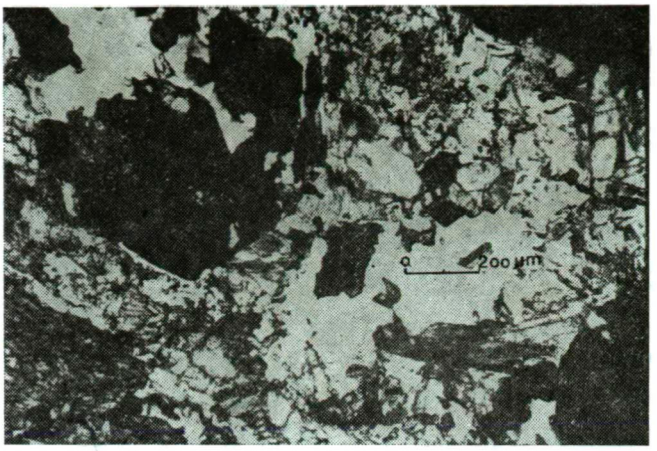

Fig. 7. Garnet, omphacite, albite, and hornblende in diaphthorized eclogite. Locality No. 1. Crossed nicols, 67x magnification

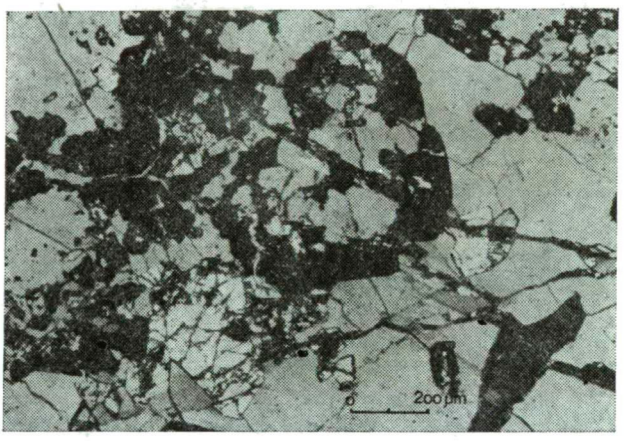

Fig. 8. Garnet relics with albite, zoisite, and chlorite. Locality No. 27, Crossed nicols, 67x magnification

position — can be recognized even after intense alteration. Consequently, the diaphthorite may inherit the textural characters of the eclogite, helping to determine its origin *(Fig. 10)*. In these metamorphites syndiaphthoritic folded structure can be observed, illustrating the relationship of this process and tectonical reactivation *(Fig. 11)*. In extreme cases the original texture is completely re-ordered due to strong alteration. The pre-altered rock is indicated by xenoblastic relic garnets *(Fig. 8)*. In these rocks the stable minerals of low-grade amphibole or greenschist facies (hornblende, actinolite, chlorite) become predominant in the case of intense diaphthoresis.

Amphibolite- and greenschist-facies rocks are not formed by diaphthoresis only. During progressive metamorphism besides eclogite a more varied metamorphic association was formed from the mafic rocks of the oceanic crust in varied amounts in each region (among others garnet-amphibolite, epidote-amphibolite, amphibole-schist, albite-zoisite-chloriteschist, actinoliteschist, chloritite, talc-schist, et.).

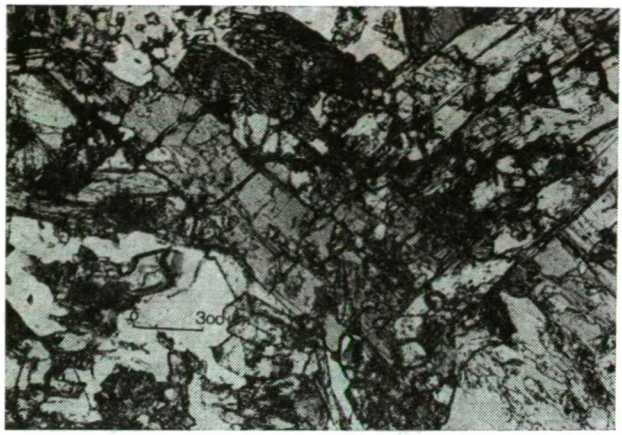

Fig. 9. Relics of hornblende, albite, and pyroxene in diaphthorized eclogite. Locality No. 27. Single nicol, 47x magnification

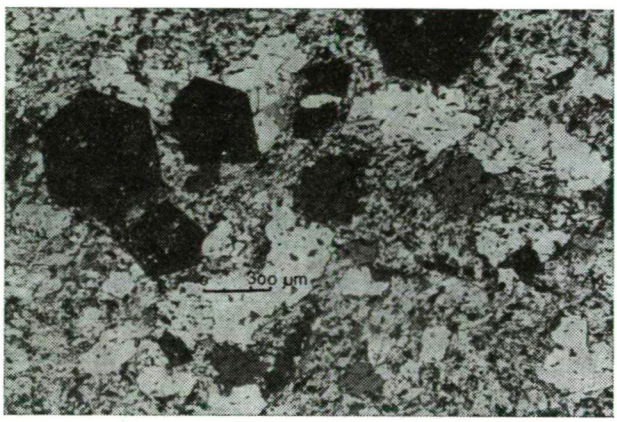

Fig. 10. Garnet, albite, and amphibole in greenschist-facies, diaphthorized eclogite. Locality No. 11. Crossed nicols, 42x magnification

Variability of eclogie diaphthoresis can be clearly observed on the blocks of the exposed stratotype *(Fig. 12)*. The most conspicuous although local metamorphic alteration was produced by an intense migration of solution post-dating the subduction (possibly connected with the uplift or obduction). The dark bluish to violet-tinted amphibole agglomerations precipitated from high-temperature solutions fill the former joints of eclogite and form dense network of mineral veinlets. These are several mm long, up to cm size and form minor nests, too. The Na-containing amphiboles form oriented clusters on both sides of the veinlets with variable density, decreasing with growing distance. This phenomenon appears as characteristic banding on the blocks *(Fig. 13)*. The amphibole — bluish green in thin section — appears in even distribution in a distance from the bands, but scattered or in rock-forming quantities depending on the intensity of the solution effect. By the growth of its ratio the amount of pyroxene decreases, and this process leads to the formation of certain garnet-amphibolite varieties.

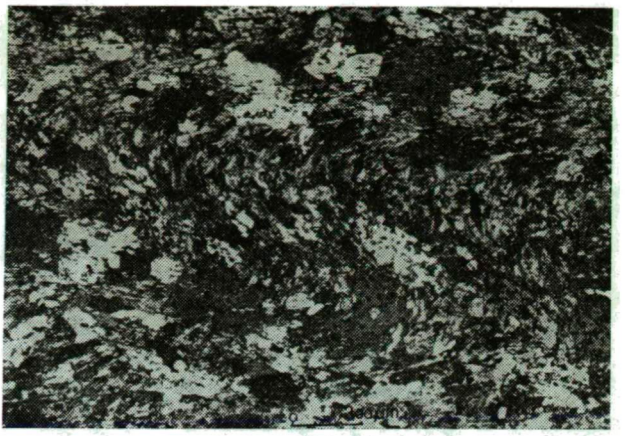

Fig. 11. Folded epidote-amphibolite with albite from diaphthorized eclogite. Locality No. 12. Crossed nicols, 42x magnification

Fig. 12. Metasomatically altered, banded eclogite SW of Gibara

The eclogite-facies metamorphites are the products of pressure (and corresponding temperature) made by the subduction of a mafic oceanic plate. Their diaphthoresis can be explained by uplift from 30 km depth to higher crustal positions and by some increase in temperature. Following this the mafic crustal rocks metamorphosed to variable grades were emplaced into the reach of obductional imbricate movements, which yielded further alterations corresponding to the new conditions, especially the characteristic metasomatic processes.

K/Ar ages of separated amphiboles from diaphthorized eclogite (locality No. 13) and from garnet-containing amphibole-schist (locality No. 20) are 103 Ma and 109 Ma, respectively. These data indicate the age of the diaphthoresis.

The schistose metamorphites are usually of mafic-ultramafic composition, with the predominance of the latter. The antigorite-schist, antigorite-talc-schist, chlorite-

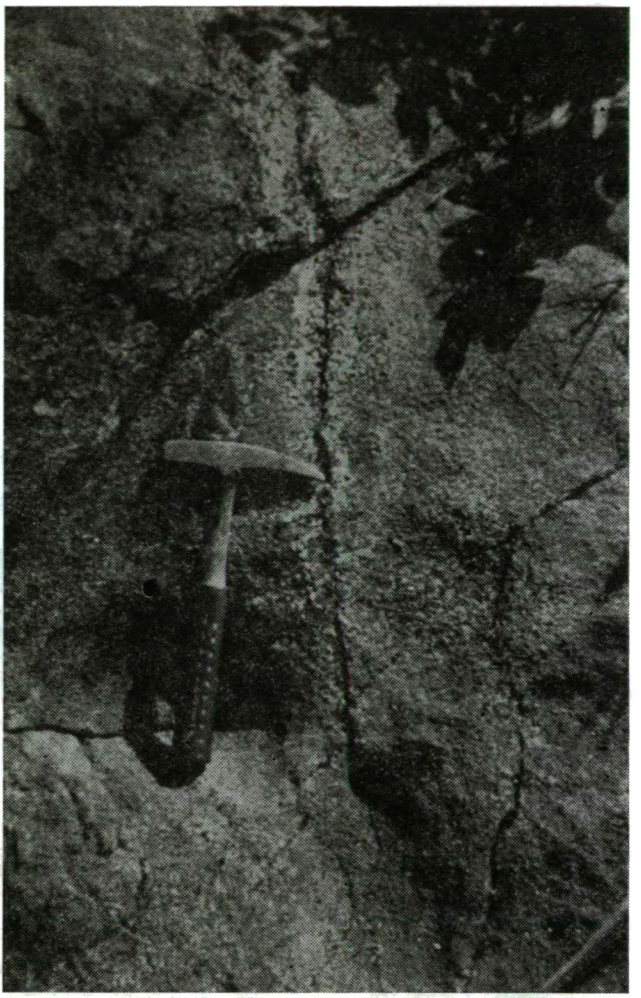

Fig. 13. Eclogite with amphibole bands. Cruce de Mateo

schist, greenschist, actinolite- and tremolite-schist, chloritic amphibole-schist and garnet-bearing epidote-amphibolite belonging to this group are products of a progressive metamorphism between greenschist and amphibolite facies. Minor diaphthoresis was observed on the amphibolites. Texture and structure of these rocks indicate a significant role of the directed pressure, while the solid phase composition demonstrates different P-T conditons. The appearance of these conditions can be explained by frictional heat and the corresponding pressure, which occurred along the shear zones below the obducting oceanic plates. An environment with higher temperature gradient was needed for the formation of the amphibolite varieties. These factors and the ultramafic-mafic chemistry of the rocks indicate that the above-mentioned strain zones may have been formed within a — then young — oceanic plate.

The muscovitic amphibolite, containing large-size (0.4—0.6 cm) garnets, is of different origin by its chemical and mineral composition ant its texture. It may have

been formed from high-MgO mafic metamorphite — possibly eclogite — or garnet-amphibolite due to greenschist-facies diaphthoresis. Its origin cannot be cleared, but its characteristic, partly relic texture, and its composition suggest an origin from a mafic-melamafic, continental deep crust. Its K/Ar age (119 Ma) measured on mescovites is older than that of the amphiboles of diaphthorized eclogites.

GEOCHEMISTRY OF METAMORPHITES OF MATEO FORMATION AND WESTERN ALPS

To determine the original and present composition and to follow the alterations (among others the diaphthoresis) chemical analyses (Geological Company, Santiago de Cuba; Department of Petrology and Geochemistry, Eötvös University, Budapest), electron microprobe analyses (Department of Petrology and Geochemistry, Eötvös University, Budapest), and REE determinations by neutron activation analysis (Budapest Technical University, Institute of Nuclear Technology) were carried out. The results are summarized as follows.

Chemical analyses (Table 1) show the mafic composition of most rocks in AFM-, and Al_2O_3—FeO^t—MgO-plots (Figs. 14—15). The AFM plot *(Fig. 14)* the eclogites, diaphthorized to varied grades, and with mafic composition are well separated from the melamafic-ultramafic schists along the F-M sied. Part of the schists display weak relationship to partially diaphthorized eclogites, while another part of them represent the types from the shear zone or the mafic deep crust. Comparing *Figs. 14* and *15* the eclogitic rocks of the formation show high similarities to mafic eclogites of tholeiitic origin in France and the Western Alps. The melamafic-ultramafic rocks of

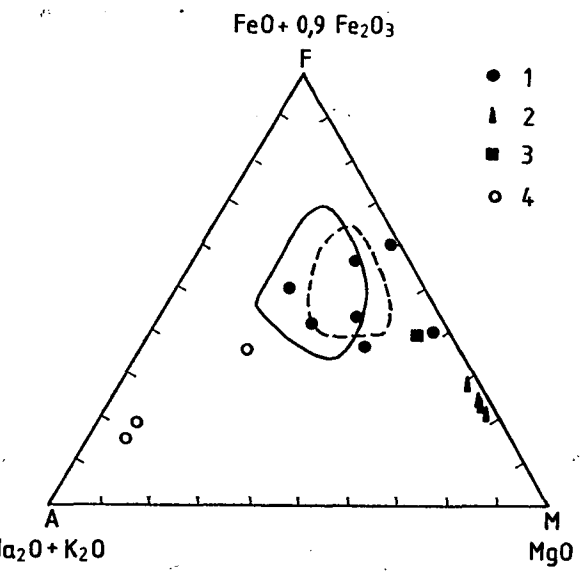

Fig. 14. AFM plot of metamorphites from NW Oriente. Legend: 1—3: Mateo Formation. 1. eclogite—diaphthorized eclogite; 2. Ophiolitic metamorphites from the overthrust zone; 3. Mafic rocks from the lower crust; 4. La Palma Formation. Continuous line: eclogite, amphibolite-bearing eclogite, and amphibolite, Mucrone Sesia Zone, Western Alps (BIINO *et al.*, 1988). Dotted line: eclogite of tholeiitic origin: Bas-Limousin, Massif Central (SANTALLIER, 1983)

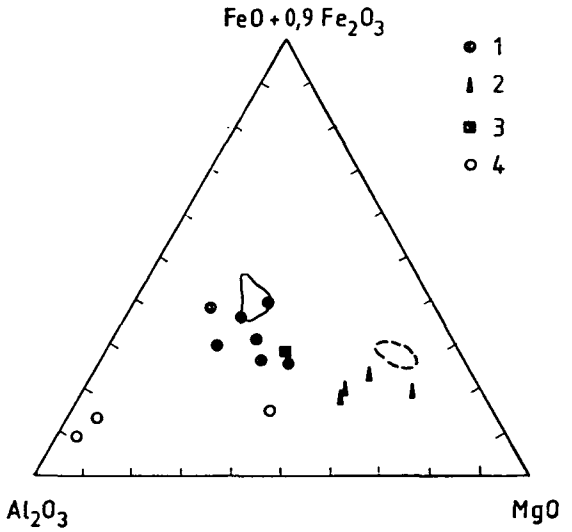

Fig. 15. Al_2O_3—FeO^t—MgO plot of the NW Oriente metamorphites. Legend of dots: see *Fig. 14*. Continuous line: Cabardés, amphibolitized eclogite (Montagne Noire, France (DEMANGE, 1985). Dotted line: Airette, eclogite-facies ultramafics, Montagne Noire, France (DEMANGE, 1985).

the formation do not fall in the field of published eclogite-facies metamorphites of mafic-ultramafic origin. This fact supports our suggestion on their different kind of formation. Garnet, pyroxene and amphibole compositions from the eclogitic series were determined by *electron microprobe.* and compared to some pyroxenes and amphiboles from weakly metamorphosed sheeted dykes and cumulates in the region.

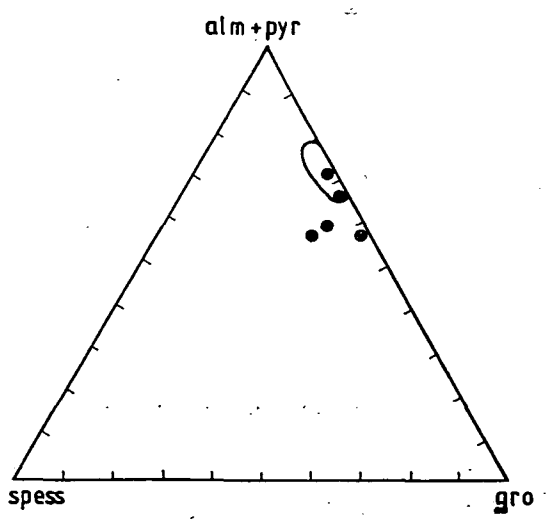

Fig. 16. Garnet compositions of NW Oriente diaphthorized eclogites in an almandine+pyrope — spessartine — grossular triangular plot. Continuous line: amphibolite containing eclogite relics, Savona crystalline massif (MESSIGA—SCAMBELLURI, 1988).

Garnets of variably diaphthorized eclogites show almost the same, mostly almandine-grossular composition, rarely with a somewhat higher ratio of spessartine molecule *(Fig. 16)*. On the Mg—Fe^2 —Ca+Mn cation number plot the garnets occupy a well-defined field, like some Western Alpine eclogites *(Fig. 17)*. However, on the grossular-almandine+spessartine-pyrope plot *(Fig. 18)* the Cuban garnets and the

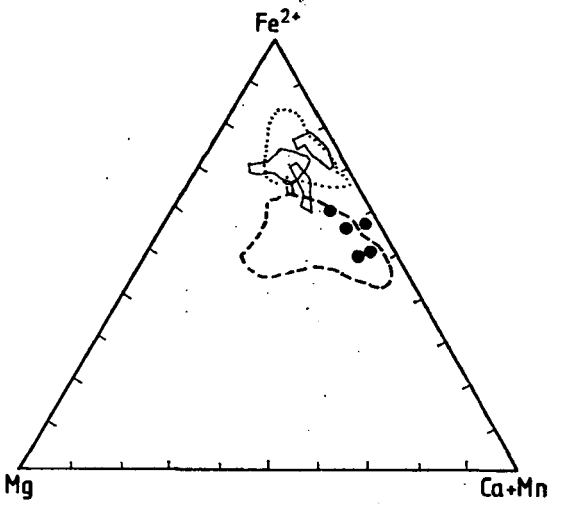

Fig. 17. Composition of NW Oriente diaphthorized eclogites in an Fe—Mg—Ca+Mn cation number plot. Continuous line: Val d'Ala, Lanzo, Western Alps; dotted line: high Mg-gabbro altered to eclogite, Voltri Massif, Western Alps. Dotted line: high Mg—Fe-gabbro altered to eclogite, Voltri Massif and Monviso, Western Alps (SANDRONE *et al.*, 1986).

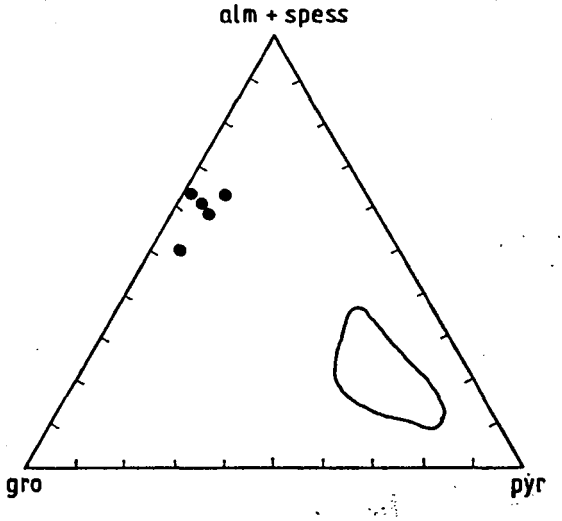

Fig. 18. Composition of garnets from NW Oriente diaphthorized eclogites in an almandine+spessartine—grossular-pyrope triangular plot. Continuous line: garnet-clinopyroxene-bearing metamorphic rocks, Bohemian Massif, Lower Austria (SCHARBERT—CARSWELL, 1983).

metamorphic garnets derived from the high-pressure granulite facies garnet-clinopyroxene-bearing rocks of the Bohemian Massif (SCHARBERT—CARSWELL, 1983) are clearly separated. *Fig. 19* illustrates the composition of the less diaphthorized eclogites of the formation compared to the pyroxenes of two metadolerites in a jadeite-aegirine-other pyroxenes triangular plot. Both types are separated by significant differences in the ratio of the aegirine-jadeite molecules. On the other hand there is definite similarity among chemical compositions of pyroxenes of eclogitic rocks from the investigated and analogous regions. *(Fig. 19).*

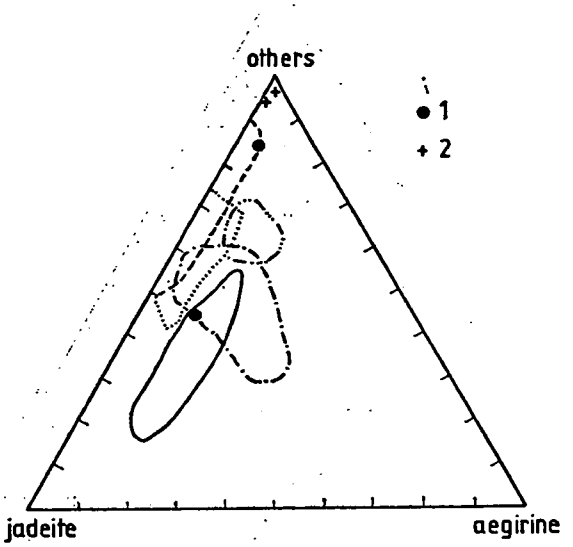

Fig. 19. Pyroxene composition of NW Oriente diaphthorized eclogites (1) and metadolerites (2) in a jadeite-aegirine-other pyroxenes triangular plot. Continuous line: omphacite from bedded eclogite, monviso, Western Alps (COMPAGNONI *et al.*, 1988). Dotted line: Cr-rich Na-pyroxene from Mg—Al-metagabbro, Monviso, Western Alps (KIENAST—MESSIGA, 1987). Dotted line: eclogite altered from high-Mg gabbro,Voltri Massif, Western Alps (SANDRONE *et al.*, 1986). ...—...—...—= =eclogite altered from high-Fe—Ti gabbro: Voltri Massif and Monviso, Western Alps (SANDRONE *et al.*, 1986). ...—...—...—=High Fe—Ti gabbro altered to eclogite, Cotti Alps (SANDRONE *et al.*, 1986)

The varied diaphthoresis grades of eclogites are indicated by the amount and chemical composition of amphiboles. Therefore the electron microprobe analysis was extended to almost all eclogite varieties and derivatives. The exact systematic position of the analysed minerals *(Fig. 20)* was determined by LAEK's (1978) method from cation numbers calculated from analytical data. The investigated minerals mostly belong to the Ca- and Na—Ca-amphibole groups. We can see, that amphiboles of eclogite diaphthorized in amphibolite- and greenschist-facies environment and of metadolerite are very similar in composition. It suggests similar chemical composition for the original rocks and similar p—T conditions, defining the amphibole chemistry for the two groups.

The above-mentioned data prove that the secondary amphiboles of Cuban metamorphites and Western Alpine eclogites are similar in composition *(Fig. 21).*

REE composition of some rock types was determined for possible grouping and for clearing genetical relationships of the different metamorphites of Mateo Forma-

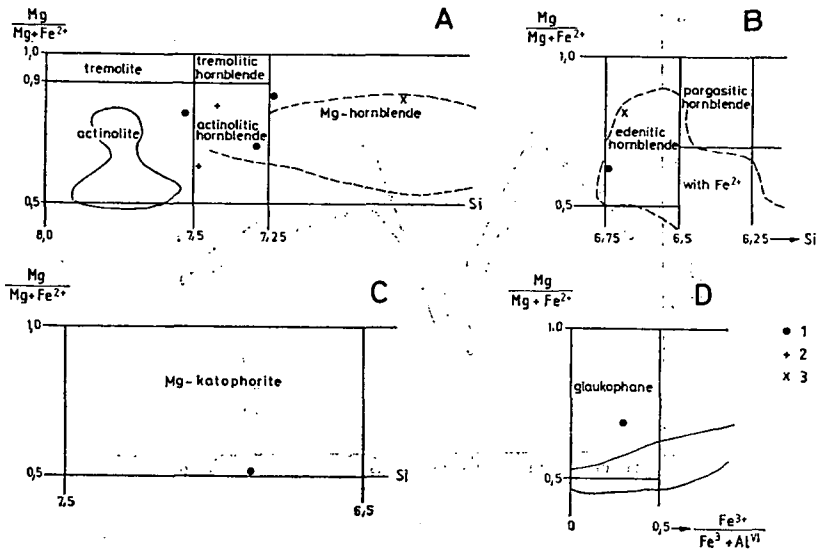

Fig. 20. Amphibole compositions in Laek's system (A, B, C, D categories). (1) from eclogite, diaphtorized eclogite, (2) metadolerite, (3) metagabbro cumulate origin. Continuous line: (A) Ca-amphibole from diaphthorized eclogite, (D) amphibole from a diaphthorized eclogite, altered from high-Fe—Ti gabbro, Voltri Massif, Western Alps (MESSIGA *et al.*, 1988). Dotted line: (A) (B) amphibolite with eclogite relics, Savona crystalline massif (MESSIGA—SCARAMBELLURI, 1988)

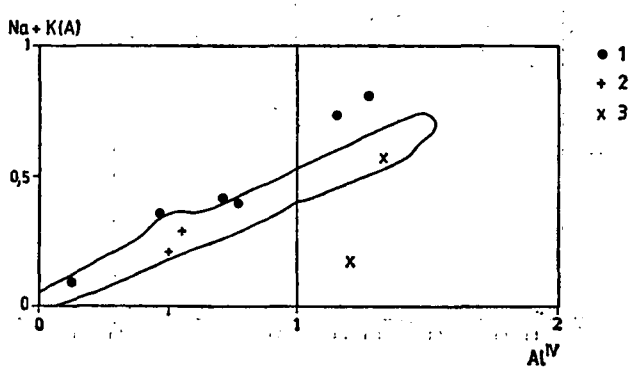

Fig. 21. Formular ratio of tetrahedral Al from eclogite and diaphthorized eclogite (1), metadolerite (2) and metagabbro of cumulate origin (3) in the function of Na+K(A). Continuous line: amphiboles of eclogites from the Sesia Zone of the Western Alps (BIINO *et al.*, 1988)

tion. The chondrite-normalized data *(Figs. 22—23)* show two types. The low average REE content of tremolite-schist *(Fig. 22)* and the shape of the curve clearly shows the connection with the serpentinized ultramafics characteristic for the region.

The other group, which contains the diaphthorized eclogites, too, has a magnitude higher REE content *(Fig. 23)*. Although the curves have similar shapes, there are significant differences in the ratio of light and heavy elements. The curve shapes resemble to that of the oceanic tholeiites, and magmatices of back-arc or intra-arc basins. Differences in La/Lu ratio suggest stronger or weaker differentiated composi-

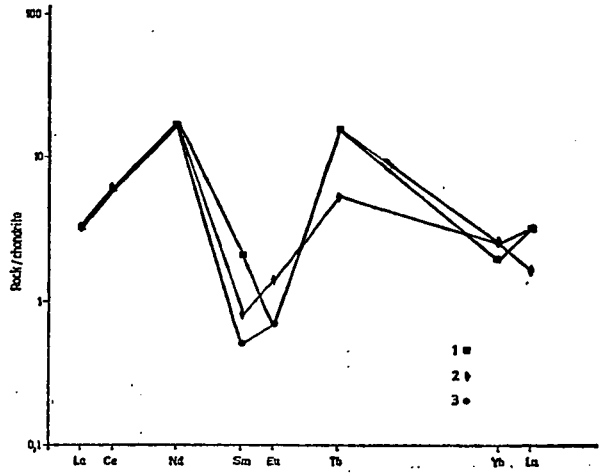

Fig. 22. Ophiolitic metamorphites and ultramafics from overthrust zones: chondrite normalized values of REE contents. 1. tremolite schist, 2—3. serpentinized ultramafics. NW Oriente.

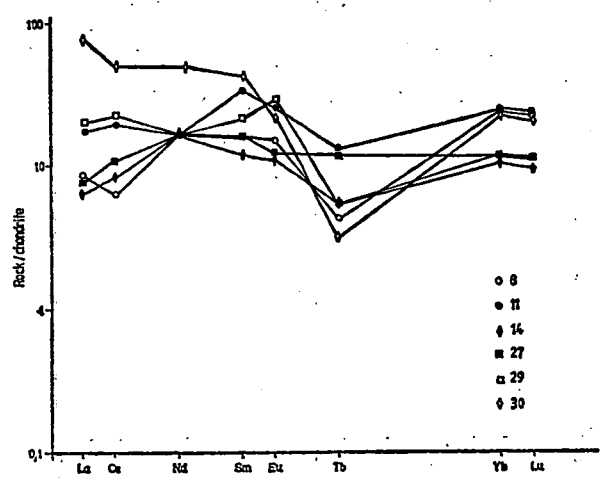

Fig. 23. Chondrite-normalized REE values of diaphthorized eclogites (locality Nos. 8, 11, 14, 27, 30) and garnet-bearing amphibolite (locality No. 29)

tions within the profiles of the investigated regions. We are aware, that REE spectrum of the muscovitic garnet-bearing amphibolite, ranegd to a separate group, is similar to that of the eclogite (except Eu). But the contrasting positive anomaly of Eu compared to that of the eclogite group can suggest significant genetical differences. This geochemical separation makes probable that the metamorphite containing large garnets may have been formed by diaphthoresis of eclogite originating from continental — or transitional — lower crust or from upper mantle of crustal origin.

CONCLUSIONS

1. There are sialic, mafic and ultramafic metamorphites of variable composition as components of tectonic melange or olistostrome-like sediment in NW Oriente. Their present spatial association reflects their allochthonous position. Their original place and composition are highly variable, as shown them MILLAN and SOMIN (1985) for other localities.

2. The La Palma Formation represents an old sialic crystalline crust and possibly Jurassic meta-terrigenous-carbonate sequence of the southern foreland of the North American continental plate. Analogous units are the crystalline and meta-terrigenous-carbonate sequences (BREZSNYÁNSZKY *et al.*, 1981) in Western Cuba, Escambray and Isla de Juventud (MILLAN, 1975; MILLAN—SOMIN, 1985).

3. The eclogitic rocks of Eastern Cuba are very similar to those of the Western Alps regarding their petrology and geochemistry.

4. Most of the mafic-ultramafic metamorphites of the Mateo Formation are considered as of oceanic origin, (see also MATTSON, 1973 and BREZSNYÁNSZKY *et al.*, 1981 for the amphibolites of Eastern Cuba).

5. The high-pressure, eclogitic formations of the Mateo Formation are correlated with the metamorphites appearing as "tectonic xenoliths" of the Northern Cuban melange zone (e.g. Sierra de los Organos, Sierra de Cristal). These are of subduction origin, as MILLÁN and SOMIN wrote (1985). The K/Ar age (upper part of Lower Cretaceous) of the diaphthorized eclogites indicate the end of the alteration, i.e. the time of uplift.

6. The greenschist-facies retrogression in the Western Alps is related to the uplift and overthrust of the high-pressure rocks. On the basis of petrological analogies the evolution of a part of the studied high-pressure rocks from Cuba also can be interpreted the similar way.

7. The formation of most of the schistose, greenschist to amphibolite-facies ultramafic-mafic metamorphic rocks is connected to shear zones of obducting, imbricated young oceanic basins with high geothermic gradient (COLEMAN, 1984). These movements sheared, then dragged the earlier subducted, then uplifted high-pressure, metamorphic rocks, too. The obducted, then overthrusted and imbricated rocks dragged blocks from the continental slope onto the foreland. (La Palma Formation, metamorphites characteristic for the mafic deep crust).

8. The North Cuban collision zone represents the products of multiple subduction, and there are probably ophiolites, which are of different age and suffered metamorphism of different grade.

REFERENCES

ANGEL, F. (1965): Retrograde Metamorphose und Diaphtorese. N. Sb. Miner. Abh. DBd. **102,** 123—176.

ANDÓ J.—KOZÁK M. (1987): La serie ofiolítica de Holguin (Cuba) y su papel en el desarollo estructural de Cretácico-Paleógeno. — Actas Facultad de Ciencias de la Tierra U. A. N. L. Lineras (México) **2,** 271—274.

BIINO, G.—COMPAGNONI, R.—LOMBARDO, B. (1988): Eclogitized granitoids, paraschists and metabasics (Sesia Zone). High pressure eclogitic reequilibration in the Western Alps: I. G. C. P. 235. Excursion to the Alps. Part **1,** Field Excursion Guidebook. 43—80.

BREZSNYÁNSZKY K.—COUTIN, D. P.—JAKUS P. (1981): Nuevos aspectos acerca del complejo basal en Cuba Oriental. — Ciencias de la Tierra y del Espacio. **3,** 23—29.

COLEMAN, R. G. (1984): Preaccretion tectonics and metamorphism of ophiolites. —Ofioliti **9.** (3), 205—222.

COMPAGNONI, R.—KIENAST, J. R.—LOMBARDO, B. (1988): The Monviso eclogitic meta-ophiolite (Cottian Alps) — High pressure eclogitic reequilibration in the Western Alps: I. G. C. P. 235. Excursion to the Alps. Part **1**, Field Excursion Guidebook 81—112.

DAL PIAZ, G. V.—HUNZIKER, J. C.—MARTINOTTI, G. (1972): La zona Sesia-Lanzo e l'evoluzione tettonico metamorfica delle Alpi nord-occidentali interne. — Mem. Soc. Geol. It. **11**, 433—460.

DAL PIAZ, G. V.—LOMBARDO, B. (1986): Early Alpine eclogite metamorphism in the Penninic Monte Rosa-Gran Paradiso basement nappes of the northwestern Alps. — Geol. Soc. Am. Mem. **164**, 249—265.

DEMANGE, M. (1985): The eclogite-facies rocks of the Montagne Noire, France. — Chemical Geology. **50**, 173—188.

DIETZ, R. S.—HOLDEN, J. C. (1970): Reconstruction of Pangea: Breakup and sidpersion of continents, Permian to present. — Journal of Geophysical Research. **75**, No 26. 4939—4956.

ERNST, W. G. (1971): Metamorphic zonation on presumably subducted lithospheric plates from Japan, California and Alps. — Contrib. Mineral. Petrol. **34**, 45—59.

ITURRALDE-VINENT, M. (1988): Naturaleza geológica de Cuba. Editorial Científico-Técnica. La Habana.

KIENAST, J. R.—MESSIGA, B. (1987): Cr-rich Mg-chloritoid, a first record in high-pressure metagabbros from Monviso (Cottian Alp), Italy. — Min. Mag. **51**, 681—687.

KOZÁK M.—ANDÓ J. (1987): Desarollo estructural del arco insular volcánico cretácico en la zona de Holguin (Cuba). — Actas Facultad de Ciencias de la Tierra U. A. N. L. Lineras (Mexico) **2**, 267—270.

LAEK B. E. (1978): Nomenclature of amphiboles. — Mineralogical Magazine. **42**, 533—563.

MATTSON, P. (1973): Middle Cretaceous nappe structures in Puerto Rican ophiolites and their relation to the tectonic history of the Greater Antilles. — Geol. Soc. Amer. Bull. **84**, 21—38.

MESSIGA, B.—SCAMBELLURI, M. (1988): The Brianconnais domain in Western Liguria — High pressure eclogitic reequilibration in the Western Alps — I. G. C. P. 235. Excursion to the Alps. Part **2**, Field Excursion Guidebook. 199—224.

MESSIGA, B.—SCAMBELLURI, M.—PICCARDO, G. B. (1988): The Voltri Massif: A section of subducted oceanic lithosphere (Internal Piedmontese zone). — High pressure eclogitic reequilibration in the Western Alps: I. G. C. P. 235. Excursion to the Alps. Part **2**, Field Excursion Guidebook. 149—198.

MILLÁN, G. (1975): El complejo cristalino mesozoico de Isla de Pinos. Su metamorfismo. — Academia de Ciencias de Cuba Serie Geológica No. **23**, 1—16.

MILLÁN, G.—SOMIN, M. L. (1985): Condiciones geológicas de la constitución de la capa granito-metamórfica de la Corteza Terrestre de Cuba. — Instituto de Geología y Paleontología, Cuidad Habana.

NAGY, E.—BREZSNYÁNSZKY, K.—BRITO, A.—COUTIN, D.—FORMELL, F.—FRANCO, G.—GYARMATI, P.—JAKUS, P.—RADÓCZ, GY. (1978): Texto explicativo del mapa geológico de la provincia de Oriente a escala 1:250 000, levantado y confeccionado por la Brigada Cubano—Húngara entre 1972 y 1976. — Memorias de Instituto de Geologia y Paleontología. Academia de Ciencias de Cuba.

PICCARDO, G. B. (ed) (1988): Geological framework of the Western Alps. — High pressure eclogitic reeguilibration in the Western Alps: I. G. C. P. 235. Excursion to the Alps. 1—88.

SANDRONE, R.—LEARDI, L.—ROSSETTI, P.—COMPAGNONI, R. (1986): P-T conditions for the eclogitic re-equilibration of the metaophiolites from Val d'Ala di Lanzo (internal Piemontese zone, Western Alps). — J. metamorphic Geol. **4**, 161—178.

SANTALLIER, D. S. (1983): Les eclogites du Bas-Limousin, Massif Central francais. Comportement de clinopyroxenes at de plagioclases antérieurement *a* l'amphibolitisation. — Bulletin de Minéralogie. **106**, (6.) 691—707.

SCHARBERT, H. G.—CARSWELL, D. A. (1983): Petrology of garnet-clinopyroxene rocks in a granulite facies environment, Bohemia massif of Lower Austria. — Bulletin de Minéralogie. **106**, (6.) 761—774.

SOMIN, M. L.—MILLÁN, G. (1981): Geology of the metamorphic complexes of Cuba. — Nauka, Moscow p. 219. (in russian)

Manuscript received, 1 December, 1989

Acta Mineralogica-Petrographica, Szeged, XXX, 55—65, 1989

GEOCHEMISTRY OF SOME HP-METAVOLCANICS FROM WESTERN ALPS METAOPHIOLITES

I. KUBOVICS and ABDEL AAL M. ABDEL-KARIM

Department of Petrology and Geochemistry, Lóránd Eötvös University

ABSTRACT

Ophiolite metavolvanics from Monviso, Arc valley and Montgenévre in the Piedmont Zone of the Western Alps are geochemically investigated and compared with data obtained from oceanic crust.

Belonging to the Zermatt-Saas and Combin (Monviso and Arc valley) units they are characterized by HP-facies metamorphism including eclogite-facies metabasalts and garnet-bearing glaucophanites that underwent into greenschist-facies metamorphism. Few metavolcanics (Montgenévre) are partly escaped from ocean-floor metamorphism, but they are overprinted by Alpine deformation. They show a large variation in the bulk rock geochemistry and roughly compare to MORB and a few of them show an IAT character. Their geochemical characters prevalently similar to that of oceanic ridge basalts and they show abyssal tholeiitic differentiation trend.

KEYWORDS: HP-Facies metavolcanics, Geochemistry, metamorphic evolution, Peidmont Zone, Western Alps metaophiolite.

INTRODUCTION

The HP-metamorphism had an effect on large bodies of the pre-Alpine continental and organic crust in the Western Alps. During the Cretaceous, most of the oceanic crust (now represented by the Piedmont ophiolite nappe) and some parts of both continental margins underwent blueschist to eclogitic conditions that are followed by the greenschist facies conditions (LOMBARDO, 1988).

The geochemistry of the metavolcanics from the Western Alps have been subjected to various studies; previous researches had carried out from Monviso in Cottain Alps (LOMBARDO *et al.*, 1978, NISIO, 1985, NISIO and LARDEAUX, 1987, COMPAGNONI *et al.*, 1988), Arc valley in the Zermatt-Saas zone (BOCQUET, 1974, DAL PIAZ *et al.*, 1981; DEN TEX, 1987; LEARDI *et al.*, 1986) and from Chenaillet in Montgenévre (MÉVEL, 1975, LEWIS and SMEWING, 1980, BERTRAND *et al.*, 1981, 1982, 1987).

FIELD RELATIONS

Field study and sampling of the metavolcanics were carried out in the eastern, central and western parts of the Piedmont ophiolite nappe in the Western Alps, e.g. Monviso, Arc valley area and Montgenévre ophiolites *(Fig. 1.)*. The Piedmont ophiolite is represented by thinned, sheared, multistage folded and metamorphosed remnants of a narrow oceanic crust and related upper mantle (DAL PIAZ *et al.*, 1981).

H-1088 Budapest, Muzeum krt. 4/a, Hungary.

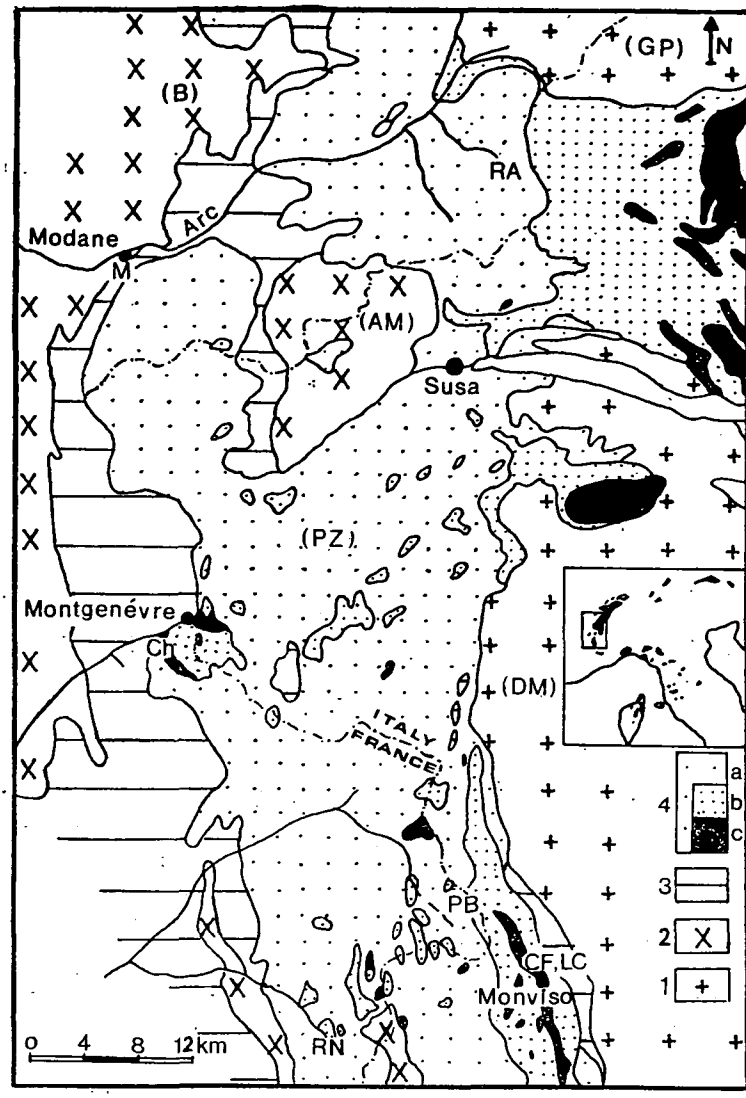

Fig. 1. Tectonic sketch map of the internal Western Alps showing the location of the main ophiolite complexes. 1. Dora-Maire (DM) and Gran Paradiso (GP) continental units (European Paleomargin), 2. Vanoise, Ambin (AM) and Brianconnais (B), continental units (European Paleomargin) Mesozoic epicontinental covers, 4. Piedmont Zones (PZ): Schistes Lustres'nappe (Mesozoic, mainly oceanic material): a. undifferentiated metasediments with subordinate ophiolites; b. ophiolite complex with minor metasediments; c. metagabbro bodies.

Location of samples: RA=Réfuge d'Averole; PC=Pre clos la Clapera; CP–MC=Carrieres du Paradis-Mont Cenis; PB=Petit Belvedere; LL=Lago Lausetto; CF=Colleto Fiorenza; C=Chenaillet

Some of these metavolcanics are partly escaped from the strong Alpine deformation while others have no primary minerals of features. Belonging to the Combin and Zermatt-Saas Units they are in different structural and stratigraphic settings compared with other parts of the ophiolite sequences (peridotite, gabbros and metasediments).

The overlying Combin unit displays pre-ophiolitic basal complex of Triassic to Liassic age with epicontinental affinity coverd by a thick volcanoclastic ophiolite bearing sequence (DAL PIAZ, 1974; DAL PIAZ *et al*, 1981; BEARTH, 1967; ETLER, 1971) which consists of metasediments and interbedded basaltic metavolcanics. This unit is also implied its relationship with other ophiolite sequences and characterized by an ocean-floor metamorphism which was overprinted by greenschist facies (HUNZIKER, 1974; DAL PIAZ *et al.* 1981).

The underlying Zermatt-Saas unit consits of basal serpentinite, gabbro capped by retrograde eclogitic basalt and garnet-bearing metasediments (BEARTH, 1973; DAL PIAZ, 1974; DAL PIAZ *et al.*, 1978, 1981). This unit has been deformed and affected by HP-metamorphism and greenschist facies conditions and are considered as oceanic crust (BEARTH, 1967, DAL PIAZ, 1974, DAL PIAZ *et al.*, 1978, 1981. e.t.c.).

The Monviso metavolcanics show three successive Alpine metamorphic stages characterized by eclogitic, blueschist and greenschist facies. They include fine grained eclogitic metabasalts and banded metabasites (garnet-bearing glaucophanites and prasinites). From few cm-s up to several dm-s thick eclogitic metabasalts collected in Colletto Fiorenza, are crosscut by smaragditic metagabbros and younger albite

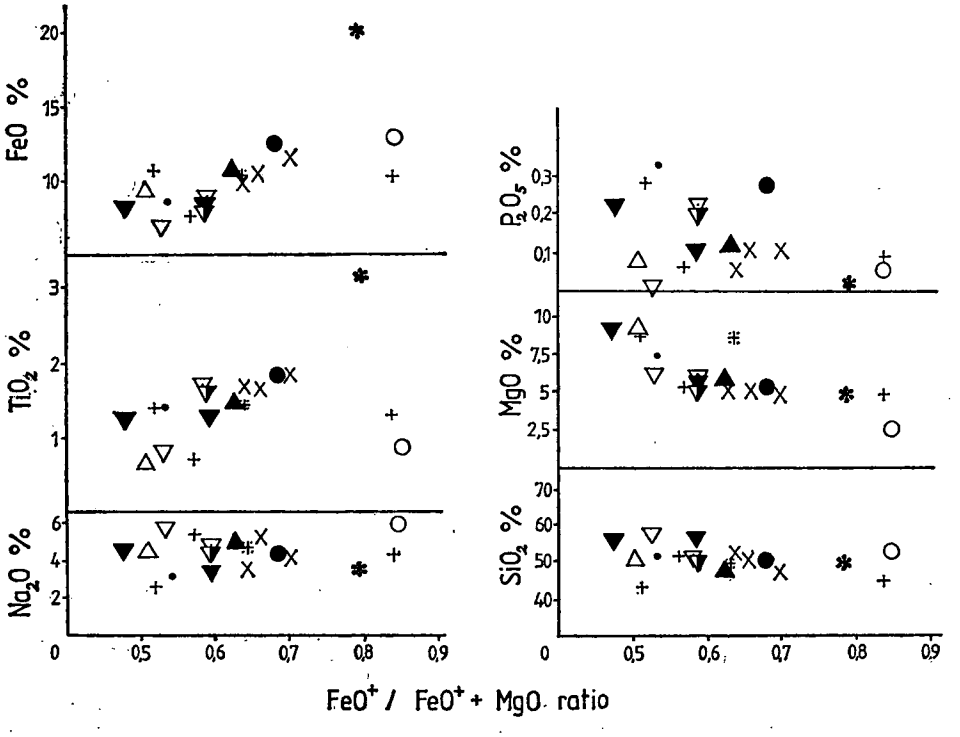

Fig. 2.: Major element oxide wt% versus $FeO^+/FeO^+ + MgO$ ratio diagram for ophiolitic metavolcanics from Western Alps. (Symbols as in Table 1)

veins. The garnet-bearing glaucophanite in Petit Belvedere is usually heterogeneous and it shows banded layering. The prasinite (Lago Lausetto) represents a homogenous thin layer (mm-scale) which differs in colour and mineral composition. The Monviso metavolcanics appear to belong to the Zermatt-Saas unit.

The Arc-valley metavolcanics of Combin unit consist of up to several hundered meters thick homogeneous prasinite which sometimes overlies on a thin ovardite level (the ovardite occurs as some thin interlations, too) and usually associate with garnet-bearing glaucophanite. They problably correspond to submarine flows, hyaloclastites and tuffites.

The metavolcanic sequence of Montgenévre represents the best preserved ophiolite complex in the Western Alps (BERTRAND *et al.*, 1987) and occurs as a separate tectonic unit. The pillow lavas are detached from the gabbros by a shear zone and sporadically contain serpentinite lenses.

PETROGRAPHY

The primary and secondary mineral assemblages, texture and metamorphic facies of the discussed metavolcanics are summarized in Table 1.

CHEMISTRY

Twelve selected metavolcanic samples collected from Monviso, Arc valley and Montgenévre in Western Alps were analysed. With the aim of the comparison we adapted six published analyses, as well. The location of samples are plotted in *Fig. 1.* and the chemical data appear in Table 2.

a) Analytical Methods

The silica was determined thermogravimetrically using the SAJO's method (1955). The ferrous Fe was analysed by HOFFMANN's method (301/87 OTH Patent). Ferric Fe was computed by the difference between FeO and total Fe, Al, total Fe, Mg, Ca, Na, K and Mn were measured by atomic absorption spectrophotometry. Other elements were determined by spectrophotometric method. H_2O, CO_2, and SO_2 were analysed by DTA method. The analyses were carried out by L. Hoffmann in the Department of Petrology and Geochemistry, Eötvös L. University, Budapest.

b) Results

The analysed HP-facies metavolcanics include 2 eclogitic metabasalts of Monviso (COMPAGNONI *et al.*, 1988) and 3 garnet-bearing glaucophanites of Monviso and Arc valley (Table 2).

The eclogitic metabasalts have large amounts of SiO_2 (50.61*/Al_2O_3/15.6*) and Mno (0.48*) and small amounts of FeO^+(8,47*) and TiO_2 (1,4*).

The garnet-bearing glaucophanite of Monviso differs from those of Arc valley in its much higher TiO_2 (3.23*) and FeO^+ (20.38*) and much lower Al_2O_3 (8.67*) and Na_2O (3.65*) content, which may be ascribed to the abundance of Fe—Ti rich

TABLE 1

Main petrographic features of representative rocks from Western Alps metavolcanics

Rock name	Texture	Main primary minerals (magmatic and late-stage primary)	Main secondary minerals (hydrothermal and metamorphic)	Metamorphic facies
		1. MONVISO: *Coletto Fiorenza*		
Eclogitic metabas.	porph, gran	cpx	omp, gar, rut, clinoz, glau, Mg-chl, leuc, ab, phen, actin, Fe-chl,tit.	Eclogitic f.
		Petit Belvedere		
Gar.-bearing glaucophanite	granone-matobl, poikil, sch.		glau, leuc, ep, chl, ab, stilp, actin, gar.	Glaucophane schist f.
Greenschist	poikil, nematobl.		actin, chl, ab, tit, clinoz, cc.	Greenschist f.
		Lago Lausetto		
Prasinite	poikil,		ab, chl, ep, glau, actin, phen, rut-tit.	Greenschist f.
		2. ARC VALLEY		
Gar.-bearing Glaucophanite	granone-matobl, poikil, sch.		glau, ep, chl, ab, gar, tit, phen, cc, qz, bio.	Glaucophane schist f.
Prasinite	poikil, sch.		ab, ep. actin, rieb, glau, chl, rut-tit, cc, phen, bio.	Greenschist f.
Ovardite	poikil, porp, gne.		ab, Fe-chl, glau, actin, ep, cc, rut-tit, phen, qz±gar.	Greenschist f.
		3. MONTGENÈVRE: *Chenaillet*		
Metabas. pill. lava	inters, porp, aphy, que, vario, arb, ves.	cpx, pl	ab, chl, preh, ep, cc±zeol, pump.	
Metabas. pill. breccia	inters, aphy, vario	cpx, pl,	epi, preh, chl, ab, hem± pump.	low-grade met.-ocean floor met.
Metadol. lava flow and dyke	vario, su-boph, interg,	ol, cpx, pl.	ab, chl, leuc, cc±preh	Prehn.-pump. and greenschist facies
Microgabbro	hypid	cpx, pl. hb.	chl, actin-trem, leuc, ap, saus.	

HP met. to low-grade met.

Abbreviations: ol: olivine; cpx: clinopyroxene; pl: plagioclase; omp: omphacite; glau: glaucophane; actin: actionlite; trem: tremolite; rieb: riebeckite; hb: hornblende; ep: epidote; clinoz: clinozoisite; chl: chlorite; preh: prehnite; cc: calcite; ap: apatite; hem: hematite; leuc: leucoxene; rut: rutile, tit: titanite; bio: biotite; phen: phengite; stilp: stilpnomelane; gar: garnet; ab: albite; qz: quartz; pump: pumpellyite; zeo: zeolite; saus: saussurite; porp: porphyroblastic; poikil: poikiloblastic; nematobl: nematoblastic; granonematobl: granonematoblastic; gran: granular; hypid: hypidiomorphic, suboph: subophitic; inters: intersertal; interg: intergranular; sch: schistose, gne: gneissose; que: quench, vario: variolitic; arb: arborescent; ves: vesicular; metabas: metabasalt; pill: pillow; metadol: metadolerite; f: facies

Locality	Arc valley								
	Carrieres du Paradis			Refuge d'Averole		Pre clos la Clapera		Carrieres du Paradis	
Rock name	Prasinites			Ovardites Bocguet 1974				Glaucophanites Bocguet 1974	
Symbols & Sample No.	×1	×2	×3	+4	+5	+6	7 (3)	⊙8	9(4)●
SiO_2	47.94	50.95	51.81	52.13	44.55	42.75	49.80	53.05	51.46
TiO_2	1.85	1.66	1.71	0.72	1.33	1.41	1.43	0.90	1.84
Al_2O_3	15.95	15.74	14.92	14.72	13.01	11.23	16.88	16.9	14.68
Fe_2O_3	3.80	3.89	0.95	0.92	7.54	2.01	5.78	10.49	5.48
FeO	7.89	6.56	9.04	6.34	2.70	8.84	4.57	2.92	6.58
MnO	0.17	0.16	0.15	0.14	0.13	0.13	0.17	0.09	0.20
MgO	4.96	5.28	5.55	5.42	5.01	9.92	5.90	2.44	5.76
CaO	8.07	3.99	4.45	5.87	11.96	11.85	6.27	5.16	6.06
Na_2O	4.12	5.32	3.57	5.39	4.32	2.56	4.90	6.02	4.45
K_2O	0.70	0.23	1.73	0.10	0.15	0.82	0.48	0.93	0.80
H_2O^+	3.10	4.20	3.58	7.60	2.30	2.85	3.52	0.73	2.09
H_2O^-	0.3	0.60	0.35	0.40	0.4	0.70	0.05	0.36	0.05
CO_2	0.7	1.60	2.14	3.0	5.76	4.28	—	—	—
P_2O_5	0.11	0.11	0.06	0.07	0.09	0.29	—	0.04	0.29
SO_2	0.10	—	—	—	—	—	—	—	—
Σ	99.76	100.29	100.01	99.82	99.25	99.64	99.75	100.03	99.74

n.d.: non detected
( ): number of analyses

oxide. As these chemical features are also recognized in some Fe—Ti rich gabbros observed in the same area (in press) and in the others within the Alpine-Apennine belt (Baccaluva *et al.*, 1977, Lomberdo *et al.*, 1978, 1982, Dal Piaz *et al.*, 1981, Bertrand *et al.*, 1987), we can expect that both the glaucophanites and Fe—Ti gabbros were probably derived from the same magma.

The analysed greenschist facies metavolcanics are as follows: 1 greenschist (Monviso), 4 prasinites (Monviso and Arc valley) and 4 ovardites (Arc valley).

The greenschist has a higher MgO (9.15*) and lower TiO_2 (0,62*) and FeO^+ (9.83*) contents.

The prasinite from Monviso is characterized by a higher Al_2O_3 (19.01*), MgO (6.01*) and K_2O (3,46*) and a lower TiO_2 (1,4*) content than that of the samples collected in the Arc valley. The higher values of Al_2O_3 and MgO may be attributed to the diluation of plagioclase and olivine accumulation. The high TiO_2 content may due to the abundant phengite. The prasinites (from Arc) cover a wide compositional ranges of SiO_2 (47.94—51.8*), FeO^+ (9.99—11.69*), CaO (3.99—8.07*) and CO_2 (0,7—2.14*) and also those elements whitch are relatively stable during the alteration, such as P_2O_5 (0.06—0.11*) and TiO_2 (1.66—1.85*). Their higher Al_2O_3

TABLE 2

volcanic sequence of Western Alps

Monviso				Montgenévre				
Petit Belvedere		Coletto Fiorenza	Lago Lausetto	Chenaillet				
	Green-schist	eclogitic metabas.	Prasinite	Metadolerite flow and dyke		Basaltic pill. lavas		
		COMPAGNONI *et al.*, 1988.		BERTRAND *et al.*, 1987		BERTRAND *et al.*, 1987		
★10	△11	·12(2)	▲13	▽14	15(9)▽	▼16	▼17	▼18(11)
50.05	50.63	50.61	47.62	57.00	51.25	56.20	56.43	50.16
3.23	0.62	1.40	1.40	0.81	1.68	1.25	1.29	1.62
8.67	13.36	15.60	19.01	13.52	15.35	10.41	11.64	15.79
12.52	2.97	1.40	10.46	1.57	2.59	1.94	2.92	2.43
7.84	6.42	7.07	n.d.	5.53	6.00	6.28	5.66	6.13
0.23	0.11	0.48	0.10	0.10	0.19	0.14	0.16	0.15
5.33	9.15	7.44	6.01	6.32	6.18	9.05	5.96	5.95
6.76	6.63	10.63	3.51	5.91	7.87	6.83	8.33	8.33
3.65	4.62	3.31	5.00	5.85	4.55	4.81	5.16	4.95
0.10	0.11	0.27	3.46	0.10	0.11	0.10	0.10	0.04
0.90	3.40	—	—	1.33	2.76	2.60	1.40	3.51
0.20	1.00	1.07	2.9	1.00	—	0.60	0.20	—
—	—	—	—	—	0.95	—	—	0.61
0.03	0.09	0.34	0.12	0.06	0.23	0.23	0.11	0.20
0.15	—	—	—	—	—	—	—	—
99.51	99.11	99.62	99.59	99.00	99.70	100.34	99.26	99.87

(14.72—15.95*) and CaO (3.99—8.07*) contents may attributed to the diluation of the plagioclase.

The Arc valley ovardites also show largely variable SiO_2 (42.75—52.13*), FeO^+ (7.26—10.85*), CaO (5.87—11.96*), P_2O_5 (0.07—0.29*) and TiO_2 (0.72—1,43*) contents. The ovardite at Pre clos la Clapera has a significantly higher MgO content (9.92%) than the other ovardites of the Arc area, which suggest their strong dilution effect by olivine accumulation or fractionation.

The chemical features of both prasinites and ovardites are well compared, however, revealed certain significant differences themselves to be excepted in view of the ovardites. MgO, CaO, CO_2 contents are higher, while TiO_2 content is lower than the mean for prasinites. This is probably ascribable to the particulary high chlorite and calcite content in the ovardites.

The analysed samples from Mongenévre represent 1 metadolerite pillow and 2 basaltic pillow lavas (margin and core) compared with their averages (BERTRAND *et al.*, 1987). The metadolerite pillow flow is characterized by higher values of SiO_2 (57.0*) and Na_2O (5.58*) and by lower values of TiO_2 (0.81*), FeO* (7.71*), Al_2O_3 (13.52*) and P_2O_5 (0.14*), than the average given by BERTRAND *et al.* (1987).

The basaltic pillow lavas have a significantly higher SiO_2 (56.2—56.43*) and lower TiO_2 (1.25—1.29*) and Al_2O_3 (10.41—11.64*) range than the average (BERTRAND *et al.* 1987).

It is interesting that the pillow lava margin has fairly higher MgO and H_2O and lower Al_2O_3, total FeO, CaO and Na_2O contents than the core has.

All these geochemical features can be attributed probably to the variant influence of the metasomatic metamorphism.

DISCUSSION

Major element composition (Table 1.) and their variation againts $FeO^+/FeO^+ + +MgO$ ratio of the metavolcanic rocks from Western Alps are shown in *Fig. 2.* Generally, the total FeO* and TiO_5 content are rapidly increased, Na_2O^* is constant while the MgO*, $P_2O_5^*$ and SiO_2^* are decreased with the increasing $FeO^+ + MgO$ ratio. The garnet-bearing glaucophanites are largely scattered which may be attributed to their different tectonic setting and mineralogic compositions.

The AFM diagram *(Fig. 3.)* applied by STRONG and MALPAS (1975) represents a tholeiitic differentiation. Some of the investigated metavolcanic rocks are tholeiitic character, while the others show calc-alkaline affinity because of their metamorphic effects and mixing with oceanic floor sediments. They mostly fall within the sheeted dyke and lava fields of the STRONG's and MALPAS's (1975) diagram. The garnet-bearing glaucophanites from Monviso, due to its higher content of total FeO which can be attributed to the dominance of the Fe-rich oxides, occur near the F-pole. Two samples of prasinites and one of dolerite flow have a more alkalic charcater than the others, indicating a more significant influence of the metamorphism.

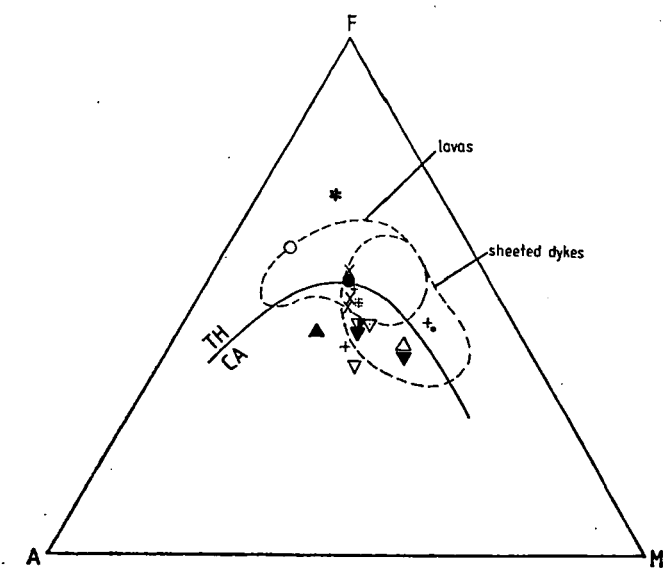

Fig. 3. AFM diagram (STRONG and MALPAS, 1975) for the ophiolitic metavolcanics from Western Alps. (Symbols as in Table 2.)

*: weight percentage $FeO^+ : FeO^* + Fe_2O_3^*$

The TiO_2 vs. P_2O_5 and the TiO_2 vs. FeO^+/MgO diagrams applied by BASS *et al.* (1973) and HEKINIAN and THOMPSON (1976), present the differentitation trend of the ophiolitic basaltic rocks *(Fig. 4.)*. In the diagram of TiO_2 vs. P_2O_5, the metavolcanic rocks are situated in the oceanic ridge basalt field showing a constant precipitation of apatite during the volcanic differentation. In the TiO_5 v. FeO^+/MgO diagram, the metavolcanics more or less correspond to the trend of the abyssal tholeiites showing an increasing TiO_2 content, together with the increasing FeO^*/MgO ratio. The garnet-bearing glaucophanite from Monviso in it higher content of TiO_2

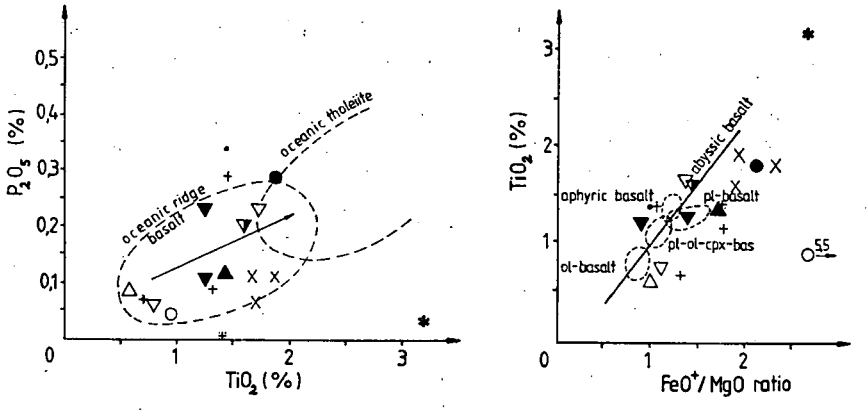

Fig. 4. (a) P_2O_5 wt% versus TiO_2 wt% diagram (HEKINIAN *et al.* 1976) and (b) TiO_2 wt% versus FeO^t/MgO ratio diagram (BASS *et al.* 1973) for the ophiolitic metavolcanics from Western Alps. (Symbols as in Table 2.)

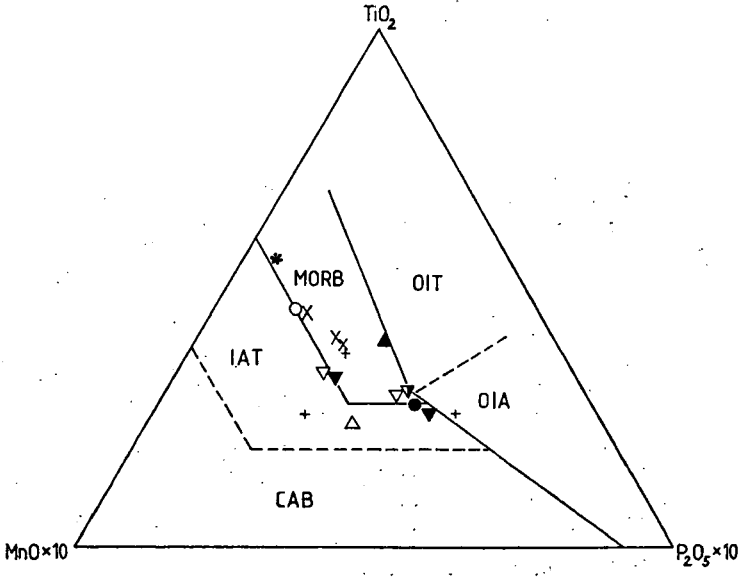

Fig. 5. $MnO \times 10$—TiO_2—$P_2O_5 \times 10$ diagram (MULLEN, 1983) for the ophiolitic metavolcanics from Western Alps. MORD=mid ocean ridge and marginal basin basalts, IAT=island arc tholeiites, CAB=calc-alkaline basalts, OIA=oceanic island alkalic basalts. (Symbols as in Table 2.)

and total FeO (which can be attributed to the abundance of Ti—Fe rich oxides) differs from that of the Arc valley rocks.

The TiO_2—$MnO \times 10 - P_2O_5 \times 10$ diagram *(Fig. 5.)* was initiated by MULLEN (1983) for the distinction of the tectonic settings of the basaltic and andesitic rocks. In this diagram, the metavolcanics of the Western Alps are almost situated in the MORB and Island Arc Tholeiites fields.

CONCLUSIONS

The Western Alps metavolcanics are distributed in both Combin and Zermatt-Saas units of the Piedmont metaophiolite. Three metavolcanic areas (Monviso, Arc valley and Montgenévre) in the Western Alps were investigated geochemicaly.

The metavolcanics of the Monviso and Montgenévre in the Zermatt-Saas unit show mostly oceanic crust origin. The Arc valley metavolcanics in the Combin unit are represented by basaltic metabasites (prasinites, ovardites and glaucophanites) and most of them probably consist of lava flows, hyaloclastites. tuffites and minor sills settled in Mesozoic calc-schists (DAL PIAZ, 1974).

The investigated metavolcanics from Western Alps, due to the significant changes in the mineral abundances, show a large variation in the bulk composition. This probably reflects an effect of the Alpine and sea-floor metamorphism. They are roughly comparable to MORB (HEKINIAN and THOMPSON, 1976; SUN *et al.*, 1979; WOOD *et al.*, 1979 b; LANGMUIR and BENDER, 1984), and a few metavolcanics belong to the Island Arc Tholeiites (as shown in MULLEN's 1983 diagram). They also show a geochemical characteristic prevalently similar to that of the oceanic ridge basalts (BASS *et al.* 1973) and differentiation path typical for abyssal tholeiites (HEKINIAN *et al.* 1976).

Morever, evidence for happened, distrinctive metamorphic and tectonic processes the oceanic stage can be recognized (MÉVEL *et al.* 1978; BERTRAND *et al.* 1985; TRICART and LEMOINE 1986).

REFERENCES

BACCALUVA, L., OHNENSTETTER, D., OHNENESTETTER, M., NENTURELL, G. (1977): The trace element geochemistry of Corsican ophiolites. — Contr. Miner. Petrol. **64,** 11—31.

BASS, M. N. et al. (1973): Volcanic rocks cored in the Central Pacific. — Leg. 17, Deep Sea Drilling Project. — In Initial Reports D. S. D. P. U. S. Govt. Prtg. Office, **17,** 429—503.

BEARTH, P. (1967): Die Ophiolite der Zone von Zermatt-Saas Fee. Beitr. Geol. Karte Schweiz, N. F. **132,** 130 p.

BEARTH, P. (1973): Gesteins- und Mineralparagenesen aus den Opthioliten von Zermatt. — Schweiz. Miner. Petrogr. Mitt. **53,** 299—334.

BERTRAND, J., COURTIN, B., VUAGNAT, M. (1981): Le massif ophiolitique du Montgenévre (Hautes-Alpes, France, et province du Turin, Italie): Données nouvelles sur un vestige de manteau supérieur et de croute océanique liguro-piemontai. — Bull. Suisse Mineral. Petrogr. **61,** 305—322.

BERTRAND, J., COURTIN, B., VUAGNAT, M. (1982): Elaboration d'un secteur de lithosphére océanique liguro-piemontais d'aprés les données de l'ophiolite du Montgenévre (Hautes-Alpes, France et province de Turin, Italie). — Ofioliti. **7,** 155—196.

BERTRAND, J., DIETRICH, V., NIEVERGELI, P., VUAGNAT, M. (1987): Comparative major and trace element geochemistry of gabbroic and volcanic rock sequences. Mongenévre ophiolite, W. Alps. — Schweiz. Mineral. Petrogr. Mitt. **67,** 147—169.

BERTRAND, J., NIEVERGELT, P., VUAGNANT, M. (1985): Interprétation paléo-oceanique d'une série pélagique *a* matériel ophiolitique: la série de Chabriére, complex de bese du massif ophiolitique du Mongenévre (Alpes occidentales). — C. R. Acad. Sc. Paris. **301,** 11/16, 1199—1204.

BOCQUET, J. (1974): Etudes mineralogiques et petrologiques sur métamorphismes d'age alpin dans les Alpes francaises. Thése Univ. Grenoble, 489 p.
COMPAGNONI, R., KIENAST, J. R., LOMBARDO, B. (1988): The Monviso eclogitic metaophiolite (Cottian Alps); in the IGCP Excursion to the Alps: HP eclogitic reequilibration in the W. Alps, Part **1**, 81—112.
DAL PIAZ, G. V. (1974): le métamorphisme de haut pression et basse temperature dans l'veolution du bassin ophiolitique alpine-apenninique (1 ére partie: considerations paléogeographiques). — Bull. Soc. Geol. It. **93**, 437—468.
DAL PIAZ, G. V., ERNST, W. G. (1978): Areal geology and petrology of eclogites and associated metabasites of the Piemonte ophiolite nappe, Breuil-St Jacques area, Italian W. Alps. — Tectonophys. **51**, 99—126.
DAL PIAZ, G. V., VENTURELLIS, G., SPADEA, P., BATTISTINI, G. Di. (1981): Geochemical features of metabasalts and metagabbros from the Piemonte ophiolite nappe, Italian W. Alps. — N. Jb. Miner. Abh. **142**, 3, 248—269.
DEN TEX, E. (1987): Two ovardite occurrence in the Piemonte Ophiolite Nappe of the Cottian Alps (NW. Italy) and their significant for the process of ovarditization. — Schweiz. Mineral. Petrogr. Mitt. **67**, 137—146.
ELTER, G. A. (1971): Schistes lustrés et ophiolites de la zone piemontaise entre Orco et Doire Baltrée Alpes Graies. — Geol. Alpine. **47**, 147—169.
HEKINIAN, R., THOMPSON, G. (1976): Comparative geochemistry of volcanics from rift valleys transforms and aseismic ridges. — Contr. Mineral. Petrol. **57**, 145—162.
HEKINIAN, R., MOORE, J. G., BRYAN, W. B. (1976): Volcanic rocks and processes of the Mid Atlantic Rift-Valley near 36° 49' N. — Contr. Mineral. Petr. **58**, 83—110.
HUNZIKER, J. C. (1974): Rb-Sr and K-Ar age determination and the Alpine tectonic history of the W. Alps. — Mem. Ist. Geol. Miner. Univ. Padova **31**, 54 p.
JEFFERY, P. D., HUTCHISON, D. (1981): Chemical Methods of rock analysis. Pergamon Press.
LANGMUIR, C. H., BENDER, J. F. (1984): The geochemistry of oceanic basalt in the vicinity of transform faults: observation and implications. — Earth. Planet. Sci. Lett. **69**, 107—127.
LEARDT, L., ROSSETTI, P., CRISCI, G. M. (1986): Greenschist altered metabasalts (ovardite) from Torre D,Ovarda (Val D'Ala, Graian Alps). — Ofioliti. **11**, (3), 263—274.
LEWIS, A. D., SMEWING, J. D. (1980): The Mongtenévre ophiolite (Hautes Alpes, France): metamorphism and trace-element geochemistry of the volcanic sequence. — Chem. Geol. **28**, 291—306.
LOMBARDO, B., COMPAGNONI, R., MESSIGA, B., KIENAST, J. R., MÉVEL, C., FIORA, L., PICCARDO, G. B., LANZA, R. (1978): Osservazioni preliminari sulle ofioliti metamorfiche del monvsio (Alpi occidentali). — Rend. Soc. It. Min. Petrol. **42**, 2, 253—305.
LOMBARDO, B., POGNANTE, U. (1982): Tectonic implications in the evolution of the W. Alps ophiolite metagabbros. — Ofioliti **2/3**, 371—394.
MÉVEL, C. (1975): les zonations chimiques dans les pillowlavas spilitiques du Chenaillet et des Gets (Alpes francaises). — Petrologie. **1**, 319—333.
MÉVEL, C., CABY, R., KIENAST, J. R. (1978): Amphibolite facies conditions in the oceanic crust: example of amphibolitized flaser-gabbro and amphibolite from Chenaillet massif (Hautes Alpes, France). — Earth. Planet Sci. Lett. **39**, 98—108.
MULLEN, D. E. (1983): $MnO/TiO_2/P_2O_5$: a minor element discriminant for basaltic rocks of oceanic environments and its implications for petrogenesis. — Earth Planet. Sci. Lett. **62**, 53—62.
NISIO, P. (1985): Les domains d'antiphase des omphacite's et la petrologie des eclogites: contribution *a* l'étude de l'evolution tectonométemorphique du Monviso (Alpes italiennes occidentales). These Univ. Claude Bernard, Lyon, 137 p.
NISIO, P., LARDEAUX, I. M. (1987): Retromorphic Fe-rich talc in low T. eclogites: example from Monviso (Italian W. Alps). — Bull. Miner. **110**, 427—437.
SAJO, I. (1955): Acta Ch. Acad. Sci. Hung. **6**, 245 p.
STRONG, D. F., MALPAS, J. G. (1975): The sheeted dyke layer of the Betts Core Ophiolites Complex does not represent spreading-further discussion. — Can. J. Earth. Sci. **12**, 844—896.
SUN, S. S., NESBITT, R. W., SHARASKIN, A. Y. (1979): Geochemical characteristics of mid-ocean ridge basalts. — Earth. Planet. Sci. Lett. **44**, 119—138.
TRICARD, P., LEMOINE, M. (1986): Mégboudinage alpine et fracturation téthysienne dans les Schistes lustrés piemontais *a* l'Ouest du Mont Viso (Alpes occidentales). — C. R. Acad. Sci. Paris. **302**, II/8, 599—604.
WOOD, D. A., TARNEY, J., VARET, J., SAUNDERS, A. D., BOUGAULT, J. R. (1979b): Geochemistry of basalts drilled in the N. Atlantic by IPOD Leg 49, — Earth. Planet. Sci. Lett. **42**, 77—97.

Manuscript received, 30 May, 1989

Acta Mineralogica-Petrographica, Szeged, XXX, 67—79, 1989

TEXTURAL FEATURES AND MODES OF ULTRAMAFIC XENOLITHS FROM SITKE, LITTLE PLAIN (HUNGARY)

Cs. SZABÓ*—O. VASELLI**

* Department of Petrology and Geochemistry, Eötvös University
** Department of Earth Sciences, University of Florence

ABSTRACT

Several upper mantle xenoliths from Sitke (Little Hungarian Plain) have been studied. This locality is one of the important sites of the Early Tertiary volcanic activity in the Little Hungarian Plain. The Sitke's volcanic apparatus is consisting of a tuff-ring which is characterized by the occurence of fragments of olivine nephelinitic host rock. The tufaceous layers and fragments are often including nodules consisting generally of spinel lherzoliths, while dunitic and harzburgitic composition occur rarely. Two special xenoliths, one with a pure spinel-vein and another with considerable amphibole and clinopyroxene content, have been found, as well.

Based on the textural investigation it can be proved that the porphyroclastic and equigranularic textures prevail and the transitional textures between them also exist. The two specific nodules are considered to be metasomatically originated in the upper mantle.

INTRODUCTION

A typical within plate basaltic activity (EMBEY-ISZTIN, 1980) took place during Pliocene in the Carpatho-Pannon region and this volcanic event lasted until the Pleistocene (JÁMBOR *et al.*, 1981; BALOGH *et al.*, 1986). The basaltic volcanism shows an alkaline character, its products contain many inclusions originated in the upper mantle and lower crust. The nodules are distributed in the following areas: (1) Graz Basin (KURAT *et al.*, 1980; DIETRICH and POULTIDIS, 1985), (2) Little Hungarian Plain (RICHTER, 1971; EMBEY-ISZTIN, 1978; SZABÓ, 1982; KUBOVICS *et al.*, 1985; EMBEY-ISZTIN *et al.*, 1989). (3) Balaton Highland (EMBEY-ISZTIN, 1976/a, 1978, 1984; BÉRCZI and BÉRCZI, 1986; EMBEY-ISZTIN *et al.*, 1989, (4) Nógrád-Gemer (Gömör) (HOVORKA, 1978; HOVORKA—FEJDI, 1980; KUBOVICS *et al.*, 1985, 1988), (5) PERSANY (PERSÁNYI) Mts. (MALDARESCU *et al.*, 1983; BÉRCZI, 1988) *(Fig. 1)*.

This paper presents the first part of a set of petrographical, petrological and geochemical studies. It describes the large suite of ultramafic xenoliths and their host rock from Sitke (Little Hungarian Plain) carrying useful information about the the nature, and the compositional feature of the upper mantle and its processes.

LOCALITY

The Sitke volcanism producting large amounts of pyroclastics *(Fig. 2)* belongs to the Little Hungarian Plain (LHP) volcanic field. Its eruptive centres are situated close to the Rába-line and in a N—S zone between Pauliberg (Pálhegy) and Güssing (Németújvár) (JUGOVICS, 1972).

* Múzeum krt 4/a H—1088 Budapest
** Via G. La Pira 4 I—50121 Florence

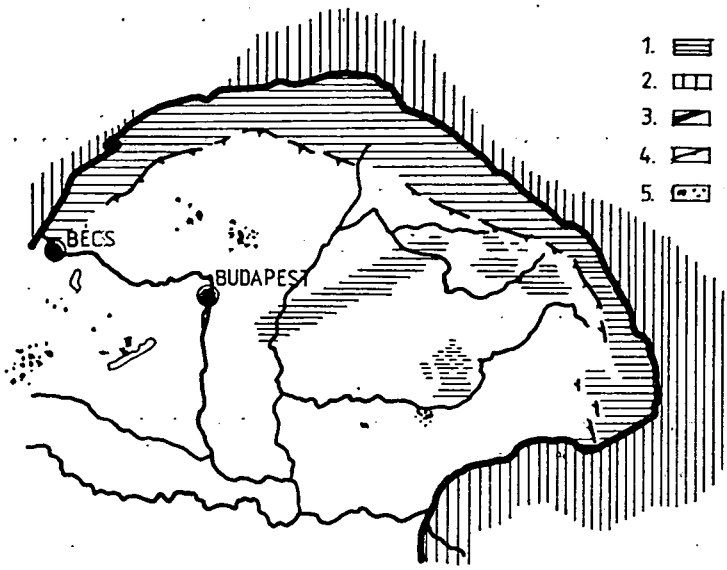

Fig. 1. Distribution of the Pliocene-Pleistocene alkaline basalt including upper mantle xenoliths in the Carpatho-Pannon region.
1 — flysh, 2 — Carpathian foredeep, 3 — contour of the Carpathian fold system, 4 — Klippen belt, 5 — alkaline basalt with upper mantle xenoliths

The Sitke volcanic activity started at least 4,25 M. y. ago. Lava flows and dikes were recognized only on the Hercseghegy *(Fig. 2)* that can be considered one of the eruptive centres (JUGOVICS, 1972). The pyroclastic series overlie the Upper Pannonian micaceous sandy and clay beds. This superposition indicates a correlation between the stratigraphical situation and radiometric data (JUGOVICS, 1972; JÁMBOR *et al.*, 1981).

The Sitke volcanic building can be studied in numerous quarries on the Belsőhegy and Hercseghegy *(Fig. 2)*. As the xenolith associations show the greatest quantity and highest variability in the Belsőhegy quarry *(Fig. 2)* we focused our investigations on this site. It is regarded as a representative outcrop of the Sitke tuffring.

The locality is a 7 m high and about 120 m long quarry front. The well-bedded host pyroclastic series (grain size is less than 4 cm) are devided into two levels by a 50 cm thick lavabreccia layer which appears in the middle part of the wall. The layers are subhorizontal. The lavabreccia consists of fragments of host rock and a lot of ellipsoidal to spheroidal shaped ultramafic xenoliths. The nodules have generally a mean size of 7 cm in diameter but they sometimes can reach 12 cm, too. Most of the lava fragments indicate high degree of carbonatization containing grains of calcite in the cracks, pores and amygdals. In addition, some small-sized (0.5 cm) olivine-rich inclusions have been recognized, as well. The series settled over and under the lavabreccia are built up by unconsolidated tuffic pyroclsatics, which are nearly barren in xenoliths, except the uppermost level where greater dimension (9 cm) nodules can be found. The nodules derived from the various levels do not show any substantial difference.

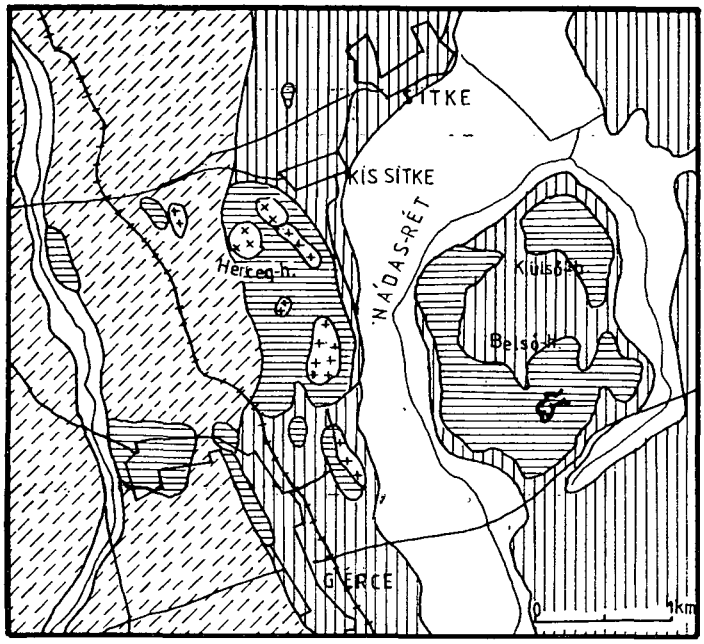

Fig. 2. Geological map of Sitke and adjacent area (JUGOVICS, 1972) 1 — Upper Pannonian sand and clay, 2 — basaltic tuffs, 3 — massiv basaltic rock, 4 — vesicular basaltic rock, 5 — Pleistocenian pebble, 6 — sampling points

HOST ROCK

Fragments of the fresh massive lava collected for the analytical purpose have a porphyritic texture with trachytic character. Proportion of the phenocrysts is 13—17 vol% and a third of them is clinopyroxene. The remaining porphyroclasts are made up olivine which is partly euhedral—hedral, partly kinked. In addition, some unhedral grains of quartz (less than 2 vol%) with undulatory extention occur in every sample. This feature proves that they originated by contamination. The mesostasis commonly contains elongated, strongly zoned crystals of augite-titanaugite. Opaque minerals are rare in the glass-rich groundmass.

The Table 1 shows the major element composition of two representative Sitke samples compared with the average of other basalt localities from the LHP.

In the *Fig. 3* the Sitke samples (Belsőhegy, Hercseghegy) appear in the tephrite and basanite field in accordance with their modal mineralogical composition, while the averages of some well-known occurences (Pálhegy, Somló, Sághegy) from the LHP fall in the trachybasalt field.

The Belsőhegy sample shows an extremly high alkali character (Table 1 No 1) and considering its high normative nepheline and olivine contents it can be regarded

TABLE 1

Major element composition, CIPW norms and some petrochemical parameters of basaltoid rocks from Sitke

	1	2	3	4	5
SiO_2	45.98	48.97	48.23	43.36	46.30
TiO_2	3.60	2.54	2.06	2.31	2.30
Al_2O_3	12.33	14.98	15.58	16.28	14.34
Fe_2O_3	7.05	2.70	4.04	1.73	4.33
FeO	4.57	6.90	5.94	7.91	6.10
MnO	0.17	0.14	0.18	0.14	0.21
MgO	8.87	7.61	6.75	10.87	8.67
CaO	9.83	8.54	8.48	9.28	9.19
Na_2O	3.27	3.68	3.71	3.07	3.83
K_2O	1.89	1.92	1.85	2.19	2.56
P_2O_5	0.97	0.47	0.70	0.15	1.17
CO_2	0.00	0.00	0.00	0.00	0.00
$+H_2O$	0.98	1.49	2.77	3.19	1.00
$-H_2O$	0.00	0.00	0.00	0.00	0.00
Sum	99.51	99.94	100.29	100.48	100.00
		CIPW norms			
or	11.17	11.35	10.93	12.94	15.13
ab	23.13	27.45	29.56	3.36	17.02
an	13.38	18.69	20.40	24.17	14.38
ne	2.46	2.00	0.99	12.25	8.33
cpx	22.61	16.53	13.64	16.76	18.70
ol	8.14	12.61	10.61	20.56	12.08
mt	4.85	3.91	5.86	2.51	6.28
il	6.84	4.82	3.91	4.39	4.37
hm	3.71				
ap	2.30	1.11	1.66	0.36	2.77
M	62.01	62.90	59.13	70.69	64.00
D. I.	36.76	40.80	41.48	28.55	40.48
S. I.	34.58	33.36	30.28	42.18	34.01

1 — Belsőhegy, Sitke
2 — Hercseghegy, Sitke (JUGOVICS, 1976)
3 — Pálhegy, (10 samples, MAURITZ, 1948; SCHARBERT *et al.* 1981; POULTIDIS and SCHARBERT, 1986)
4 — Somló, (13 samples, JUGOVICS, 1976)
5 — Sághegy, (22 samples, JUGOVICS, 1976)

as an olivine nephelinite composition. Whereas its petrochemical patameters (Table 1, mg-value, D. I., S. I.) resemble to that of more evolved basaltoid rocks of Pálhegy, Somló and Sághegy and show a lot of differences from the primitive, undifferentiated Hercseghegy sample (Table 1 No 2). The above-mentioned apparent contradiction can be explained by effect of the qartz grains originated by contamination in the Belsőhegy sample, that increased the normative orthoclase and albite content. A neglecting proportion of the quartz grain in the Belsőhegy olivine nephelinite can be found this rock may have been derived from a primitive, undifferentiated melt similar to lavas which are characteristic at the Hercseghegy.

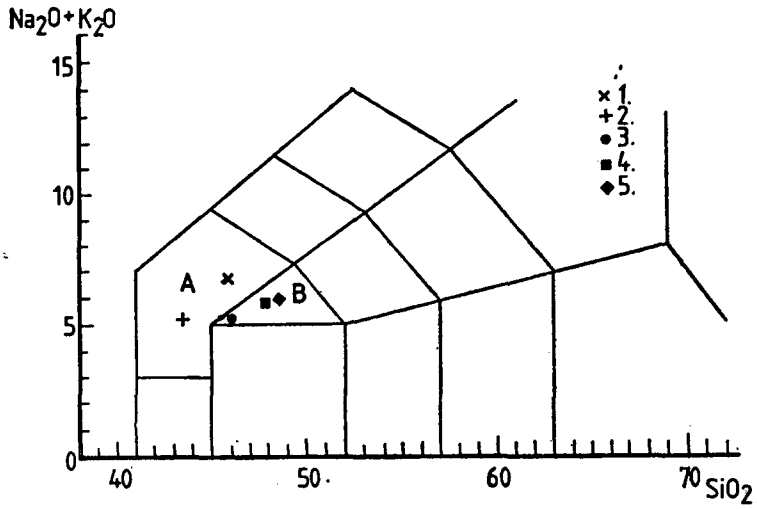

Fig. 3. TAS-diagram of the Little Hungarian Plain basaltoid rocks A — Tephrite and basanite. B — Trachybasalt, 1, 2, 3, 4, 5 symbols as in Table 1

PETROGRAPHY OF THE ULTRAMAFIC XENOLITHS

We have collected about 150 xenoliths from the Sitke tuffring situated south from the village. This sampling was completed by some specimens from Hercseghegy and from Gérce *(Fig. 2)* where some nodules have been previously studied by EMBEY-ISZTIN (1978, 1984), SZABÓ (1982), EMBEY-ISZTIN *et al.* (1989). A large amount (99%) of the studied samples described in this paper are derived from the quarry of Belsőhegy.

Modal compositions of about 40 representative xenoliths were calculated from least-squares analyses of bulk rock. The nodules display a relatively limited mineralogical variation (Table 2) and they are principally made up of olivine (40—80 vol%), orthopyroxene (9—36 vol%), clinopyroxene (5—17 vol%) and spinel (<5,5 vol%). This composition resembles to Cr-diopside group (Type I) of xenoliths (WILSHIRE and SHERVAIS, 1975), except for 3 dunites (sample No BH—60, —78, —79) and a

TABLE 2

Modal composition of some representative xenoliths from Sitke

Sample Texture	BH—04 Porphyr	BH—09* Equigr	BH—15 Equigr	BH—55 Porphyr	BH—60 Second	BH—81 Equigr	BH— 58 Porphyr
Ol	53	20	68	68	85	30	48
Opx	36	72	11	16	12	7	34
Cpx	7	4	17	8	2	36	11,5
Sp	4	4	4	8	1	10,5	4
Amph	—	—	—	—	—	6	0,5
Glass	—	—	—	—	—	10,5	2

* without spinel-rich vein.

special spinel- rich composite xenolith (sample No BH—09). In addition we have found 4 nodules (sample No BH—74, —81, —85, —90) containing amphibole grains. In the BH—81 ample the quantity of amphibole reach >6 vol%. No trace of primary plagioclase neither relic garnet were observed in the studied xenoliths.

The majority of analysed xenoliths is spinel lherzolite and harzburgite; other rock types [dunites (BH—60, —78, —79), composite xenoliths (BH—09) and amphibole-rich material (BH—81)] are rare *(Fig. 4)*.

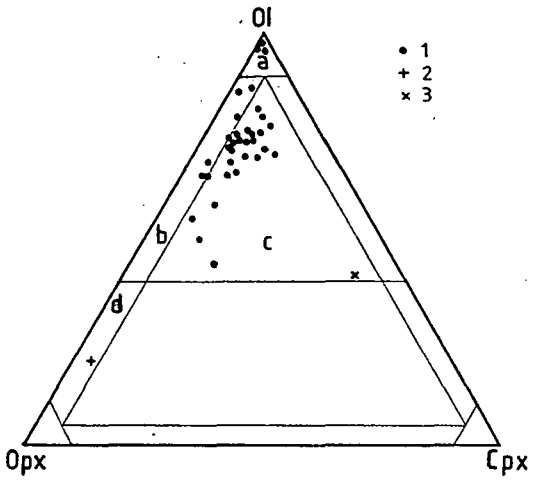

Fig. 4. Ol—Opx—Cpx diagram (STRECKEISEN, 1974) of ultramafic xenoliths from Sitke, 1 — common xenolith, 2 — composite xenolith, 3 — amphibole lherzolite xenolith, a — dunite, b — harzburgite, c — lherzolite, d — olivine orthopyroxenite

Among the secondary minerals calcite and hematite are common in the Sitke xenoliths, but the quantity of these materials is restricted. Hematite is found as a film around olivine and pyroxene grains, whereas calcite can mostly replaces a part of the olivine crystals. Both of these secondary minerals are the products of subsequent alteration.

The xenoliths commonly show an evidence of minor partial melting process along some grain boundaries or in patches. These melted zones consist of euhedral clinopyroxene and olivine crystals with euhedral spinel and yellow or red glass *(Fig. 5)*; plagioclase microlites, calcite and xenomorphic amphibole are very subordinate. The above-mentioned minerals and glass may be common in the ultramafic xenoliths (FREY and PRINTZ, 1978) and result from melting of amphibole (or phlogopite) during the rapid eruption of the host magma (FREY and GREEN, 1974; BEST, 1974).

Based on the textural studies of spinel peridotite xenoliths derived from the upper mantle four principal types were usually identified (MERCIER and NICOLAS, 1975; PIKE and SCHWARZMAN, 1977; HARTE, 1977): (1) protogranular or allotriomorphic-granular or coarse, (2) porphyroclastic, (3) equigranular or granuloblastic, and (4) secondary recristallized. (In this paper we used the Mercier-Nicolas's classification.) The main characters which permit distinction among their textural types are the following: grain size, presence or absence of porphyroclasts and their deformation, grain boundary of the silicate phases (linear, curved, ragged), shape and position

Fig. 5. Photomicrograph showing in melted zone glass, euhedral fine clinopyroxene, olivine, spinel and resorbed amphibole (amph) [BH—85, Sitke]. 1N, M=33x

of the spinel grains. Textures of the Sitke xenoliths are porphyroclastic, equigranular and transitional between these two types. In addition secondary recrystallized textures also exist. EMBEY-ISZTIN (1978) described xenoliths have protogranular-porphyroclastic transitional texture, but we have not recognized this type yet.

36% of the xenoliths display a typical porphyroclastic texture *(Fig. 6)* which is wide-spread type in upper mantle peridotites. Porphyroclasts of olivine and orthopyroxene are up to 6 mm in diameter; boundaries of these minerals are ragged and curved. Olivines have kink bends or undulatory extenction. Orthopyroxenes are usually strained and often show fine clinopyroxene exsolution lamellae in the inner part of the grains *(Fig. 7)*. Sometimes a few small euhedral olivines are enclosed by large sized othopyroxenes resembling to poicilitic texture. Neoblasts of olivine and orthopyroxene also appear in the equigranular matrix (which contains clinopyroxene and spinel). The grain boundaries of the neoblasts are linear, and the triple point

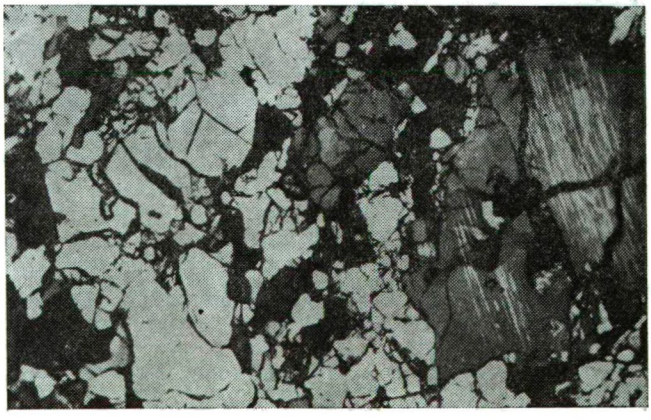

Fig. 6. Photomicrograph showing porphyroclastic texture in spinel lherzolite xenolith from Sitke [BH—74]. +N, M=20x

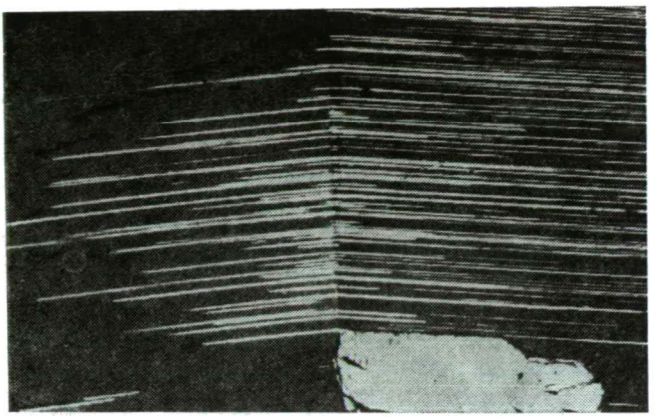

Fig. 7. Photomicrograph showing clinopyroxene exsolution lamellae and olivine inclusion in orthopyroxene in spinel lherzolite xenolith from Sitke [BH—04]. +N, M=33x

junction is characteristic. This texture appears to be the result of a polygonisation and recrystallization of the coarser grained assemblages. These minerals are very rarely strained. Spinels are chestnut brown and form holly-leaf shaped grains in the interstitial position. Xenoliths with this mentioned texture type comprise a few grains of probably pargasitic amphibole.

Relatively high ratio (22%) of the studied inclusions exhibit a typical granuloblastic texure *(Fig. 8)*. In these nodules minor olivine and/or orthopyroxene porphyroclasts occur. These grains have similar textural features to those which have been described at the previous textural groups. Excluding the rare porphyroclasts (flattening character), the average grain size of these nodules is generally less than 1.0 mm. Neoblasts of olivine and orthopyroxene have straight or smoothly curved borders and often show 120° triple point junctions. Such a feature (strain-free grains) indicate the recristallization after strong deformation. Spinel forms generally small near-spherical opaque or redbrown grains in the silicate phases, however, some of

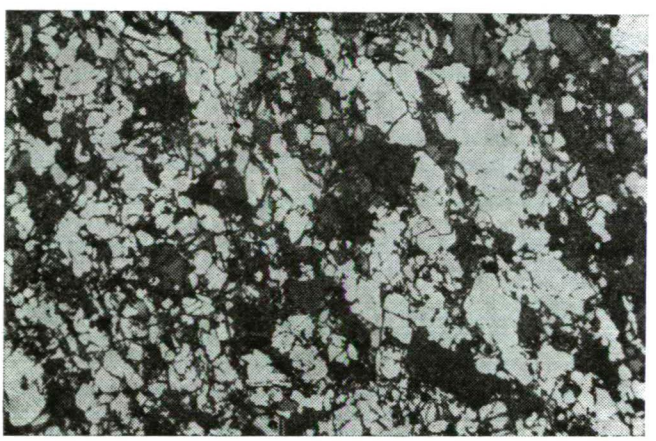

Fig. 8. Photomicrograph showing equigranular texture in spinel lherzolite xenolith from Sitke [BH—33]. +N, M=20x

them can occur as translucent holly-leaf shaped crystals surrounded with an opaque rim in the interstitial position, associated with the melted areas containing unhedral spongy clinopyroxene grains as well. In some of equigranular xenoliths the mineral grains define a weak foliation and show two dimensions markedly more flattened than the third one. So it means that the equigranular nodules can be divided into two groups: tabular and mosaic equigranular ones.

22% of the xenoliths show transitional features between porphyroclastic and equigranular types. Grain size of the strained olivine and orthopyroxene is smaller than those of porphyroclastic textured xenoliths. These nodules display no signs of foliation. The neoblasts have curvilinear boundaries and the triple point junctions are characteristic.

The proportion of pure secondary recristallized nodules compared to the primary types is subordinate (18%). Grain-size of olivine and orthopyroxene is less than 2 mm and these crystals are generally unstrained. Mineral borders are curved and linear with triple junctions. Small grains of spinel constitute spherical inclusions in olivines and orthopyroxenes. Larger spinels show amoeboid-like shape and appear in interstitial position.

Only two nodules display conspicuous differences in mineralogical composition and textural features. One is a composite xenolith (BH—09), in which an olivine orthopyroxenite is intruded by a spinel-rich vein. The olivine orthopyroxenite has mosaic equigranular texture. Among the polygonal neoblasts we found only a few strained orthopyroxene porphyroclasts with fine clinopyroxene lamellae. Several small opaque grains of spinel appears as spherical inclusion in the silicate phases. Large opaque spinel crystals form a fine vein (its width is about 1 cm) crosscutting and consuming the host peridotite *(Fig. 9)*.

The other special xenolith (BH—81) contains abundant amphibole crystals. This amphibole lherzolite has a characteristic equigranular texture with typical olivine and orthopyroxene porphyroclasts and neoblasts *(Fig. 10)*. Grains of clinopyroxene are polygonal and have sometimes display twinning and inclusion of Cr-rich spinel. The grain-size of amphiboles is less than 1.2 mm. They are brown colour and anhedral in shape. They appear in intersitial position defining nearly parallel bands. These bands also contain spinel and considerable clinopyroxene and their

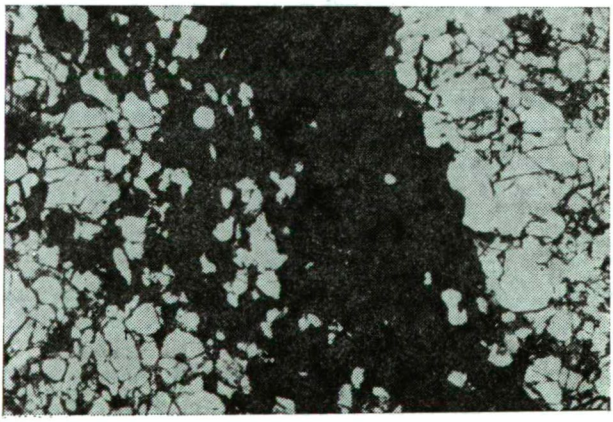

Fig. 9. Composite xenolith [BH—09], showing thin spinel vein in olivine orthopyroxenite xenolith from Sitke. 1N, M=20x

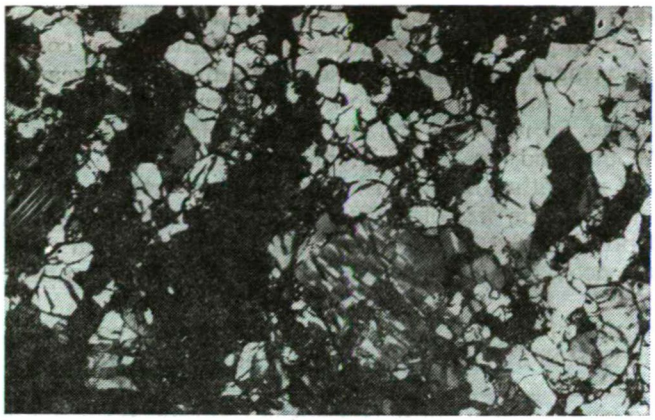

Fig. 10. Amphibole lherzolite xenolith [BH—81], showing olivine porphyroclast and nearly parallel band consisting mainly of amphibole, clinopyroxene and spinel in a typical equigranular texture. 1N, M=20x

position suggests close textural relationships. The spinels are brown. The large amoeboid shaped grains (about 2 mm) are covered by a fine opaque rim. Large amount of spinel occur close to the amphiboles; the interstitial spinel is typically absent in this amphibole lherzolite. The overprinting of these bands on the normal recrystallized texture indicates that the amphiboles were formed after the polygonization and recrystallization of this xenolith.

These two special nodules can be considered as an evidence of modal metasomatism (HARTE, 1983; DAWSON, 1984) in the upper mantle. This metasomatism has already been proved beneath the Carpatho-Pannon region by EMBEY-ISZTIN (1976/b), KURAT *et al.* (1980) based on the young basaltoid suite and by SZABÓ (1985), KUBOVICS *et al.* (1989) based on the Early Cretaceous lamprophyre.

CONCLUSIONS

The Sitke tuffring encloses four textural types of upper mantle xenoliths.

Textural analyses of the xenoliths show that high porportion of the nodules has porphyroclastic and equigranular texture. We have found many transitional textures as well, proving that the nodules are products of a continous metamorphic process (MERCIER and NICOLAS, 1975). Textural relationship of these inclusions confirms NICOLAS and MERCIER's theory suggesting that a volcanic vent carries out one predominant nodule-type.

The strained elements in the texture indicate that the upper mantle had a long, complex previous deformational history. The straining may has occurred during the development of the diapir (COISY and NICOLAS, 1978) or during the shearing due to the decoupling of the mantle from the crust. Mantle diapirs in Neogene are demonstrated by geophysical methods (STEGENA *et al.*, 1975). Development of upper mantle diapir beneath the LHP has also been proposed by EMBEY-ISZTIN (1984).

Two special types of xenoliths were collected. One contains bands rich in amphibole, clinopyroxene and spinel and the other is a composite nodule with spinel-vein. They suggest that the upper mantle beneath the LHP has been undergone a modal metasomatism after the deformation. This process has facilitated the formation of

the basaltic melt. The amphibole-bearing (Cr-diopside group) mantle nodules are wide-spread in the world (e.g. WHITE, 1966; BEST, 1974; FREY and GREEN, 1974; FRANCES, 1976; TAKAHASHI, 1980; WILSHIRE *et al.*, 1980) and occurence of them are regarded as an important volatile-containing phase within the upper mantle (e.g. OXBURGH, 1964; DAWSON and SMITH, 1982). It should be mentioned that some amphibole lherzolites have been recognized in the Carpatho-Pannon region by EMBEY-ISZTIN, (1974); KURAT *et al.*, (1980); KUBOVICS *et al.*, (1989).

The Sitke xenoliths may have contained more amphiboles than at present and some part of them may have been partially melted during the ascent to the surface in the host magma.

ACKNOWLEDGMENTS

Authors are grateful to Professor. I. KUBOVICS (Department of Petrology and Geochemistry, Eötvös University, Budapest) for his help in field work and for his helpful criticism of the manuscript.

REFERENCES

BALOGH K., ÁRVA-SÓS E., PÉCSKAY Z., RAVASZ-BARANYAI L. (1986): K/Ar dating of Post-Sarmatian alkali basaltic rocks in Hungary. Acta Min. Petr. Szeged. **XXVIII,** 75—93.

BÉRCZI Sz. (1988): Proofs for the existence of anorthite-spinel-garnet peridotite series of inclusions in basalts of Persányi Mts., Transylvania, Rumania. Reminescent of an old book. Acta Min. Petr. Szeged. **XXIX,** 139—143.

BÉRCZI Sz., BÉRCZI J., (1986): Rare earth element content in the Szentbékkála series of peridotite inclusions. Acta Min. Petr. Szeged. **XXVIII,** 61—74.

BEST M. G. (1974): Mantle-derived amphibole within inclusions in alkali-basaltic lavas. J. Geoph. Res. **79,** 2107—2113.

COISY P., NICOLAS A. (1978): Regional structure and geodynamics of the upper mantle beneath the Massif Central. Nature. **274,** 429—432.

DAWSON J. B. (1984): Contrasting types of mantle metasomatism. In: Kimberlites I. The mantle and crust-mantle relationships. Ed. KORNPROBST J. Elsevier. Amsterdam—Oxford—New York—Tokyo, 289—294.

DAWSON J. B. (1982): Upper-mantle amphiboles: a rewiev. Min. Mag. **45,** 35—46.

DIETRICH H., POULTIDIS H. (1985): Petrology of ultramafic xenoliths in alkali basalt from Klöch and Stadner Kogel (Styria, Austria). N. Jahr. Min. Abh. **151,** 131—140.

EMBEY-ISZTIN A. (1976/a): Felsőköpeny eredetű lherzolit zárványok a magyarországi alkáli olivin bazaltos, bazanitos vulkanizmus kőzeteiben (Lherzolite nodules of upper mantle origin in the oliviné basaltic, basanitic rocks of Hungary). Földt. Közl. **106,** 42—51. (in Hungarian with English abstract).

EMBEY-ISZTIN A. (1976/b): Amphibolite-lherzolite xenolith from Szigliget, North of the Lake Balaton, Hungary. Earth Planet. Sci. Lett. **31,** 297—304.

EMBEY-ISZTIN A. (1978): Texture types and their relative frequencies in ultramafic and mafic xenoliths from Hungarian alkali basaltic rocks. Annls hist.-nat. Mus. natn. hung. **76,** 27—42.

EMBEY-ISZTIN A. (1980): Major element patterns in Hungarian basaltic rocks: an approach to determine the tectonic settings. Annls. hist.-nat. Mus. natn. hung. **72,** 19—31.

EMBEY-ISZTIN A. (1989): Petrology and geochemistry of peridotite xenoliths in alkali basalts from the Transdanubian Volcanic Region, West Hungary. J. Petrol. **40,** 79—105.

FRANCIS D. M. (1976): Amphibole pyroxenite xenolith: cumulate or replacement phenomena from the upper mantle, Ninuvak Island, Alaska. Cont. Min. Petr. **58,** 51—61.

FREY F. A., GREEN D. H. (1974): The mineralogy, geochemistry and origin of lherzolite inclusions in Victorian basanites. Geochim. Cosmochim. Acta. **36,** 1023—1059.

FREY F. A., PRINZ M. (1978): Ultramafic inclusions from San Carlos, Arizona: petrological and geochemical data bearing on their petrogenesis. Earth Planet. Sci. Lett. **38,** 129—176.

HARTE B. (1977): Rock nomenclature with particular relation to deformation and recrystallization textures in olivine-bearing xenoliths. J. Geol. **85,** 279—288.

HARTE B. (1983): Mantle peridotites and processes the kimberlite sample. In: Continental basalt and mantle xenoliths. Eds. HAWKESWORTH C. J., NORRY M. J. Shiva Publ. Ltd. Leicester, 46—91.

HOVORKA D. (1978): Uzavrevy spinellovych peridotitov v basanite pri Maskovej-reziduum vrchneho plasta? (Xenoliths of spinel peridotite in basanite near Maskova [West Carpathian Mts.] — Upper mantle residuum?). Min. Slov. **10,** 97—112. (in Slovak with English abstract).

HOVORKA D., FEJDI P. (1980): Spinel peridotite xenoliths in West Carpathian late tectonic alkali basalts and their tectonic significance. Bull. Volc. **43,** 95—105.

JÁMBOR Á., PARTÉNYI Z., SOLTI G. (1981): A dunántúli bazalt vulkanitok földtani jellegei (Geological feature of the basalt volcanics in Transdanubia, W Hungary). MÁFI Évi Jel 1979-ről, 225—239. (in Hungarian with English abstract).

JUGOVICS L. (1972): A Kisalföld bazalt és bazalttufa előfordulásai (Die Basalt- und Basalttuffvorkommen der Kleinen Ungarischen Tiefebene)MÁVI Évi Jel. 1970-ről, 79—103. (in Hungarian with German abstract).

JUGOVICS L. (1976): A magyarországi bazaltok kémiai jellege (Chemical features of the basalts in Hungary) MÁFI Évi Jel. 1974-ről, 431—470. (in Hungarian with English abstract).

KUBOVICS I., ÁRGYELÁN B. G., SZABÓ CS., SÓLYMOS G. K. (1988): Geochemical investigation of olivines from alkali basalt and their xenoliths (Nógrád-Gömör region, Hungary). Acta Min. Petr. Szeged. **XXIX,** 35—46.

KUBOVICS I., SÓLYMOS G. K., SZABÓ CS. (1985): Petrology and geochemistry of ultramafic xenoliths in mafic rock of Hungary and Burgenland (Austria). Geol. Carp. **36,** 433—450.

KUBOVICS I., SZABÓ CS., JÁNOSI M., GÁL-SÓLYMOS K. (1989): Comparative geochemistry of amphiboles from xenoliths and megacrysts of alkali basalts in the Carpathian Pannonian Region. XIV. Congress CBGA. Extended Abstract, 222—225.

KURAT G., PALME H., SPETTEL B., BADDEBHAUSE H., HOFMEISTER-PALME CH., WANKE H. (1980): Geochemistry of xenoliths from Kapfenstein, Austria: Evidence for a variety of upper mantle processes. Geochim. Cosmochim. Acta. **44,** 45—60.

MALDARESCU I., ATANASIU M., SECLANAN M. (1983): Significations de le présence de certains nodules de péridotites dans les basaltes de Racosul de Jos. Rév. Rum. Géol. Géoph. Géogr. Géologie. **27,** 9—14.

MAURITZ B. (1948): A Dunántúli bazaltok kőzetkémiai viszonyai (Die petrologischen Verhalthissen der Transdanubian Basaltgesteine. Földt. Közl. **78,** 134—169. (in Hungarian with German abstract).

MERCIER J. C. C., NICOLAS A. (1975): Textures and fabrics of upper mantle peridotites as illustrated by basalt xenoliths. J. Petrol. **15,** 454—487.

OXBURGH E. R. (1964): Petrological evidence for the presence of amphibole in the upper mantle and its petrogenetic and geophysical implications. Geol. Mag. **101,** 1—19.

PIKE J. E., SCHWARZMAN E. (1977): Classification of textures in ultramafic xenoliths. J. Geol. **85,** 9—61.

POULTIDIS H., SCHARBERT H. G. (1986): Bericht über geochemisch-petrologische Untersuchungenan basaltische Gesteinen des österreichischen Teils der transdanubuschen vulkanischen Region. Anz. Öst. Akad. Wiss. math.-natw. Kl. **123,** 65—76.

RICHTER W. (1971): Ariegite, Spinell-Peridotite und Phlogopit-Klinopiroxenite aus dem Tuff von Tobaj im Südlichen Burgenland. Tscherm. Min. Petr. Mitt. **16,** 227—251.

SCHARBERT H. G., POULTIDIS C., HÖLLER H., KOLMER H., WIRSCHING U.: (1981): Vulkanite im Raume Burgenland — Oststeiermark. Fschr. Min. **59,** 69—88.

STEGENA L., GÉCZY B., HORVÁTH F. (1975): A Pannon-medence kainozoos fejlődése (The Late Cenozoic evolution of the Pannonian basin). Földt. Közl. **105,** 101—123. (in Hungarian with English abstract).

STRECKEISEN A. (1974): Classification and nomenclature of plutonic rocks. Geol. Rundschau. **63,** 773—786.

SZABÓ A. (1982): Vulkanológiai vizsgálatok a Kisalföldön (Volcanological studies from the Little Hungarian Plain). M. Sc. thesis. Eötvös University, Budapest, Manuscript. (in. Hungarian).

SZABÓ Cs. (1984): Az Alcsutdoboz—2 (AD—2) fúrással harántolt alkáli bázit zárványainak ásvány-kőzettani és geokémiai vizsgálata, eredete, genetikai jelentősége (Mineralogy, petrology and geochemistry of ultramafic nodules in alkali basic rocks of Alcsutdoboz—2 borehole [Bakonyi-kum, Hungary]: their origin and genetic implication). M. Sc. thesis. Eötvös University, Budapest, Manuscript. (in Hungarian with English abstract)

TAKAHASHI E. (1980): Thermal history of lherzolite xenoliths-I. Petrology of lherzolite xenoliths from the Ichonomegata crater, Oga peninsula, Western Japan. Geochim. Cosmochim. Acta. **44**, 1643—1659.

WHITE R. W. (1966): Ultramafic inclusions in basaltic rocks from Hawaii. Contr. Min. Petr. **12**, 245—314.

WILSHIRE H. G., PIKE J. E. N. (1975): Upper mantle diapirism: Evidence from analoguos features in alpine peridotite and ultramafic inclusions in basalts. Geology. **3**, 467—470.

WILSHIRE H. G., SHERVAIS J. W. (1975): Al-augite and Cr-diopside ultramafic xenoliths in rocks from western United States. Phys. Chem. Earth. **9**, 257—272.

WILSHIRE H. G., PIKE J. E. N., MEYER C. E., SCHWARZMAN E. C. (1980): Amphibole-rich veins in lherzolite xenoliths, Dish Hill and Deadman Lake, California. Am. J. Sci. **280-A**. 576—593.

Manuscript received, 4 November, 1989

Acta Mineralogica-Petrographica, Szeged, XXX, 81—92, 1989

THE POSITION AND PETROCHEMISTRY OF THE RHYOLITE IN THE RUDABÁNYA MTS. (NE HUNGARY)

SZAKMÁNY GYÖRGY*—MÁTHÉ ZOLTÁN**—RÉTI ZSOLT***

Dept. of Petrology and Geochemistry L. Eötvös University,
Mecsek Ore Mining Enterprise, Hungarian Geological Survey

ABSTRACT

The work was focussed to the position-origin and petrology of the rhyolite in the Rudabánya Mts. Our basic intention aimed to make exact determinations of the feldspars; their structure and chemical composition by electron microscope as well as electron microprobe analyses. According to these results the original rock-forming feldspars were sanidines and the minor plagioclase have been transformed to albite, by the effect of secondary sodium-metasomatism. Besides this transformation the rhyolite suffered silicification and carbonatisation. The relation and position of the Jurassic black shale and the intercalated rhyolite blocks, have also been analysed in detail. The methods were the following: trace element geochemistry (B, Li), vitrinite reflectance and macro- and microscopic analysis. All these data show, that the not completely cooled rhyolite entered to the unconsolidated Middle Jurassic sediments, so its age is probably the same or perhaps a little younger than that of these sediments.

INTRODUCTION

Vienna school geologists — the first surveyors of the area — determined the material of the small hillock on the flank of the Dunna hill, as a melaphire (FOETTERLE 1868, 1869, WOLF 1869). Firstly KOCH A. (1904) determined this rock as a metarhyolite (quartz porphyry) as the product of the coeval eruption with the sedimentation of the Lower Triassic (Werfenian shales). According to later studies of BALOGH K.—PANTÓ G. (1949) these rhyolites are younger than the Szepes-Gömör porphyries, and they dated the shales and the volcanism to the Ladinian stage. According to JUHÁSZ Á. (1964) all the chemically and mineralogically slightly varying rhyolites of the Rudabánya Mountains have the same origin, and represent a long time span of acid volcanism.

The latest research conducted by the Hungarian Geological Survey from 1979 to 1985 revaluating the structural position and determining radiolarians in the black shales, dated the rhyolites to the Middle Jurassic (GRILL *et al.* 1984).

Rhyolite outcrops in the Rudabánya Mts. *(Fig. 1)* are as follows:

1. Szalonna-Perkupa roadcut (Geol. Basic Section). This section is an olistostroma (KOVÁCS S. 1987), containing olistolites, (boulders and cobbles of limestone, sandstones and rhyolite in black shale of Jurassic age.)
2. Telekes valley — On the slope SE of the hunting box (vadászház) — There is a 150 m long outcrop of rhyolite in black shale environment.

* H-1088 Budapest, Muzeum krt. 4/A.
** H-7673 Kővágószőlős
*** H-1143 Budapest, Népstadion Népstadion u. 14.

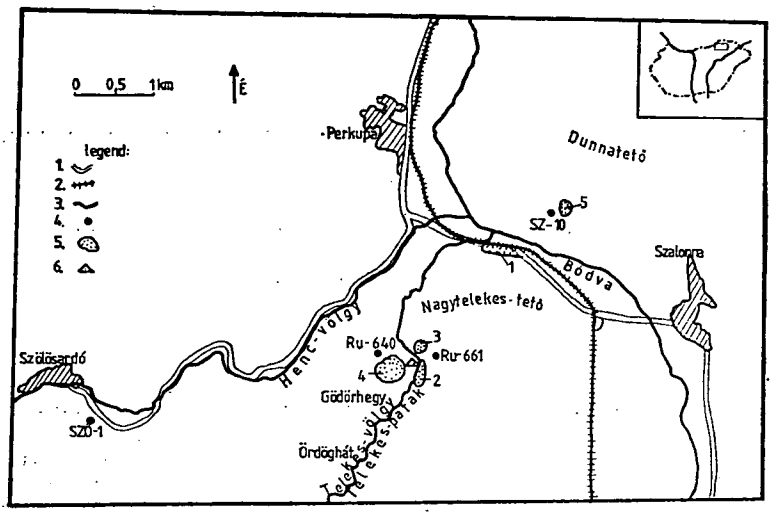

Fig. 1. Rhyolitic rocks in the Rudabánya Mts. 1=road, 2=railroad, 3=creek, 4=borehole, 5= =outcrop, 6=Vadászház (hunting box)

3. Southern side of the Balázs peak, — in black shale.
4. NW-from hunting box on the hillside the rhyolite crops out in some artificial research trenches.
5. On the southern slope of the Dunna hill crops out a rhyolite body.

Besides the outcrops boreholes cored the rhyolite: Szalonna—10, Rudabánya—640 and 661. The Szőlősárdó—1 penetrated greyish-green rhyodacitic tuff between 464.2—464.9 m — in BALOGH K.—KOVÁCS S. (1981).

MINERALOGY OF THE RHYOLITE

On the surface the color of the relatively fresh samples is greyish-green to light green. The weathered rhyolites of outcrops No. 5 are yellow. The core samples are generally fresh, with greyish color. The texture is dominantly porphyric, with macroscopically two minerals determinable (quartz and feldspar). The length of the elongated feldspars frequently is exceeding 1 cm. Their color is dominantly pink, but some samples (Dunna hill, Szalonna—10) have white feldspars, too.

The lathy feldspars and the 0.5 cm patchy quartz crystals are surrounded mostly by chlorite mass in this porphyric rock. On the surface the rock is well fragmented. The cracks are refilled up with dark green chlorite. The massive, thick (1—10 cm) quartz veins also filled up with pyrite. The siderite pseudomorphs filled with limonite. The pseudomorphs had probably been formed by the migration of secondary solutions, which oxidized the pyrite and siderite. The veins infiltrate the surrounding black shale, too.

With this method the following minerals were determined: quartz, feldspar, biotite, accessories (zircon, apatite) and secondary minerals (calcite, chlorite, sericite, clay-minerals and hematite). The euhedral quartz crystals are dominating with triangular, quadrangular and hexagonal shape. Some quartz crystals are broken, and the fragments are pulled away to some millimeters and also suffered superficial resorption (Fig. 2). The reaction rim around them consist of microcrystalline quartz, calcite, albite, sericite, chlorite (Fig. 3.). The devitrified glass and the calcite frequently appear inside large quartz crystals. This way, it is evident that the quartz phenocrysts are first generation rock forming high temperature dihexaedric crystals. The biotite is low quantity constituent, which dominantly has elongated habit of crooked platy forms. Strongly alterated to bauerite or kaolinite. Frequently has zircon inclusions. The first determinations of the feldspar were contradictory. JUHÁSZ Á. (1964) determined to orthoclase, and mentioned sanidine, too. GATTER I. (1976) determined

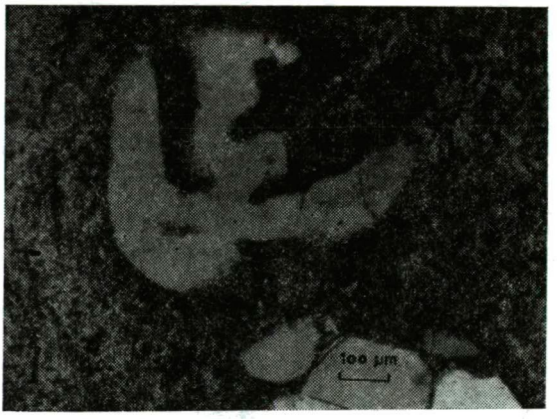

Fig. 2. Resorbed quartz from Szalonna—10 borehole (66.0): magn. 100X Crossed polarizers

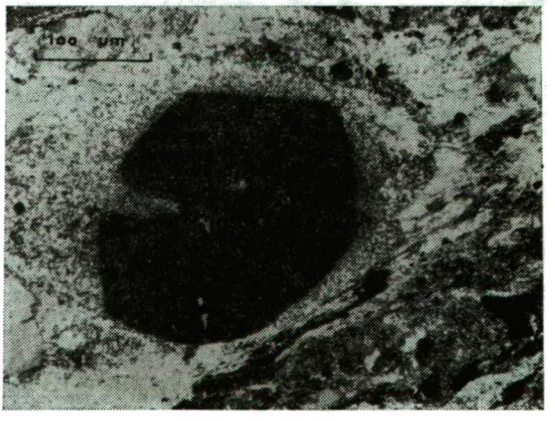

Fig. 3. Resorbed fine grain quartz surrounded by sericite, chlorite reaction rim-from Szalonna—10 borehole (31.8 m): magn. 40X. Crossed polarizers

anorthoclase by universal stage. ÁRKAI P.—KOVÁCS S. (1986) determined low albite from the same rock by X-ray diffractometry. Searching for exact data (besides traditional microscopy) Transmission Electron Microscope (I. DÓDONY) and Electron Microprobe Analysis (K. GÁL—SOLYMOS) were also used.

In thin sections two different feldspar generations were distinguished: (1) The first original volcanic generations are sanidine and plagioclase. (2) The secondary albites appearing in veins. The first generation euhedral, subhedral crystals have generally platy and rarely lathy habites. A great part of the crystals are broken and some places these fragments are dispersed to 1—2 mm distance. The resorption is also dominant, as well as the cluster forming of the wealded feldspars. These feldspars were determined by microscope to sanidine. These biaxal, optically (—) crystals have maximum 2V of 15—20°, and form Karlsbad twins *(Fig. 4)*. Rarely they also form hour-glass twins *(Fig. 5)*. The secondary calcite and albite veins, are frequent in the feldspars. On the less altered part mosaic (domenic) structure exists, too *(Fig. 4)*. About 5% of the plagioclase formed during the first (volcanic) crystallization

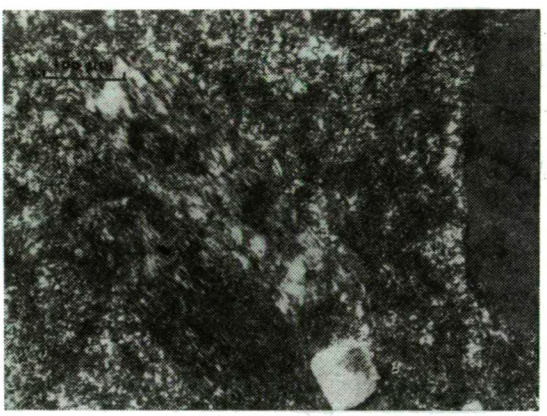

Fig. 4. Carlsbade twinned feldspar from Vadászház NW outcrop: magn. 65X Crossed polarizers

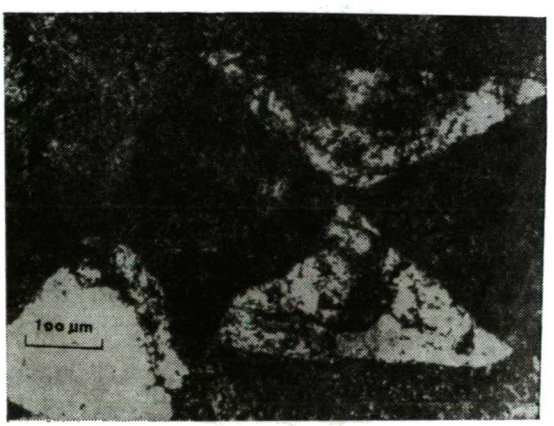

Fig. 5. Hour-glass structure feldspar from Szalonna—10 borehole (66.8 m): magn. 65X Crossed polarizers

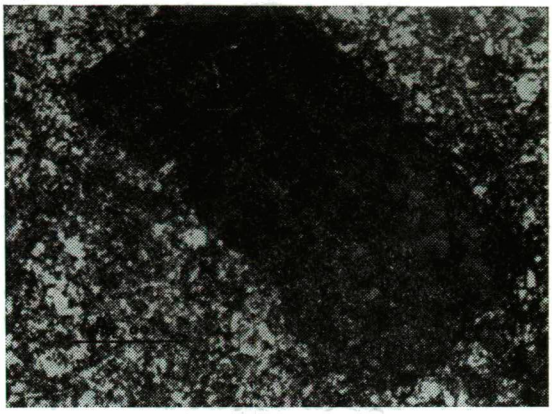

Fig. 6. Strongly altered feldspar, Vadászház NW outcrop: magn. 40X Crossed polarizers

phase. This original feldspars are already altered, and only some twinned crystal remains can be found by optical microscope. According to their optical character, albite-oligoclase were determined *(Fig. 6)*.

The more exact method (TEM) shows, that these domenic feldspars don't form twins, neither show intermingling. In this way the mosaic structure is neither the result of twinning, nor intermingling. For getting exact chemistry of the feldspars, Electron Microprobe Analyses were carried our on a couple of feldspar grains. Using this method the Si, K, Na and Ca were measured. All the feldspars are rich in Na. Potassium appears just in the narrow cracks. The Ca is definitely low. The wt% of the mean oxides are the following:

SiO_2	Al_2O_3	CaO	Na_2O	K_2O
68.7	19.2	0.13	11.9	0.07

The calculated feldspar is 99.05% albite, 0.59% K-feldspar, 0.36% anortite.

This way it is clear, that the feldspars of the meta-rhyolite are dominantly low temperature albites (pseudomorphs) and a few original plagioclase grains still exist. It shows that the rhyolite suffered Na-metasomatism, formed the second generation of albites, stable in low grade metamorphic condition.

The albite one way enmeshes the feldspars and the porphyric quartz crystals and also forms clusters in the mass and inside some feldspar crystals. It also forms reaction rims around quartz crystals. Generally the secondary albite forms clean platy crystals. The albite veins frequently infiltrate the nearby black shale, too.

The high sodium content of 6.6 wt% Na_2O is much more then the average for the calc-alkaline rhyolites; it is suggesting certain sodium metasomatism, too. The Na-rich solutions exhanged the potassium content of the sanidine to sodium, and this way it transformed to albite. A considerable portion of the K probably remained in the volcanite and formed sericite (K_2O=0.73—4.64 wt%).

The CaO content is generally low (1.5 wt%), only the secondary calcite veins elevates it in some samples. It shows that the original basic plagioclase content was low, so the plagioclase was nearly pure albite.

The few accessory minerals are zircon, apatite and opaques. The zircon appears with the opaques as scattered crystals in the mass, and as inclusion in the feldspars

TABLE 1

Chemical analyses of rhyolitic rocks of the Rudabánya-Mts (wt %)

Sample	SiO_2	TiO_2	Al_2O_3	Fe_2O_3	FeO	MnO	MgO	CaO	Na_2O	K_2O	P_2O_5	$-H_2O$	$+H_2O$	SO_3	CO_2	total
1	68.45	0.08	11.09	0.45	1.16	—	3.02	2.24	3.15	4.64	—	0.79	3.92	0.09	—	99.08
2	75.91	0.08	10.76	0.45	1.16	—	1.20	0.84	5.65	1.61	—	0.38	1.63	0.16	—	99.83
3	71.05	0.07	12.65	0.80	0.72	—	1.01	0.56	5.81	4.35	—	0.27	1.63	0.29	—	99.21
4	77.45	0.08	10.73	0.50	0.87	—	0.21	1.02	6.61	0.73	—	0.25	0.73	0.13	—	99.31
5	73.32	0.15	12.78	0.62	1.30	—	2.41	0.58	3.07	2.07	—	0.59	2.56	0.10	—	99.55
6	65.61	0.51	16.80	0.50	1.74	—	3.78	0.58	3.19	3.01	—	0.51	3.79	0.10	—	100.12
7	66.34	0.20	17.27	0.40	1.74	—	3.25	1.17	2.95	2.52	—	0.72	3.59	0.23	—	100.38
8	59.47	0.65	16.23	0.57	4.28	—	3.04	2.92	2.98	3.04	—	0.50	4.33	0.08	1.54	99.63
9	45.73	0.24	14.67	0.27	4.35	—	3.04	11.99	2.26	3.37	—	0.32	3.87	0.12	9.36	99.59
10	64.55	0.11	15.73	0.04	2.32	—	2.52	2.92	3.03	2.23	—	0.44	4.22	0.13	1.58	99.82
11	71.49	0.20	13.77	0.15	2.46	—	2.94	0.87	2.39	2.27	—	0.32	3.15	0.23	0.14	100.38
6R	71.02	0.22	15.42	1.21	1.06	0.01	1.06	0.85	2.62	3.27	0.17	0.70	2.62	—	0.50	100.73
7R	77.91	0.18	12.22	0.70	0.60	0.01	0.57	0.23	2.91	2.12	0.05	0.54	1.52	—	—	99.56
13R	79.45	0.15	11.23	0.69	0.57	0.01	0.44	0.30	3.29	0.96	0.05	0.56	1.93	—	—	99.63
14R	83.26	0.17	5.83	0.84	0.22	0.01	0.35	0.36	4.93	1.48	0.07	0.36	1.32	—	—	99.20

Analyses: 1—11: Laboratory of OFKFV, Komló
6R, 7R, 13R, 14R: L. Hoffmann, Department of Petrology and Geochemistry, Eötvös Univ., Budapest

1. Sz—10 5.25—5.40 m; 2. Sz—10 15.50—15.60 m; 3. Sz—10 25.10—25.20 m; 4. Sz—10 35.50—35.60 m; 5. Sz—10 45.00—45.10 m; 6. Sz—10 55.50—55.60 m; 7. Sz—10 65.80—65.90 m; 8. Sz—10 70.40—70.50 m; 9. Sz—10 87.80—87.90 m; 10. Sz—10 123.20—123.30 m; 11. Sz—10 130.00—130.10 m

6R; 13R; Telekes-valley, on the slope SE of the hunting box.

7R; Telekes-valley, on the slope SE of the hunting box; near of the contact of the shale.

14R; Telekes-valley, NW from hunting box on the hillside.

and biotites. Two different generations of the zircon exist (GATTER, 1976). The first is short tetragonal pyramidic, and the second is elongated ditetragonal dipyramidic crystals.

In accordance with the low opaque (magnetite, ilmenite) mineral content, the TiO_2, Fe_2O_3 and FeO are lower than the rhyolite mean (Table 1).

Two kinds of apatite have been distinguished by microscope. The first one exists in the rhyolite outcroping NW of the Vadászház and it is found together with zircon and opaques in sericitic patches, and is optically tipical apatite. The other type of apatite existing in small quantity in all samples but it is abundant in the Sz—10 4R sample which had been determined by X-ray diffractometry as fluor-apatite. It will be discussed later in detail, in a separate paper.

The basic material of the rhyolite is devitrified glass containing the other components: sericite, chlorite, calcite and patches of clay minerals.

As a result of secondary silicification the quartz veins are frequent. Reflecting this secondary process some samples have extremely high silica content (SiO_2= =83 wt%) (Table 1). A part of the chlorite has probably been formed by the effect of silicic solutions from the groundmass, and the other is a secondary product derived from the mafic minerals.

The original texture of the rhyolite had been vitrophyric. Devitrification of the groundmass as well as the chloritisation and sericitisation transformed the original texture to spherulitic-felsitic one.

STUDY OF THE RHYOLITE-SHALE CONTACT

The precise age of the rhyolite and black shale is still not to be determined. The Telekes valley and Bódva pass black shale series (containing the bodies of rhyolite) was dated to Jurassic. According to the determined Unuma echinatus radiolarian zone the age of the shale is Middle Jurassic (GRILL—KOZUR 1986). In this way the age of the black shale is exact, however, that of the rhyolite is not. Two alternatives were raised recently: (1) Coeval formation of the rhyolite and the black shale (GRILL *et al.* 1984). (2) According to KOVÁCS (1987) the Perkupa-Szalonna roadcut (Telekes oldal) outcrop represents an olistostroma with sandstone and rhyolite olistoliths in the Jurassic shale. In such a case the age of the rhyolite can be Middle to Upper Triassic.

Macroscopic observations

In the Sz—10 borehole the rhyolite and the black shale alternate. At the contact these rock-types are mixing. The quartz and the calcite veins infiltrate both rock types. As the exocontact zone of the rhyolite the shale in also silicified. The veins of the shale entered the cracks of the volcanite. This kind of contact appears twice in the cores at 66.8 m the whitish-grey shale, and at 121.4 the black shale are mixing with the rhyolite. Similar phenomena can be found in Rudabánya—640 and Rb—661 boreholes, too.

In the outcrop "Vadászház SE" at the contact a 1 cm thin dark hard fragile contact rock band can be found. Leaving the contact at 1.5 cm a spotted shale, at 4 cm a dark gray shale and between 4 and 10 cm a confusedly bedded yellowish rock are found. Thickness of the exocontact does not exceed 10 cm.

Microscopy

The contacts are generally very sharp in thin sections but some places micro-interfingering and mixing of the two different rocks are visible *(Fig. 7, 8, 9)*.

On the sharp contact the phenocrysts (quartz, feldspar) are touching the shale. On these places are not contact alterations at all. There are plenty of veins in microscopic dimensions on contact surfaces. The mineral content of these veins is characteristic, as the center is filled with calcspars and the vein walls are covered by chlorite and albite. The chlorite shows a light green pleochroism with irregular brown or blue interference colour *(Fig. 10)*. Near the contact small fragments of rhyolite can frequently be found among the shreds of the shale *(Fig. 7, 8, 9)*. On these spots (between the shale and rhyolite) chlorite and calcite vein as well a sericite stripes are found. There has not been found thermal contact index minerals, just all the material is darker near the contact, and sericite is more abundant. There is a sedimen-

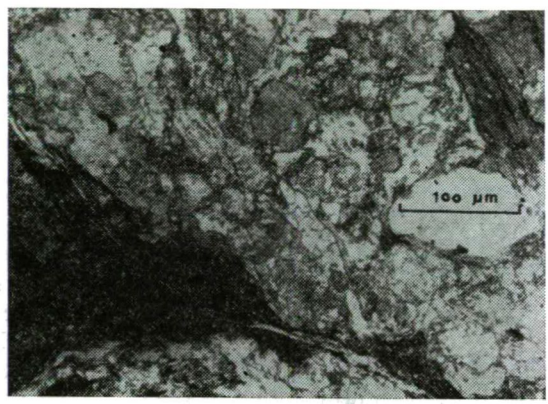

Fig. 7. Rock mixing at the rhyolite-shale contact from Szalonna—10 borehole (66.8 m): magn. 40X Crossed polarizers

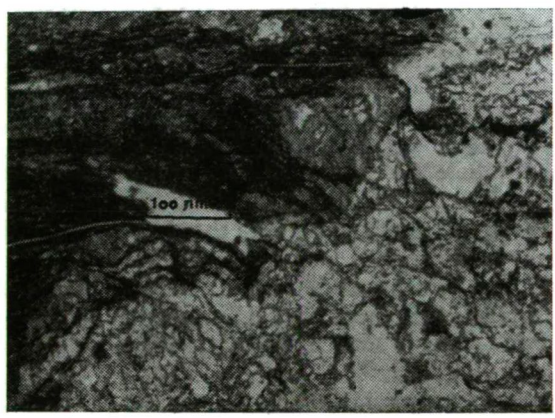

Fig. 8. Contact of rhyolite and shale from Szalonna—10 borehole (66.8 m): magn. 60X Crossed polarizers

tary inhomogeneity also, close to the contact. The chlorite and albite veins are continuing on the other side of the rock. The albite appears not only in veins, but also in flakes and in druses. So, this way it is evident that the Na-metasomatism affected not only the rhyolite but the shale, too.

The characteristic minerals are fine grained quartz forming fine layers, muscovite, biotite, feldspar, zircon, opaques and a few tourmaline. On the rhyolite side of the contact zone the minerals are the same as were mentioned earlier. Thin black shale fragments also appear in the rhyolite either as isolated patches, or as vein-like forms that are connected to the main body of the shale. There is always a chlorite enrichment around them. Near this shreds the volcanite shows its original texture and structure and there are no marks of any tectonic fragmentation. It is best shown by the fact, that the porphyric minerals are the same on the contact and far from it.

Accordingly, tectonic dislocation between these two consolidated rock body is considered to be impossible. A single change is noticed in the groundmass of the

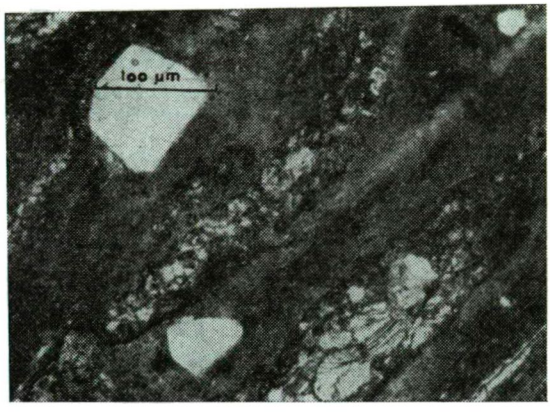

Fig. 9. Alteration of rhyolite and shale zones at the contact from Szalonna—10 borehole (66.8 m): magn. 40X one polarizer

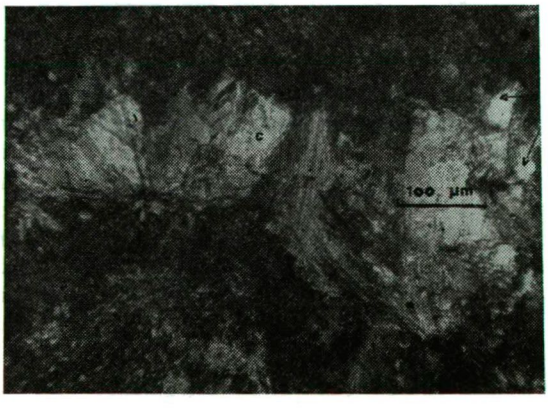

Fig. 10. Calcite (c), albite (a), chlorite (chl)-filled vein on the contact from Szalonna—10 borehole (121.4 m): magn. 160X Crossed polarizers

rhyolite, namely, it has more sericite and chlorite near the contact than far from it. In the light of these data the interpretation of the contact remained ambigous, so other type of analyses had been necessary (Trace element geochemistry and vitrinite reflectance).

Trace element geochemistry

The B and Li content were analysed by sensitive OES in the supposed thermal contacts, since these elements migrating to the direction of the heat source are perfect indicators of the thermal effects. This analysis was carried out on the „Vadászház outcrop" samples and borehole Szalonna—10, 121.4 m core sample (Table II.).

TABLE 2

The B and Li content in the shale and the rhyolite near the contact (ppm)

	Distance from the contact	B	Li	B	Li
		1.		2.	
	background	80	80	—	—
Shale	20 cm	60	75	—	—
Shale	10 cm	95	75	—	—
Shale	4 cm	80	105	—	—
Shale	2 cm	75	110	125	90
Shale	1 cm	75	85	130	80
	contact	220	80	130	80
	contact	35	105	85	110
rhyolite	1 cm	40	105	80	90
rhyolite	2 cm	20	110	75	85
rhyolite	4 cm	40	110	—	—
rhyolite	8 cm	25	85	—	—
rhyolite	20 cm	50	110	—	—
rhyolite	40 cm	35	85	—	—
	background	60	80	—	—

1. Vadászház SE — outcrop on the hillside
2. Szalonna—10 borehole (121.4 m)
Analyser: Mrs. VIGH. MÁFI spectroscopic laboratory.

Analysing the contact of the rhyolite and the shale, the B content in the volcanite is constant (40 ppm), and 220 ppm in the shale, which is dropping immediately at the contact to one third (B=75 ppm) within 1.5 cm and there is no any significant difference farther. The Li content remains constant around the contact, and it is the same (110—130 ppm) in the surface and the core samples. In case of the Sz—10 core the heat effect was definitely less, so the Li content in the contact is the same, and the B is slightly higher than the average of the rhyolite and the sediment.

Concludingly, on the basis of trace element enrichment pattern a typical thermal contact can not be defined. Probably they were not any appropriate pressure conditions for the pyrometamorphic recristallisation (open system).

VITRINITE REFLECTANCE MEASUREMENTS

Determination of R_{max}, R_{min} and R_{random} was carried out in MTA Geochemical Lab. by Z. A. HORVÁTH at 548 nm wavelenght in oil immersion using a reflection prism series of standards of the Bitumenous Coal Research Inc.... The samples are collected from the Sz—10/e borehole (121.4 m) and from the outcrop SE of Vadászház.

The samples contain 1—10 μm sized coal granules which are in relation to the original organic content of the sediment. Besides these, allochtonous graphite scales with pyrite are also abundant. In the Sz—10/e sample 16 granules were measured by this method.

The mean reflection is $(R_{random})=4.745\%$, the standard deviation is $(S_x)=0.133$. From the surface exposure 28 granules were measured: ($R_{random}=4.565\%$, $S_x=0.178$).

Interpretation of the data

In the metamorphic petrological study of the Aggtelek—Rudabánya and Slovakian Karst mountains by ÁRKAI P.—KOVÁCS S. (1986), correlations between the results of petrological data of very-low grade metamorphic rocks and conodont studies as well as carbonate microfacies analyses were carried out. According to their studies, these Jurassic shales suffered only diagenetic effects (250 °C), near to the conditions of the very-low grade regional metamorphism. Mean value of the illite crystallinity (IC) of <2 μm fraction shows a diagenetic transition alteration just below the anchi zonal metamorphism.

The R_{random} — values for the samples SE from Vadászház (Telekes oldal) are as follows:

$$R_{random}\,(\%) = \frac{\bar{x}}{S_x} = \frac{4.533}{(0.432)} \quad \text{mean of 13 anal.}$$

$$\frac{\bar{x}}{S_x} = \frac{4.630}{(0.144)} \quad \text{mean of 30 anal.}$$

Contrary the IC results according to ÁRKAI and KOVÁCS (1986) these values are fitting to the anchi metamorphic zone. The higher R values can probably be explained by short time heat effect.

Comparing these high R_{random} values with that of the contact [$X/S_x=4.745/0.133$ and $X/S_x=4.565/0.178$], those it can be seen that are even higher. In this case we could also explain it with this short time thermal effect.

Summarising the results of vitrinit reflectance measurements, and the B and Li geochemistry, we found that a sharp rhyolite-shale thermal contact could not be proved, but according to these data the partly cooled rhyolite lava entered the Jurassic unconsolidated sediment, so these materials were partially mixed. It can be studied best on the core samples of the Szalonna—10 borehole (Fig. 7). This way the partially cooled lava coudn't produce a real contact effect. Consequently, this rhyolite is a result of a Jurassic or a little younger volcanism.

REFERENCES

ÁRKAI, P.—KOVÁCS, S. (1986): Diagenesis and Regional Metamorphism of the Mesozoic of Aggtelek—Rudabánya Mountains (Northeast Hungary) — Acta Geol. Hung. **29,** 349—373.

BALOGH, K.—KOVÁCS, S. (1981): A Szőlősardó 1. sz. fúrás. (The Triassic Sequence of the borehole Szőlősardó 1. (N Hungary). Ann. Rep. of Hung. Geol. Inst. of 1981. 39—63. (in Hungarian with English abstract).

BALOGH, K.—PANTÓ, G. (1952): A Rudabányai-hegység földtana. (La géologie de la montagne de Rudabánya). Ann. Rep. of Hung. Geol. Inst. of 1949. 135—154. (in Hungarian with French abstract).

FOETTERLE (1868): Das Gebiet zwischen Forró, Nagy-Ida, Torna, etc. Verhandl. d. K. K. geol. Reichsanst. **276.**

FOETTERLE (1869): Vorlage der geologischen Detailkarte der Umgebung von Torna und Szendrő. — Verhandl. d. K. K. geol. Reichsanst. **147.**

GATTER, I. (1976): A Rudabányától ÉÉK-re levő Telekesi-völgy kalkopirit, hematit, mangánérc indikációinak ásványtani vizsgálata. (Mineralogical investigation of the chalcopyrite, hematite and manganese ore mineral indications in the Telekes-valley, NNE of Rudabánya, Hungary). M. Sc. thesis. Library of Dept. Petrol. Geochem. of Univ. Loránd Eötvös, Budapest. Manuscript (in Hungarian).

GRILL, J.—KOVÁCS, S.—LESS, GY.—RÉTI, ZS.—RÓTH, L.—SZENTPÉTERI, I. (1984): Az Aggtelek—Rudabányai-hegység földtani felépítése és fejlődéstörténete. (Geological constitution and history of evolution of the Aggtelek—Rudabánya Range). Földt. Kutatás. **XXVII 4,** 49—56. (in Hungarian with English abstract).

GRILL, J.—KOZUR, H. (1986): The first evidence of the Unuma echinatus Radiolarian zone in the Rudabánya Mts (Northern Hungary). Geol. Paläont. Mitt. Innsbruck. **13,** 239—275.

JUHÁSZ, Á. (1964): A Rudabányai-hegység kvarcporfir kőzeteinek összehasonlító vizsgálata. (Examen comparatif des roches de porphyre quartzifère de la montagne de Rudabánya.) — Földt. Közl. **94, 3,** 321—326. (in Hungarian with French abstract).

KOCH, A. (1904): A Rudabányai-Szent-Andrási hegyvonulat geológiai viszonyai. (Geology of the Rudabánya-Szent András Mountains, Hungary). Mat. und Naturwissenschaft. Anzeiger **22,** 132—145. (in Hungarian).

KOVÁCS, S. (1987): Olisztosztrómák és egyéb, víz alatti, gravitációs tömegszállítással kapcsolatos üledékek az északmagyarországi paleo-mezozoikumban, I—II. (Olisthostromes other deposits connected to subaqueous mass-gravity transport in the Nort-Hungarian Paleo-Mesozoic I—II.). — Földt. Közl. **117,** 61—69 and 101—119. (in Hungarian with English abstract).

PÁLFY, M. (1924): A Rudabányai-hegység geológiai viszonyai és vasérctelepei. (Geology and iron ore deposits of the Rudabánya Mountains, Hungary.) Ann. Inst. Geol. Publ. Hung. **XXVI, 2,** 1—24. (in Hungarian).

WOLF, H. (1869): Das Kohlenvorkommen bei Somodi und das Eisensteinvorkommen bei Rákó im Tornaer Comitate — Verhandl. d. K. K. geol. Reichsanst. Jahrg. **217.**

Manuscript received, 1 November, 1989

Acta Mineralogica-Petrographica, Szeged, XXX, 93—101, 1989

PETROGRAPHIC STUDY OF THE MÓRÁGY-TYPE GRANITOID AND THE CSERDI CONGLOMERATE AT NYUGOTSZENTERZSÉBET (MECSEK MTS., SOUTH HUNGARY)

T. FEHÉR, A. MOLNÁR

Department of Petrology and Geochemistry, L. Eötvös University

ABSTRACT

The Upper Carboniferous Mórágy-type granitoids were formed by anatectic and metasomatic processes. The two macroscopically different types (medium grained granite and aplite) have the same origin. The aplite was developed in the fracture zones where the crushed rocks were potash-metasomatized more thoroughly than the surrounding granite. It has higher microcline, lower mafic mineral content and well developed cataclastic texture with more fine grained matrix than the enclosing granite.

Studies of the morphology of zircon grains provided a well detectable evolutional trend from the anatectic restites to the medium grained granite. In the course of anatexis the zircon grains developed the typical low temperature types from high temperature ones.

The source rocks of the Middle Permian Cserdi Conglomerate were Lower Permian rhyolites and granitoids of unknown age. The latter ones are strongly mylonitized but show the same metasomatic phenomena as the Mórágy-type granitoids.

The zircon types of the granitoid pebbles of the conglomerate are anatectic ones. Our opinion is that they derived from an upper part of the Mórágy-type granitoid complex.

INTRODUCTION

In the summer of 1987 the authors and LÁSZLÓ BUJTOR mapped a 6 km^2 area north of Nyugatszenterzsébet in the western part of the Mecsek Mts., South Hungary, on a scale of 1:10 000 *(Fig. 1.)*. This area was recently surveyed by the geological and geophysical team of the MÉV (Mecsek Ore Mines Company) on a 1:25 000 scale (KONRÁD and KONRÁD—DOBOSI, 1982).

The oldest rock is the Upper Carboniferous Mórágy-type granite. It was previously studied by JANTSKY (1979), who emphasized its anatectic origin, and by BUDA (1968, 1971, 1984, 1985) who first attributed great role to the rock-forming potash-metasomatism. BUDA has found close relationship between the granitoids occurring in the Western and also in the Eastern part of Mecsek Mountains.

The pebbles of the Cserdi Conglomerate were described by JÁMBOR (1964), KONRÁD and KONRÁD—DOBOSI (1980) and FAZEKAS (1979, 1987). Their studies showed a denudation area built up principally by rhyolites and, in a lesser amount, metamorphic rocks and granites.

In the Pliocene sandy sequence deposited here.

In the Quarternary about 30 m thick loess covered the whole area. Recent waterflows cut their valleys mainly into this loess hence the older rocks are poorly represented on the surface.

H-1088 Budapest, Múzeum krt. 4/a,

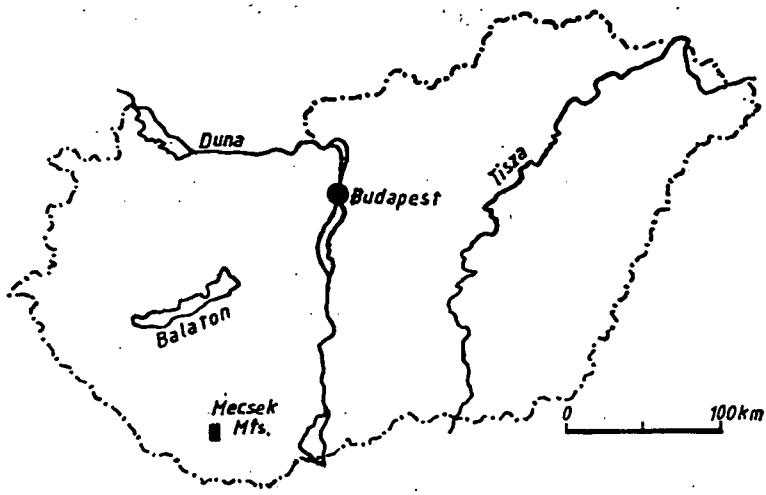

Fig. 1. Location of the mapping area

PETROGRAPHY

Mórágy-type granitoids

In the outcrops two granitoid types occur: in greater part strongly weathered granite of medium grain size (granite auct.) and in smaller part fresh fine grained granite with very small amount of biotite (aplite auct.). The latter forms dykes of varying width in the former.

The microscopic studies show that both are composed of more or less sericitized plagioclase, fresh microcline, quartz, altered biotite (colourless mica and opaques)

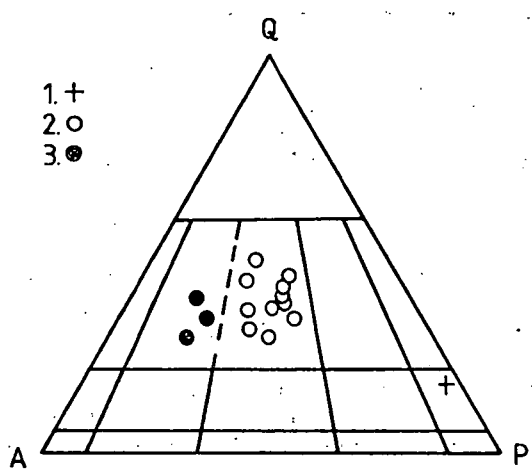

Fig. 2. The modal compositions of the different granitoid types in the QAP diagram of STRECKEISEN (1978).

1. granitoid from the outcrop 1 km north of Nyugotszenterzsébet 2. medium grained granite (Nagyváty Valley) 3. fine grained granite (Nagyváty Valley).

and apatite, zoned zircon and pyrite as accessory minerals. All samples were affected by potash-metasomatism (BUDA, 1968, 1971, 1984, 1985): sericitized myrmekitic plagioclase; plagioclase replaced by microcline.

Due to the strong weathering biotitization of amphibole, chloritization of biotite etc. (BUDA, 1985) can't be properly recognised. In fact the biotite or any other presumably original mafic mineral was opacitized or altered to a point to be unidentifiable in both rock types. The anorthite content of the plagioclase is 34—35% (universal stage results) in all samples independently of the rock type. The quartz in the medium grained variety has always wavy extinction and fragmented or crushed crystals are not uncommon. The fine grained rock type contains cataclastic matrix of recrystallized or nonrecristallized quartz.

The modal composition of the medium grained granite is monzogranitic in the diagram of STRECKEISEN (1978) with 1—5% biotite. An exception is an outcrop 1 km North of Nyugotszenterzsébet which is probably a great restite (similar inclusions were described by BUDA, 1984, from the cores of deep drilling holes) and which has 2.7% microcline and 37% biotite content. The fine grained granite ("aplite") is syenogranite with less than 1% biotite *(Fig. 2)*.

Cserdi Conglomerate

The colour of the rock is purple brown with variable grain size and pebble content. The pebbles are less rounded; 94—95% of them are rhyolites and 6—5% are granitoids. The matrix is coarse to medium grained sandstone with a weakly developed stratification dipping about 15° NNE.

The rhyolite pebbles are principally red and purple coloured and more or less silicified. Rarely the original fluidal texture can be seen in thin section. Sometimes a green coloured variety occurs with finely distributed glauconite-like mica. The phenocrysts of the rhyolite are more or less sericitized plagioclase (in the green coloured type it is always strongly altered), fairly fresh orthoclase containing patch perthite frequently with albite twins, quartz, faded and opacitized biotite sometimes with sagenitic rutile. These phenocrysts are always resorbed. In the green rhyolite pebbles there are some quartz-glauconite pseudomorphs formed presumably after pyroxene. In this rock type the alteration of the biotite is fading also just in the red variant. Accessory minerals are apatite, unzoned zircon, rutile and rarely garnet, monazite (enclosed in apatite with zircon, EMA result) in both types.

The matrix of the rhyolite is nearly always fine grained quartz, sometimes with chalcedony spherules with glauconite or limonite pigment according to the rock colour.

Dynamothermally metamorphosed pebbles, mentioned in earlier works, do not occur in this area. In these rock types, with few exceptions, we can identify the effects of potash-metasomatism just as in the granitoids now on surface.

According to the macroscopic and microscopic studies five main source rock types can be distinguished: (1) granitoid rock with pink coloured feldspar porphyroclasts (mineral assemblage: plagioclase: An_{24-28}, quartz, microcline, biotite, muscovite, apatite, titanite, zoned zircon); (2) aplite (mineral assemblage: plagioclase: An_{25-27}, microcline, quartz, muscovite, biotite, chlorite, apatite, zircon, titanite, zoisite, garnet); (3) mylonite with abundant mica (mineral assemblage: plagioclase: An_{18-22}, quartz, biotite, muscovite, apatite, zircon, garnet, titanite); (4) coarse grained quartz-plagio-

clase rock (mineral assemblage: quartz, plagioclase, muscovite); (5) medium grained granite (mineral assemblage: quartz, plagioclase, microcline, biotite, apatite, zircon).

As mentioned above potash-metasomatism strongly affected these rocks except mylonite and the coarse grained quartz-plagioclase rock. This appears as: plagioclase replaced by microcline; sericitized, myrmekitic and sometimes saussuritic plagioclase; chloritization, baueritization, vermiculitization (?) of biotite.

DISCUSSION OF THE PETROGRAPHY

Microscopic study of the Mórágy-type granitoid proves the macroscopically well distinguishable "aplite" and "granite" to be of the same origin. The potash-metasomatic phenomena appear in both rock types and the composition of the plagioclase are the same. The sericitization of plagioclases depend mainly on the strength of metasomatism and not on weathering. We attribute the higher microcline, lower mafic mineral content and the well develoned cataclastic texture of the "aplite" only to a more complete metasomatism in fracture zones. It would explain the cataclastic texture of the rock and we needn't suppose any magmatic differentiation.

The granitoid pebbles of the Cserdi Conglomerate show the same potash-metasomatic effects as the Mórágy-type granitoid. The main difference from the granitic rocks now on surface (except the medium grained granite pebbles) is the strongly mylonitic or cataclastic texture of the pebbles. The mylonitic texture occurs in the mica bearing types while the cataclastic one appears in the mica-poor varieties.

During the mylonitization the temperature didn't reach the degree needed for recrystallization as seen on the anomalous optical properties of the minerals (SPRY 1969), and neither was it enough for the crystallization of metamorphic index minerals.

The exact identification of the original rock types is impossible and the relationships between them are obscure because of the detrital occurrence. However we emphasize that these pebbles derive from Mórágy-type granitoid rocks and possibly from the non-granitized aureole and have been mylonitized before Middle Permian time.

ZIRCON TYPOLOGY

We followed the method of PUPIN (1980) in general but additionally we didn't cover the crystals and used a universal stage (without the upper hemisphere just for turning the crystals to every direction) and a strong table lamp for illuminating from above. With this arrangement it was possible to get a proper three-dimensional view of the grains.

We identified zircons from the following rocks: the "granite" 1 km North of Nyugotszenterzsébet; the "granite" from the Nagyváty Valley (2 km NE from Nyugotszenterzsébet); the granitoid pebbles with rose coloured feldspar porphyroclasts from the conglomerate; the rhyolite pebbles from the conglomerate.

Zircons from all granitoid types were colourless or pinkish coloured. P and S types with high T indice were mainly pinkish and were slightly resorbed while those of having lower T indice were pure, colourless and bright. This distribution didn't appear in the rhyolite though these zircons were also variably coloured and resorbed.

The zircon populations of the granites now on surface show high T indices *(Fig. 3* and *4)*. The distribution of zircon types of the granites of typically anatectic

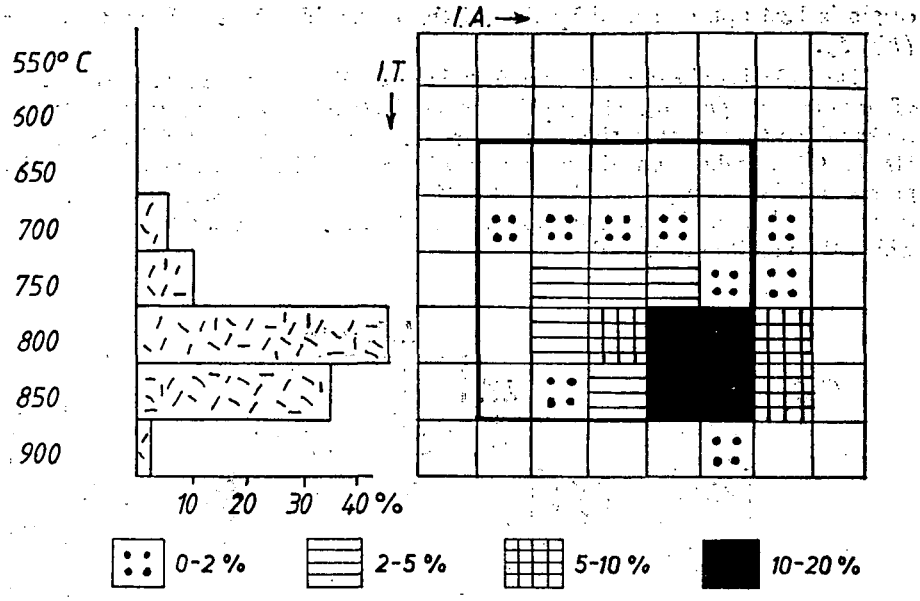

Fig. 3. Distribution of zircon types of restite (100 grains), (outcrop 1 km north of Nyugotszenterzsébet)

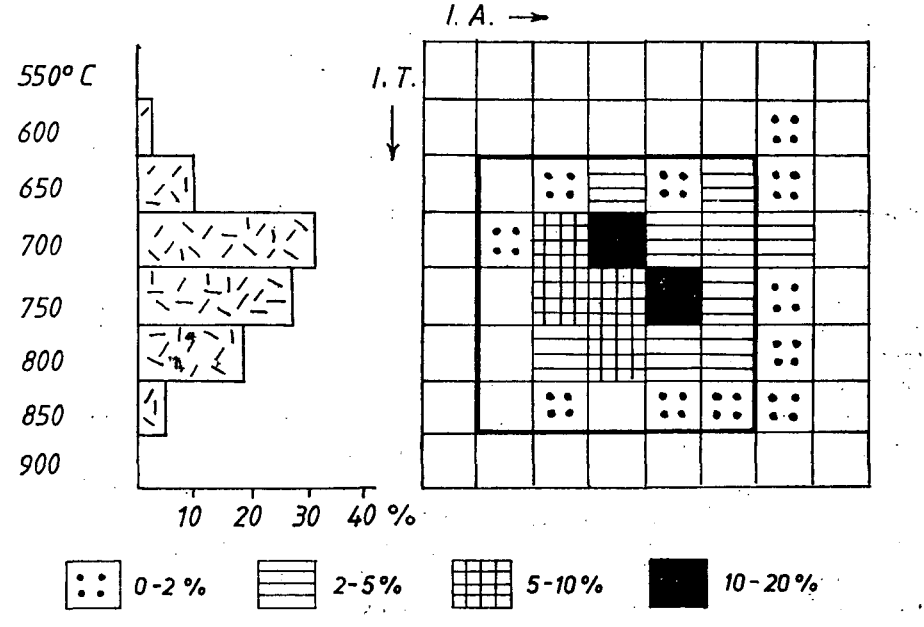

Fig. 4. Distribution of zircon type of the medium grained granite (Nagyváty Valley), 100 grains observed

origin is best approximated by that of the granitoid pebbles of the conglomerate *(Fig. 5)*.

The linked projection points make a line parallel with the longer axis of the field of granodiorites *(Fig. 6)*. The populations of the granites contain zircons of the source rocks which took part in the anatectic process. It is corroborated by GBELSKY and HATÁR (1982) who studied the zircons of the granitized metabasite and nebulitic granite of the same granitoid complex 40 km east from this occurrence. In these rocks abundant mafic inclusions represent the amphibolite facies host rocks from which the granite originated.

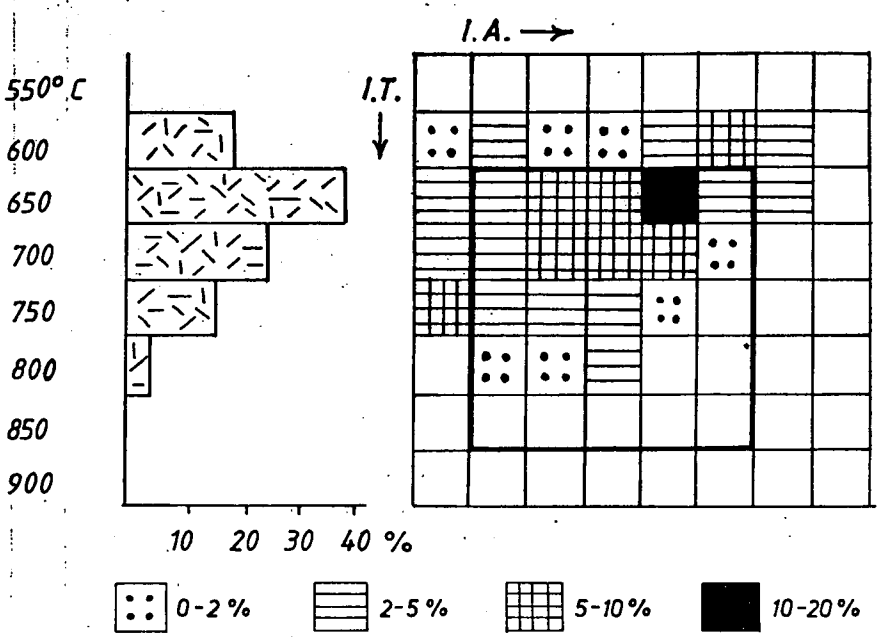

Fig. 5. Distribution of zircon types of the granitoid pebbles of Cserdi Conglomerate, 100 grains observed

Zircon morphological distribution given by GBELSKY and HATÁR (1982) is nearly the same as we got from the granitoid 1 km North of Nyugotszenterzsébet *(Fig. 3)*. This fact and the mineralogical composition provide evidence that this outcrop display a large restite (see BUDA, 1984).

More zircon types characterizing anatectic granites have been found in the rocks of the Nagyváty Valley where we haven't found any xenoliths.

As mentioned above we got the best fitting anatectic granite zircon distribution from the granitoid pebbles of the Cserdi Conglomerate *(Fig. 5)*. Comparing this and also the similar mineralogical composition and phenomena with the granitoids now on surface we think that these pebbles have been derived from an upper level of the Mórágy-type granitoid complex (see *Fig. 6*).

The zircon population of the rhyolite pebbles of the Cserdi Conglomerate covers a large area in the typological diagram *(Fig. 7)*. Some of these grains were inherited

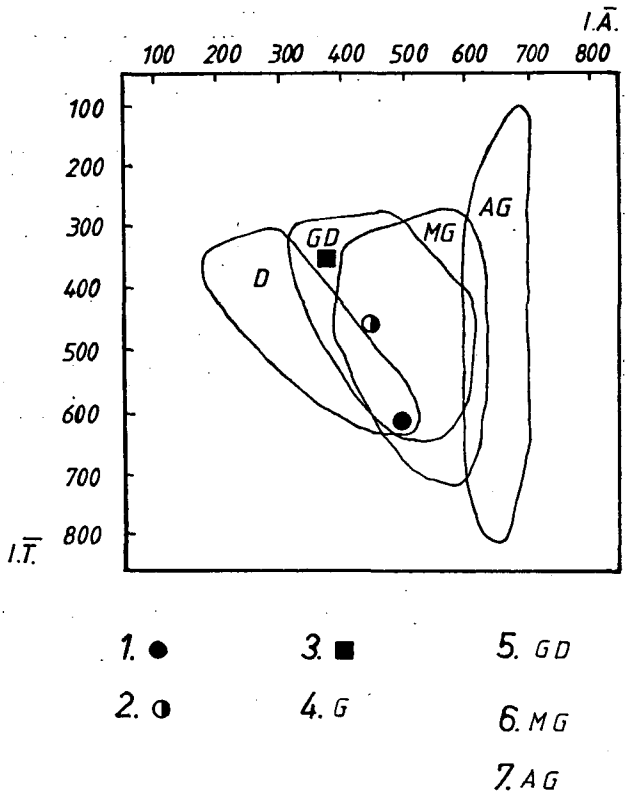

Fig. 6. Location of the projection points of the different zircon populations in the PUPIN (1980) diagram

1. restite 2. medium grained granite 3. granitoid pebbles 4. the field of diorites and tonalites 5. the field of granodiorites 6. the field of monzogranites 7. the field of alkalic granites

from the surrounding granitoid as, in some cases, the rhyolite contains small xenoliths observed in thin sections. Nevertheless, these zircons do not affect the location of the projection point of the population that is still lying in the field of calc-alkalic rhyolites *(Fig. 8)*.

CONCLUSIONS

The Mórágy-type granitoids are typical anatectic and metasomatic rocks. This is supported by microscopic studies which revealed the effects of potash-metasomatism and also the distribution of their zircon types. The different rock types (aplite-looking variety and medium grained granite) have the same origin because the former is only a more thoroughly potash-metasomatized rock body which suffered cataclasis in a fracture zone.

The granitoid pebbles of the Cserdi Conglomerate were eroded from an upper level of this granitoid complex during the Middle Permian. The source rock of these pebbles were potash-metasomatized just as the Mórágy-type granitoids. Zircon mor-

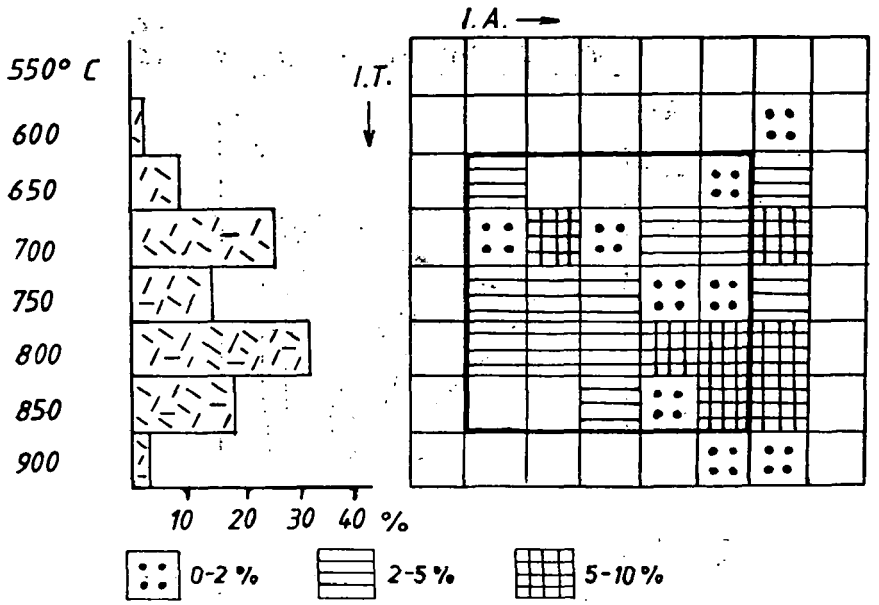

Fig. 7. Distribution of zircon types of the rhyolite pebbles of Cserdi Conglomerate

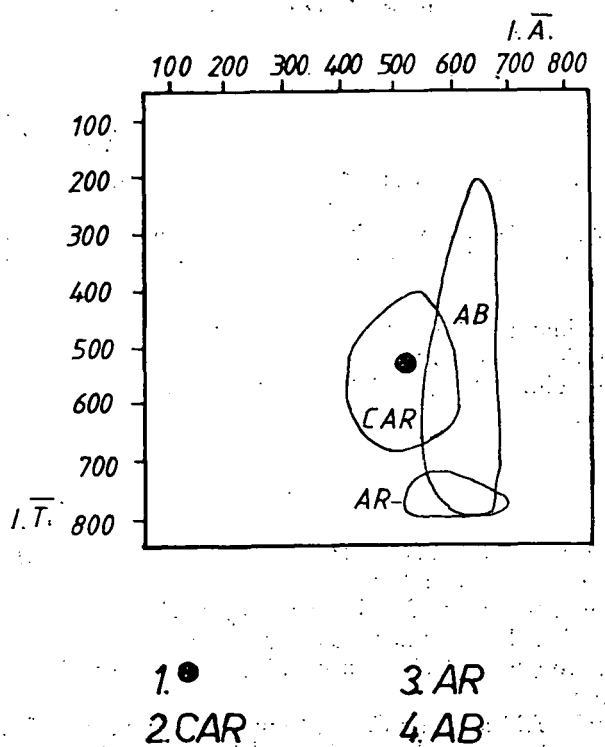

1. ● 3. AR
2. CAR 4. AB

Fig. 8. Location of the projection point of the zircon population of the rhyolite pebbles. 1. projection point of the zircon population 2. calc-alkalic rhyolites 3. alkalic rhyolites 4. alkalic basalts'field (PUPIN, 1980)

phology also links these rocks together because continuous development of zircon types was observed from restite to the granitoid pebbles of the conglomerate.

The zircon types of the rhyolite pebbles differ from those of the granitoid originated ones. This may help to identify the source rock area of the finer grained detrital deposits of the same age.

ACKNOWLEDGEMENT

We would like to thank the valuable help of the Mecsek Ore Mines Company and especially of BÉLA WÉBER and VIA FAZEKAS. Our study was supported by the Department of Petrology and Geochemistry of Eötvös L. University (Budapest). We thank the valuable help of GYÖRGY BUDA and Prof. JÁNOS KISS in the interpretation of our results and MIKLÓS KÁZMÉR and ATTILA DEMÉNY for their advices.

REFERENCES

BUDA, GY. (1969): Optical and X-ray study of the feldspars of granitoid rocks of Mecsek and Velencei Mts. Unpublished Univ. Doctorate dissertation, ELTE Petr. and Geochem. Dept. Library, mauscript (in Hungarian).

BUDA, GY. (1971): Report on the mineralogical and petrographical study of the granitoid rocks investigated with deep drillings in Dunántúl. MÉV Library, manuscript (in Hungarian).

BUDA, GY. (1984): Report on the mineralogical and petrographical study of the granitoid rocks occur in the Western part of Mecsek Mts. MÉV Library, manuscript (in Hungarian).

BUDA, GY. (1985): Origin of collision granitoid rocks (Variscian Age) on the examples of Hungary, West Carpathians, and Bohemian Massif. Unpublished Ph. D. thesis, ELTE Petr. and Geochem. Dept. Library, manuscript (in Hungarian).

FAZEKAS, V. (1979): Mineralogical and petrographical study of the Lower Permian detrital formations of Mecsek Mts. and their comparison with the Kővágószőlős and Jakabhegy Formations. Survey report, MÉV Library, manuscript (in Hungarian).

FAZEKAS, V. (1987): Mineralogical composition of the Permian and Lower Triassic detrital formations of Mecsek Mts. Földtani Közlöny. **117,** 11—30. (in Hungarian).

GBELSKY, J., HATÁR, J. (1982): Zircon from some granitoid rocks of the Velenc eand Mecsek Mts. (Hungary). Geol. Carpathica. **33/3,** 343—363.

JANTSKY, B. (1979): Geology of the granitized crystalline basement of Mecsek Mts. MÁFI Évk. **60,** (in Hungarian).

JÁMBOR, Á. (1964): Lower Permian formations of the Mecsek Mts. MÉV Library, manuscript (in Hungarian).

KONRÁD, GY., KONRÁD—DOBOSI, I. (1980): Report on the pebble-study of the mineralized area in 1979. MÉV Library, manuscript (in Hungarian).

KONRÁD, GY., KONRÁD—DOBOSI, I. (1982): Documentation of the 1:25 000 scale geological map of Bükkösd area. MÉV Library, manuscript (in Hungarian).

PUPIN J. P. (1980): Zircon and granite petrology. Contribution to Mineralogy and Petrology. **73,** 207—220.

SPRY, A. (1969): Metamorphic textures. Pergamon Press, p. 350.

STRECKEISEN, A. (1978): Classification and nomenclature of volcanic rocks, lamprophyres, carbonatites and melilitic rocks. Neues Jahrbuch für Mineralogie Abh. **134,** 1—14.

Manuscript received, 15 December, 1989

Acta Mineralogica-Petrographica, Szeged, XXX, 103—113, 1989

STRUCTURAL ORDERING OF CARBONACEOUS MATTER IN PENNINIC TERRANES

A. DEMÉNY*

Dept. of Petrology and Geochemistry, L. Eötvös University

ABSTRACT

This paper presents a study of relations between graphitization processes and metamorphic conditions in the easternmost windows of the Alpine Penninic system (Eastern Austria, Western Hungary). Samples for comparison were collected from the Tauern Window, too. From XRD investigations it can be concluded that strong shearing could result in development of graphite in greenschist facies conditions. The mobility of metamorphic fluids also plays a determining role in graphitization.

KEYWORDS: Penninic units, graphitization, XRD study.

INTRODUCTION

This paper will deal with the Easternmost outcrops of the Alpine Penninic unit. These areas lie on or near the Hungarian—Austrian border as indicated in *Fig. 1.* As the major part of the unit is on the Austrian side the whole system will be called "Burgenland Penninic".

Several geologists have mapped the distribution of different rock types, amongst them were BANDAT (1928, 1932), FÖLDVÁRY *et al.* (1948) and KISHÁZY and IVANCSICS (1976, 1984). A recent summary can be found in the work of KOLLER and PAHR (1980). According to them this Penninic terrane consists mainly of metapsammites-pelites, metacarbonates and metamagmatic rocks. KUBOVICS (1983) and KOLLER (1985) have dealt with the latter ones and showed a possible ophiolitic origin.

The age of the sediments has been determined by SCHÖNLAUB (1973) who described Mid-Cretaceous sponge spiculae in some metacarbonate rocks.

Three metamorphic events have affected the sequence: an oceanic hydrothermal, a subduction-related HP/LT type and a young Alpine influence (LELKES—FELVÁRY, 1982; KOLLER, 1985). In the metasediments only the latest effect can be observed which is characterized by about 350 °C in the northern and 430 °C in the southern part of the area. These temperature data have been obtained from evaluation of mineral parageneses (KOLLER, 1985) and from preliminary fluid inclusion studies (DEMÉNY, unpublished results). The pressure had a maximum of 0.3 GPa during this late event.

At least two deformation phases can be determined (KISHÁZY and IVANCSICS, 1984) that created two imbrications with different fold axes (HERRMANN and PAHR, 1988).

Present address: Lab. for Geochem. Res., Hung. Acad. Sci., Budapest, Budaörsi út 45.

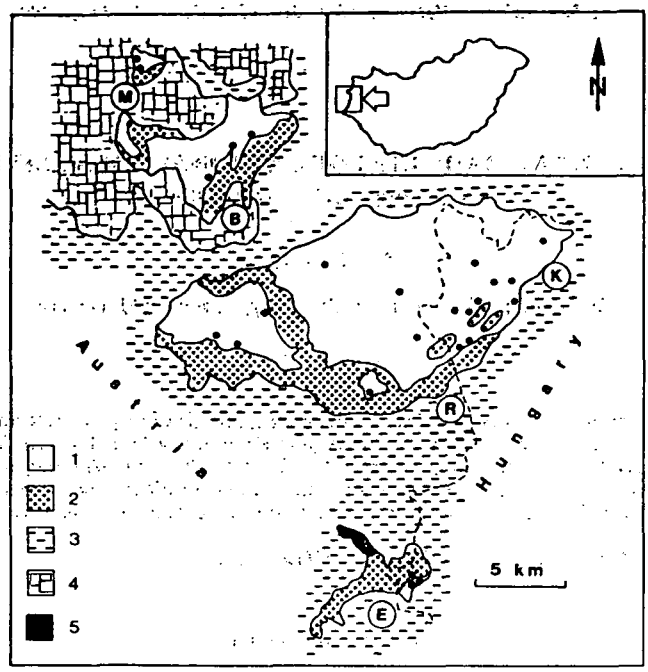

Fig. 1. Geological sketch map of the easternmost Penninic windows, with sample localities. 1. Penninic metasediments, 2. Penninic metamagmatites, 3. Tertiary sediments, 4. lower eastalpine nappes, 5. upper eastalpine nappes (after KOLLER, 1985). M: Möltern, B: Bernstein, R: Rechnitz, K: Kőszeg, E: Eisenberg

Some samples were collected for comparison from the Tauern Window *(Fig. 2)* following the guide-book written by MATURA and SUMMESBERGER (1980). According to them the metamorphic temperatures were between 450 and 550 °C, while the pressure was around 0.4—0.6 GPa in the study area *(Fig. 2)*.

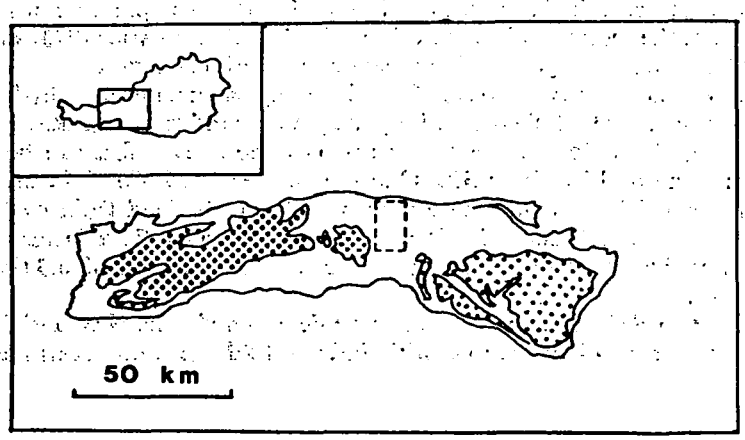

Fig. 2. Geological sketch map of the Tauern Window. Spotted area: Central Gneiss. The study area is indicated by dashed lines. After DROOP (1985)

Here I intend to discuss the relations between graphitization processes and metamorphic influences in these Penninic terranes by means of XRD investigations on the structural ordering of carbonaceous matters.

EXPERIMENTAL AND THEORETICAL APPROACHES OF GRAPHITE FORMATION (A SHORT REVIEW)

Detailed descriptions of graphitization processes appeared in the 60 s, but at first they based mainly on laboratory experiments. During this work several authors proved that the main factor is the temperature, but the pressure, stresses and catalizing materials also play an important role (BRAGG *et al.*, 1964; NODA *et al.*, 1968a, b; MARSH and WARBURTON, 1976).

The bases of X-ray diffraction investigations on graphites of metamorphic rocks were established by FRENCH (1964) and later GRIFFIN (1967) and GREW (1974) made some contributions to the newly recognised problems.

Detailed investigations on the relations between graphitization and metamorphic influences have been made by DIESSEL and OFFLER (1975), DIESSEL *et al.* (1978), and OKUYAMA—KUSONOSE and ITAYA (1987). WINTSCH *et al.* (1981) discussed variable effects of metamorphic fluids, while ITAYA (1981) recognised the dependence of graphitization on the duration of metamorphism. He also managed to determine detrital graphite together with graphitizing carbonaceous matter.

Finally, comparisons between X-ray diffraction results and other methods (TEM, SEM: LANDIS, 1971, BONIJOLY *et al.*, 1982, BUSECK and HUANG, 1985, illite crystallinity: PESQUERA and VELASCO, 1988) elucidated the processes that can cause development of graphites. The temperature dependence of the structural change of this mineral has been determined by SHENGELIA *et al.* (1977) applying heating experiments.

According to these authors graphitization takes place in three steps: (1) development of hexagonal rings (2) appearance of two dimensional layers (3) formation of three dimensional structure.

During this process volatiles are released creating bubbles and pores in the carbonaceous matter which pores promote development of preferred orientation in case of shear stresses. The next step is the so called "turbostratic structure" in which we have hexagonal layers, but they are random rotated. Further heating can cause partial graphitization forming "transitional material". At even higher temperature (about 500—550 °C) pure graphite will develop.

As it was mentioned before, shear stresses play a great role, but different catalizing materials (SiO_2, FeS_2, Fe, Co, Ni, $CaCO_3$, etc.) can also enhance the graphitization process. In contrast, trapped volatiles inhibit the development of graphite.

The present work is based on the feature that the X-ray diffraction pattern of graphite changes during the structural ordering, namely the 2Θ value and half-height width ($W_{1/2}$) of the d_{002} peak vary with the metamorphic degrees. Previous results have been published in a short abstract form (KUBOVICS *et al.*, 1988).

ANALYTICAL PROCEDURES

As quartz and micas make the investigation of the d_{002} peak of the graphite impossible the graphitic matter had to be separated. Powdered rock samples were treated with hot concentrated HCl and HF at least 5—8 hours long and this proce-

dure was repeated when necessary. After this treatment saturated $AlCl_3$ solution was used with minor amount of HCl to remove the artificial products (GREW, 1974). This stage was followed by washing with destilled water until reaching neutral pH.

Beside graphitic matter, tourmaline, pyrite, zircon and rutile remained in the samples.

The X-ray diffraction patterns were measured with a Siemens D500 type diffractometer using graphite filtered CuK_α emission. Scanning speed was 0.5°/min and chart speed was 1 cm/min. Corrections were made using silicon as internal standard.

Reproducibilities of the calculated "c" values were between ±0.013 Å and ±0.002 Å (±0.005 Å on the average). The precisity of the measured $W_{1/2}$ values was ±0.01—0.17 °2Θ (±0.08 °2Θ on the average).

RESULTS

The localities of samples studied in this paper are shown in *Figs. 1* and *2*. Sample numbers (see also Tables 1 and 2) beginning with "A" stand for Austrian localities, while "K" and "Fcs" mean Kőszeg Mts. and Felsőcsatár (Eisenberg—Vashegy window), respectively.

Having measured the X-ray diffraction patterns of these samples, I have calculated the "c" values (Table 1) and plotted them against the metamorphic temperatures *(Fig. 3)*. The temperature data were obtained from interpolation of values mentioned in the Introduction. It is obvious for the first glance that the graphitic matter in the Easternmost Penninic system is generally well developed, but one sample group — at about 400 °C — has higher values than usual in this terrane. As most of the sample points fall in this temperature interval, sampling bias can not be ruled out off-hand. It means that in case of larger number of samples, bigger scatter of results would be expected. On the other hand the areal distribution of sample localities and "c" values

TABLE 1

Lattice parameter values ("C", in Å) of carbonaceous matter in the easternmost Penninic windows and in the Tauern Window

Easternmost Penninic windows

sample	"C"	sample	"C"	sample	"C"
A13	6.72	A18	6.70	A44	6.73
A50	6.73	A51	6.71	A64	6.70
A77	6.69	A80	6.73	A91	6.71
A101	6.71	K12	6.73	K13A	6.74
K16	6.63	K21	6.74	K33	6.74
Fcs—203B	6.73	Fcs—203F	6.70	Kő—6/1	6.77
Kő—6/2	6.76	Bo—8/2	6.74	Fcs—74/96	6.72
B—2	6.74	V15B	6.71	V17B	6.77
V15C3	6.72 and 6.79				

The Tauern Window

sample	"C"	sample	"C"	sample	"C"
A113	6.70	A123	6.72	A125	6.72
HM	6.72				

TABLE 2

Half-height width ($W_{1/2}$, in °2Θ) values of carbonaceous matter in the easternmost Penninic windows and in the Tauern Window

Easternmost Penninic windows

sample	$W_{1/2}$	sample	$W_{1/2}$	sample	$W_{1/2}$
A51	1.0	A54	1.55	A67	1.4
A79	1.3	B10/4K	0.8	B10/4Ab	1.0
V15C3	1.26	Fcs—203B	0.61	Kő—6/1	1.05
Kő—6/2	0.65	Bo—8/2	0.98	K16	0.52
K21	1.07	K29	0.9	K33	0.65

The Tauern Window

sample	$W_{1/2}$	sample	$W_{1/2}$	sample	$W_{1/2}$
A109	0.41	A113	0.58	A116	0.85
A121	0.7	A123	0.45	A125	0.42
HM	0.42				

(Fig. 1 and *5)* point to the importance of geological conditions as the main causes of the observed scatter in "c" values. Detailed interpretation of this areal variability is discussed in the next part of the paper.

The comparative samples of the Tauern window provided the general values around 6.70—6.72 Å.

The half-height width values of graphites of the Burgenland Penninic unit range from 0.6 to 1.2 °2Θ, while the samples collected from the Tauern window gave data between 0.4 and 0.85 °2Θ (Table 2). Plotting these $W_{1/2}$ data against the metamorphic temperatures it is apparent that the $W_{1/2}$ values show decreasing tendency with increasing T *(Fig. 4)*. This feature hints at the increasing crystallite-size of the the graphites (KWIECINSKA, 1980).

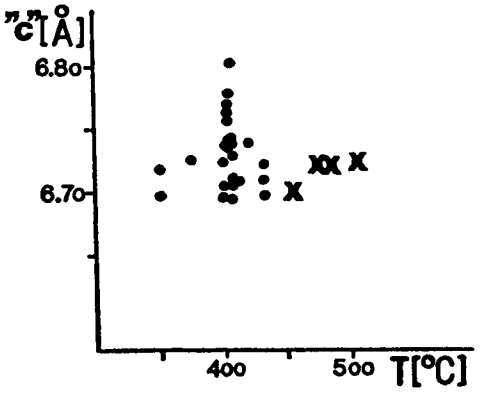

Fig. 3. Lattice parameter dara („C") of graphites versus metamorphic temperatures inferred from results of KOLLER (1985) and MATURA—SUMMESBERGER (1980). o: Burgerland Penninic; x: Tauern Window

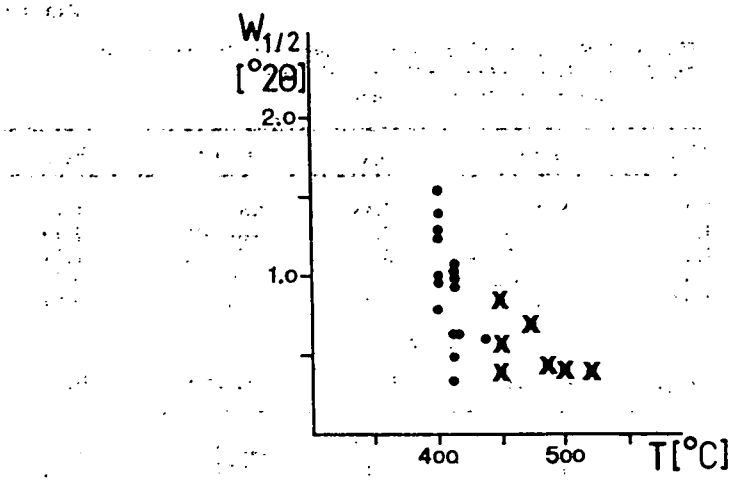

Fig. 4. Plot showing half-height width ($W_{1/2}$) values against metamorphic temperatures for carbonaceous matter of Penninic terranes. Tauern Window: (x), Burgerland windows: (o). The temperature data are the same as in *Fig. 3.*

RELATIONS BETWEEN GRAPHITIZATION AND METAMORPHIC CONDITIONS

Plotting the "c" values on the map of the study area a systematic distribution can be observed *(Fig. 5)*. It is apparent that these data are higher in the Kőszeg Mts. (Western Hungary) than in other parts of the windows. On the other hand, there is no distinct trend from lower to higher metamorphic degrees. This latter observation points to the role of sheart stresses that were effective enough to produce well developed graphite even at 350—400 °C. This feature is not unique, as ÁRKAI *et al.* (1981) have mentioned that shearing can promote graphitization even under very low-grade metamorphic conditions.

There is another factor that can also enhance this effect: the composition of the starting organic matter. DEMÉNY and KREULEN (1989) have described an areal variability having normal marine organic matter in the Mölltern and Bernstein windows and detrital carbonaceous material in the Kőszeg—Rechnitz area. It is well known that the former material is much more sensitive to metamorphic influences than the latter one (MCKIRDY—POWEL, 1974). As the metamorphic temperatures were higher in the area of the Kőszeg—Rechnitz window where detrital organic matter is predominant than in the Mölltern and Bernstein windows with normal marine material, no surprise that there are graphites with about the same "c" values throughout the whole unit.

The explanation of the high "c" data of the Kőszeg Mts. can be found in the difference in deformations and fluid behaviours. Several samples of this area contain trapped carbonaceous material that structurally poorly developed (DEMÉNY, 1986, KUBOVICS *et al.*, 1988), such as sample V15C3. This observation hints at a locally closed system that prevented the release of volatiles which inhibited the structural ordering of graphites. As it has been pointed out by WINTSCH *et al.* (1981) such trapped fluids can prevent the complete graphitization resulting in lower degree of ordering.

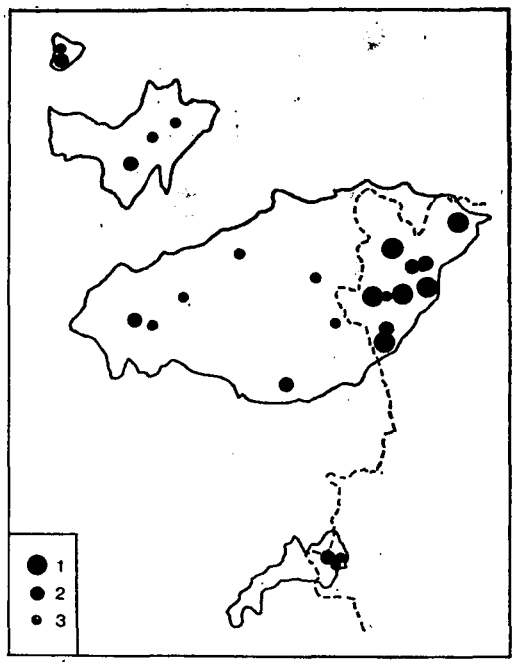

Fig. 5. Areal variability of „C" lattice parameter data in the easternmost Penninic windows. 1. values higher than 6.74 Å, 2. values between 6.74 and 6.71 Å, 3. values lower than 6.71 Å. See *Fig. 1.* for comparison

After these considerations I intended to correlate the "c" data with the graphite geothermometer of SENGELIA *et al.* (1977), but I had difficulties in the interpretation. To solve this problem I have collected the data of several authors mentioned before and plotted them in the diagram given by SHENGELIA *et al. (Fig. 6)*. It is apparent that the experimental curve greatly differs from the others. In my oppinion the reason is that the laboratory conditions of Shengelias'work didn't follow properly the natural processes, hence the graphite "geothermometer" should be reevaluated. The curves for different metamorphic regimes (HP/LT type to LP/HT one) prove that the pressure has a determining role during natural graphitization as has been mentioned before.

The results presented in this paper show a relationship with the curves of the high pressure and regional dynamothermal metamorphic terranes *(Fig. 7)* which connection is in a good agreement with the geological facts (see Introduction).

Finally it can be concluded that in the rock sequence studied here the structural ordering of graphites doesn't serve as a good geothermometer, but it can provide valuable information for the metamorphic evolution.

CONCLUSIONS

The "c" values of graphites of the Burgenland Penninic system show a distinct areal distribution which seems to be independent of the increasing metamorphic degrees. It would mean that about 350—400 °C well developed graphite has been

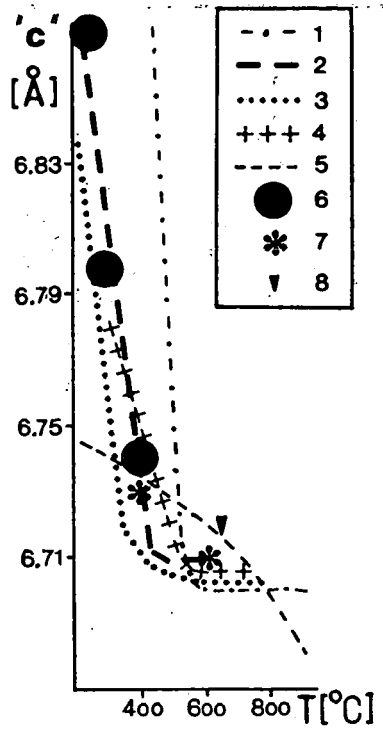

Fig. 6. Lattice parameter data („C") of graphites versus metamorphic temperatures. „C" values are from: 1. OKUYAMA—KUSONOSE and ITAYA (1987), 2. DIESSEL *et al.* (1978), 3. GREW (1974), 4. DIESSEL—OFFLER (1975), 5. SHENGELIA *et al.* (1977), 6. ITAYA (1981), 7. FRANK (1983), 8. KATZ (1987)

formed which can be attributed to the effect of strong deformation and shearing. This process is enhanced by differences in the starting organic compositions as we have more sensitive matter in the areas with lower metamorphic degrees than in the areas of higher temperatures. As a consequence of these compositional differences the same "c" values have been determined in areas with slightly different metamorphic temperatures.

The metamorphic fluids may have also affected the process of graphitization. The poor development of carbonaceous matter in some rocks of the Kőszeg Mts. indicates a locally closed system in which trapped organic compounds prevented the complete ordering.

On the contrary, the $W_{1/2}$ values show good correlation with the metamorphic temperatures that points to increasing crystallite size of graphites regardless of deformation and fluid mobility.

I applied the graphite "geothermometer" to the studied samples on the base of literature data. It has turned out during the interpretation that — at least in this case — this method can provide useful information for the effects of deformation, shearing and fluid behaviours rather than for the metamorphic temperatures.

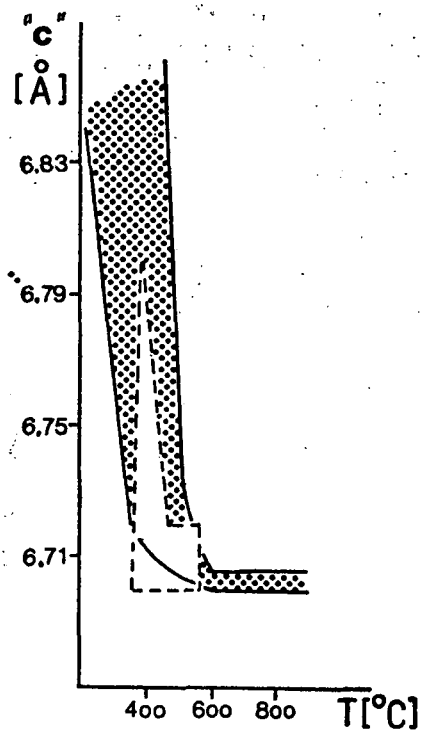

Fig. 7. „C" parameter distributions of literature data and the Penninic carbonaceous matter. Spotted area: data shown in *Fig. 6.* The area indicated by dashed lines consists of the "c" values of Penninic samples

ACKNOWLEDGEMENTS

I should like to express my thanks to professor IMRE KUBOVICS for rendering my work at his department possible. Valuable help of my colleagues at the Dept. of Petrology and Geochemistry and the Dept. of Mineralogy, ELTE is also gratefully acknowledged. Fruitful discussions with dr. P. ÁRKAI greatly improved the paper. The field work in Austria was financially supported by the Soros Foundation, New York (87-D116, 1180).

REFERENCES

ÁRKAI, P., HORVÁTH, Z. A., TÓTH, M. (1981): Transitional very low- and low-grade regional metamorphism of the Paleozoic formations, Uppony Mountains, NE-Hungary: mineral assemblages, illite-crystallinity, -b and vitrinite reflectance data. Acta Geol. Acad. Sci. Hung. **24,** 265—294.

ARNETH, J. D., SCHIDLOWSKY, M., SARBAS, B., GEORG, V., AMSTUTZ, G. C. (1985): Graphite content and isotopic fractionation between calcite-graphite pairs in metasediments from the Mgama Hills, Southern Kenya. Geochimica et Cosmochimica Acta. **49,** 1553—1560.

BANDAT, H. (1928): Geological conditions of the western part of the Kőszeg-Rohonc Mts. Földtani Szemle. **I. 3,** 1—24. (in Hungarian).

BANDAT, H. (1932): Die geologische Verhaltnisse des Kőszeg-Rechnitzer Schiefergebirge. Földtani Szemle. **I. 2,** 140—186.

BONIJOLY, M., OBERLIN, M., OBERLIN, A. (1982): A possible mechanism for natural graphite formation. International Journal of Coal Geology. **1,** 283—312.
BRAGG, R. H., CROOKS, D. D., FENN Jr., R. W., HAMMOND, M. L. (1964): The effect of applied stress on the graphitization of pyrolitic graphite. Carbon. **1,** 171—179.
BUSECK, P., HUANG, B. (1985): Conversion of carbonaceous material to graphite during metamorphism. Geochimica et Cosmochimica Acta. **49,** 2003—2016.
DEMÉNY, A. (1986): Petrological and geochemical investigations on the parametamorphites of the Kőszeg Mts. Diploma work. Dept. of Petrology and Geochemistry. ELTE, Budapest. pp. 68. (in Hungarian).
DEMÉNY, A., KREULEN, R. (1989): Carbon isotope ratios of graphites in Alpine Penninic rocks: origin of organic matter and facies correlation between the Tauern Window and the easternmost Penninic windows (Austria and W. Hungary). In prep.
DIESSEL, C. F. K., Offler, R. (1975): Change in physical properties of coalified and graphitized phytoclasts with grade of metamorphism N. Jb. Mineral. Mh. **1975,** 11—26.
DIESEL, C. F. K., BROTHERS, R. N., BLACK, P. M. (1978):: Coalification and graphitization in high-pressure schists in New Caledonia. Contributions to Mineralogy and Petrology **68,** 63—78.
DROOP, G. T. R. (1985): Alpine metamorphism in the south-east Tauern Window, Austria: 1. P-T variations in space and time. J. metamorphic Geol. **3,** 371—402.
FÖLDVÁRY, A., NOSZKY, J., SZEBÉNYI, L., SZENTES, L. (1948): Geological observations in the Kőszeg Mts. Jel. Jöv. Mélykút. 1947/48 évi Munk. 5—31. (in Hungarian).
FRANK, E. (1983): Alpine metamorphism of calcareous rocks along a cross-section in the Central Alps: occurrence and breakdown of muscovite, margarite and paragonite. Schweiz. Min. Petr. Mitt. **63,** 37—93.
FRENCH, B. M. (1964): Graphitization of organic material in a progressively metamorphosed Precambrian Iron Formation. Science. **146,** 917—918.
GREW, E. (1974): Carbonaceous material in some metamorphic rocks of New England and other areas. Journal of Geology. **82,** 50—73.
GRIFFIN, G. M. (1967): X-ray diffraction techniques applicable to studies of diagenis and low-rank in humic sediments. Journal Sediment. Petrol. **37,** 1006—1019.
HERRMANN, P., PAHR, A. (1988): Erlauterungen zu Blatt 138 Rechnitz. Geologische Karte der Republik österreich 1:50 000. Wien (Geol. B.-A.), 1988.
ITAYA, T. (1981): Carbonaceous material in pelitic schists of the Sangabawa metamorphic belt in Central Shikoku, Japan. Lithos. **14,** 215—224.
KATZ, M. B. (1987): Graphite deposits of Sri Lanka: a consequence of granulite facies metamorphism. Mineralium Deposita. **22,** 18—25.
KISHÁZY, P., IVANCSICS, J. (1976): Standard investigation on the metamorphites of Western Hungary. II. The Rechnitz (Rohonc) metamorphic complex. Manuscript. MÁFI Adattár, Budapest. (in Hungarian).
KISHÁZY, P., IVANCSICS, J. (1984): A guide to the geological study of the outcrops of the Kőszeg crystalline schist sequence. Manuscript. MÁFI Adattár. (in Hungarian).
KOLLER, F. (1985): Petrologie und Geochemie der Ophiolite des Penninikums am Alpenostrand. Jb. Geol. B.-A. **128,** 83—150.
KOLLER, F., PAHR, A. (1980): The Penninic ophiolites of the Eastern end of the Alps. Ofioliti. **5,** 65—72.
KUBOVICS, I. (1983): Petrological characteristics and genetics of the crossitite of Western Hungary. Földtani Közlöny. **113,** 207—224. (in Hungarian).
KWIECINSKA, B. (1980): Mineralogy of natural graphites. Prace Mineralogiczne. **67,** Polska Akademia Nauk. pp. 79.
LANDIS, A. (1971): Graphitization of dispersed carbonaceous material in metamorphic rocks. Contributions to Mineralogy and Petrology. **30,** 54—67.
LELKES-FELVÁRY, GY. (1982): A contribution to the knowledge of the Alpine metamorphism in the Kőszeg-Vashegy area (Western Hungary). N. Jb. Geol. Palaont. Mh. **1982. 5.** 297—305.
MARSH, H., WARBURTON, A. P. (1976): Cataliting graphitization of carbon using titanium and zirconium. Carbon. **14,** 47—52.
MATURA, A., SUMMESBERGER, H. (1980): Geology of the Eastern Alps. Abh. Geol. B.-A. 26° CGI. **34,** 103—170.
MCKIRDY, D. M., POWELL, T. G. (1974): Metamorphic alteration of carbon isotopic composition in ancient sedimentary organic matter: new evidence from Australia and South Africa. Geology. **2,** 591—595.
NODA, T., INAGAKI, M. (1964): Effect of gas phase on graphitization of carbon. Carbon. **2,** 127—130.
NODA, T., KAMIYA, K., INAGAKI, M. (1968 a): Effect of pressure on graphitization of carbon. I. Heat treatment of soft carbon under 1, 3 and 5 kbar. Bull. Chem. Soc. Japan. **41,** 485—492.

NODA, T., INAGAKI, M., HIRANO, S., AMANUMA, K. (1968 b): Effect of coexisting minerals on graphitization of carbon. I. Heat treatments of carbon under 3 kbar in the presence of limestone. Bull. Chem. Soc. Japan. **41,** 1245—1248.

OKUYAMA-KUSONOSE, Y., ITAYA, T. (1987): Metamorphism of carbonaceous material in the Tono contact aureole, Kitakami Mountains, Japan. Journal of Metamorphic Geology. **5,** 121—139.

PESQUERA, A., VELASCO, F. (1988): Metamorphism of the Palaeozoic Cinco Villas massif (Basque Pyrenees): illite crystallinity and graphitization degree. Mineralogical Magazine. **52,** 615—625.

SCHÖNLAUB, H. P. (1973): Schwamm-Spiculae aus dem Rechnitzer Schiefergebirge und ihr stratigraphiser Wert. Jb. Geol. B.-A. **116,** 35—48.

SHENGELIA, D. M., AKHVLEDIANI, R. A., KETSKHOVELI, D. N. (1977): The graphite geothermometer. Doklady. Earth Sci. Sect. **235,** 132—134.

WINTSCH, R. P., O,CONELL, A. F., RANSOM, B. L., WIECHMANN, M. J. (1981): Evidence for the influence of f_{CH4} on the crystallinity of disseminated carbon in greenschist facies rocks, Rhode Island, USA. Contributions to Mineralogy and Petrology. **77,** 207—213.

Manuscript received, 1. November, 1989

Acta Mineralogica-Petrographica, Szeged, XXX, 115—126, 1989

FLUID INCLUSION STUDY OF THE GNEISS FROM THE BOREHOLE NAGYATÁD K—1, 11, SW TRANSDANUBIA [HUNGARY]

KÁLMÁN TÖRÖK

Department of Petrology and Geochemistry, L. Eötvös University

ABSTRACT

Fluid inclusions in synkinematic quartz lenses, segregations and those in the matrix quartz were studied from the 11-th core of the Nagyatád-K-1 borehole. This one is bored in the Somogy—Dráva Basin, SW-Hungary. It explored a polymetamorphic staurolite-kyanite-garnet gneiss mass. The studied fluid inclusions can be divided into three groups according to their compositoin: (1) $H_2O+1.7$—14.3 NaCl equivalent weight % salt, (2) $CO_2+/-CH_4$ and/or N_2 [$X_{CH_4-N_2} \leqq 0.1$], (3) mixed CH_4—N_2—CO_2.

The peak P—T conditions of two metamorphic phases were inferred from geothermobarometric data of ÁRKAI [1984] and the obtained fluid inclusion data. The inferred P—T conditions of the first metamorphic phase were about 890—900 MPa and 550 °C. The fluid, existed at these P—T conditions, was a CO_2 rich one. The maximum pressure and temperature, reached during the second stage of metamorphism was determined by the method of intersecting isochores of two immiscible fluids, trapped simultaneously. On the basis of this method the obtained pressure was 240—260 MPa and the temperature about 540 °C. All the three compositional types were present during the second metamorphic event. The third metamorphic stage was a very low-low grade one with a simple, dilute aqueous solution.

INTRODUCTION

The studied Nagyatád-K-1-11. sample derives from a hydrocarbon exploratory well of the National Oil and Gas Industrial Trust. The exposed staurolite-kyanite-garnet gneiss belongs to the crystalline basement of the Somogy Dráva Basin. The exact location of the borehole is shown on the *Fig 1* after ÁRKAI [1984].

The aim of this paper is to provide further data on the polymetamorphic P—T history and fluid evolution of the crystalline basement of the Somogy—Dráva Basin on the basis of fluid inclusion study. This paper is a first attempt in this topic in Hungary.

The obtained fluid inclusion data and the available geothermo-barometric results made it possible to construct a P—T path for the polymetamorphic history of the basement.

GEOLOGY AND PREVIOUS DATA

The Somogy—Dráva Basin is situated in south western Transdanubia, as it is shown on the *Fig. 1.* Its crystalline basement is known only by hydrocarbon exploratory wells, because it is covered by thick neogene-quarternary sediments.

H-1088 Budapest, Múzeum krt. 4/a

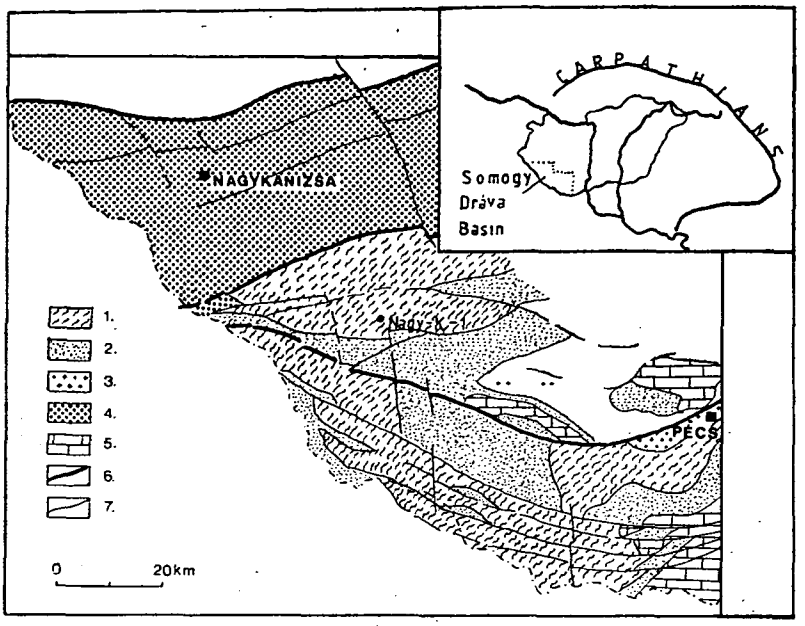

Fig. 1. Simplified geologic sketch of the pre-Tertiary formations of the Somogy—Dráva Basin with the locality of the Nagyatád-K-1 borehole taken from ÁRKAI [1984]. 1. = polymetamorphic basement, 2. = Paleozoic in general, 3. = granitoid rocks, 4. = Permian-Mesozoic sedimentary rocks of the northern part of the Somogy—Dráva Basin, 5. = Mesozoic in general, 6. = major tectonic lines, 7. = subordinate tectonic lines

The crystalline basement of the Somogy—Dráva Basin is connected with the Slovenian Papuk—Jankovac migmatite-metamorphite and the Psunj—Katjevo granite-metamorphite complexes towards south-southwest. On the opposite direction it is in connection with the Transsylvanian Midmountains through the Görcsöny—Mórágy complex and the polymetamorphic basement of the Hungarian Great Plain [SZEDERKÉNYI, 1974; JANTSKY, 1979; ÁRKAI ET AL., 1985].

The most frequent rock types are micaschist, gneiss or milonite, blastomilonite originated from the rocks mentioned above. The amphibolite and amphibole-gneiss is subordinate. The detailed description of the different rock types and a more detailed geologic map of the crystalline basement is published by ÁRKAI [1984], see this study for details.

The rock forming minerals of the studied Nagyatád-K-1, 11 staurolite-kyanite-garnet gneiss are plagioclase, quartz, biotite, muscovite. The rock contains garnet, kyanite, staurolite, carbonate minerals, chorite, zircon, rutile, apatite, pyrite, and dispersed graphite as accessory minerals.

The case history of the Somogy—Dráva Basin and the adjoining areas can be summarized according to SZEDERKÉNYI [1974, 1976], JANTSKY [1979], LELKES—FELVÁRY and SASSI [1981], and ÁRKAI [1984], ÁRKAI *et al.* [1985].

The parent rock of the different micaschist and gneiss types may have been pelitic-psammitic sediment. However, in case of some gneiss types of mainly potash feldspar-plagioclase-quartz composition, the magmatic origin cannot be excluded either. The precursor of the amphibolite and amphibole-gneiss may have been a

certain kind of basic-neutral magmatic rock. The exact age of the parent rocks is unknown. According to suppositions it might be precambrian or early paleozoic.

The first metamorphic event was a Barrovian type one with kyanite-staurolite-garnet-biotite-muscovite-plagioclase [sometimes with sillimanite] mineral assemblage. ÁRKAI [1984], ÁRKAI *et al.* [1985] determined the peak P—T conditions of this event from 5 samples, belonging to the crystalline basement of the Somogy—Dráva Basin, using a plagioclase-garnet-biotite-muscovite geothermobarometer [GHENT and STOUT, 1981] and a hornblende-plagioclase geothermobarometer presented by PLJUSNINA [1982]. He obtained 590—890 MPa pressure and 550—600 °C for the micaschist and gneiss samples and 750 MPa and 507 °C for the amphibolite. The age of the first metamorphic event is thought to be Precambrian, Caledonian or early Hercynian.

The second stage of the metamorphism was a low pressure, medium grade one which can be caracterized by andalusite-staurolite-garnet-biotite-muscovite mineral assemblage. During this event a migmatitisation and a granitisation took place in the Mórágy unit and in some places of the crystalline basement of the Hungarian Great Plain. The age of the second stage is defined by isotope geochronological data [BALOGH *et al.* 1981]. The inferred age of the metamorphism and the granitisation is Hercynian. BUDA [1972] reported late hercynian potash metasomatism.

The first two metamorphic events were followed by a low-very low grade one which locally caused milonitisation of the preexisting rocks. The typical mineral assemblage of this phase is quartz-sericite-chlorite and carbonate minerals. The age of the third event may have been late Hercynian.

SELECTING OF SAMPLES, SAMPLE PREPARATION

The fluid inclusion studies were carried out on synkynematic quartz segregations, which are concordant with the schistosity. Besides these inclusions 20 aqueous inclusions were also measured from the matrix quartz grains. Fluid inclusions in other minerals than quartz were not observed. The selection and preparation of the samples were carried out in accordance with the method proposed by HOLLISTER *et al.* [1981].

All measurements were conducted on doubly polished 100—150μ thick samples, using a Chaixmeca heating-freezing stage [POTY *et al.* 1976] at the Department of Mineralogy of the Eötvös Loránd University. The reproducibility of the measurements was +/−0.1 °C in the negative and +/−0.2 °C in the positive temperature interval. All microthermometric measurements were made during the heating cycles. The correction of the obtained data was carried out using the Inc. calc- computer program of GATTER and MOLNÁR [unpubl.].

The Raman spectroscopic analyses were run in Novosibirsk at the Institute of Geology and Geophysics of the Siberian Branch of Academy of Sciences of the Sovietunion by A. SHEBANIN on a Jobin Yvon instrument.

MODE OF OCCURENCE AND TRAPPING SEQUENCE

The trapping sequence and the following grouping of inclusions were deduced from textural observations on the basis of textural criteria, published by SWANENBERG [1980], TOURET [1981], ROEDDER [1984] and OLSEN [1987]. The fluid inclusions were grouped in four categories from the oldest [group A] to the youngest ones

[group D]. The trapping sequence of the inclusions is not always clear; there are overlaps between the four groups. An example for the mode of occurence of the A, B and C type CO_2 inclusions is presented on the *Fig. 2.*

Type A: Solitary inclusions and those in small groups both in the synkinematic quartz lenses and in the matrix quartz grains are considered to belong to this group. Both CO_2 and H_2O inclusions belong to the type A. The observed clusters of inclusions in all cases were intragranular. The inclusions are rounded or have negative crystal shape. The negative crystal shape is more caracteristic for the CO_2 inclusions than for the H_2O rich ones. The CO_2 inclusions are between 5 μm and 10 μm in size, while the H_2O-rich ones range from 8 μm to 12 μm in longest dimension.

Type B: Both CO_2 and H_2O rich inclusions belong to this group. The inclusions are similar in size to those being in the group A. The shape of the inclusions tends to be more sperical or ellipsoidal and there are less negative crystal like inclusion than are found in the group A. The inclusions form trails along healed microcracks which do not cross grain boundaries. There are no CO_2 rich and aqueous inclusions together along the same trail.

Type C: All of the compositional groups are observed in this type. There are CH_4—N_2—CO_2, aquaeous and CO_2 rich inclusions along healed fractures which cross the grain boundaries and show the features of a mature fracture OLSEN [1987].

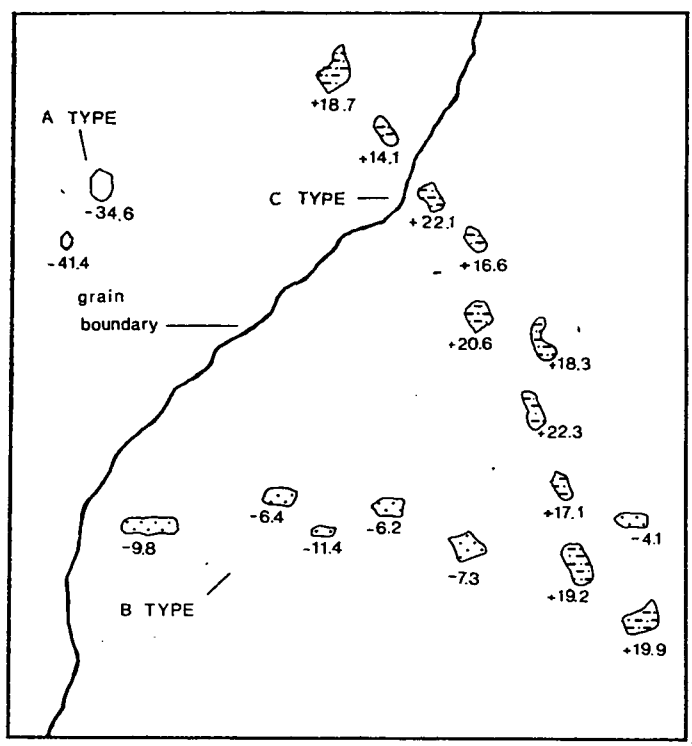

Fig. 2. An example for the mode of occurence of the A, B, and C type CO_2 inclusions. The numbers indicate the homogenisation temperature of the inclusions in °C

O=A type CO_2 inclusions,
....=B type CO_2 inclusions,
—.—.—=C type CO_2 inclusions.

The inclusions are ellipsoidal or irregular in shape and their size ranges from 9 μm to 16 μm. The C type CO_2 rich inclusion trails crosscut the B type ones at the angle of 50°—70°.

Type D: There were only H_2O-rich inclusions observed in this group. The trails of inclusions along immature healed fractures [OLSEN 1987] crosscut the grain boundaries and contain sometimes hundreds of well oriented, irregular or amoeba-like inclusions of various size, up to 50 μm.

FLUID INCLUSION DATA

CO_2-rich inclusions

The CO_2 rich inclusions were identified by melting temperatures close to −56.6 °C Most of the inclusions show freezing point depression to a minimum of −59.4 °C *[Fig. 3b]*. They may contain a minor amount of either CH_4 or N_2 up to 0.1 mol% [BURRUSS, 1981; KERKHOF, 1988]. However, the highest density CO_2 inclusion measured by Raman spectroscope, does not contain any CH_4 or N_2 [Table 1]. The homogenisation temperature of the CO_2-rich inclusions range from −41.4 °C up to +26.5 °C *[Fig. 3a]*. All inclusions homogenized to liquid phase. There are no CO_2-rich inclusions observed in the matrix quartz, they seem to be restricted to the quartz segregations where they tend to separate from the H_2O-rich ones.

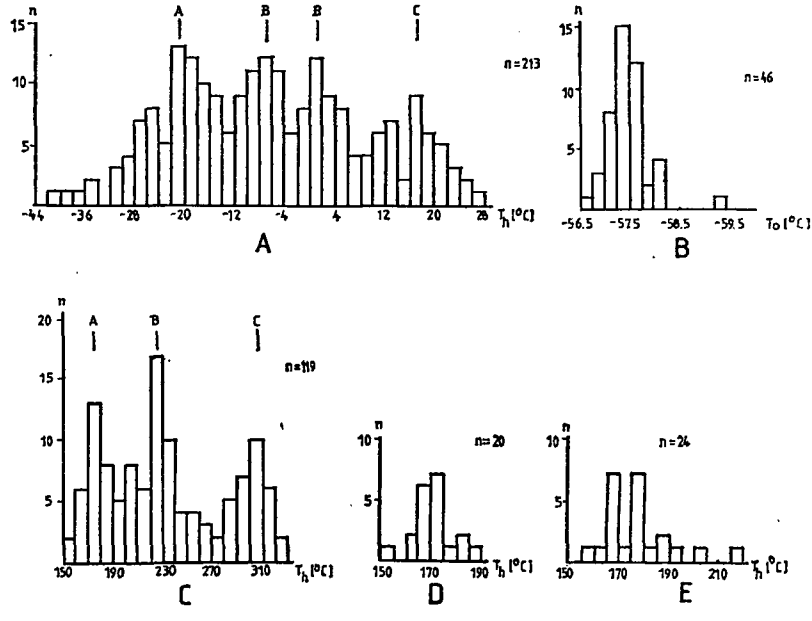

Fig. 3. Distribution diagrams: n — number of measurements, T_h — homogenisation temperature, T_0 — melting temperature. A: T_h distribution diagram of A, B and C type CO_2 inclusions. B:- Distribution diagram of melting temperatures of CO_2 inclusions. C: Distribution diagram of homogenisation temperatures of A, B and C type aqueous inclusions in the quartz segregations. D: The dis ribution diagram of H_2O inclusions in the matrix quartz. E: T_h distribution diagram of D type aqueous inclusions

TABLE 1

Results of the laser Raman spectroscopic analyses.
Analyst: A. SHEBANIN

Sample	T_h(°C)	T_0(°C)	CO_2	CH_4	N_2
N—2/8	−41,4	−56,9	100	n.d.	n.d.
N—II/1	−63,9C	−75,0	25	39	36

T_h = homogenisation temperature, T_0 = CO_2 melting temperature, C = critical homogenisation, n.d. = not determinable. All compositional units are given in mole percent.

A computer program, "CO_2", published by NICHOLLS and CRAWFORD [1985], utilizing the equation of state of ANGUS *et al.* [1976], was used to determine the densities and the isochores of the CO_2-rich inclusions. The isochore of the most dense CO_2 inclusion and those of belonging to the maxima of the histogram *[Fig. 3a]* are presented on the *Fig. 4*. Though there are overlaps in the homogenisation temperatures of the different inclusion types, but the maxima of the histogram roughly correspond to the types listed above.

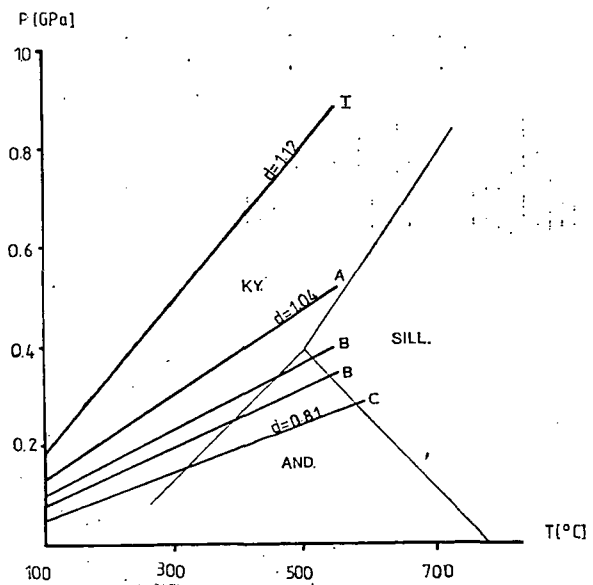

Fig. 4. Representative isochores of CO_2 inclusions. I = isochore of the most dense CO_2 inclusion, A, B, C = isochores, calculated from the adequate peaks of the distribution diagram *[Fig. 3a.]*. ky. = kyanite, and. = andalusite, sill. = sillimanite. The Al_2SiO_5 stability fields were drawn after HOLDAWAY [1971]

H_2O-rich inclusions

The H_2O-rich inclusions are less common in the quartz segregations than the CO_2-rich ones. The homogenisation temperatures [T_h] of the A, B, C type aqueous inclusions range from +154.8 to +325.8 °C with three maxima *[Fig. 3c]*. These inclusions contain more or less dilute solutions with 1.7—14.3 wt.% NaCl equivalent salt content. There is no correlation between the salinity and the homogenisation temperature of the inclusions.

The maximum of the homogenisation temperatures of the aqueous inclusions in the matrix quartz gives a good coincidence with that of the A type H_2O inclusions in the quartz segregations. The salinity of the matrix quartz H_2O inclusions ranges from 3.2 to 4.6 NaCl equivalent wt% and the homogenisation temperature is between +155 °C and +188 °C *[Fig. 3d]*. The H_2O inclusions found in the matrix quartz grains may represent a fluid originated from metamorphic reactions taking place soon after the peak P—T conditions of the first metamorphic stage. The relative scarcity of H_2O inclusions, as compared with the quartz segregations, may be due to the H_2O consuming mineral reactions, such as the formation of biotite and muscovite during different stages of metamorphism on one hand and to the possible destruction of inclusions by later recrystallisation on the other. The homogenisation temperature and salinity range of H_2O inclusions in the matrix quartz is less broad than those of the type A aquaeous inclusions in quartz segregations, which may refer to the fact that these fluids were closer to the equilibrium with the host rock than the aqueous fluids trapped in the quartz segregations [YARDLEY, 1983]. The lack of CO_2 inclusions in the matrix quartz may be due to the lack of CO_2 producing reaction during the metamorphism. The CO_2-rich fluids were probably introduced along the quartz segregations.

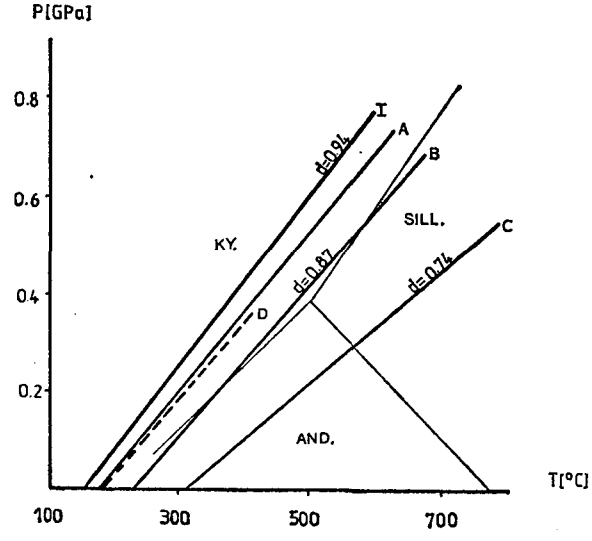

Fig. 5. Representative isochores of the aquaeous inclusions. I = isochore of the most dense H_2O inclusion, A, B, C, D — Isochores, calculated from the adequate peaks of the distribution diagram *[Fig. 3c* and *3e]*. ky = kyanite, and. = andalusite, sill. = sillimanite. The Al_2SiO_5 stability fields are after HOLDAWAY [1971]

Most of the T_h values of the D-type, late aquaeous inclusions fell within the interval between 160 °C and 180 °C, but the whole measured T_h range is from 155.4 °C up to 217.2 °C *[Fig. 3e]*. The salinity of the D-type aquaeous inclusions ranges from 1.9 to 4.2 wt% NaCl equivalent.

Calculation of the isochores was made by computer program of GATTER and MOLNÁR [unpubl.] based on the equation of state published by TALANTCHEV [1978]. Pressure results, exceeding 300 Mpa were obtained by extrapolation. The representative isochores of the most dense A-type aquaeous inclusion [I] as well as those belonging to the three maxima of the histogram *[Fig. 3c]* and to the D-type H_2O-rich inclusions are presented on the *Fig. 5.*

CH_4—N_2—CO_2 inclusions

The CH_4—N_2—CO_2 inclusions were observed along distinct healed mature fractures which always cross grain boundaries. All these inclusions belong to the C-type considering textural criteria. They were identified by critical homogenisation between −83 °C and −63.9 °C. The measured melting temperatures of the solid CO_2 range from −75 °C up to −73.6 °C. The exact composition of a CH_4—N_2—CO_2 inclusion was determined by Raman spectroscopy [Table 1j. The measured intermediate composition between these three fluids is quite rare. According to KERKHOF [1988], most of the metamorphic fluid inclusions in the CH_4—N_2—CO_2 system can be approached as binary CO_2—N_2, CO_2—CH_4, or CH_4—N_2 systems, though TOMILENKO and CHUPIN [1983] also report mixed CH_4—N_2—CO_2 inclusions with various proportions of the three fluids in high grade metamorphic rocks of the Aldan shield.

Besides the inclusion types listed above, some one phase inclusions could be observed that failed to show any phase change in the temperature interval of −180 °C and +350 °C. These inclusions may contain some kind of low pressure gas or metastable fluid [HOLLISTER *et al.*, 1981]. Decrepitated inclusions of all compositional types were observed as well.

DISCUSSION

If we want to evaluate the nature of the fluid existed at peak metamorphic conditions we have to consider the followings: (1) The isochore of the most dense CO_2 inclusion marks higher pressure than that of the most dense aqueous inclusion, (2) In spite of thorough study of several samples, mixed CO_2—H_2O inclusions were not observed at all, (3) The earlier published miscibility-immiscibility relations in the system CO_2—H_2O—NaCl [see TAKENOUCHI and KENNEDY, 1965; GEHRING *et al.*, 1979; HENDEL and HOLLISTER, 1981; SISSON *et al.*, 1981; BOWERS and HELGESON, 1983a, b; among others].

Considering the observations and available literature data, the existence of a pure or almost pure CO_2 fluid is the most probable at peak P—T conditions of the first metamorphic stage. However, H_2O may be present in minor amount that cannot be observed optically in the CO_2 inclusion up to 20 mol% [CRAWFORD and HOLLISTER, 1986]. The presence of more than 20 mol% water cannot be proved because of the lack of mixed CO_2—H_2O inclusions. The causes of separated CO_2 and H_2O inclusions can be as follows:

(1) Decrepitation of preexisting mixed CO_2—H_2O inclusions and redistribution of the fluid under P—T conditions where the mixed CO_2—H_2O fluid was no more miscible.
(2) Sampling problems, due to the little amoung of core sample.
(3) The immiscibility may account for distinct CO_2 and H_2O inclusions as well, but only under lower P—T regions of the metamorphism. The two fluids should have been miscible at higher metamorphic grades regarding the data published in the studies listed above.
(4) Physical separation of the two fluids at higher P—T regions of metamorphism [CRAWFORD and HOLLISTER, 1986].
(5) The recrystallisation of the host quartz due to the later stages of the metamorphism also may have contributed to the elimination of the mixed CO_2—H_2O inclusions.
(6) The fluids were introduced separately along distinct fractures.

The peak P—T conditions of the first stage of the metamorphism, marked by the most dense CO_2 isochore [see isochore I on the *Figure 4*] are in good agreement with those, determined by ÁRKAI [1984], P=890 MPa, T=550 °C, on the basis of plagioclase-garnet-biotite-muscovite geothermobarometer [GHENT and STOUT, 1981]. After the peak of the metamorphism, the fluid enriched in H_2O, but the two fluids trapped separately. The representative isochores of the A and B-type CO_2 and H_2O inclusions *[Fig. 4* and *5]* show a continuous drop in the pressure and temperature. The aqueous inclusions in the matrix quartz formed during the early stage of the retrogression at the same time with the A-type aquaeous inclusions.

There were three different fluids, CO_2, H_2O, and CH_4—N_2—CO_2 present during the second, low pressure metamorphic stage. On the basis of intersecting isochores

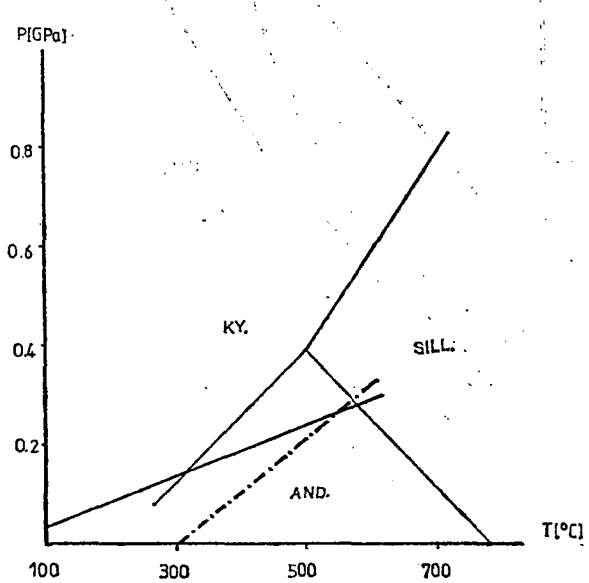

Fig. 6. Intersection of isochores of representative C type aquaeous and CO_2 inclusions, taken from *Fig. 4* and *5*.
—·— representative C type H_2O isochore,
——— representative C type CO_2 isochore

of two immiscible fluids trapped simultaneously, the P—T conditions of the second metamorphic stage can be determined. The intersecting isochores of the C-type H_2O and CO_2 inclusions, calculated from the adequate maxima of the histograms *[Fig. 3a* and *3c]*, show 240—260 MPa pressure and approximately 540 °C temperature *[Fig. 6]*. The pressure and temperature inferred for the second metamorphic phase fall within the stability field of the andalusite [HOLDAWAY, 1971]. Though andalusite was not found in this sample, but it is present in several localities of the crystalline basement of the Somogy—Dráva Basin, giving an evidence on the existence of the second, low pressure metamorphic phase [LELKES—FELVÁRI and SASSI, 1981, ÁRKAI 1984].

The D-type aqueous inclusions, sealed along immature healed fractures, mark a late fluid influx after the second, low pressure metamorphic stage. They are probably due to the third, very low-low grade metamorphic phase. The representative isochore of the D-type aquaeous inclusions *[Fig. 5]* show a similar temperature gradient as the A-type aquaeous inclusions do. According to ÁRKAI [1984], the P—T conditions of this metamorphic event did not reach those of the biotite isograde, that means, the temperature remained below 450 °C [WINKLER, 1976]. If the temperature is considered to be about 300—400 °C, the pressure should have increased during this metamorphic stage.

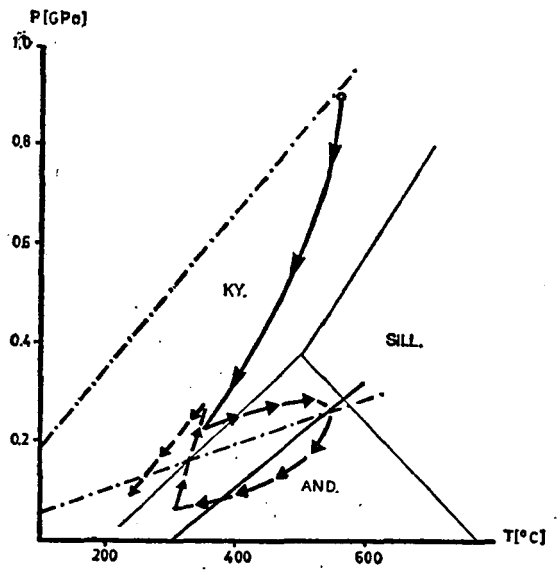

Fig. 7. A possible metamorphic P—T history of the Nagyatád K—1 gneiss on the basis of geothermobarometric data of ÁRKAI [1984, 1985] and fluid inclusion data.

O — peak P—T conditions of the first metamorphi stage,
→ = peak P—T conditions of the first metamorphic stage,
→ = P—T path of the second stage,
—→ = P—T path of the third stage,
—·— = CO_2 isochores [isochore of the most dense CO_2 inclusion and the representative isochore of the C type ones are taken from the *Fig. 4.*],
— = representative isochore of the C type H_2O inclusions taken from the *Fig. 5.*

CONCLUSIONS

The peak metamorphic P—T conditions, marked by the densest CO_2 inclusion, are in good agreement with those, which are calculated from plagioclase-garnet-biotite-muscovite geothermobarometer [GHENT and STOUT 1981] by ÁRKAY [1984], ÁRKAI ET AL. [1985]. The fluid, existed at the peak of the first metamorphic stage was a CO_2-rich one, perhaps with a minor amount of aqueous solution. After the peak P—T conditions CO_2-rich and aqueous fluids existed together and formed separate inclusions during the whole period of metamorphism. The decreasing density of A and B-type fluid inclusions is due to the pressure and temperature drop during the retrogression. When the temperature decreased as low as 300—400 °C at approximately 200—300 MPa pressure, due to uplift, the temperature began to rise again, but the pressure did not change considerably. This increase in the temperature was probably due to a heat influx from below. The pressure and temperature of the second low pressure metamorphic event, inferred from the method of intersecting isochores of two immiscible fluids are about 240—260 Mpa and 540 °C. Besides the temperature increase, the fluid composition became more difficult than it was previously. Three different kinds of fluid existed during this metamorphic stage: a CO_2-rich-, an aqueous- and a mixed CH_4—N_2—CO_2 one. After the peak of the second metamorphism the temperature dropped faster, than the pressure did. During the third phase, the thermal gradient decrased again, i.e. the pressure increased quicker than the temperature did. The fluid composition became simple, only a dilute aquaeous solution was present during the third metamorphism. A possible uplift path, concluded from the obtained data, is presented on the *Figure 7.*

ACKNOWLEDGEMENTS

The author wishes to thank to DR. A. A. TOMILENKO for his helpful instructions and discussions, to DR. A. SHEBANIN for laser Raman analyses, to professor I. KUBOVICS, to DR. I. GATTER and to DR. CS. SZABÓ for critical review of the manuscript. Thanks are also due to DR. J. KÓKAI, the Chief geologist of the National Oil and Gas Trust, who made it possible to collect core samples, to T. SZALAI for adopting the CO_2 computer program, and to MRS. G. SZILÁGYI for her help in drawing the figures.

REFERENCES

ANGUS, S., ARMSTRONG, B., DE REUCK, K. M. [1976]: International thermodynamic tables of the fluid state. Carbon dioxide. Pergamon Press, 67 p.

ÁRKAI, P. [1984]: Polymetamorphism of the crystalline basement of the Somogy—Dráva Basin [Southwestern Transdanubia, Hungary] Acta Miner. Petr. Szeged. **26,** 129—153.

ÁRKAI, P., NAGY, G., DOBOSI, G., [1985]: Polymetamorphic evolution of the South Hungarian crystalline basement, Pannonian Basin: geothermometric and geobarometric data. Acta Geol. Hung. **28,** No. [3—4], 165—190.

BALOGH, K., ÁRVA-SÓS, E., BUDA, GY. [1981]: Chronology of granitoid and metamorphic rocks of Transdanubia [Hungary]. Annuarul Inst. Geol. Geophys., Bucuresti. **61,** 359—364.

BOWERS, T. S., HELGESON, H. C. [1983a]: Calculation of the thermodynamic and geochemical consequences of nonideal mixing in the system H_2O—CO_2—NaCl on phase relations in geologic systems: Equation of state for H_2O—CO_2—NaCl fluids at high pressures and temperatures. Geochim. Cosmochim. Acta **47,** 1247—1275.

BOWERS, T. S., HELGESON, H. C. [1983b]: Calculation of the thermodynamic and geochemical consequences of nonideal mixing in the system H_2O—CO_2—NaCl on phase relations in geologic systems: Metamorphic equilibria at high pressures and temperatures. Amer. Mineral. **68,** 1059—1075.

BUDA, GY. [1972]: Genetic and tectonic classification of the granitoid rocks of Hungary, with special regard to the feldspar investigations. Proceedings of the X. th Dept. of Acad. Sci. Hung. **5,** 21—26. [in Hungarian].

BURRUSS, R. C. [1981]: Analysis of fluid inclusions: phase equilibria at constant volume. Amer. Jour. Sci. Vol. **281.** Oct., 1104—1126.

CRAWFORD, M. L., HOLLISTER, L. S. [1986]: Metamorphic fluids: The evidence from fluid inclusions. In: WALTHER, J. V., WOOD, B. J. [eds.] Fluid-rock interactions during metamorphism. Springer, New York, 1—35.

GEHRIG, M., LENTZ, H., FRANCK, E. U. [1979]: Thermodynamic properties of water-carbon dioxide-sodium chloride at high temperatures and pressures. In: TIMMERHAUS, K. D., BARBER, M. S. [eds.] High pressure science and technology, I, Physical properties and material synthesis. Plenum, New York, 539—542.

GHENT, E. D., STOUT, M. Z. [1981]: Geobarometry and geothermometry of plagioclase-biotite-garnet-muscovite assemblages. Contrib. Mineral. Petrol. 76, 92—97.

HENDEL, E. M., HOLLISTER, L. S. [1981]: An empirical solvus for CO_2—H_2O—2.6 wt% salt. Geochim. Cosmochim. Acta. **45,** 225—228.

HOLDAWAY, M. J. [1971]: Stability of andalusite and the aluminium silicate phase diagram. Amer. Journ. Sci. Vol. **271,** 97—131.

HOLLISTER, L. S., BURRUSS, R. C. [1976]: Phase equilibria in fluid inclusions from Khtada Lake metamorphic complex. Geochim. Cosmochim. Acta. **40,** 163—175.

HOLLISTER, L. S., CRAWFORD, M. L., ROEDDER, E., BURRUSS, R. C., SPOONER, E. T. C., TOURET, J. [1981]: Practical aspects of microthermometry. In: HOLLISTER, L. S., CRAWFORD, M. L. [eds.]: *Short course in fluid inclusions: applications to petrology.* Mineral. Assoc. Canada, Calgary, 278—304.

JANTSKY, B. [1979]: Geology of the granitized crystalline basement of the Mecsek Mts. Annual Geol. Inst. Hung. Vol. **60,** 1—385. [in Hungarian].

KERKHOF. A. M. VAN DEN [1988]: Phase transitions and molar volumes of CO_2—CH_4—N_2 inclusions. Bull. Mineral. **111,** 257—266.

LELKES-FELVÁRI, GY., SASSI, F. P. [1981]: Outlines of the pre-Alpine metamorphisms in Hungary. IGCP Project No. 5, Newsletter **3,** 89—99.

NICHOLLS, J., CRAWFORD, M. L. [1985]: FORTRAN programs for calculation of fluid properties from microthermometric data on fluid inclusions. Comput. Geosci. **11,** 619—645.

OLSEN, S. N. [1987]: The composition and role of the fluid in migmatites: a fluid inclusion study of the Front Range rocks. Contrib. Mineral. Petrol. 96, 104—120.

PLYUSNINA, L. P. [1982]: Geothermometry and geobarometry of plagioclase-hornblende bearing assemblages. Contrib. Mineral. Petrol. **80,** 140—146.

POTY, B., LEROY, J., JACHIMOWITZ, L. [1976]: Un nouvel appareil pour la mesure des temperatures tous le microscope: L'installation de microthermometrie Chaixmeca. Bull. Soc. Fr. Mineral. Cristallogr. **99,** 182—186.

ROEDDER, E. [1984]: Fluid inclusions. Reviews in Mineralogy Vol. **12,** Mineral. Assoc. Amer. p. 644.

SISSON, V. B., CRAWFORD, M. L., THOMPSON, P. H. [1981]: CO_2-brine immiscibility at high temperatures, evidence from calcareous matesedimentary rocks. Contrib. Mineral. Petrol. **78,** 371—378.

SWANENBERG, H. E. C. [1980]: Fluid inclusions in high-grade metamorphic rocks from SW Norway. Geologica Ultraiectina, Utrecht No. **25,** p. 146.

SZEDERKÉNYI, T. [1974]: Rare element research on the early Paleozoic rocks of SE Transdanubia. Unpubl. Candidate theses. [in Hungarian].

SZEDERKÉNYI, T. [1976]: Barrow type metamorphism in the crystalline basement of south-east Transdanubia, Hungary. Acta Geol. Acad. Sci. Hung. **20,** 47—61.

TAKENOUCHI, S., KENNEDY, G. C. [1965]: The solubility of carbon dioxide in NaCl solution at high temperatures and pressures. Amer. Journ. Sci. **363,** 445—454.

TALANCHEV, A. C. [1978]: An equation for calculation of isochores of gas-liquid inclusions, homogenizing into liquid phase. Dokl. Akad. Nauk. SU, ser. Geochem. Vol. **240,** No. 1. 185—188 [in Russian].

TOMILENKO, A. A., CHUPIN, V. P. [1983]: Thermobarogeochemistry of metamorphic complexes. Nauka, Novosibirsk [in Russian].

TOURET, J. [1981]: Fluid inclusions in high grade metamorphic rocks. In: HOLLISTER, L. S., CRAWFORD, M. L. [eds.]: Short course in fluid inclusions: application to petrology. Mineral. Assoc. Canada. Calgary, 182—208.

WINKLER, H. G. F. [1976]: Petrogenesis of metamorphic rocks. Springer, New York.

YARDLEY, B. W. D. [1983]: Quartz veins and devolatilization during metamorphism. Journ. Geol. Soc. London. Vol. **140,** 657—663.

Manuscript received, 1 November. 1989

Acta Mineralogica-Petrographica, Szeged, XXX, 127—136, 1989

DETRITAL FRAMEWORK ANALYSIS OF LOWER CRETACEOUS TURBIDITE SEQUENCE OF NESZMÉLY—4 BOREHOLE (W. GERECSE MTS., HUNGARY)

GIZELLA B. ÁRGYELÁN

Dept. of Petrology and Geochemistry, L. Eötvös University

ABSTRACT

Lower Cretaceous (Berriasian to Lower Aptian) turbidite sequence of W. Gerecse Mts. formed within the Bakony unit in norheastern part of the Transdanubian Mts.

On the basis of detrital framework grain analysis a possible history of the source area can be inferred. The sedimentation started by erosion of oceanic crust and continued dominantly by erosion of continental basement. The serpentinite, chloritite, gabbro and dolerite lithic fragments, as well as the greenschist facies rock fragments and volcanic glass have been derived from the erosion of an ophiolite complex. The sandstone is rich in quartz and sedimentary, metasedimentary lithic fragments originated from mature sedimentary rocks or slightly metamorphosed rocks. In the heavy mineral assemblage chromian spinel is predominant suggesting ophiolitic provenances, too.

KEYWORDS: Neszmély Sandstone Formation, Lower Cretaceous turbidite sequence, detrital, framework grain analysis, heavy minerals, provenance area

INTRODUCTION

The Lower Cretaceous clastic formations of Gerecse Mts. are situated in Bakony unit, in northeastern part of the Transdanubian Mts.

The formations of W. Gerecse Mts. differ considerably from that of the E Gerecse Mts. The western region consists mostly of sandstone sequence with a few thin conglomerate intercalations, while the eastern part is characterized by Bersek Marl, Lábatlan Sandstone and Köszörűkőbánya Conglomerate Formations (FÜLÖP, 1958). The paleogeographic connection between the E. and W. Gerecse is uncertain.

The studied Neszmély—4 (N—4) borehole explored the W. Gerecse Clastic Complex (CSÁSZÁR and HAAS, 1984) which was lately called Neszmély Sandstone Formation (CSÁSZÁR, pers. comm.), *Fig. 1.*

According to FÜLÖP (1958) the geological features of E. Gerecse Mts. show similarity to that of Rossfeld Formation, and show some criteria of flysch sediments (flute casts, trace fossils, graded bedding)(CSÁSZÁR and HAAS, 1979). It was deposited in a prograding submarine fan (KÁZMÉR, 1987) from Lower Berriasian to Upper Aptian — Lower Albian (SZTANÓ, 1989). On the basis of stratigraphic and tectonic observations of KÁZMÉR and KOVÁCS (1985), and KÁZMÉR (1988) the sedimentary basin was formed within the Bakony unit in the Alps during the Mesozoic time.

This work forms part of a new research program being carried out by the Hungarian Geological Institute to clarify geological similarities between the two parts of Gerecse Mts., as well as to establish their connection to the clastic developments of Alp-Carpathian-Dinarian region.

H-1088. Budapest, Múzeum krt. 4/a

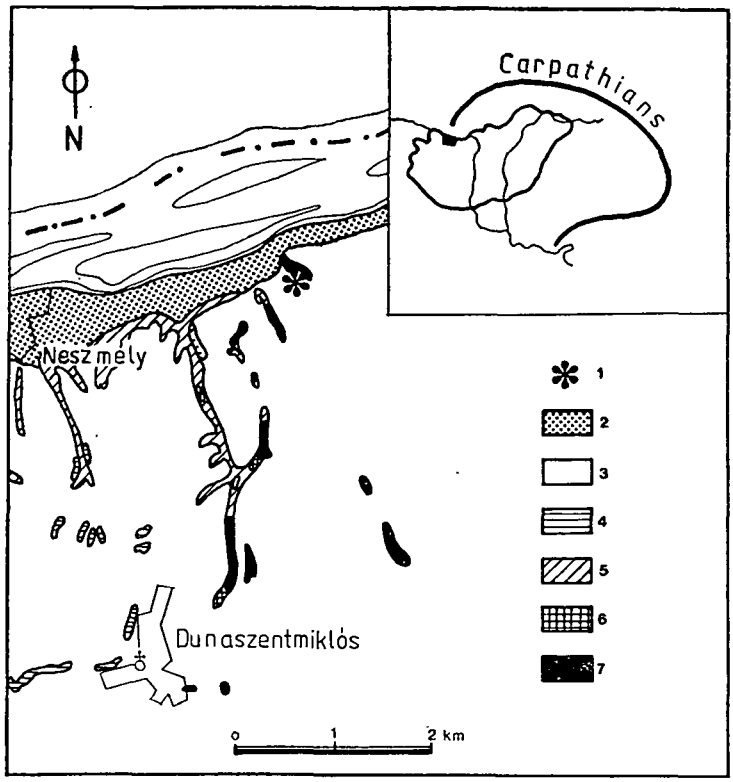

Fig. 1. Locality of Neszmély—4 (N—4) borehole and geology of surrounding area: 1. Neszmély—4 borehole; 2. Pleistocene terrace sand; 3. Pleistocene loess; 4. Pleistocene freshwater limestone; 5. Pannonian sand and mud; 6. Eocene sandstone and mudstone; 7. Neocomian sandstone

STRATIGRAPHY

Neszmély—4 borehole consists of alternating mudstone, marl, fine- and coarse grained sandstones and matrixsupported conglomerate, deposited by turbidite current. The sandstone facies are sublitharenite-litharenite or lithic arenite-lithic wacke (terminology after FOLK (1968) and DOTT (1964)), see further discussion below. On the basis of available Ammonites fossiles the sequence was formed from Lower Berriasian i to Lower Aptian (HORVÁTH, pers. comm).

Fig. 2 shows the stratigraphy, lithology, carbonate content and characteristic clastic components in the sequence.

HEAVY MINERALS

In the heavy mineral assemblage the grains of chromian spinel are predominant in association of augite, chlorite and a few kinds of metamorphic minerals such as garnet, staurolite, kyanite, epidote, actinolite (tremolite), apatite as well as stable minerals such as rutile, tourmaline, zircon *(Fig. 3a)*. Some opaque grains with hematized and goethitized surface show ilmenite-magnetite exsolution. Pyrite is also

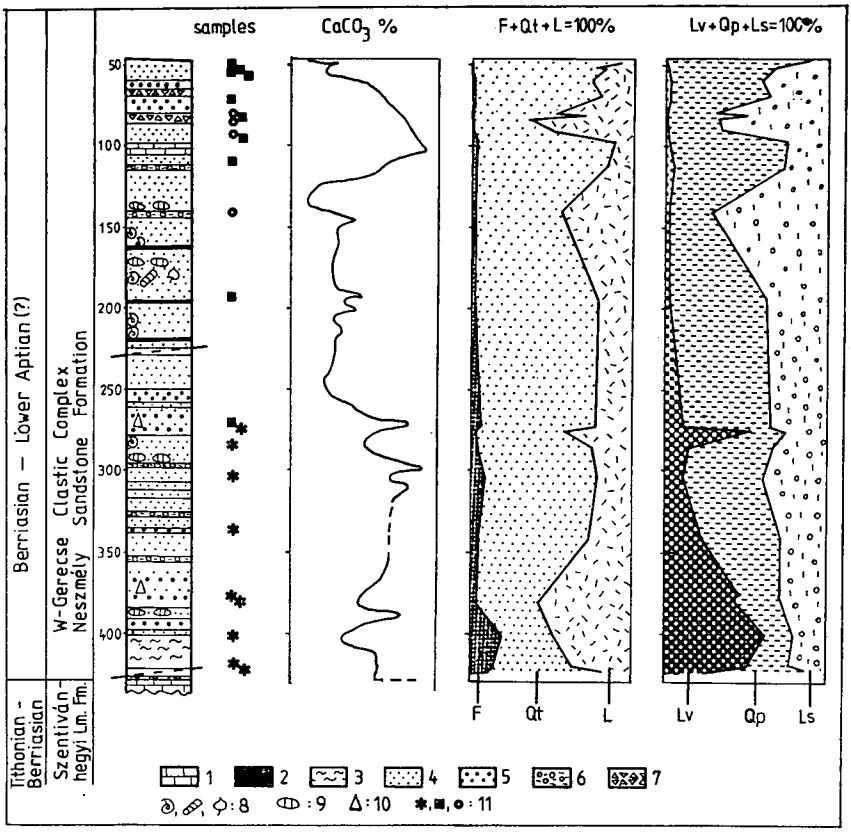

Fig. 2. Lithological section, carbonate contents and relative abundance of the main detrital components: 1. Limestone; 2. Mudstone; 3. Marl; 4. Fine to medium-grained sandstone; 5. Coarse grained sandstone; 6. Matrixsupported conglomerate; 7. Breccia; 8. Ammonites, trace fossils, plant fragments; 9. Carbonate nodules; 10. Normal gradation; 11. Samples from facies „a", „b", „c", respectively (explonation in the text)

enriched in certain levels. According to my preliminary microprobe analysis the chemical composition of chromian spinel is $Cr/(Cr+Al) \approx 0.7$ and $Mg/(Mg+Fe^{2+}) \approx 0.4$—0.5. The chromian spinel and orthopyroxene ((?) (which are not documented yet by microprobe analysis) grains may hint at an ophiolitic source area which must have been on the surface during the erosion.

Comparing the heavy mineral composition with that of the Oštrc Fm. (ZUPANIČ *et al.*, 1981) and the Rossfeld Fm. (POBER and FAUPL, 1988) a great similarity can be seen among them *(Fig. 3b)*. The exotic detritus of Rossfeld Formation (chromian spinel) originated from the Tethys' sutura belt which was to the south of the Northern Calcareous Alps (DECKER *et al.*, 1988; POBER and FAUPL, 1988).

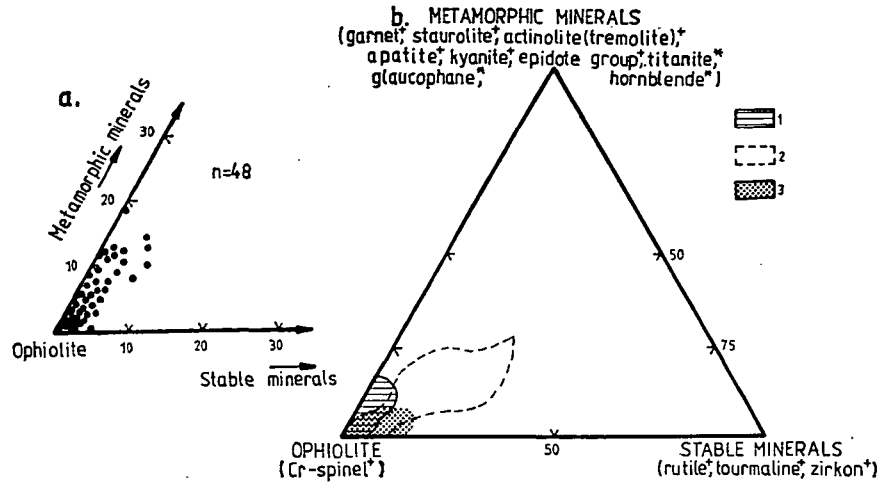

Fig. 3. Heavy mineral composition of N—4 borehole (a) compared to analogous sequences (b): 1. N—4 borehole; 2. Rossfeld Formation (POBER and FAUPL, 1988); 3. Oštrc Formation (ZUPANIČ *et al.*, 1981); + Heavy minerals in N—4 borehole; * additional heavy minerals in analogous sequences. (Studied interval: 0.063—0.250 mm)

FRAMEWORK ANALYSIS

Method

A standard framework grain analysis was done by Dickinson's method using the ribbon counting technique on monomineralic and unstable lithic sandy grains, 0.0625 to 2 millimeter (e.g. GRAHAM *et al.*, 1976; MOORE, 1979; ZUFFA *et al.*, 1980; WINKLER, 1984, 1988; GARZANTI, 1985). Table 1. contains the classification and symbols of main grain types. These are the basis for the petrological F-Qt-L, Lv-Qp-Ls, F-Qm-Lt and P-Qm-K diagrams (DICKINSON and SUCZEK, 1979; DICKINSON, 1985). and the secondary petrological parameters, Qt(=C)/Q, P/F and Lv(=V)/L (DICKINSON, 1970).

The crucial point of this method is the exact identification of detrital grains. In this work the optical analysis of secondary and diagenetic processes (MCBRIDE, 1985) proved to be very useful. Heavy minerals are ignored because of their different hidrodynamic behavior and geochemical resistance (MORTON, 1985). The intrabasinal grains are ignored, too (terminology after ZUFFA, 1980). Distinction between the extrabasinal and intrabasinal carbonate grains are difficult because of the different diagenetic effects (micritization, recrystallization, oxidized contours). Therefore the extrabasinal carbonate grains or detrital limeclasts (intraclasts, ooids, peloids, bioclasts) are not recalculated with other lithic fragments (DICKINSON, 1970, 1985), (Lc, Table 1.). Special counting technique can minimize the dependence of rock composition on grain-size (ZUFFA, 1980, 1985). Accordingly, the monomineralic crystals and other grains of sand size occuring in larger lithic fragments (e.g. granite) are classified as crystals rather than rock fragments. Inspite, the microcrystalline lithic fragments (e.g. phyillites) preserve their original texture during transportation. INGERSOLL *et al.* (1984) described in details that the using of Gazzi—Dickinson method on unsorted and different grain size fractions of the same sample is produce same results. Otherwise the sieving and multiple counts of different fractions are unnecessary.

TABLE 1

Classification and symbols of grain types
(slightly modified after DICKINSON *1970, 1985)*

A) Quartzose grains (Qt = Qm + Qp)
   Qt = total quartzose grains
   Qm = monocrystalline quartz (>0.0625 mm)
   Qp = polycrystalline quartz (or chalcedony)
B) Feldspar grains (F = P + K)
   F = total feldspar grains
   P = plagioclase grains
   K = kalifeldspar grains
C) Unstable lithic fragments (L = Lv + Ls)
   L = total unstable lithic fragments
   Lv = volcanic/metavolcanic lithic fragments
   Ls = sedimentary/metasedimentary lithic fragments
D) Total lithic fragments (Lt = L + Qp)
E) Lc = extrabasinal detrital limeclasts (not included in L or Lt)
   Note: Lc is not recalculated in plots (explonation in the text)

The advantages of the used ribbon counting method over the line- and point-countig method are as follows (VAN DER PLAS, 1962): (1) the studied bands are as wide as the largest grain diameter or even wider; (2) the center of particles are counted in the bands representing a random sampling; (3) if stratification is visible in thin section the homogneous areas can be separated and treated the results separately.

Using the above mentioned criteria 23 samples were analyzed, 400—500 grains per thin section. The grain distribution is Poisson-like, therefore the relative error is $1/\sqrt{n}$ ($\lesssim 5\%$ in our cases).

Results

On the basis of optical analysis the main detrital components of turbidite sequence are as follows:

(a) *Calcareous detritus.* The carbonate particles are micritized and hematized extraclasts of platform facies origin. They are mainly angular shaped, encrusting and calcareous algae detritus can also be seen. They originated by the erosion of older Mesozoic calcareous rocks and resedimented already in lithified condition. Bryozoan and Echinoid fragments are present.

(b) *Non-calcareous detritus.* Quartz is increasingly abundant upwards in the sequence *(Fig. 2)* Deformed monocrystalline quartz grains are dominant in the upper part of the profile and originated from mature sedimentary rocks (BASU *et al* 1975; YOUNG, 1976). Dissolution and diagenetic overgrowth are frequent.

Plagioclase usually ranges in composition from oligoclase to andezine. Chloritization, carbonatization and albitization are present by the effect of diagenetic processes. Orthoclase and microcline are rare.

(c) *Rock fragments.* In the lower part of the sequence dolerite with ophitic texture, serpentinite, chloritite, gabbro and greenschist facies rock fragments are characteristic *(Fig. 2, Fig. 4).* Similar ophiolitic and ultramafic fragments were found in Oštrc Formation and Rossfeld Formation. VASKÓ—DÁVID (1988) noted that radial chlorite, serpentinite and detrital chromite are also abundant in Lower Cretaceous sandstones of the Tatabánya basin.

Serpentinite fragments are too small for exact identification of texture. Inpenetrating type of nonpseudomorphic texture can be found on fragments referring to ser-

pentinization in higher grade metamorphic condition. The pseudomorphic texture showing lower P, T conditions is absent except for a few fragments explained as bastite. The rocks containing the above mentioned texture type may consists of only antigorite, antigorite+chrysotile or antigorite+chrysotile+lizardite (PAPP, pers. comm.).

Volcanic glass *(Fig. 5)*, chlorite precipitating in radial symmetry in amygdales or chlorite with mozaic structure are rare, but they may reflect the basaltic parts of ophiolite complex. Epidote, clinozoizite, albite and actinolite may have been the fragments of greenschist facies layers of ophiolite complex, too.

In the upper part of the sequence the sedimentary and sightly metamorphic rock fragments are predominant *(Fig. 2)*, such as sandstone, shale, phyllite, quartzite and red radiolarite.

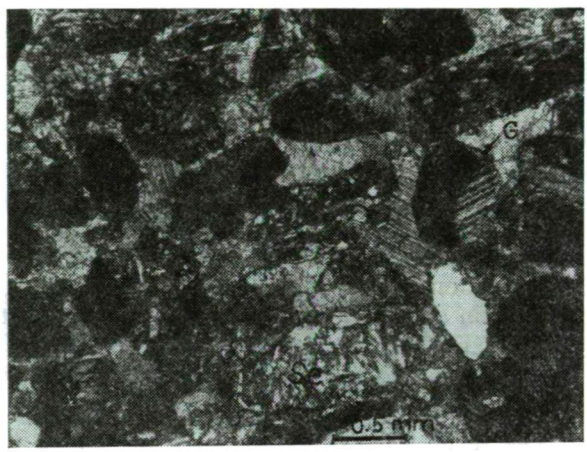

Fig. 4. Photomicrograph showing gabbro (G) and serpentinite (Se) fragments. In the gabbro fragment the plagioclase is albitized and the dark minerals are chloritized. XN.

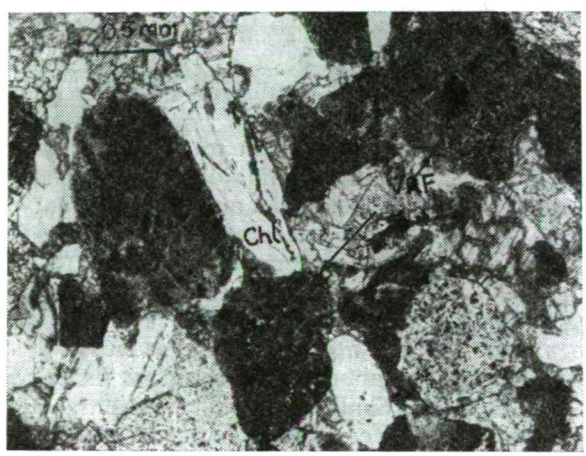

Fig. 5. Photomicrograph showing limonitized and parcially chloritized fragment of volcanic glass with typical vitreous texture. Close to it there are chloritite (Chl) and chloritized dolerite fragments (VRF). Only the plagioclase can be identified from the original texture. The groundmass is chloritized and hematized. According to the former nomenclature its name is diabase. 1N

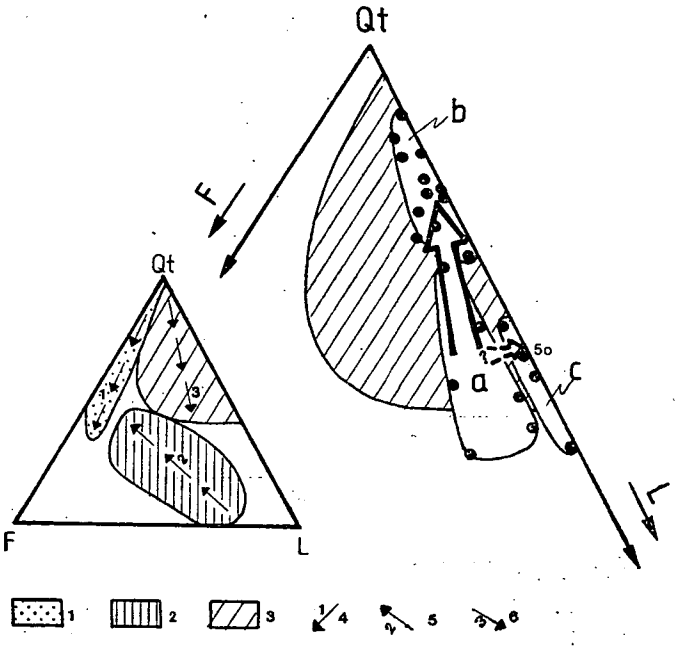

Fig. 6. Triangular plots of framework grain analysis (DICKINSON's method, 1970, 1979, 1985) F-Qt-L diagram: F, Qt, L see Table 1.; 1. Continental block provenances; 2. Magmatic arc provenances; 3. Recycled orogen provenances; 4. Decreasing maturity or stability; 5. Increasing ratio of plutonic to volcanic sources; 6. Increasing ratio of oceanic to continental materials; a, b, c different petrological fields in each plots; bold and dashed arrows show the petrological development trends upwards in the sequence in each plots

Three petrological facies were recognized among the arenite samples *(Fig. 2, Fig. 6, Fig. 7)*:

— Facies "a" is litharenite with average composition $F_7Qt_{57}L_{36}$. The quartzose grains are mostly chert. They contain a lot of remnants of ultramafic bodies of the ophiolite complex.

— Facies "b" rich in quartz and sedimentary rock fragments is sublitharenite with average composition $F_1Qt_{80}L_{19}$, reflects continental source area.

— The average composition of very coarse grained facies "c" is $F_1Qt_{48}L_{51}$. Red radiolarite fragments are abundant in this facies.

Petrographic transition between the above-mentioned facies "a" and "b" is continuous, but between facies "a" and "c" is questionable, *(Fig. 6, Fig. 7)*. The starting point of the facies evolution trend is doubtful considering that remnants of magmatic arc provenances may have also been preserved in some other submarine fans of the basin. The percentage of total feldspar is very low in all sample. Polycrystalline to total quartz ratios (Qp/Qt) are around 0.4 in facies "a" and 0.6 in facies "b". In facies "c" it is highly variable from 0.3 to 0.9, while volcanic to unstable lithic rock fragments and plagioclase to total feldspar ratios are 0.1—0.7 in facies "a" and under 0.1 in facies "b" *(Fig. 8)*. Variability of composition is more characteristic in Lv-Qp-Ls diagram than in F-Qt-L, therefore the former plot is more useful for determining the provenance area than the latter one.

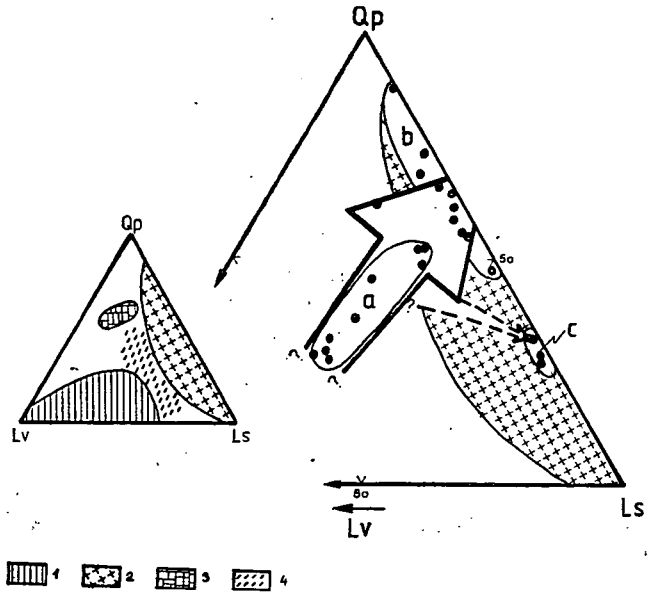

Fig. 7. Lv-Qp-Ls diagram: Lv, Qp, Ls see Table 1.; 1. Arc orogen sources; 2. Collision suture and fold-thrust belt sources; 3. Subduction complex sources; 4. Mixed orogenic sands; bold and dashed arrows see Fig. 6.

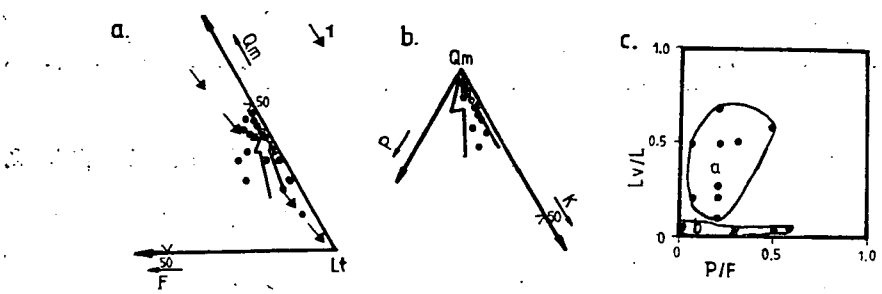

Fig. 8. F-Qm-Lt (a), P-Qm-K (b) diagrams and Lv/L to P/F ratio (c): F, Qm, Lt, P, K, Lv, L see Table 1.: 1. Increasing ratio of chert to quartz; a, b in Fig. 8c see *Fig. 6.*

SANDSTONE PETROGRAPHY AND GEODYNAMIC FRAMEWORK

The appearance and relative abundance of detrital components of arenites are in good correlation with source area(s) (DICKINSON, 1970, 1985; DICKINSON and SUCZEK, 1979; INGERSOLL and SUCZEK, 1979; VALLONI and MAYNARD, 1981; SCHWAB, 1981). Certainly, the provenance types of DICKINSON and SUCZEK are strongly generalized and can only by used with other stratigraphic considerations, otherwise they may lead to recognition of incorrect population (MACK, 1984). On the basis of triangular plots the provenance areas can be determined, however, further studies are inevitably required to reliably interpret the possible tectonic position of the depositional basin.

Our flysch data points fall into the "recycled orogen provenances" field (F-Qt-L diagram, see *Fig. 6*) and "collision suture and fold — thrust belt sources" field as well as "mixed orogenic sands" field (Lv-Qp-Ls diagram, see *Fig. 7*), consequently. It can be well correlated with the previous note of Lower Cretaceous paleotectonic events. Thus the evolution of W. Gerecse Mts. in that time was probably connected with the collision event in the Eastern Alps, that produced the Rossfeld Formation, and the clastic sequence of E. Gerecse Mts. as well.

CONCLUSIONS

On the basis of framework grain analysis a possible history of the source area can be inferred.

The Jurassic calcareous sedimentation was replaced by siliciclastic turbiditic sedimentation in Berriasian. The sedimentation started by erosion of the oceanic crust and continued dominantly by erosion of the continental basement evidenced by increasing quantity of quartz and sedimentary rock fragment and by decreasing ophiolitic one. We considered, that greenschist facies rock fragments, serpentinites, dolerite and gabbrofragments, volcanic glass as well as chlorite and detrital chromian spinel grains have been derived from the erosion of an ophilitic complex *(Fig. 7,* facies "a"*)*.

The intensity of ultramafic material supply was changing *(see Fig. 2)*. In periods of diminishing ultramafic material supply the outer self and continental slope or uplifted continental crust might have been eroded by the effects of slight geotectonic uplifts and their fragments could have been transported to the basin *(Fig. 7,* facies "c"*)*

At last, the sandstone is rich in quartz and sedimentary lithic fragments which were formed by erosion of the continental basement containing sedimentary and metamorphic rocks *(Fig. 7,* facies "b"*)*.

Two analogous series can be found in Ivanščica Mts. (Oštrc Fm.) and in Northern Calcareous Alps (Rossfeld Fm.). Ophiolitic detritus (lithic fragments and chromian spinel) are present in large quantities in both regions.

On the basis of our present studies of Neszmély—4 borehole we could manage to reconstruct the history of the source area, however, the tectonic position of the microplates remained questionable.

ACKNOWLEDGEMENTS

I am grateful to G. Császár, S. Kovács and I. Kubovics for their help.

REFERENCES

Basu, A., Young, S. W., Suttner, L. J., James, W. C., Mack, G. H. (1975): Re-evolution of the use of undulatory extention and polycrystallinity in detrital quartz for provenance interpretion. Jour. Sed. Petrology. **45**, 873—882.

Császár, G., Haas, J. (1979): Review of facies and paleogeography of the Cretaceous in Hungary, In: Wiedmann, J. (ed): Aspecte der Kreida Europas, IUGS Ser. A, No. 6, 413—424, Schweizerbart, Stuttgart.

Császár, G., Haas, J. (1984): The Cretaceous in Hungary: a review, Acta Geol. Hungarica. **27**, 417—428.

Decker, K., Faupl, P., Müller, A. (1987): Synorogenic Sedimentation on the Northern Calcareous Alps During the Early Cretaceous. In: Flügel, H. W., Faupl, P. (eds) (1987): Geodynamics of the Eastern Alps, Vienna, (Deuticke).

DICKINSON, W. R. (1970): Interpreting detrital modes of grauwacke and arkose, Jour. Sed. Petrology. **40,** 695—707.
DICKINSON, W. R. (1985): Interpreting provenance from detrital modes of sandstones. in: ZUFFA, G. G.: Provenance of Arenites NATO ASI Series, Series C. **148,** 333—361.
DICKINSON, W. R., SUCZEK, C. A. (1979): Plate tectonics and Sandstone Compositions, AAPG Bull. **63,** 2164—2182.
DOTT, R. L. (1964): Wacke, graywacke and matrix — What approach to immature sandstone classification?, Jour. Sed. Petrology. **34,** 625—632.
FOLK, R. L. (1968): Petrology of sedimentary rocks, 170 p., Austin, Texas, Hemphill's.
FÜLÖP, J. (1958): Die kretazeischen Bildingen des Gerecse-Gebirges, Geologica Hungarica, Ser. Geologica. **11,** 124 p., Budapest.
GARZANTI, E. (1985): The sandstone memory of the evolution of a Triassic volcanic arc in the Southern Alps, Italy, Sedimentology. **32,** 423—433.
INGERSOLL, R. V., BULLARD, T. F., FORD, R. L., GRIMM, J. R., PICKLE, J. D. and SARES, S. W. (1984): The effect of grain size on detrital modes: A test of Gazzi-Dickinson pointcounting method. Jour. Sed. Petrology. **54,** 103—116.
INGERSOLL, R. V., SUCZEK, C. A. (1979): Petrology and provenance of Neogene sand from Nicobar and Bengal fans, DSDP sites 211 and 218, Jour. Sed. Petroloyg. **49,** 1217—1228.
KÁZMÉR, M. (1987): A Lower Cretaceous submarine fan sequence in the Gerecse Mts., Hungary Annales Univ. Sci. Budapest, Sectio Geologica. **27,** 101—116.
KÁZMÉR, M. (1988): Lower Cretaceous facies zones in the Bakony unit of Hungary, Annales Univ. Sci. Budapest, Sectio Geologica. **28,** 116—168.
KÁZMÉR, M., KOVÁCS, S. (1985): Permian Paleogene paleogeography along the eastern part of the Periadriatic Lineament: Evidence for continental escape of the Bakony-Drauzug, Unit, Acta Geol. Hungarica. **28,** 69—82.
MACK, G. H. (1984): Exceptions to the relationship between plate tectonics and sandstone composition. Jour. Sed. Petrology. **54,** 212—222.
MCBRIDE, E. F. (1985): Diagenetic processes that affect provenance determinations in sandstone, in: ZUFFA, G. G.: Provenance of Arenites NATO ASI Series. Series C. **148,** 95—115.
MOORE, G. F. (1979): Petrography of subduction zone sandstones from Nias Island, Indonesia, Jour. Sed. Petrology. **49,** 71—84.
MORTON, A. C. (1985): Heavy minerals in provenance studies, in: ZUFFA, G. G.: Provenance of Arenites, NATO ASI Series. Series C. **148,** 249—279.
POBER, E., FAUPL, P. (1988): The chemistry of detrital chromian spinels and its implications for the geodynamic evolution of the Eastern Alps, Geol. Rundschau. **77,** 641—670.
SCHWAB, F. L. (1981): Evolution of the western continental margin, French-Italian Alps: sandstone mineralogy as an index of plate tectonic setting, Jour. Geology. **89,** 349—368.
SZTANÓ, O. (1989): Submarin fan-channel conglomerate of Lower Cretaceous Gerecse Mts., Hungary, Neues Jahrbuch (in press).
VALLONI, R., MAYNARD, J. B. (1981): Detrital modes of recent deep-sea sands their relation to tectonic setting: a first approximation, Sedimentology. **28,** 75—83.
VAN der PLAS, L. (1962): Preliminary note on granulometric analysis of sedimentary rocks, Sedimentology. **1,** 145—157.
VASKÓ-DÁVID, K. (1988): Studies on chromite and their implications in the Lower and Middle Cretaceous of the Tatabánya Basin and Vértes Foreland, Magyar Áll. Földt. Int. Évi Jel. **1986i.** évről, 241—261.
WINKLER, W. (1984): Palaeocurrents and petrography of the Gurnigel — Schlieren flysch: a basin analysis, Sed. Geology. **40,** 169—189.
WINKLER, W. (1988): Mid- to Early Late Cretaceous Flysch and Melange Formations in the Western Part of the Eastern Alp. Palaeotectonic Implication. Jb. Geol. B-A. **131,** 341—389.
YOUNG, S. W. (1976): Petrographic textures of detrital polycrystalline quartz as an aid to interpreting crystalline source rocks, Jour. Sed. Petrology. **46,** 595—603.
ZUFFA, G. G. (1980): Hybrid arenites: their composition and classification, Jour. Sed. Petrology. **50,** 21—29.
ZUFFA, G. G. (1985): ed.: Provenance of Arenites NATO ASI Series, Series C. **148,** 393 p. D. Reidel Publishing Company, Dordrecht) Boston/Lancaster.
ZUFFA, G. G., GAUDIO, W. and ROVITO, S. (1980): Detrital mode evolution of rifted continental-margin Longoducco Sequence (Jurassic), Calabrian Arc, Italy, Jour. Sed. Petrology. **50,** 51—61.
ZUPANIČ, L., BABIĆ, L. and CRNJAKOVIĆ, M. (1981): Lower Cretaceous basinal clastics (Oštrc Formation) in the Mt. Ivanščica (Northwestern Croatia), Acta Geol. **11,** 1—44. Zagreb.

Manuscript received, 1 November, 1989

Acta Mineralogica-Petrographica, Szeged, XXX; 137—147, 1989

HYDROCARBON GENERATIVE FEATURES OF THE UPPER TRIASSIC KÖSSEN MARL FROM W. HUNGARY

M. HETÉNYI*

Department of Mineralogy, Geochemistry and Petrography, Attila József University

ABSTRACT

The organic matter of the Kössen Marl accumulated in an anoxic environment is supposed to be an oil prone sequence. A verification of this assumption is attempted in this paper by determining its organic facies and its petroleum potential.

The relationship lithology and hydrocarbon generative features of the Kössen Marl was studied. One part of the samples was chosen from a shallow corehole consisting of mainly dolomite. The other part of the samples originated from three subdivisions of a corehole drilled in the vicinity of the previous one. The subdivisions were the following: calcareous marl, marl and silstone.

The petroleum potential and the hydrogen index of the dolomite indicated a good source rock of Organic Facies B. The calcareous marl proved to be a typical example of the excellent oil producing matter. It had high petroleum potential and its organic facies was nearly AB. The marl also seemed to be a very good source rock. However, its petroleum potential was less than half of the value measured in the previous subdivision and its organic facies was BC. The siltstone of Organic Facies D was found to be a nongenerative rock.

The hydrocarbon generative features mentioned above were checked on two selected samples by simulating the catagenesis under laboratory conditions by performing a thermal degradation.

KEYWORDS: hydrocarbon generative features, kerogen types, organic facies, petroleum potential, source rock, thermal degradation

INTRODUCTION

The Upper Triassic Kössen Marl from West Hungary is considered to be a good oil source rock. A relationship is supposed to exist between its organic matter and the Nagylengyel oil field which contains heavy and sulfur-rich crude oil. On the basis of sulfur content, stable isotope ratios and trace elements KONCZ (1984) suggested that there is a Triassic carbonate source rock for the crude oil of the Nagylengyel field. Two shallow coreholes located in the vicinity of this oil field — Rezi 1 (referred to as R) and Zalaszentlászló 1 (referred to as Z) — were studied by BRUKNER-WEIN and VETŐ (1985). They investigated the relationship between lithology and organic matter in anoxic sediments. Results of their work — organic carbon content, the quantity of iron and that of different forms of sulfur, as well as detailed geochemical analysis of extracts — indicated that the examined sequence of Kössen Marl is an excellent oil source rock. The fine-laminated structure and the absence of benthic remains were evidences of an anoxic depositional environment.

Microscopic examination of the amorphous kerogen revealed that the precursor biomass was algae and associated bacteria in various stages of decomposition In core R Botryococcus remnants could be identified. In core Z strongly degraded palynomorphs were found (GÓCZÁN, unpublished data).

* H-6701 Szeged, P. O. Box: 651

The conclusions of works mentioned above could be confirmed further by some data concerning the type of kerogen, the organic facies and petroleum potential. The aim of the present paper was to determine these geochemical parameters of the selected sequence of Kössen Marl, as well as to study in detail its hydrocarbon generative features by thermal degradation.

Simplified lithologic logs of the Kössen Marl in wells R and Z (after BRUKNER-WEIN and VETŐ, 1985) are shown in *Fig. 2.* Lithology of the sequence selected for study varies from carbonates to siltstones. The carbonate mineral in core R is mainly calcite, in core Z is mainly dolomite.

EXPERIMENTAL

The total organic carbon content (TOC) was measured at 1000 °C under intense oxygen flow by combusting in Carmograph—8 equipment.

The hydrocarbon generative (petroleum) potential, the maturity of the kerogen the hydrogen- and oxygen-indices were determined by Rock Eval pyrolysis (ESPITALIÉ *et al.*, 1977).

Experimental assay of thermal evolution was carried out in a temperature-programmed furnace under nitrogen atmosphere. Temperatures of the experimental evolution were 350°, 375°, 400°, 450° and 500° C. At each temperature the heating period lasted for 1, 5, an 10 hours. Volatile bitumens were collected in cooled traps, soluble bitumens were extracted by chloroform. The residue of thermal degradation (unconverted kerogen) was characterized by Rock Eval pyrolysis and by CR/CT ratio measured according to the ASTM standard (CUMMINS *et al.*, 1972).

RESULTS

1. *The quality of organic matter*

The quality of organic matter was characterized by the organic facies and the type of kerogens. "The organic facies is specific body of sedimentary rocks identified by the same organic features" (JONES, 1987). The same organic facies may contain a variety of kerogen types in different mixtures. One of the bases of classification is the hydrogen index measured at a vitrinite reflectance $\simeq 0.5\%$. Immaturity of the kerogen is an essential condition for determining the organic facies. As it is shown in Table 1 and 2, as well as in *Fig. 1* maturity of the organic matter in each examined sample meets this requirement. So the maturity level of kerogens in both of the coreholes is the most favourable to state their type and organic facies, as well as to compare them to each other.

The type of kerogen. Nearly all the types of kerogen can be found among the 72 examined samples *(Fig. 1)*. The hydrogen indices change from 38 mgHC/gTOC (type III) to 968 mgHC/gTOC (type I). On the basis of the average value of the hydrogen indices both wells contained kerogen of type II. In corehole Z the average HI was 413 mgHC/gTOC while it was 454 mgHC/gTOC in corehole R. The PC/TOC ratios were also very characteristic of the kerogen of type II (36% and 40%, respectively).

In corehole Z almost each core contained kerogen of type II (Table 2 and *Fig. 1*).

In contrast, the quality of organic matter in three subdivisions of corehole R was very different *(Fig. 1* and Table 1*)*. In calcareous marl, although the kerogen

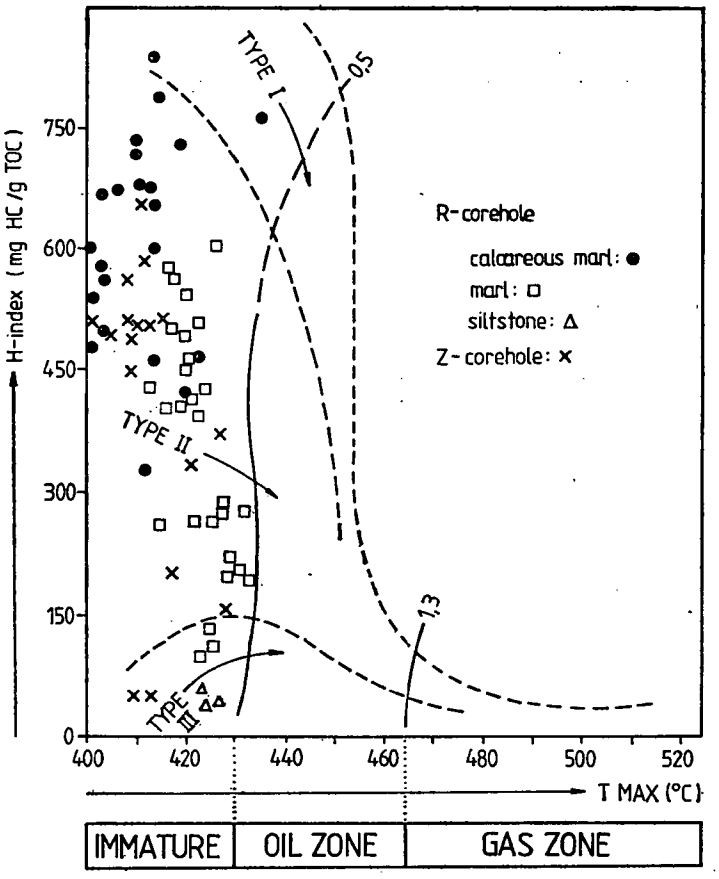

Fig. 1. HI – T_{max} diagram showing type and maturity of kerogen of Kössen Marl in wells R and Z

was type II, the values of HI and PC/TOC ratio approached the boundary between the kerogen of type I and II. Most of the studied kerogen in this section proved to be pronouncedly type I—II (Table 1).

The kerogen of marls changed from one type to another at a depth of about 110—120 m (dotted line in Table 1). The average value of HI decreased from 444 mgHC/gTOC to 198 mgHC/gTOC and the PC/TOC ratio decreased from 39% to 17%.

Not only the quantity, but the quality of the organic matter of siltstone turned out to be very poor. These kerogens showed low HI and low PC/TOC ratio, too.

Organic facies. The general organic facies of both examined wells is B. The organic facies B is considered to be the predominant source of the world's oil. The precursor biomass of the examined Kössen Marl consisted mainly of Botryococcus algae and associated bacteria in various stages of decomposition (GÓCZÁN, unpublished data). However, some terrestrially derived organic matter varying in amount and in type was present, too. Depending on the ratio of aquatic and terrestrially

TABLE 1

Organic geochemical characterization of core Rezi 1 (southwest part of Transdanubian Mid-Mountains, Hungary) by Rock Eval pyrolysis

Depth (m)	TOC (%)	T_{max} (°C)	HC-pot kgHC/ton of rock	S2/S3	PC/TOC (%)	HI mgHC/g TOC	OI $mgCO_2/g$ TOC	Type of kerogen	Org. fac.
1	2	3	4	5	6	7	8	9	10
44.0	0.84	426	0.37	0.85	3.57	42	50	III	D
49.1	0.78	424	0.30	0.90	2.56	37	41	III	D
59.8	0.72	423	0.39	1.00	4.17	52	52	III	CD
82.4	0.67	432	1.94	2.30	23.88	279	120	II	BC
88.4	1.06	425	1.56	2.22	12.26	138	62	III	C
88.6	1.51	433	2.95	4.11	15.89	190	46	II	w
92.6	1.06	426	1.16	1.92	8.49	103	53	III	CD
93.6	1.17	423	1.20	1.73	8.55	93	53	III	CD
99.8	1.72	431	3.58	5.17	16.86	201	38	II	C
101.3	1.92	429	4.30	4.90	18.23	217	44	II	C
102.6	1.39	428	2.79	2.65	16.55	194	73	II—III	C
107.6	1.83	427	5.21	3.95	23.50	276	69	II	BC
113.2	1.62	427	4.80	3.92	24.70	288	73	II	BC
122.6	4.76	426	29.96	16.52	51.89	607	36	II	B
129.6	3.46	420	19.27	9.54	46.24	540	56	II	B
136.6	5.01	417	26.70	13.06	44.31	503	38	II	B
147.6	3.13	420	16.41	9.54	43.45	494	51	II	B
148.6	7.92	416	48.65	19.67	51.14	578	29	II	B
149.6	1.94	424	8.79	5.54	37.63	422	76	II	B
151.6	6.08	423	33.54	17.57	45.89	517	29	II	B
156.6	3.72	419	15.63	9.77	34.95	401	41	II	B
162.5	5.53	417	32.13	15.61	48.28	558	35	II	B
171.6	3.03	421	14.97	9.80	40.93	468	47	II	B
175.5	1.66	426	4.45	3.82	22.29	257	67	II	BC
177.5	2.25	415	6.42	4.15	23.56	271	65	II	BC
179.5	3.55	423	14.94	9.06	34.93	403	44	II	B
180.5	3.41	421	15.19	8.14	36.95	422	51	II	B
181.5	2.66	418	11.10	7.83	34.59	400	51	II	B
187.5	2.76	420	13.14	9.04	39.50	458	50	II	B
190.5	1.62	422	4.34	3.50	22.22	254	72	II	BC
192.5	2.15	413	9.90	5.83	38.14	433	74	II	B
202.7	2.69	419	21.53	11.53	66.54	737	63	I—II	AB
211.9	3.73	404	22.74	10.58	50.67	570	53	II	B
213.8	10.34	415	86.84	25.97	69.92	788	30	I—II	AB
215.9	4.43	414	39.59	11.99	74.27	833	69	I	AB
216.6	8.65	414	56.73	17.09	54.56	604	35	II	B
217.4	6.05	436	62.82	18.65	86.44	968	51	I	A
218.0	4.02	414	28.43	9.37	58.70	653	69	I—II	AB
220.9	4.12	423	19.88	8.26	40.04	469	56	II	B
223.8	2.72	420	11.76	7.58	36.02	420	55	II	B
225.8	8.57	412	31.54	8.02	30.57	326	40	II	BC
227.4	5.59	410	45.71	17.30	67.98	740	42	I—II	AB
229.5	4.01	407	32.04	17.42	66.58	715	40	I—II	AB
230.5	5.76	413	42.04	15.19	60.70	672	44	I—II	AB
234.7	8.60	411	33.94	11.69	61.30	676	57	I—II	AB
235.7	2.72	401	16.08	8.52	49.26	535	62	II	B
240.4	2.90	401	15.45	5.22	44.14	479	91	II	B
241.4	6.49	400	42.46	15.72	54.39	608	38	II	B
242.0	6.58	403	40.20	14.39	50.91	568	39	II	B
250.0	2.97	414	14.77	6.56	41.41	464	70	II	B
251.6	2.04	403	15.56	8.42	63.23	664	78	I—II	AB
253.6	3.60	407	27.41	11.02	63.33	670	60	I—II	AB
266.3	2.60	436	20.21	10.48	64.61	762	72	I—II	AB
269.0	2.81	404	15.28	8.71	45.19	499	57	II	B
Average values	3.57	411	20.54	9.13	40.31	454	55	II	B

derived organic matter, different organic facies could be recognised in the two wells and in the three subdivision.

In the corehole Z there were two samples of Organic Facies D. Their organic matter consisted primarily of inertinite maceral groups and this facies is non-generative. Except for these two cores the organic facies of almost each sample was B (Table 2).

In corehole R the organic facies changed with the depth. The oil prone Organic

TABLE 2

Organic geochemical characterization of core Zalaszentlászló 1 (southwest part of Transdanubian Mid-Mountains, Hungary) by Rock Eval pyrolysis

Depth (m)	TOC (%)	T_{max} (°C)	HC-pot kgHC/ton of rock	S2/S3	PC/TOC (%)	HI mgHC/g TOC	OI $mgCO_2$/g TOC	Type of kerogen	Org. fac.
1	2	3	4	5	6	7	8	9	10
304.9—307.0	31.5	412	22.53	16.09	59	653	40	I—II	AB
317.6—318.4	4.56	408	25.09	19.40	46	510	26	II	B
322.0—325.0	0.17	427	0.67	0.85	29	370	435	II	BC
337.6—340.7	1.11	416	5.90	5.56	44	511	91	II	B
341.5—344.0	0.17	417	0.36	0.70	18	200	282	II	C
349.1—352.0	2.25	405	11.74	13.85	43	498	36	II	B
354.8—360.0	2.48	412	15.36	19.79	52	590	29	II	B
360.2—363.0	2.25	413	11.78	15.01	44	507	33	II	B
363.0—366.8	5.23	408	30.33	23.38	48	554	23	II	B
375.0—378.5	2.09	401	11.23	15.22	45	510	33	II	B
378.5—381.4	2.98	410	15.62	22.75	44	504	22	II	B
381.4—383.0	2.45	409	12.65	20.33	43	489	24	II	B
383.0—386.0	0.72	409	3.37	6.69	39	455	68	II	B
387.0—388.0	1.85	413	9.88	14.33	44	507	35	II	B
407.8—408.8	0.86	421	3.02	3.05	29	337	110	II	BC
410.9—413.0	0.65	428	1.05	1.36	12	155	113	II—III	C
421.5—425.5	0.33	413	0.14	0.30	3	42	139	III	D
434.0—436.8	0.40	409	0.24	0.25	5	47	187	III	D
Average values:	1.87	413	10.05	11.06	36	413	166	II	B

Facies AB and B were followed by mixed Organic Facies BC, then by the gas prone Organic Facies C and finally, by the non-generative Organic Facies D (Table 1).

The average HI of the calcareous marl reached almost the beginning of the Organic Facies AB (HI=650 mgHC/gTOC). Numerous samples even exceeded this value. Within the marls of Organic Facies BC two sections could be distinguished Organic Facies B (HI=444 mgHC/gTOC) and Organic Facies C (HI=198 mgHC/gTOC).

2. *Source rock considerations*

The organic carbon content and the petroleum potential of the examined samples indicated that the Kössen Marl was a good source rock. Their organic carbon content ranged from 0.2% to 10.3 and their petroleum potential varied from 0.3 kgHC/ton of rock to 86.8 kgHC/ton of rock *(Fig. 2)*.

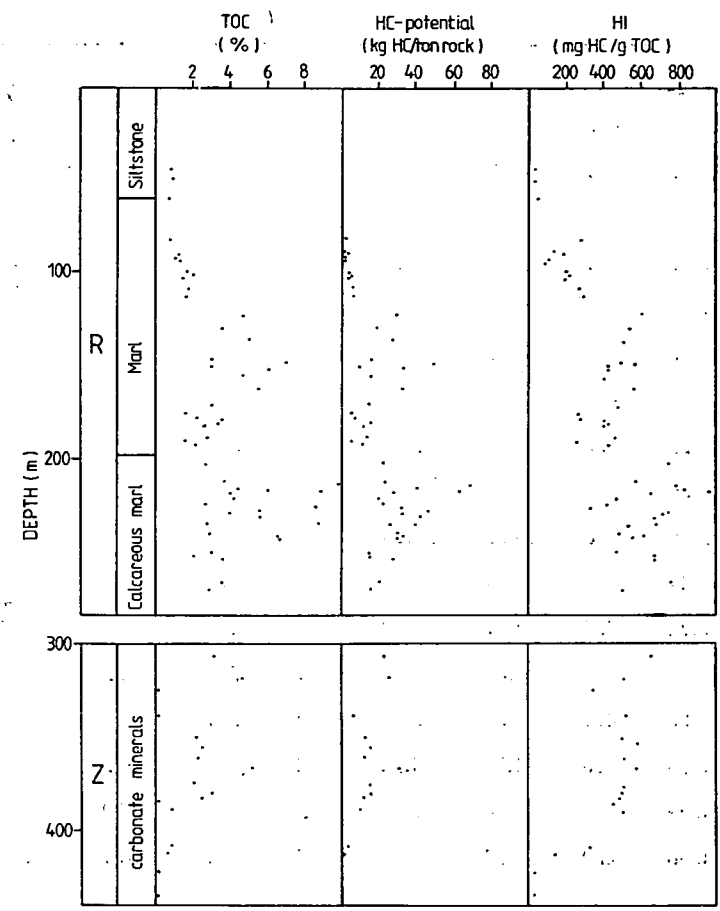

Fig. 2. Simplified lithologic logs of Kössen Marl in wells R and Z as well as hydrocarbon generative features vs. depth

On the average values of these parameters (Table 2) core Z of Organic Facies B proved to be a "good source rock". According to PETERS (1986) the organic carbon content of a "good source rock" is 1—2% and its hydrocarbon generative potential is 6—12 kgHC/ton of rock.

The other studied core (R), which also contained Organic Facies B, seemed to be a "very good source rock" its TOC being higher than 2% and its petroleum potential higher than 12 kgHC/ton of rock (Table 1).

In addition to their average organic carbon content and their petroleum potential the high S2/S3 ratio of the calcareous marl (Table 3) also showed an excellent oil producing source rock.

On the basis of average values mentioned above the total section of marls also seemed to be a very good source rock (Table 3). However, similarly to the other geochemical parameters studied in this paper, the S2/S3 ratio also revealed two zones within the marl sequence. The average value of S2/S3 ratio (9.89) of the deeper zone of marl characterized an excellent oil producing source rock. On the other hand, this parameter (3.29) marked only a gas prone source rock in the upper zone (Table 1).

Siltstones containing a small quantity of organic carbon and being a non-generative facies cannot be regarded as a source rock.

TABLE 3

Average values of some quantitative and qualitative features of the organic matter in core Rezi 1

Lithological subdivisions	Depth (m)	TOC (%)	HC-pot kgHC/ ton of rock	S2/S3	PC/TOC (%)	HI mgHC/g TOC	Type of kerogen	Organic facies
Siltstone	44.0—59.8	0.78	0.35	0.92	3.43	44	III	D
Marl	82.4—192.5	2.81	13.04	7.53	30.92	356	II	BC
Calcareous marl	202.7—269.0	4.87	32.30	12.16	56.55	627	II	B

3. Results of thermal degradation

Experimental assay of thermal degradation was performed on two samples.

The core of Organic Facies B selected from well Z (depth=317,6—318.4 m) contained a very good oil producing kerogen. TOC=4.56%, HC-potential=25.09 kgHC/ton of rock, S2/S3=19.40, HI=510 mgHC/gTOC.

The core of Organic Facies AB selected from well R (depth=213.8 m) contained an excellent oil producing kerogen, too. TOC=10.34%, HC-potential= 86.84 kgHC/ton of rock, S2/S3=25.97, HI=788 mgHC/gTOC.

The quantity of total bitumens yielded by the two samples during the thermal degradation changed both in function of heating period and in function of temperature (Table 4).

The thermal degradation properties of core Z proved to be similar to those of the kerogen of type II. Evolution properties of the core R of high generating capacity,

on the other hand, were revealed to be close to the kerogen of type I. A higher percent of the organic matter in sample R was converted to oil than in sample Z. Independently of the experimental conditions much more bitumen developed from sample R than sample Z (Table 4).

TABLE 4

Quantity of bitumens yielded by thermal degradation of two Kössen Marl samples (R: a sample of Organic Facies AB from core Rezi 1 and Z: sample of organic Facies B, from core Zalaszentlászló 1)

Temperature (°C)	Heating period (hours)	Soluble bitumen		Volatilized bit. mg/gTOC		Total bitumen	
		R	Z	R	Z	R	Z
350	1	222.4	197.4	106.4	43.8	328.8	241.2
	5	261.1	65.8	145.1	43.8	406.2	109.6
	10	299.8	43.8	193.4	43.8	493.2	87.6
375	1	164.4	65.8	116.1	43.8	280.5	109.6
	5	222.4	43.8	203.1	109.6	425.5	153.4
	10	251.5	21.9	270.8	109.6	522.3	131.5
400	1	348.2	197.4	145.1	109.6	493.3	307.0
	5	174.1	43.8	222.4	153.5	396.5	197.3
	10	280.5	21.9	560.9	175.4	841.4	197.3
450	1	154.7	43.8	435.2	131.6	589.9	175.4
	5	19.3	21.9	560.9	219.3	579.9	241.2
	10	48.4	21.9	647.9	175.4	696,3	197.3
500	1	19.3	21.9	647.9	263.1	667.2	285.0
	5	9.7	21.9	686.6	219.3	696.3	241.2
	10	9.7	21.9	715.7	285.1	725.4	307.0

TABLE 5

Change of some characteristics of unconverted kerogen type I—II (from core R) during the thermal degradation

Temperature (°C)	Heating period (hours)	CR/CT	T_{max}	S2/S3	HC-pot kgHC/ton of rock	HI mgHC/gTOC
Unheated sample		—	415	25.97	86.84	788
350	1	0.61	418	25.22	65.29	696
	5	0.66	422	24.05	51.43	695
	10	0.78	423	21.97	46.72	639
375	1	0.59	416	24.90	54.12	710
	5	0.74	424	21.23	38.82	573
	10	0.76	430	14.22	26.74	443
400	1	0.80	425	16.34	31.91	641
	5	0.87	436	7.51	16.45	382
	10	0.91	441	6.47	11.21	260
450	1	0.95	443	4.74	7.45	263
	5	0.96	455	1.17	2.21	70
	10	0.99	456	0.54	1.08	27
500	1	0.95	463	0.70	1.32	34
	5	0.98	>465	0.15	0.41	21
	10	0.99	>465	0.13	0.36	8

The kerogen of type I, however, requires higher temperature for generating oil than the other types. Moreover, the main formation of petroleum starts at a somewhat higher temperature (TISSOT and WELTE, 1978). As it is shown in Table 7 the hydrocarbon generating potential of sample R reduced to 1% of its original value at 450 °C.

TABLE 6

Change of some characteristics of unconverted kerogen type II (from core Z) during the thermal degradation

Temperature (°C)	Heating period (hours)	CR/CT	T_{max} (°C)	S2/S3	HC-pot kgHC/ton of rock	HI mgHC/gTOC
Unheated sample		—	408	19.40	25.09	510
350	1	0.62	416	21.45	17.63	349
	5	0.88	426	8.75	8.13	172
	10	0.96	434	3.52	3.30	72
375	1	0.77	417	22.10	15.92	346
	5	0.85	436	6.27	4.54	101
	10	0.99	437	1.56	1.95	33
400	1	0.88	426	12.13	9.00	213
	5	0.93	440	1,78	2.64	42
	10	0.94	448	0.16	0.07	1
450	1	0.84	443	1.90	1.26	33
	5	0.93	>465	0,00	0.09	0
	10	0.93	>465	0.00	0.07	0
500	1	0.90	>465	0.03	0.15	0
	5	0.93	>465	0.10	0.18	0
	10	0.94	>465	0.00	0.09	0

TABLE 7

Decreasing of the hydrocarbon generative potential during the thermal degradation
(R: a sample of Organic Facies AB from core Rezi 1
Z: a sample of Organic Facies B, from core Zalaszentlászló 1)

Temperature (°C)	Heating period (hours)	Decreasing of HC-pot. %	
		R	Z
350	1	25	32
	5	41	68
	10	46	84
375	1	38	38
	5	55	82
	10	69	92
400	1	63	65
	5	81	90
	10	87	99
450	1	91	95
	5	97	100
	10	99	100
500	1	92	99
	5	100	100
	10	100	100

In contrast, residual petroleum potential of the sample Z, which required lower activation energy, was 1% at 400 °C. A significant difference was found between the two examined rocks regarding the decrease of their petroleum potential at the beginning of the catagenesis, which was simulated by thermal degradation at 350 °C for 10 hours. While the hydrocarbon generative potential of sample R fell to 56% of that of the unheated matter, the residual potential of sample Z was only 16%.

The so called "oil death line" (vitrinite reflectance=1.35% and $T_{max} \cong 465$ °C) was reached at 500 °C and at 450 °C by sample R and sample Z, respectively (Table 5 and 6).

CONCLUSION

1. On the basis of the results presented in this paper the Upper Triassic Kössen Marl (W. Hungary) had very good hydrocarbon generative features.
2. Both of the studied wells (R and Z) represented organic rich (TOC=0.2—10.3%) shallow marine sequences. All types of kerogen occurred among the examined samples. In *Fig. 1* kerogen of type II in siltstone (core R) and in core Z could be recognized. The calcareous marl (core R) contained a kerogen of high quality, about type I—II.
3. The total zone of the catagenesis could be simulated by thermal degradation. This fact and the low T_{max} suggested that the organic matter was in the early stage of maturation
4. The ratio of the organic carbon content in the three lithological subdivisions of core R (siltstone, marl and calcareous marl) was 1:3.6:6.2 and that of the petroleum potential was 1:37:92.
5. The calcareous marl of Organic Facies B (even nearly AB) proved to be an excellent oil producing matter. Its average petroleum potential was 32.30 kgHC/ton of rock.
   The marl of Organic Facies BC was found to be a very good source rock, its petroleum potential was 13.04 kgHC/ton of rock.
   As the siltstone of Organic Facies D had a very low petroleum potential (0.35 kgHC/ton of rock) it was naturally a non-generative rock.
   The core Z of Organic Facies B seemed to be a good source rock. Its petroleum potential was 10.05 kgHC/ton of rock.
6. On the basis of organic facies, petroleum potential and type of kerogen two zones were distinguished in the marl of core R. These differences may reflect variations in the depositional environment. Further investigation is necessary to compare these two zones to each other.
7. The thermal degradation properties of samples from core Z and from calcareous marl of core R corresponded to those of the kerogen type II and the kerogen type I, respectively. A lower percent of the organic matter of core Z was converted to oil and a smaller quantity of bitumen developed from it than from core R. At the same time the kerogen of core R required higher activation energy for generating volatile bitumen. So, its main oil producing zone began, as well as ended temperature 50 °C below than that of the other sample.

ACKNOWLEDGEMENT

The author expresses her gratitude to G. Solti making available the samples investigated.

REFERENCES

BRUKNER-WEIN, A. and VETŐ, I. (1986): Preliminary organic geochemical study of an anoxic Upper Triassic sequence from W. Hungary. Org. Geochem., **10,** 113—118.

CUMMINS, J. J. and ROBINSON, W. E. (1972): Thermal degradation of Green River kerogen at 150° to 350° C. U. S. Bur. Mines Rep. Invest. **7620,** 15.

ESPITALIÉ, J., MADEC, M., TISSOT, B., MENNIG, J. J. and LEPLAT, P. (1977): Source rock characterization method for petroleum exploration. Offshore Technology Conf., Paper no. **2935,** 11th Annual OTC,. Houston.

DEMAISON, G. J. and MOORE, G. T. (1980): Anoxic Environments and Oil Source Bed Genesis. AAPG. Bull., **64/8,** 1179—1209.

JONES, R. W. (1987): Organic Facies. Advances in Petroleum Geochemistry, **2,** 1—90.

KONCZ, I. (1984): Nagylengyel és környéke kőolajelőfordulásainak eredete. Földt. Közl. (In press).

PETERS, K. E. (1986): Guidelines for evaluating petroleum soure rock using programmed pyrolysis. AAPG Bull., **70,** 318—329.

TISSOT, B. P. and WELTE, D. H. (1978): Petroleum Formation and Occurrence. Springer Verlag, 185—200, 500—510.

Manuscript received, 5 July, 1989

Acta Mineralogica-Petrographica, Szeged, XXX, 149—159, 1989

DIAGENETIC MODEL OF A REEF COMPLEX, AQRA-BEKHME FORMATION (LATE CRETACEOUS), NORTHEASTERN IRAQ

BASIM AL-QAYIM

Department of Geology, Salahudine University, Arbil, Iraq

ABSTRACT

The extensive reef complex of Aqra-Bakhme Formation on northeastern Iraq consists of massive rudist-dominated limestone which characterizes the central part, and a periferial, medium to thick-bedded limestone and dolostone representing the detrital part of complex. Petrographic examination of rock samples of six esposed section from different localities reveal a variety of diagenetic products that results from long and complicated diagenetic history. The significant diagenetic processes were: micritization, cementation, recrystallization, leaching, silification, dolomitization and oil dissipation.

The diagenetic history of these processes are reviewed in term of changes in diagenetic environments and tectonic setting of the area. A diagenetic model is suggested to classify these processes into two stages. (A) The early diagenetic model (prior to final burial) which includes micritization, cementation, recrystallization, leaching, selective dolomitization and bitumene seepage. (B) The late diagenetic model (post final burial) which includes intensive dolomization, dolomite cementation, leaching as well as interstitial oil impregnation.

INTRODUCTION

The Aqra-Bekhme Formation of northeast Iraq represents an elongated, bank-type reef complex. It extends in a northwest-southeast direction parallel to the tectonic strike of northeast Iraq *(Fig. 1)*. The huge carbonate body is more than 75 km. long and about 20 km. wide. The age of its rocks range between Upper Campanian to Maastrichtian. The reef body is rudistdominated limestone which is commonly surrounded by detrital limestone and massive dolostone. Outcrops of the complex exposed throughout the high folded zone of north Iraq, displaying its estensive distribution as well as variable lithologic association. The complex is remarkably associated with hydrocarbon which shows either in the form of oil impregnation (Aqra, Bekhme Shaqlawa and Harir localities or bituminous fragments or seeps (Aqra, Bekhme localities). Because of this and due to its stratigraphic position within the Upper Cretaceous cycle which is developed during the tectonic climax of the Zagros orogenic belt, the formation earn considerable attention of geologists and sedimentologists, respectively.

Early investigations of these rocks goes back to the fifties when HENSON (1950) examined their stratigraphic and paleontological aspects. DUNNINGTON (1958) discussed their stratigraphic relation to hydrocarbon accumulation of north Iraq. The stratigraphic status is defined formally by BELLEN *et al.* (1959). Detailed sedimentological studies which include microfacies analysis were given by SADIK and AL-OMARI (1977), AL-RAWI and a AL-HAMADANI (1985), and AL-AMERI and LAWA (1986). However, most of these works are confined to the Aqra area. Recently Al-

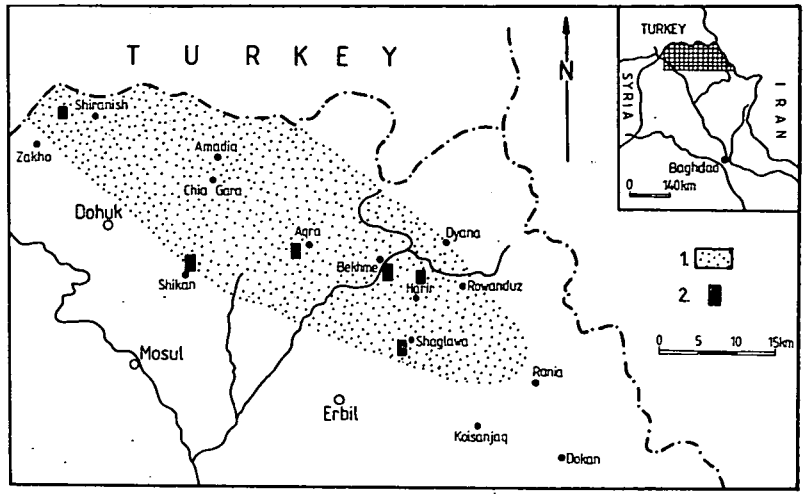

Fig. 1. Index map of studied area and examined localities.
1 = Areal extent of the reef complex, 2 = studied localities

Quayim and SAADALAH (1989) had given regional account to the sedimentary facies type and distribution of the complex compiling data from several localities. Little attention is given to the diagenetic characters of these rocks. This study deals with examination of the diagenetic aspects and its role in the development of the lithologic characters of the reef complex. Various diagenetic processes had influenced these rocks including micritization, cementation, leaching, recrystallization, silicification, and dolomitization. The nature, distribution, and possible origin of these processes is reviewed here to understand better their relations to the reef complex.

About 150 rock samples were collected from exposures of six localities. These localities are Aqra, Bekhme, Harir, Shiranish, Sheikhan, and Shaqlawa areas *(Fig. 1)*. Polished slabs and thin sections were prepared from the studied samples for detailed petrographic examination. Alizarinred staining solution is used to differentiate the dolomite from the calcite, and X.R.D analysis were conducted for further mineralogical differentiation specially for some sampless insoluble residue's.

STRATIGRAPHY AND FACIES

The Aqra-Bekhme Formation is defined by BELLEN *et al.* (1959) as two different stratigraphic units. The Aqra Formation represents a massive reef limestone mass of the complex, and the Bekhme Formation consists of dolomitic detrital limestone which is closely associated with the former. Due to their mutula origin and complex lithologic interrelation BUDAY (1980) had unified then into one single unit, namely the Aqra-Bekhme Formation. The formation represents the extensive carbonate body of the Upper Campanian-Maastrichtian cycle of north Iraq. It has been interfingering with the flysch sediments of Tanjero Formation northeastward and with the basin-origined marl of Shiranish Formation southward *(Fig. 2)*. The Aqra-Bekhme Formation is usually underlies unconformably the middle Cretaceous Qamchuqa Formation, and conformably and transgressively is overlain by the Shiranish Formation. However, in certain areas i.e. Aqra and Sheikhan, the

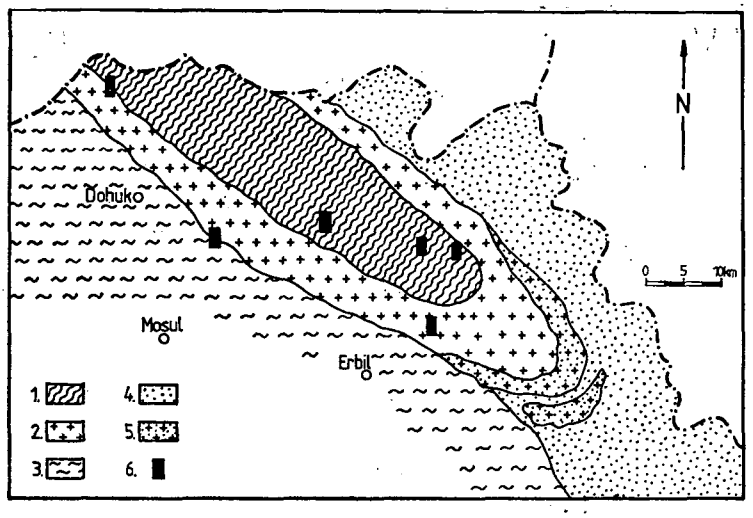

Fig. 2. Facies map of Upper Cretaceous Sedimentary Cycle of Northeastern Iraq showing regional facies belts of Aqra-Bekhme Formation (from AL-QAYIM and SAADALAH, 1989).
1 = Reef body, 2 = Reef apron, 3 = Shiranish basinal limestone, 4 = Tanjero flysch, 5 = Reef apron within Tanjero Sediments, 6 = Studied localities

upper contact of the formation is unconformable and erosinal, whereby the Paleocene-Lower Eocene marine clastics of the Kolosh Formation is succeeded.

According to AL-QAYIM and SAADALAH (1989), the Aqra-Bekhme reef complex consists of two closely associated but regionally distinctive parts. The central reef body, and the periferial detrital shade which surrounds it, is known as a reef apron facies *(Fig. 3A)*. The reef body is a massive limestone buildup which constitutes the core of the complex *(Fig. 2)*. Three distinctive facies have been recognized within the reef body, as follows: reef core, interior lagoon, and fore-reef facies *(Fig. 3B)* Below there is a brief description of the reef complex facies.

a) Reef core facies

It is characterized by massive rudist-dominated limestone. Other skeleta constituents, such as algae, bryozoa, and echinoderms. are also occured. These rocks are variably oil impregnated and recrystallized and selectively domomitized and/or leached.

b) Interior lagoon facies

This facies is represented by peloidal-miliolid rich gray limestone. It shows patchy distribution within the reef core facies *(Fig. 3B)*. It is strongly influenced by recrystallization and cementation with occasional occurrence of selective dolomitization.

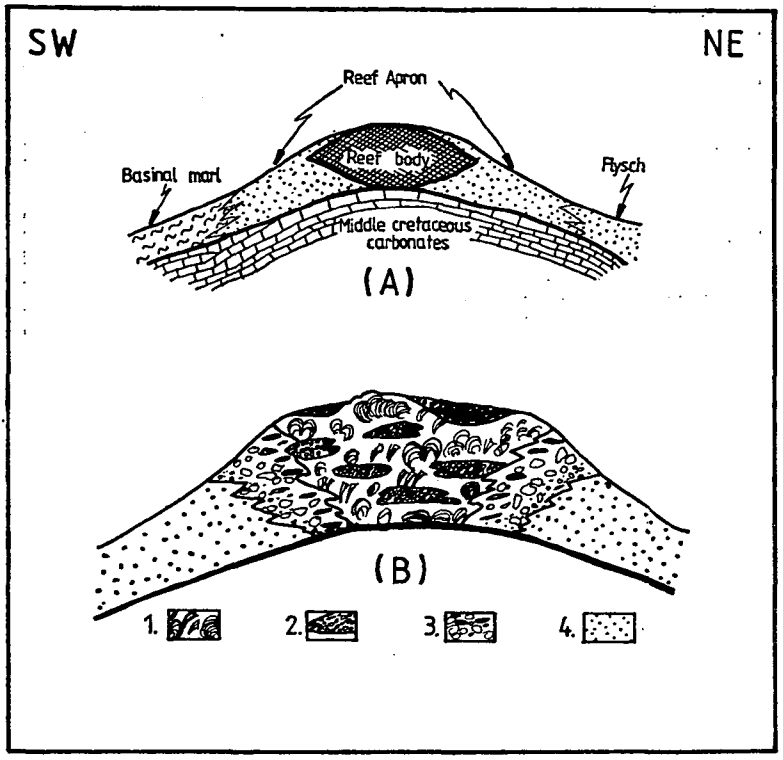

Fig. 3. Schematic cross section illustrating the Aqra-Bekhme Facies types. (A) regional belts, (B) facies types in detail (from AL-QAYIM and SAADALAH, 1988).
A = Reef core, 2 = interior lagoon, 3 = Fore reef, 4 = Reef apron

c) Fore-reef facies

This facies is used here to designate the reef talus sediments which represent a narrow belt developed around the reef core and characterized by massive to thick bedded bituminous limestone. Fragments are reef-derived with characteristic fauna includes Laftosia, Acteonella, and Orbitolina. Recrystallization, dolomitization and to less extent silicification are characteristic diagenetic processes in this facies.

d) Reef apron facies

The sediments of this facies is characterized by medium to thick bedded reef-derived calcarenite type detrital limestone. This facies is deposited in a relatively deep water and spreads distantly from the reef body into the surrounding deep marine basin sediments. Intensive dolomitization had commonly altered these rocks into a massive and thick sequence of sucrosic dolostone which is often impregnated with oil. Other diagenetic processes including silicification, dolomite cementation and leaching are also recognized.

DIAGENETIC PROCESSES

Several diagenetic processes have had influenced the Aqra-Bekhme rocks. Among these processes micritization, leaching, recrystallization, silicification, cementation, dolomitization, fracturing and oil impregnation are noticed. Below is the discussion of the most important ones.

Cementation

Several type of cement have been recognized. These types are as follows: (1) *Syntaxial cement* is developed as thin clear rim surrounding the echinodermal bioclasts *(Fig. 4a)*. It is recognized within the detrital limestone of fore-reef facies and adjacent part of the reef apron facies. Such an early diagenetic cementation is probably took place during the shallowing periods and upon the meteoric influences (LONGMAN 1980). (2) *Intragranular cement* is the spary calcite which fills foram chambers and other skeletal cavities. Miliolids of the interior lagoon facies are often contain such cements *(Fig. 4b)*, as well as cavities of reef-derived macrofossils. However the succeeding leaching couldreduce the amount of this cement by the dissolution. (3) *Intergranular cement* represents the sparite, microsparite subhedral calcite mosaic which fills mainly the intergranular spaces of the skeletal limestone of interior lagoon and reef core facies *(Fig. 4f, 5a)*. The close association of this cement to these two facies implies marine vadose to meteoric conditions (LONGMAN, 1980) which could prevealed during or shortly after the deposition, i.e. early diagenetic stage.

Recrystallization

This process affects both skeletal grains and micrite of the reef body facies. The reef core and the interior lagoon facies are most affected *(Fig. 4d, e)*. The extent of this process is hard to be evaluated because products of the cementation might be incorporated in the groundmass.

Inversion of skeletal fragments into coarse crystalline calcite are common especially within parts which are rich in unstable (high Mg calcite) skeletal grains i.e. the reef core, fore reef facies *(Fig. 4f, 5a)*. Neomorphism of these shallow marine sediments could have been occurred within a meteoric phreatic environment during the early stages of diagenesis (LONGMAN, 1980).

Micritization

It is recognized as thin dark film surrounding reefderived skeletal fragments *(Fig. 5a)*. The extent of this process is limited to certain parts and often associated with samples from fore reef facies.

Micritization is believed to have been developed during postdepositional algal and bacterial activities (BATHURST, 1977 and REIJERS and HSU, 1986).

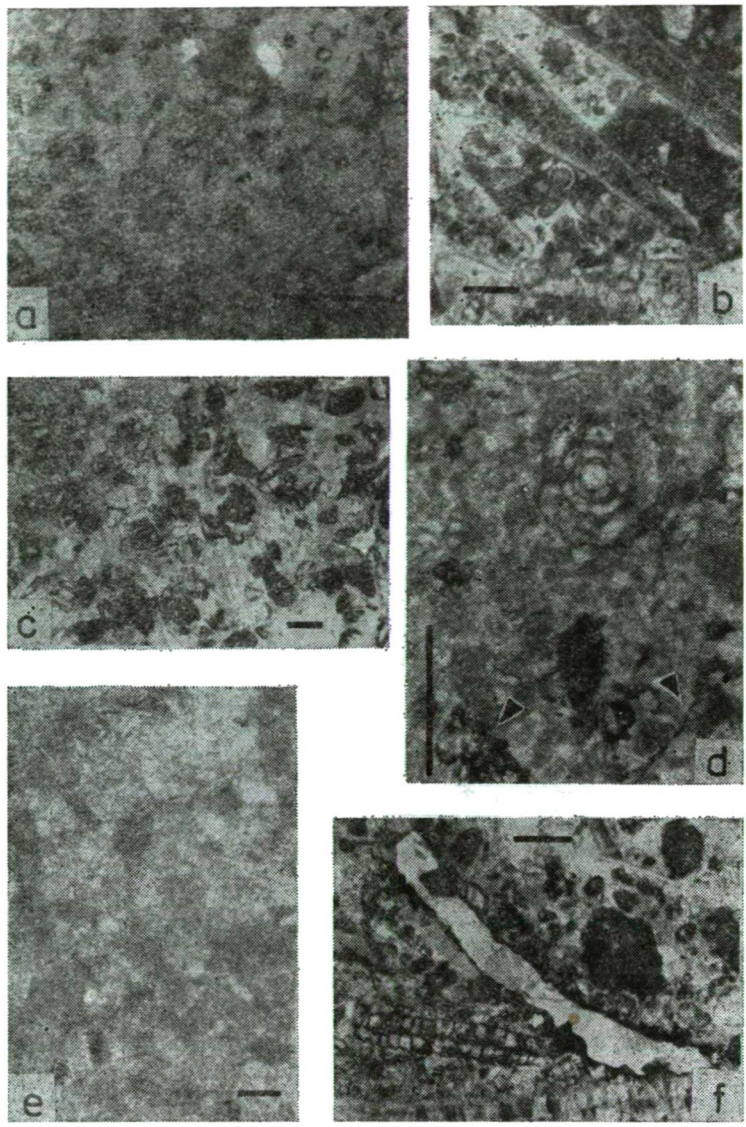

Fig. 4. (a) Photomicrograph of nondolomitized detrital limestone of the reef apron facies. Grains are dominated by fine sand size echinodermal bioclasts showing syntaxial rim cement (arrows). (XN) Fore reef rudstone with spary intergranular calcite cement filling skeletal cavities. (XN) (c) Miliolid pelcidal packstone of reef interior facies showing intergrabular spary calcite cement. (d) Miliolid peloidal packstone which shows cementation and recrystallization of both grains and matrix. Note microcracks and vugs filled with oil (arrows). (e) Intensive recrystallization of peloidal wackestone of the interior lagoon facies. (XN). (f) Gastropod fragments which is totally inverted into spary calcite mosaic. Note oil impregnation in leached out micritic envelope of the fragment. (Bar is 0.5 mm)

Leaching

Influence of this process have been recognized on samples from different facies. It is noticed in samples from reef core and interior lagoon facies producing moldic or vugs porosity which is frequently replaced by oil impregnation *(Fig. 4d, 5b)*. Other samples from dolostone of the reef apron facies show large (2—10 cm. wide) irregular vugs which are partially filled by white dolomite cement *(Fig. 5f)*.

Paragenesis of leached material and replaced substances suggest two mode of leaching occurred during successive subearial conditions and consequent meteoric vadose environment which is the most favourable for leaching phenomena (HECKEL, 1983).

Silicification

Silica replacement is observed in a limited distribution. It is recognized in the field as elongated, up to 10 cm. wide, dark brown chert nodules. In these cases no evidences of the precursor limestone is preserved. In other cases where partial replacement occur the original detrital limestone fabric is recognized *(Fig. 5e)*. However, both cases the silicification seems to have been associated with the reef apron facies and in particular near its upper part. The deep water environment of these sediments and its transgressive upbulding (AL-QAYIM *et al.* 1986) rule out the mixing zone origin. Silicification of these sediments seem to have been developed during late diagenesis and probably in association with intensive dolomitization.

Dolomitization

Dolomitization affect the different facies of the Aqra-Bekhme reef complex in different ways suggesting different mode of origin. Three distinctive type of dolomite is recognized: (1) *Selective floating dolomite* occurs as dissiminated, euhedral silt size dolomite rhombs within specific skeletal grains or rarely within the matrix. It is generally associated with the grains of reef core and interior lagoon facies and matrix of reef apron facies. The fabric of this dolomite suggests early stage of dolomitization (RANDAZZO and ZACHUS, 1984) and could be generated by concentration of Mg^{++} ion within sediment particles (MATHEWS, 1974). (2) *Intensive sucrosic dolomite* is the most common and extensive type of dolomite and it is strongly associated with the detrital limestone of the reef apron facies and often obliterate its original fabric. The resulting dolomite is sucrosic in type and consists of silt size, euhedral and interlocking *(Fig. 5e)*, or subhedral sutured *(Fig. 5d)* mosaic. The resulting intercrystalline prosity is often impregnated with oil *(Fig. 5e)*. The pervasive nature, subrosic fabric and association w th relatively deep marine facies suggest a late diagenetic and deep burial origin (MATTES and MOUNTJOY, 1980, and RANDAZZO and ZACKUS 1984). (3) *White dolomite cement* is locally developed as white euhedral coarse crystalline dolomitic patches or pods especially associated with intensively dolomitizized rocks *(Fig. 5f)*. It is often line vugs and cavity walls that have been developed within the sucrosic dolostone. Dolomite of such characters is believed to represents a late diagenetic phenomena which post dates the sucrosic dolomite (MATTES and MOUNTJOY, 1980).

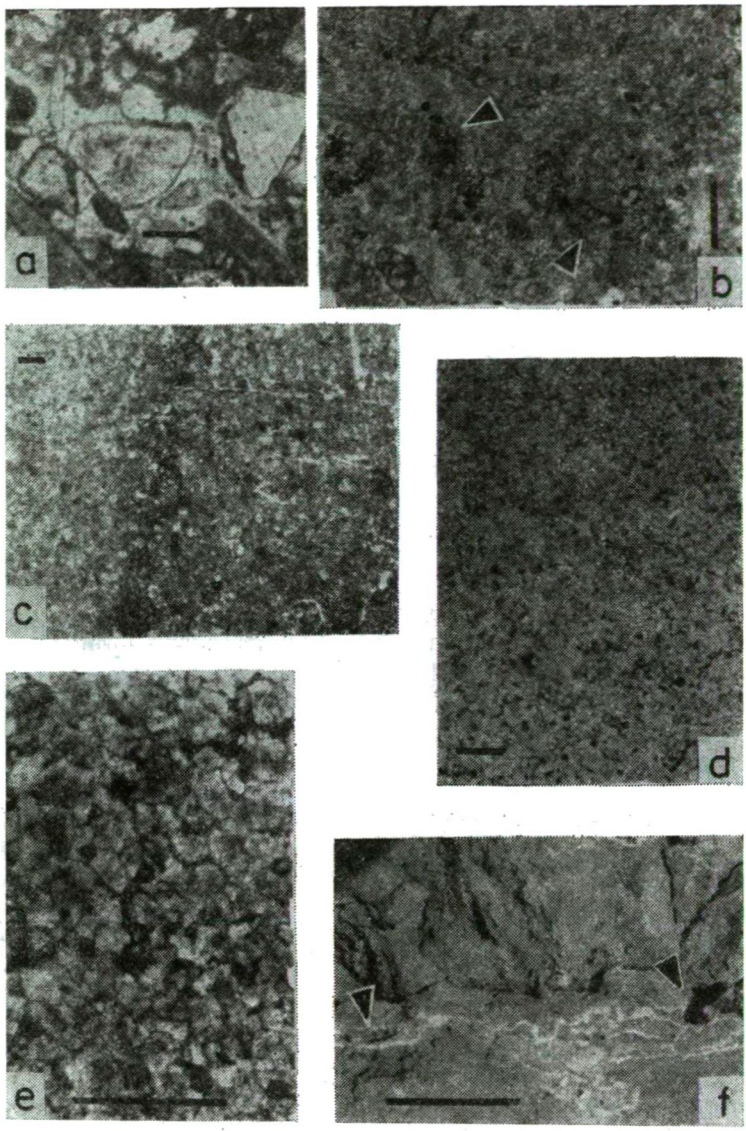

Fig. 5. (a) Fore reef bioclastic calcarenite showing neomorphosed skeletal grains with micritic envelope. Intergranular spaces partially filled by spary calcite (XN). (b) Interior lagoon packstone which is selectively leached into small irregular vugs. Both vugs and micro-cracks (arrows) filled with oil (c) Detrital limestone of the reef apron facies showing partial silicification of matrix (XN). (d) Subhedral silt size sutured mosaic dolomite of the reef apron facies. (e) Silt size, euhedral, and interlocking dolomite mosaic of the reef apron facies with intercrystalline porosity filled with oil. (f) White irregular pod of coarse crystalline dolomite cement within the sucrosic dolomite of the reef apron facies. Note secondary vugs that associated with these pods (arrows). (Bar is 0.5 mm except for f is 15 cm.).

DIAGENETIC MODEL

From the preceding description of the diagenetic products and processes that had affect the Aqra-Bekhme reef complex and its distribution and relation to the different facies, and based on their paragenetic relationships, a diagenetic model which depicts the evolution and sequence of these processes is attempted. The suggested model is schematically presented in *Figure 6A, B* and discussed below in term of changes in diagenetic environment and tectonic setting.

The sediment of the Aqra-Bekhme Formation is deposited under marine water of various environmental condition. The reef core and interior lagoon facies represent a shallow marine environment which could be interupted by subaerial conditions. This situation would conceivably provide an alternating marine phreatic — marine vadose and even meteoric environments. Development of such conditions obviously would intiate early diagenetic processes such as micritization, inversion, leaching, cementation (intragranular, intergranular & syntaxila) as well as early stage of oil seepage and butumine fragmentation. The sequence and distribution of these processes would depends on local water chemistry and circulation as well as type and composition of specific sediments particle *(Fig. 6A)*. Simultaneously, the fore-reef and reef apron facieses show little or no response to most of these processes. This is probably due to deposition under relatively deep water, whereby inactive water circulation would yield passive marine phreatic reactions (LONGMAN, 1980). As accumulation of sediments continue and probably prior to lithification partial dolomitization might be generated selectively depending on grain type and matrix mineralogy.

Prior to significant burial and after early lithification stage the whole reef body is believed to be uplifted forming an emerging ridge (DUNNINGTON, 1958). Such a tectonic event is believed to cause the early cracking phase which characterizes the already lithified parts of the complex. The whole complex is drown again upon the transgression of the paleocene which causes its burial under the paleogene marine sequence.

The burial history of the area is not the subject of this paper, however, it semingly contribute to the late diagenetic history and possible hydrocarbon disspiation within the complex. The intensive dolomitization which is associated with the reef apron facies could have been developed by reactions of compaction fluids which might be expelled from surrounding marl and shale basins *(Fig. 2)*. These fluids which could be enriched with Mg ion required for dolomitization (ILLING, 1959 and JODRY, 1969) might migrate laterally towards the reef body through the detrital limestone the reef apron facies causing its dolomitization *(Fig. 6B)*. Similar mechanism for the development of the intensive dolostone which is associated with the Miette buildup of Alberta is suggested by MATTES and MOUNJOY (1980). Oil migration and dissipation could have occured along with migration of these fluids or later on. The oil impregnation which fills this dolomite intercrystalline porosity *(Fig. 5e)* as well as microcracks *(Fig. 4d, 5b)* suggests post-dolomitization emplacement.

Successive deep burial changes in chemical environment would conceivably cause the leaching and vugs as well as the white dolomite cementation of reef apron facies *(Fig. 6b.)*.

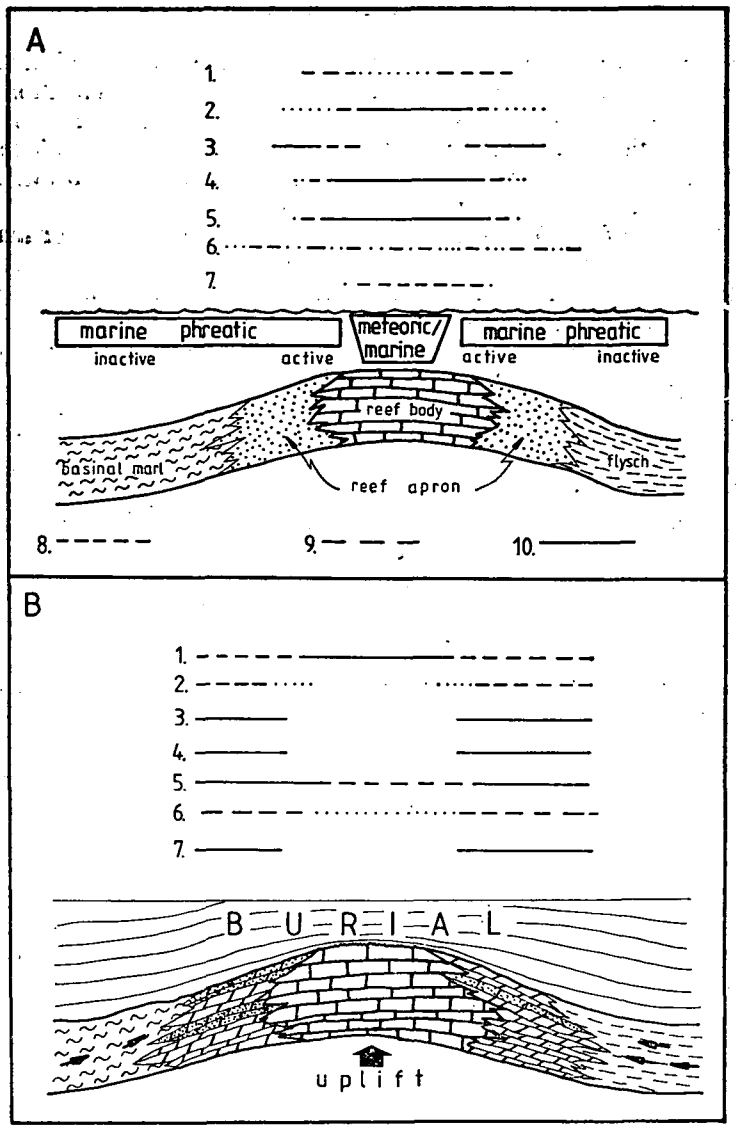

Fig. 6. Diagenetic model for the Aqra-Bekhme reef complex showing type and distribution of diagenetic products interm of sedimentary facies and diagenetic environments. (A) Early diagenetic sequence. 1 = micritization, 2 = cementation, 3 = syntaxial rim, 4 = recrystallization, 5 = oil seepage, 6 = selective dolomitization, 7 = leaching, 8 = weak, 9 = moderate, 10 = strong. (B) Late diagenetic sequence. 1 = cracking, 2 = silification, 3 = intensive dolomitization, 4 = intercryst porosity, 5 = oil impregnation, 6 = leaching and vugs, 7 = dolomite cement

REFERENCES

AL-AMRI, T., LAWA, F. (1986): Paleoecological model and faunal interaction within Aqra Limestone Formation, north Iraq.-Jour. Geol. Soc. Iraq. **19,** 121—142.

A -QAYIM, B., HABIB, R., AL-DYNI, N. (1986): Petrology and geochemistry of Shiranish Formation (type section) towards sedimentary facies interpretation. Jour Geol. Soc. Iraq. **19,** 164—180.

AL-QAYIM, B., SAADALAH, A. (1988): Sedimentary facies and stratigraphic evolution of Aqra—Bekhme reef complex (Upper Cretaceous) of north Iraq. Jour. Geol. Soc. Iraq. (in press).

AL-RAWI, D., AL-HAMDANI, T. (1985): Microfacies study of Aqra limestone in the type section and Gelizenta section and reconstruction of paleoclimate. Jour. Geol. Soc. Iraq. **18,** 115—161.

BATHURST, R. (1977): Carbonate sediments and their diagenesis, 2nd ed., Elsevier Pub. Co., Amsterdam, 658 p.

BELLEN, V., DUNNINGTON, H. V., WETZEL, R., MORTON, D. (1959): Lexique stratigraphique international, Asia, Fase 9a (Iraq), Paris, 333 p.

BUDAY, T. (1980): Regional geology of Iraq, V. I: Stratigraphy and paleogeography, S. O. M., Baghdad, 447 p.

DUNNINGTON, H. V. (1958): Generation, migration, accumulation and dissipation of oil in northern Iraq. In: WEEKS, L. C. (ed.): Habitat of oil, AA. P. G. Publication, 1194—1251.

HECKEL, P. H. (1983): Diagenetic model for carbonate rocks in mideontinent Pennsylavnian eustatic cyclothems. Jour. Sed. Pet. **53,** 733—759.

HENSON, F. R. (1950): Cretaceous and Tertiary reef formations and associated sediments in the middle east: A. A. P. G. **34,** 215—238.

ILLING, L. V. (1959): Deposition and diagenesis of some upper paleozoic carbonate sediments in western Canada. 5th Wor. Pet. Cong. Proc. Section **1,** 23—52.

JODRY, R. L. (1969): Growth and dolomitization of Silurian reef, St. clair county, Michigan, A. A. P. G. **53,,** 957—981.

LONGMAN, M. V. (1980): Carbonate diagenetic texture from nearshore diagenetic environments. A. A. P. G. **64,** 461—487.

MATHEWS, R. K. (1974): A process approach to diagenesis of reefs and reef associated limestone. In: LAPORTE, L. E. (ed.): Reefs in time and space, S. E. P. M. Spec. Pub. 18, 234—256.

MATTES, B. W., MOUNTJOY, E. W. (1980): Burial dolomitization of the Upper Devonian Miette buildup, Jasper natural park, Alberta. In: ZENGER, O. H., DUNHAM, J. B., ETHINGTON, R. L. (eds.): Concepts and Models of Dolomitization. S. E. P. M. Spec. Pub. **28,** 259—297.

PANDAZZO, A. F., ZOCHOS, L. G. (1984): Classification and description of dolomite fabrics of rocks from the Floridon aquifer, U. S. A. Sed. Geol. **37,** 151—162.

REIJERS, T. J., HSÜ, K. J. (1986): Manual of carbonate sedimentology, Academic press, London, 302 p.

SADIK, A., AL-OMARI, F. (1977): Microfacies studies of some Late Cretaceous Seiments (Aqra Formation) from northern Iraq. Revista Espanola of micropaleontologia, 9, 251—157.

Manuscript received, 26 October, 1989

Acta Mineralogica-Petrographica, Szeged, XXX, 161—171, 1989

COASTAL EROSION IN RELATION TO SEA LEVEL CHANGES, SUBSIDENCE AND RIVER DISCHARGE, NILE DELTA COAST

NABIL M. EL-FISHAWI

Geology Department, Institute of Coastal Research, Alexandria

ABSTRACT

The Nile Delta coast has been dynamically unstable for centuries. Before 1900, its delta front was prograding seaward but after it began to retreat. Examination of the 1988 shoreline survey in relation to the 1909 shows that the total loss of land was 14.7 km² for Rosetta, 0.44 km² for Burullus and 21.0 km² for Damietta. The maximum rate of erosion was found to be 58 m/year at west of Rosetta.

Sea level gauges were installed for records along the coast. The tides are semi-diurnal in nature with two high and two low water levels in a tidal day. A considerable difference was found between water levels of summer and winter seasons. The swell action at Burullus during summer seasons and the effect of winter waves at Rosetta may cause the increasing of sea level and hence coastal erosion. Many evidences indicate that subsidence is partly responsible for erosion.

A significant difference occurred in the Nile load prior and after 1900. The Nile flood levels became lower and the annual sediment load decreased. Furthermore, the closure of the Aswan High Dam in 1964 has reduced the flow and sediment load of the River Nile to insignificant quantities.

Sea level rise and/or subsidence possibly coupled with reduction of the sediment load of the River Nile became paramount importance in recent coastal erosion along the Nile Delta coast.

INTRODUCTION

The coastline of the Nile Delta is a part of the low sandy shore bordering the southeastern part of the Mediterranean sea. The total length of the Nile Delta coastline is about 260 km from Alexandria to Port Said *(Fig. 1)*. Coastal dunes with elevations up to 30 m act as barriers against the action of the sea waves along the eastern part of the Burullus coast. The hydrodynamic factors affecting the coast are the waves, currents and winds. The predominant direction of the waves is NNW with an average height of 80 cm. The eastward littoral current predominates with an average velocity of 36 cm/sec. The prevailing wind comes from the WNW, NW, W and N. The majority of the daily readings range between 9—23 knots/hour. The average tidal changes along the delta coast are small and not exceeding 26 cm.

The stability of coastline depends upon the balance between the quantity of sediment supplied to the coast and that carried away. Formerly, because of the large amounts of sediments brought to the coast by the Nile, depositional forces prevailed near the main discharge points of Rosetta and Damietta. Erosional processes are confined to the coast since 1909 and accelerated after the construction of the Aswan High Dam in 1964 due to reduced Nile sediment inputs.

An increasing body of evidences (HICKS, 1978; HICKS *et al.*, 1983; HULL and TITUS, 1986) suggests that in the coming 100 years a global warming due to the

Inst. of Coastal Research, 15 Faraana st., El-Shalallat, Alexandria, Egypt.

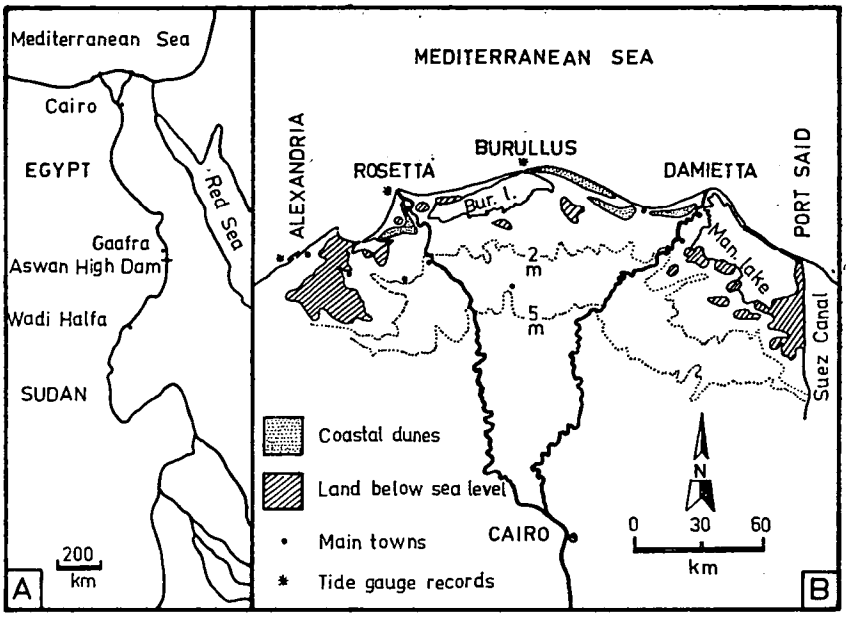

Fig. 1. Location map for the River Nile (A) and the Nile Delta coast (B)

greenhouse effect will lead to a rise in sea level from 0.5 m to 3.5 m. The sea level rise in future coupled with a possible increase in storm surges would cause severe erosion, flooding of reclaimed lands, salt water intrusion and public health risks as well as direct damage to ports, towns and roads of the Nile Delta coast. Over 20% of the coastal land in the Nile Delta could be flooded with a 2 m rise in sea level.

The present study on the Nile Delta coast aims to investigate the the recent coastal erosion in relation to sea level changes, subsidence and reduction of the River Nile inputs. The impacts of future sea level rise in aquifers and estuaries of the northern coast are also discussed.

RATE OF COASTAL EROSION ON HEADLANDS

Erosion of the Nile Delta beaches has been observed long before the construction of the Aswan High Dam. Severe coastal erosion is predominating on the Rosetta, Burullus and Damietta headlands. Many summer houses located on the beach have been destroyed by the sea advance. A cut of about 1 m high in the beach sediments characterizes the eroded area. Coastal dunes are severely eroded due to the attack of waves.

The changes in coastal areas and length were investigated for Rosetta, Burullus and Damietta headlands from the beginning of erosion in 1909 to 1988 *(Fig. 2)*. The total area of erosion in square meters for the three headlands is calculated by comparing the shoreline of 1909 with that of 1988 (Table 1). The loss of coastal lands was about 14.7×10^6 m^2 for Rosetta, 0.44×10^6 m^2 for Burullus and 21.0×10^6 m^2 for Damietta. On each headland, it is observed that the eastern part is eroded faster than the western one. The slow erosion at Burullus may be related to its extension

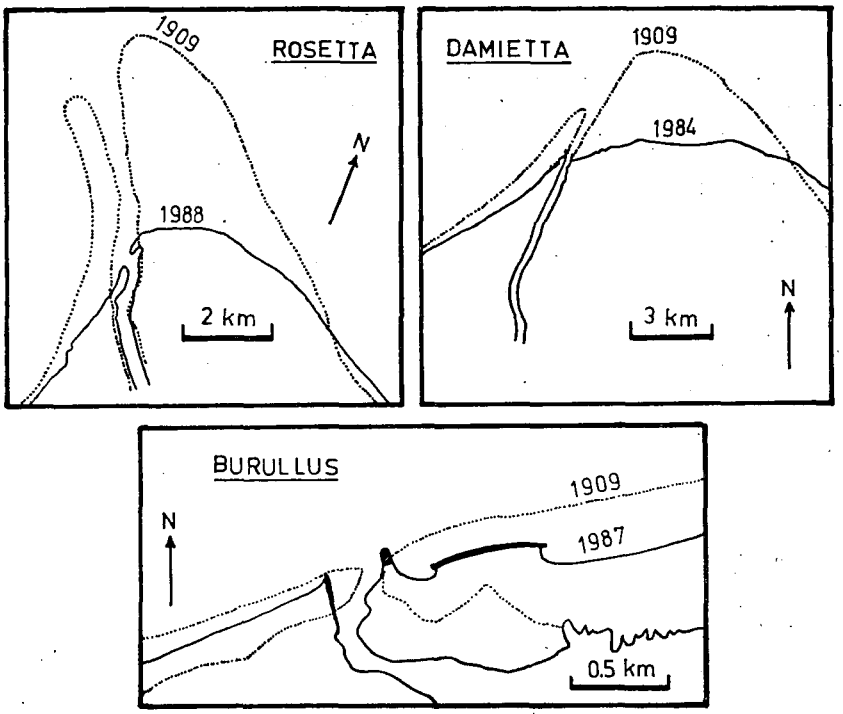

Fig. 2. Shoreline changes at Rosetta, Burullus and Damietta headlands during 1909—1988

and less curved shape than on the other headlands. The rate of erosion was calculated to be 184.000 m²/yr for Rosetta, 5.500 m²/yr for Burullus and 263-000 m²/yr for Damietta. The decrease in maximum length from the extremity of the point during the period 1909—1988 was found to be 4.6 km for Rosetta, 0.3 km for Burullus and 3.3 km for Damietta. The fastest rate of shoreline receding was observed at Rosetta (58 m/yr) if it is compared to 41 m/yr for Damietta and 3.8 m/yr for Burullus.

TABLE 1

Changes in areas and length of Rosetta, Burullus and Damietta, headlands during 1909—1988

Stretch	Eroded area ($\times 10^6$ m²)	Erosion rate (m²/yr)	Decrease in max length (m)	Dc. rate in length (m/yr)
West Rosetta	3.50	44,000	4.600	58.0
East Rosetta	11.20	140,000	4.250	53.0
West Burullus	0.09	1,100	100	1.3
East Burullus	0.35	4,400	300	3.8
West Damietta	4.20	53,000	1.900	24.0
East Damietta	16.80	210,000	3.300	41.0

Sea level change is essential in delineating the position of shoreline. Automatic water level gauges were installed for records along the Nile Delta coast in different times an at different areas. Continuous reading of the water level was made 24 hours a day. In order to define the sea level change, the following levels and their variability were determined: (1) The mean water level (MWL). (2) The mean high water level (MHWL). (3) The highest high water level (HHWL). (4) The mean low water level (MLWL). (5) The lowest low water level (LLWL).

Sea level records were available at Alexandria for the period 1985—1986, at Rosetta for the period 1982—1983 and at Burullus for the period 1984—1985 *(Figs. 3, 4* and *5)*. The sea level characteristics are referred to the Survey Department Zero Level in Egypt. Harmonic analysis of the water level records along the Nile Delta coast indicated that the tides are semi-diurnal in nature with two high and two low water levels in a tidal day with comparatively little diurnal inequality.

At Alexandria and Burullus, a considerable difference was found between water levels of summer and winter seasons *(Figs. 3* and *5)*. It is indicated that the summer

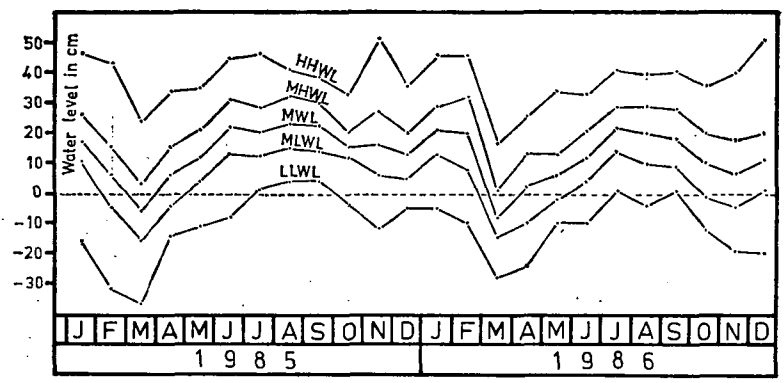

Fig. 3. Sea level changes at Alexandria, 1985—1986

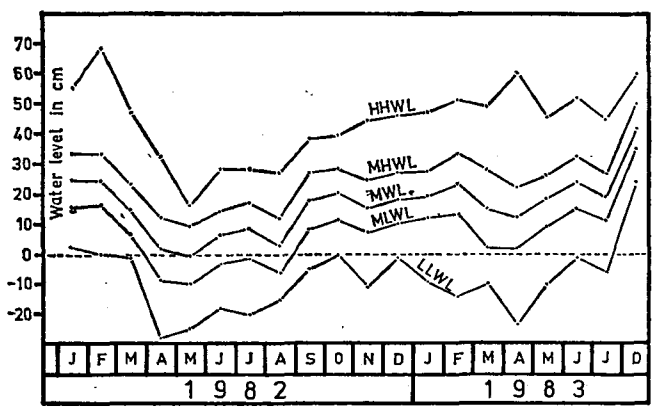

Fig. 4. Sea level changes at Rosetta, 1982—1983

seasons have higher water levels than that in winter ones. The swell action (MANOHAR, 1976) during summer months of June, July, August and September may cause the increasing of the water levels considerably during those months. These high water levels during summer seasons may explain the severe erosion of the beach and coastal dunes at Burullus.

On the other hand, water levels of summer and winter seasons at Rosetta show contrast situation *(Fig. 4)*. Water levels become high in winter and low in summer. Consequently severe coastal erosoion at Rosetta headland may be related to the effect of the winter waves to increasing the water levels and hence erosion became excessive.

TABLE 2

Sea level characteristics and tidel range at Alexandria, Rosetta and Burullus (in cm)

Stretch	HHWL	MHWL	MWL	MLWL	LLWL	Tidal range
Alexandria	51	22	13	4	−37	18
Rosetta	68	26	17	8	−28	18
Burullus	68	36	28	20	−35	16

Table 2 illustrates the characteristics of water level at Alexandria, Rosetta and Burullus. It is clear that the average tidal changes along the coast are small; the difference between MHWL and MLWL ranges from 16 cm to 18 cm. However, the monthly tidal range not exceeding 24 cm most of the time.

Water level characteristics were drawn in order to investigate the variations along the western coast of the Nile Delta *(Fig. 6)*. It is indicated that the water levels increase from Alexandria to Burullus. The mean water levels at Alexandria, Rosetta and Burullus were found to be 13 cm, 17 cm and 28 cm respectively. The difference in MWL from Alexandria to Rosetta was 4 cm and from Alexandria to Burullus it was 15 cm. Such eastward increase in the sea level coincides with the predominate direction of longshore current which feeding the coast from west to east.

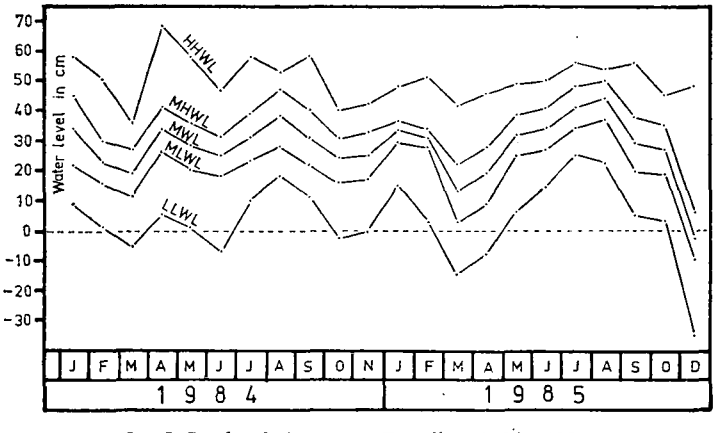

Fig. 5. Sea level changes at Burullus, 1984—1985

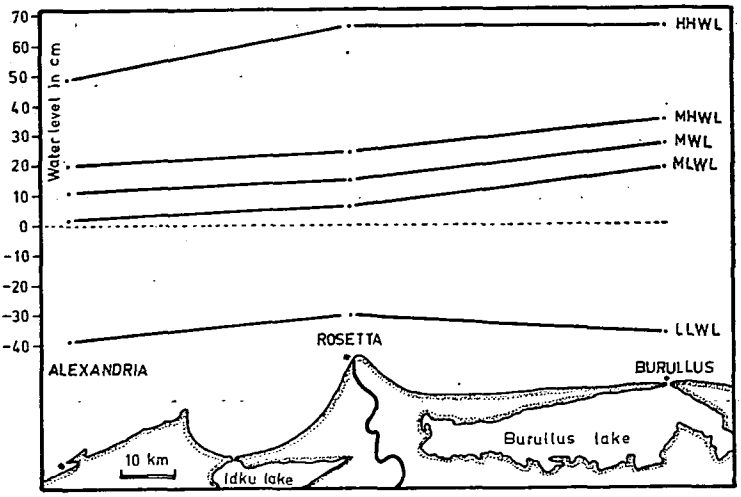

Fig. 6. Sea level variations between Alexandria and Burullus

Impacts of sea level rise in aquifers and estuaries

EL-FISHAWI and FANOS (1989) reported that the rise in sea level along the Nile Delta coast was estimated to be 10 cm for the period 1926—1973 with a rate of 2.2—2.9 mm/year. HICKS (1978) and HICKS *et al.* (1983) estimated an average rised of 2.6—3.7 mm/year along the Atlantic coast for the period 1921—1975. The predicter sea level rise in future will have an important impact on society. As ground water is removed and aquifer approaches equilibrium with current sea level, the salt front will move farther inland from the sea to recharge aquifers and hence increase the salinity. HULL and TITUS (1986) estimated that a 73 cm rise in sea level would increase the maximum thirty-day chlorinity at Delaware River from 135 mg/l to 305 mg/l. High concentrations of sea salts at water intakes would create public health risks, increase the cost of water treatment and damage plumbing and machinery. High salinity could also upset the ecology of the estuary.

Recently, many wells were drilled along the northern coast of Egypt for land reclamation, irrigation and industrialization. Therefore, it is recommended to:

1. Control the ground water exploitation in the northern coast to reduce subsidence and salt water intrusion in fugure.
2. Use a mathematical model to study salinity changes in the estuaries and aquifers of the Nile Delta.

SUBSIDENCE OF COASTAL LANDS

Evidences for continued subsidence during the last 2000 years could be seen in Alexandria, Burullus lake, Manzale lake and Sinai. In the western part of the Nile Delta coast, Ptolemaic and Roman settlements are now found at depths between 5—8 m below sea level (TOUSSOUN, 1934). Of course, the site of these settlements is deeper than can be accounted for by a sea level rise of 1.5 cm/100 years. The ancient

monuments between Alexandria and Abu Quir, originally were built on land, had been submerged by the sea water. The coastal lakes could owe its existence to subsidence caused by earthquakes (COASTAL PROTECTION STUDIES, 1978). The structure in a sheltered embayment and such soil layers could be susceptible to subsidence of 1—2 m or more due to collapse of the loose soil structure under vibration. Also ruins of ancient villages on numerous islets in the coastal lakes show clearly the invation the sea to the agricultural land that had been utilised by the ancient inhabitants of these villages. The base of the ruins of Tennis were said to be below the level of Manzala lake. Furthermore, the remnants of two forts near Burullus outlet were visible below the sea in 1930, but they have now disappeared. The old site of Burg El-Burullus village is now about 2 km in the sea.

Published informations on the subsidence rate along the Nile Delta coast are few and show wide variation. In the Suez Canal stretch, a steady sinking of 1.2 mm/year since 1860 has been documented by GOBY (1952). Archeologists have calculated a definite rise of sea level relative to the land of 2.6 m in the last 18 centuries, corresponding ot an average of 1.4 mm/year (IBRAHIM, 1963). The eastern part of the Nile Delta indicated subsidence of some 10 m over at least 20,000 years (0.5 mm/year) and subsidences of few centimeters only during the last 2,000 years (COASTAL PROTECTION STUDIES, 1978). Considerable subsidence of the coastal zone is indicated by the 10—50 m thick layer of post 8,000 BP nearshore marine, lagoonal and deltaic sediments in the NE part of the Nile Delta (CONTEULLIER and STANLEY, 1987). At Port Said, an independent record of neotectonic motion for the period 1922—1950 indicated a subsidence of 4.8 mm/year (EMERY *et al.*, 1987). The Holocene thickness map points to the considerable subsidence in the coastal lower delta plain in the last 6,000 years (SESTINI, 1988), dated sequences suggest rate of subsidence of 1.5 mm/year. Higher subsidence rates ranging from about 4.5 mm/year to 5.0 mm/year for at least 7,500 years are calculated by STANLEY (1988). In fact, long-term subsidence rates of 5 mm/year are higher compared to rates at other much larger and thicker delta deposits, i.e. the rate of subsidence of the lower part of the Mississippi River Delta is found to be less than 2 mm/year as mentioned by STANLEY (1988).

To sum up, evidences indicate that erosion may be partly related to subsidence. However, more detailed work could answer the question of whether-eroded areas along the coast have subsided or the sea level has steadily increased.

CHANGE IN THE RIVER NILE LOAD

The relationship between the recent coastal erosion and the changes in the River Nile load can be traced if one of the important questions that the scientists try to answer: how much discharge and sediment were brought down by the Nile to Egypt from its upper reaches. Therefore, an attempt was made to show if noticeable change has occurred in the Nile levels, discharge and load during the recording period, then their repercussions must be related to the climatic change over the Nile basin.

It has been stated that the Nile flood levels *(Fig. 7)* were particularly high in the period 1840—1900 and that they have been significantly lower in the period 1900—1944 (QUELENNEC and KRUK, 1976). These features will be considered with the variations of the annual discharge and sediment load brought down the delta by the Nile.

Time series of total annual discharge of the Nile at Aswan (Fig. 8) was discussed by the COASTAL PROTECTION STUDIES (1978). The variation in the natural river flow

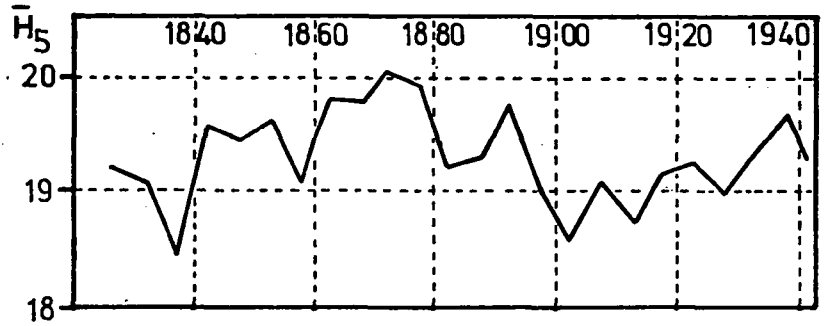

Fig. 7. Five years averages of the Nile maximum levels at Rodah (Cairo), 1825—1944 (after QUELENNEC and KRUK, 1976)

at Aswan indicated a difference of 27% between two sub-series during 1870—1971. The average annual discharge was estimated to be 107×10^9 m^3/yr during the period 1870—1902 and 84.4×10^9 m^3/yr during the period 1903—1971. Someone may relate this difference to the effect of the Low Aswan Dam constructed in 1902. In fact, a comparison between the annual Nile discharge recorded at Wadi Halfa (upstream) and Aswan (downstream) indicates an overestimation at Wadi Halfa to be of an order of magnitude of about 10%. But this overestimation of 10% can not explain the 27% difference in the two published sub-series during 1870—1902 and 1903—1971.

The averages of the yearly Nile sediment load at Gaafra *(Fig. 9)* have been estimated (COASTAL PROTECTION STUDIES, 1978) to be 200 million tons/yr for the period 1825—1902 and 160 million tons/yr for the period 1903—1963 (25% decrease). It is quite clear that the Nile suspended sediment load was heavier in the 19th Century during the periods 1860—1883 and 1890—1898 than it has been since 1900. In addition, the quantities of silt deposited in the Egyptian irrigated areas in 1886 was estimated to be 37 million tons; it decreased to be 22 million tons in 1959. Moreover, the amount of the sediments brought to the Mediterranean through the Rosetta and Damietta branches decreased with an average of 25%. During the period 1825—1902, an average of 162—175 million tons of sediments would annually reach the Mediterranean and then decreased to be 130—140 million tons during 1903—1963.

To sum up, a significant difference occurred in the Nile load prior and after 1900. The Nile flood levels became lower and the annual discharge and sediment load

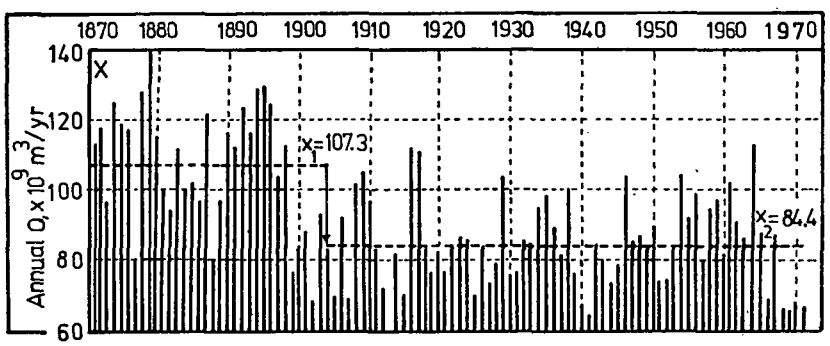

Fig. 8. Natural annual discharge of the Nile at Aswan, 1871—1971 (after COASTAL PROTECTION STUDIES, 1978)

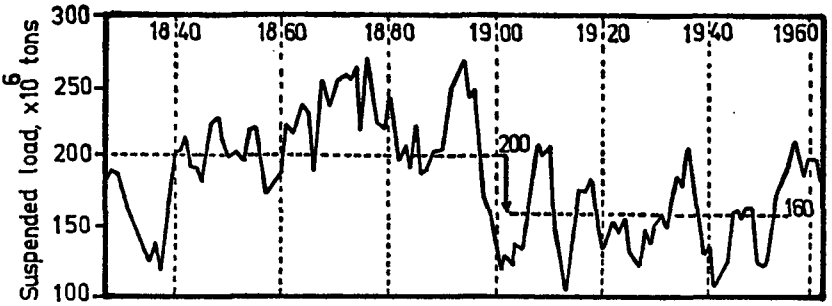

Fig. 9. Estimated suspended sediment load at Gaafra (Nile), 1825—1963 (after COASTAL PROTECTION STUDIES, 1978)

particularly decreased. The decrease of the Nile discharge and load due to reduced monsoonal rainfall over eastern Africa (ROSSIGNOL—STRICK, 1983) initiated a period of coastal instability and of headland recession. The cyclic variability of the Nile floods (HASSAN, 1981; HAMID, 1984) related to climate and precipitation change in east Africa had resulted during Dynastic times (3050—330 BC) in periods of economic stagnation. It is most likely that the changes occurred in the River Nile at Aswan since the beginning of the 20th century is the consequence of a slow climatic oscillation of more than 100 years period. On the other hand, HARRIS (1979) mentioned that the annual mean discharge decreased from 43.5 km³/yr to 4.4 km³/yr and the suspended load decreased from 60 million tons/yr to 5 million tons/yr after the construction of the Aswan High Dam in 1964. Therefore, the High Dam may play a minor part in the changing coast because the coastal erosion has been observed long before its construction.

CONCLUSIONS

1. Recent coastal erosion of the Nile Delta has been observed since 1909. The loss of coastal lands for the period 1909—1988 at Rosetta, Burullus and Damietta was about 14.7, 0.44 and 21.0 million square meters respectively. The fastest rate of shoreline receding was found at Rosetta (58 m/yr) if it is compared to 41 m/yr for Damietta and 3.8 m/yr for Burullus.

2. Sea level change is essential in the problem of coastal erosion. The average tidal changes along the Nile Delta coast are small and range between 16 and 88 cm and not exceeding 24 cm for the monthly readings.

3. Summer seasons at Burullus have higher sea levels than those in winter ones. The summer swells may increase the sea level causing erosion of the beach and coastal dunes near Burullus. In contrast, sea levels of Rosetta become higher in winter than those in summer. Severe coastal erosion at Rosetta headland therefore may be related to the effect of the winter waves to increasing the sea level.

4. The sea level increases from Alexandria to Rosetta and up to Burullus; the mean sea level for each area is 13, 17 and 28 cm respectively. Such eastward increase in the sea level coincides with the predominant direction of longshore current which feeding the coast from west to east.

5. Evidence for continued subsidence could be seen in many areas along the coast. The subsidence rate on published studies ranges between 0.5 and 5.0 mm/yr and will increase the predicted sea level rise.

6. A significant difference occurred in the Nile load piror and post 1900. The Nile flood levels became lower and the annual discharge and sediment load particularly decreased. Such phenomena may explain the cause of erosion on the Nile Delta coast since 1900. On the other hand, the construction of the Aswan High Dam in 1964 has reduced the Nile discharge and sediment load to insignificant quantities and hence causing accelerated erosion.

7. Causes of recent erosion along the Nile Delta coast may be related to the action of the following factors together: (a) Decrease of Nile discharge and sediment load since 1900. (b) The part played by the Aswan High Dam. (c) Continued subsidence of the coastal areas. (d) Sea level rise.

REFERENCES

COASTAL PROTECTION STUDIES (1978): Final Technical Report. UNDP (EGY) **73/063**, UNDP/UNESCO, Paris, 483 p.

COUTELLIER, V. and STANLEY, D. J. (1987): Late Quanternary stratigraphy and paleogeography of the eastern Nile Delta, Egypt. Mar. Geology. **77**, 257—275.

EL-FISHAWI, N. M. and FANOS, A. M. (1989): Prediction of sea level rise by 2100, Nile Delta coast. INCUA **11** (in press).

EMERY, K. O., AUBREY, D. G. and GOLDSMITH, V. (1987): Coastal neo-tectonics of the Mediterranean from tide-gauge levels. Mar. Geology. **81**, 41—52.

GOBY, J. E. (1952): Histoire des nivellements de l'Isthme de Suez. Bull. Soc. Etudes Hist. Geogr. de l'Isthme de Suez. **5**, 23—43.

HAMID, S. (1984): Fourier analysis of Nile flood levels. Geophysical Res. Letters. **11**, 843—858.

HARRIS, F. R. (1979): Master planning and infrastructure development for the Port of Damietta. Consultants Reports to Ministry of Reconstruction and New Communities, Egypt. Prepared by F. R. Harris, Inc., Consulting Engineers.

HASSAN, F. A. (1981): Historical Nile floods and their implications for climatic change. Science. **212**, 1142—1145.

HICKS, S. D. (1978): An average geopotential sea level series for the United States. Jour. Geophys. Res. **83**, 1377—1379.

HICKS, S. D., DEBOUGH, H. A. and HICKMAN, L. E. (1983): Sea level variation for the United States, 1855—1980. Rockville, MD: National Ocean Service.

HULL, C. H. J. and TITUS, J. G. (1986): Greenhouse effect, sea level rise and salinity in the Delaware Estuary. U. S. Environmental Prot. Agency, Washington, D. C. 20 460, EPA 230—05—86—010. 88 p.

IBRAHIM, M. M. (1963): The last subsidence movement of land on the Mediterranean coast. Unpublished paper, Mineral Wealth and Ground Water, Ministry of Scientific Research, Egypt. 6 p.

MANOHAR, M. (1976): Dynamic factors affecting the Nile Delta coast. In: Proc. Semin. on Nile Delta Sedimentology. UNDP/UNESCO/ASRT, Alexandria, 25—29 Oct. 1975. 104—129.

QUELENNEC, R. E. and KRUK, C. B. (1976): Nile suspended load and its importance for the Nile Delta morphology. In: Proc. Semin. on Nile Delta Sedimentology. UNDP/UNESCO/ASRT, Alexandria, 25—29 Oct. 1975. 130—144.

ROSSIGNOL-STRICK, M. (1983): African monsoons, an immediate climatic response to orbital insulation. Nature. **303**, 46—49.

SESTINI, G. (1988): Nile Delta: a review of depositional environments and geologic history. In: M. K. G. Whateley and K. T. Pickering (eds): Deltas, sites and traps for fossil fuels. Geol. Soc. London, Spec. publ. Blackwell Scientific Publications (in press).

STANLEY, D. J. (1988): Subsidence in the northern Nile Delta: Rapid rates, possible causes and consequences. Science. **240**, 497—500.

TOUSSOUN, O. (1934): Les ruines sous-marines de la baie d'Abuquir. Bull. Soc. Roy. Arch. Alexandria. **29**, 342—354.

Manuscript received, 18 May, 1989

ANNOUNCEMENT

EUROPEAN ASSOCIATION OF PETROLEUM GEOSCIENTISTS

On Tuesday 30 May 1989 the European Association of Petroleum Geoscientists (EAPG) was formally launched at its Inuagural Meeting in the International Congress Centre in Berlin (West).

For some time the need was felt among European earth scientists for a professional organisation which would bring together the various earth-science disciplines used in the search for and the production of oil and natural gas.

About two years ago some o *f*cers and members of the European Association of Exploration Geophysicists took the initiative to prepare the launch of the EAPG. More than 400 petroleum professionals joined as Founder Members and have now installed an initial Executive Committee.

The Association aims to bring together the many thousands of petroleum geoscientists in East and West Europe. W. F. STEENKEN, the Chairman of the new Executive Committee said in his inaugural speech: "Europe, more actively than in the past, is looking for its own identity. Not only the move towards an "EEC without frontiers' in 1992, also the exciting developments in other parts of the continent increase the awareness of a common European destiny. It seems only logical for the European oil industry to respond to this trend of integration."

The new Association held a four-day conference to which many scientists from East and West Europe contributed. Its theme was "Multidisciplinary Petroleum Geoscience: Generation, Accumulation and Production of Europe's Hydrocarbons". This conference ran parallel to a similar one of the EAEG and it is the intention to coordinate closely also future activities of the two sister organisations.

Applications for active and student membership will now be processed. Application forms can be obtained from the EAPG Business Office, PO Box 298, 3700 AG Zeist, The Netherlands, telephone: +31.3404.56997, fax: +31.3404.62640.

90-1433 — Szegedi Nyomda
Felelős vezető: Kónya Antal mb. igazgató

Illustrations

Figures should be used only where they are essential to elucidate the text.

The illustrations should be numbered according to their sequence in the text, and in the text references should be made to each figure.

All illustrations should be given separately, not stuck on sheets and not folded. The number of the figure and the authors name should be noted on the reverse side of the photographs and on the lower frontside of drawings, indicating at the same time the top of the figure where it is necessary.

Captions for all figures should be given typewritten on a separate list at the end of the manuscript. Drawn text in the figures should be kept to a minimum.

Drawings should be made on tracing paper by Indian ink. The thickness of the lines and the size of the lettering should be big enough to allow a necessary reduction.

Photographs of good contract and intensity on glossy paper are only acceptable. Colour photographs or drawings cannot be accepted.

Use bar scale on all illustrations instead of numerical scales that must be changed if reduction in necessary.

References

All references to publications made in the text should be made by quoting the author's name (without initials) and year of publication in parenthesis.

The list of references at the end of the manuscript should be arranged alphabetically by author's names and chronologically per author.

If the referred publications are written by more than two authors, in the text only the name of the first author should be indicated, the other co-authors are denoted by "et al.", however, in the list of references the names of authors and all co-authors should be mentioned.

In the list of references all references should be written, e.g. Balogh, K., A. Barabás (1972): The Carboniferous and Permian of Hungary. Acta Miner. Petr., Szeged, XX/2, 191—207.

At references to books beside the author's name, year of publication, title and the publishing house should also be mentioned.

In the case of references for symposium volumes, special issues or multi-authors books, the following system should be used: Roser, B. P., C. W. Childs, and G. P. Glasby (1980); Manganese in New Zealand. In: I. M. Varentsov and Gy. Grasselly (Editors): Geology and Geochemistry of Manganese, Vol. II. Akadémiai Kiadó, Budapest, 199—211.

Manuscript that are not adequately prepared will be returned to the author(s).